U.S. Department
of Commerce

Volume 109
Number 2
April 2011

Fishery Bulletin

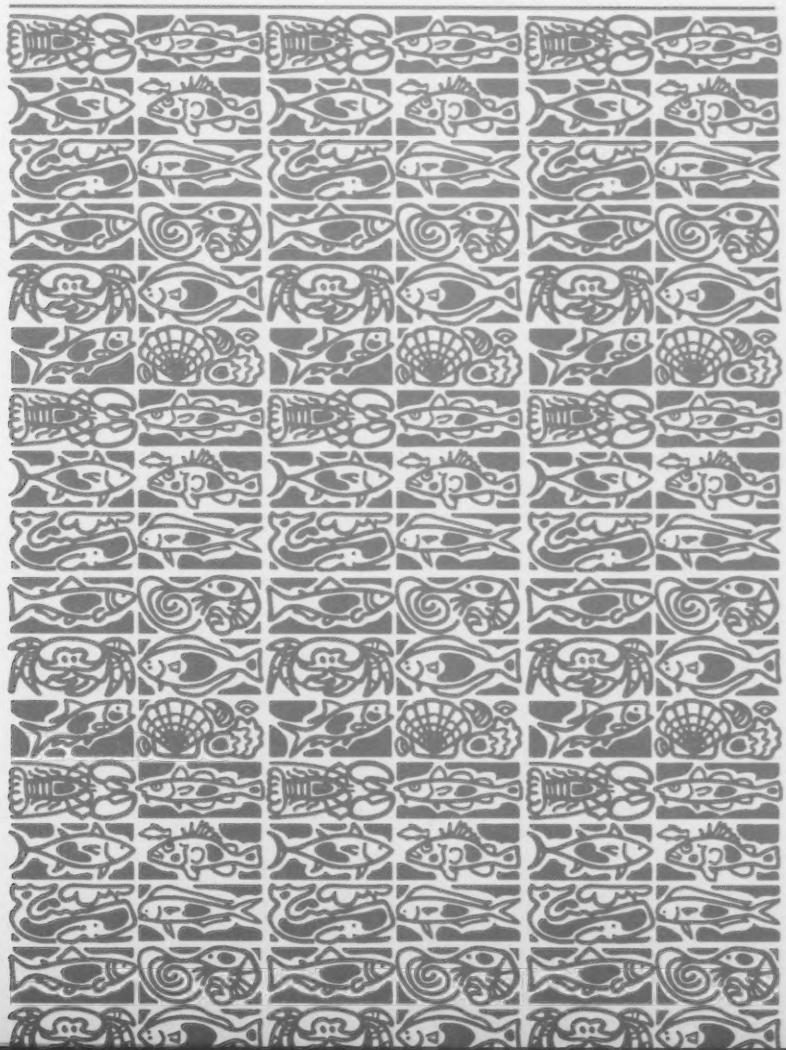

U.S. Department of Commerce
Gary Locke
Secretary of Commerce

National Oceanic and Atmospheric Administration
Jane Lubchenco, Ph.D.
Administrator of NOAA

National Marine Fisheries Service
Eric C. Schwaab
Assistant Administrator for Fisheries

Fishery Bulletin

Scientific Editor
Richard D. Brodeur, Ph.D.

Associate Editor
Julie Scheurer

National Marine Fisheries Service
Northwest Fisheries Science Center
2030 S. Marine Science Dr.
Newport, Oregon 97365-5296

Managing Editor
Sharyn Matriotti

National Marine Fisheries Service
Scientific Publications Office
7600 Sand Point Way NE
Seattle, Washington 98115-0070

Editorial Committee

John Carlson	National Marine Fisheries Service, Panama City, Florida
Kevin Craig	Florida State University, Tallahassee, Florida
Jeff Leis	Australian Museum, Sydney, New South Wales, Australia
Rich McBride	National Marine Fisheries Service, Woods Hole, Massachusetts
Rick Methot	National Marine Fisheries Service, Seattle, Washington
Adam Moles	National Marine Fisheries Service, Auke Bay, Alaska
Frank Parrish	National Marine Fisheries Service, Honolulu, Hawaii
Dave Somerton	National Marine Fisheries Service, Seattle, Washington
Ed Trippel	Department of Fisheries and Oceans, St. Andrews, New Brunswick, Canada
Mary Yoklavich	National Marine Fisheries Service, Santa Cruz, California

***Fishery Bulletin* web site: www.fisherybulletin.noaa.gov**

The *Fishery Bulletin* (ISSN 0090-0656) is published quarterly by the Scientific Publications Office, National Marine Fisheries Service, NOAA, 7600 Sand Point Way NE, BIN C15700, Seattle, WA 98115-0070. Periodicals postage is paid at Seattle, WA. POSTMASTER: Send address changes for subscriptions to Fishery Bulletin, Superintendent of Documents, Attn.: Chief, Mail List Branch, Mail Stop SSOM, Washington, DC 20402-9373.

Although the contents of this publication have not been copyrighted and may be reprinted entirely, reference to source is appreciated.

The Secretary of Commerce has determined that the publication of this periodical is necessary according to law for the transaction of public business of this Department. Use of funds for printing of this periodical has been approved by the Director of the Office of Management and Budget.

For sale by the Superintendent of Documents, U.S. Government Printing Office, Washington, DC 20402. Subscription price per year: $36.00 domestic and $50.40 foreign. Cost per single issue: $21.00 domestic and $29.40 foreign. **See back for order form.**

The *Fishery Bulletin* carries original research reports and technical notes on investigations in fishery science, engineering, and economics. It began as the Bulletin of the United States Fish Commission in 1881; it became the Bulletin of the Bureau of Fisheries in 1904 and the *Fishery Bulletin* of the Fish and Wildlife Service in 1941. Separates were issued as documents through volume 46; the last document was No. 1103. Beginning with volume 47 in 1931 and continuing through volume 62 in 1963, each separate appeared as a numbered bulletin. A new system began in 1963 with volume 63 in which papers are bound together in a single issue of the bulletin. Beginning with volume 70, number 1, January 1972, the *Fishery Bulletin* became a periodical, issued quarterly. In this form, it is available by subscription from the Superintendent of Documents, U.S. Government Printing Office, Washington, DC 20402. It is also available free in limited numbers to libraries, research institutions, State and Federal agencies, and in exchange for other scientific publications.

U.S. Department of Commerce
Seattle, Washington

Volume 109
Number 2
April 2011

Fishery Bulletin

Contents

Articles

139–146 **Sanchez-Rubio, Guillermo, Harriet M. Perry, Patricia M. Biesiot, Donald R. Johnson, and Romuald N. Lipcius**
Climate-related hydrological regimes and their effects on abundance of juvenile blue crabs (*Callinectes sapidus*) in the northcentral Gulf of Mexico

147–161 **Fry, Brian**
Mississippi River sustenance of brown shrimp (*Farfantepenaeus aztecus*) in Louisiana coastal waters

162–169 **Duffy-Anderson, Janet T., Deborah M. Blood, and Kathryn L. Mier**
Stage-specific vertical distribution of Alaska plaice (*Pleuronectes quadrituberculatus*) eggs in the eastern Bering Sea

170–185 **Prista, Nuno, Norou Diawara, Maria José Costa, and Cynthia Jones**
Use of SARIMA models to assess data-poor fisheries: a case study with a sciaenid fishery off Portugal

186–197 **Reum, Jonathan C. P., and Timothy E. Essington**
Season- and depth-dependent variability of a demersal fish assemblage in a large fjord estuary (Puget Sound, Washington)

198–216 **He, Xi, Stephen Ralston, and Alec D. MacCall**
Interactions of age-dependent mortality and selectivity functions in age-based stock assessment models

The National Marine Fisheries Service (NMFS) does not approve, recommend, or endorse any proprietary product or proprietary material mentioned in this publication. No reference shall be made to NMFS, or to this publication furnished by NMFS, in any advertising or sales promotion which would indicate or imply that NMFS approves, recommends, or endorses any proprietary product or proprietary material mentioned herein, or which has as its purpose an intent to cause directly or indirectly the advertised product to be used or purchased because of this NMFS publication.

The NMFS Scientific Publications Office is not responsible for the contents of the articles or for the standard of English used in them.

217–231 **Ralston, Stephen, André E. Punt, Owen S. Hamel, John D. DeVore, and Ramon J. Conser**
A meta-analytic approach to quantifying scientific uncertainty in stock assessments

232–242 **Collins, Angela B., and Richard S. McBride**
Demographics by depth: spatially explicit life-history dynamics of a protogynous reef fish

243 Errata

244 Guidelines for authors

Subscription form (inside back cover)

Climate-related hydrological regimes and their effects on abundance of juvenile blue crabs (*Callinectes sapidus*) in the northcentral Gulf of Mexico

Guillermo Sanchez-Rubio (contact author)[1]
Harriet M. Perry[1]
Patricia M. Biesiot[2]
Donald R. Johnson[1]
Romuald N. Lipcius[3]

Email address for contact author: guillermo.sanchez@usm.edu

[1] The University of Southern Mississippi
Center for Fisheries Research and Development
Gulf Coast Research Laboratory
703 East Beach Drive
Ocean Springs, Mississippi 39564

[2] The University of Southern Mississippi
Department of Biological Science
118 College Drive
Hattiesburg, Mississippi 39406

[3] Virginia Institute of Marine Science
The College of William and Mary
Department of Fisheries Science
P.O. Box 1346
Gloucester Point, Virginia 23062

Abstract—The abundance of juvenile blue crabs (*Callinectes sapidus*) in the northcentral Gulf of Mexico was investigated in response to climate-related hydrological regimes. Two distinct periods of blue crab abundance (1, 1973–94 and 2, 1997–2005) were associated with two opposite climate-related hydrological regimes. Period 1 was characterized by high numbers of crabs, whereas period 2 was characterized by low numbers of crabs. The cold phase of the Atlantic Multidecadal Oscillation (AMO) and high north-south wind momentum were associated with period 1. Hydrological conditions associated with phases of the AMO and North Atlantic Oscillation (NAO) in conjunction with the north-south wind momentum may favor blue crab productivity by influencing blue crab predation dynamics through the exclusion of predators. About 25% (22–28%) of the variability in blue crab abundance was explained by a north–south wind momentum in concert with either salinity, precipitation, or the Palmer drought severity index, or by a combination of the NAO and precipitation.

Manuscript submitted 22 February 2010.
Manuscript accepted 5 January 2011.
Fish. Bull. 109:139–146 (2011).

The views and opinions expressed or implied in this article are those of the author (or authors) and do not necessarily reflect the position of the National Marine Fisheries Service, NOAA.

Nonlinear oceanic-atmospheric oscillations have been linked to hydrological conditions in the continental United States. Individual and combined nonlinear oceanic-atmospheric oscillations, such as the Pacific Decadal Oscillation (PDO), Atlantic Multidecadal Oscillation (AMO), North Atlantic Oscillation (NAO), and El Niño Southern Oscillation (ENSO) have been shown to modulate Mississippi, Atchafalaya, Pearl, and Pascagoula river flows in their lower basins (Sanchez-Rubio et al., 2011). Discharge from the Mississippi and Atchafalaya rivers represents over 90% of the total river discharge in Louisiana (Perret et al., 1971). The Pascagoula and Pearl rivers account for more than 90% of the freshwater discharge into the Mississippi Sound (Eleuterius, 1978). High river flows in northern Gulf of Mexico (GOM) estuaries have been linked to increased commercial landings of blue crabs (*Callinectes sapidus*) in Texas (More, 1969) and Florida (Wilber, 1994) and to both commercial landings and abundance of juvenile crabs (<40 mm carapace width [CW]) in Louisiana (Guillory 2000). River discharge enhances wetland nursery areas by increasing the geographic extent of marsh-edge habitat and by providing nutrients that facilitate growth of vegetation. The quantity and quality of coastal marsh habitat have been linked to the successful production of blue crabs. Flooding events directly influence the degree of accessibility of marsh habitats (Rozas and Reed, 1993; Minello and Webb, 1997; Castellanos and Rozas, 2001). Vegetated and ephemeral structured habitats provide chemical cues for settlement, food, and refuge to juvenile crabs (Williams et al., 1990; Heck et al., 2001; Rakocinski et al., 2003).

The blue crab is a conspicuous member of coastal ecosystems along the Atlantic and Gulf coasts and the species supports important recreational and commercial fisheries for both hard and soft crabs (Guillory et

Table 1

Meteorological and hydrological parameters and sources for juvenile blue crab (*Callinectes sapidus*) abundance data used in data analyses. Data for climate-related hydrological regimes, oceanic-atmospheric indices, and Mississippi and Pascagoula river flows were adopted from Sanchez-Rubio et al. (2011).

Parameter	Annual period	Source
Kessler east-west and north-south wind momentum, (dynes/cm^2)h	Sep–Aug	http://cdo.ncdc.noaa.gov/qclcd/QCLCD?prior=N&state=MS&wban=13820 (accessed Mar 2007).
Coastal Louisiana and Mississippi Palmer drought severity index and precipitation, mm		http://www7.ncdc.noaa.gov/CDO/CDODivisionalSelect.jsp (accessed Mar 2008).
Louisiana coastal water level, m		http://www.mvn.usace.army.mil/eng/edhd/watercon.htm (accessed Feb 2008).
Trawl sampling salinity, ppt		Louisiana Department of Wildlife and Fisheries, Gulf Coast Research Laboratory-Mississippi Department of Marine Resources
Catch per unit of effort	Jan–Dec	

al., 2001). The ability to predict adult population size and thus annual available harvest has been limited by an incomplete understanding of the impact of biotic and abiotic variables as they relate to recruitment and survival of juvenile blue crabs. Although the oceanic-atmospheric oscillations have been associated with the amount of Mississippi River and Pascagoula River discharge (Sanchez-Rubio et al., 2011), they have not been related to the periodicity of blue crab population levels in the northcentral GOM. The purpose of the present study is to examine the relationship between nonlinear oceanic-atmospheric oscillations and juvenile blue crab abundance in the northcentral GOM and to elucidate underlying mechanisms involved in that association. This article also addresses the relevance of this study for the management of blue crab in the northcentral GOM.

Materials and methods

Data acquisition

Sanchez-Rubio et al. (2011) examined combinations of oceanic-atmospheric oscillations related to river flow in the northcentral GOM and determined that two regime occurred during the period covered in this study: I) the AMO (cold)–NAO (positive[=high water flow]) and II) the AMO (warm)–NAO (negative[=low water flow]). These regimes were used to examine the relationship between climate and juvenile blue crab abundance. Individual oceanic-atmospheric indices and river-flow anomalies were also adopted from that study. Other meteorological (wind momentum) and hydrological (precipitation, Palmer drought severity index [PDSI], water level, and salinity) data and the biological data (crab abundance) used in the present study are described and illustrated in Table 1 and Figure 1, respectively. The annual environmental data were calculated from September to August because that period incorporates the time of peak settlement of megalopae in the northern GOM and these megalopae are an important link in determining early year-class strength. Perry and Stuck (1982) noted that the large catches of blue crab megalopae in August and September were followed by an increased catch of juvenile crabs (10.0 to 19.9 mm) in October or November in Mississippi estuaries. Thus the chosen period for examination follows the dominant modal group responsible for year-class strength. Blue crabs recruit to trawls at ~30 mm CW and are abundant at this size in the winter. The January to December time frame covers the period of juvenile development and it is this period when year-class success is established.

Daily coastal water-level data were obtained from two U.S. Army Corps of Engineers gauges along the Louisiana coast (Fig. 1: see Cocodrie [1969–2000], and Rigolets [1966–2005]). Daily water-level data from the Rigolets gauge were averaged to obtain monthly water-level values. The monthly water-level values were averaged to obtain an annual water-level data set for the years 1973–2005. An annual water level anomaly was calculated by subtracting the average value by year from the yearly values of water level. Hourly wind data were obtained from the National Climatic Data Center, Asheville, NC. Hourly records of wind speed and direction were taken from the Kessler Airport, Biloxi, MS, with an anemometer mounted at 10 m height. The direction of the winds was subdivided into winds from the east (67.5–112.5°), west (247.5–292.5°), north (337.5–22.5°), and south (157.5–202.5°). Wind stress values were calculated for the four directions in dynes/cm^2. For each direction of the winds, the monthly average of wind stress was multiplied by the number of hours (wind momentum = [dynes/cm^2]h) and then, annual values of wind momentum were calculated from 1973 through 2003. To compare climate-related periods of blue crab

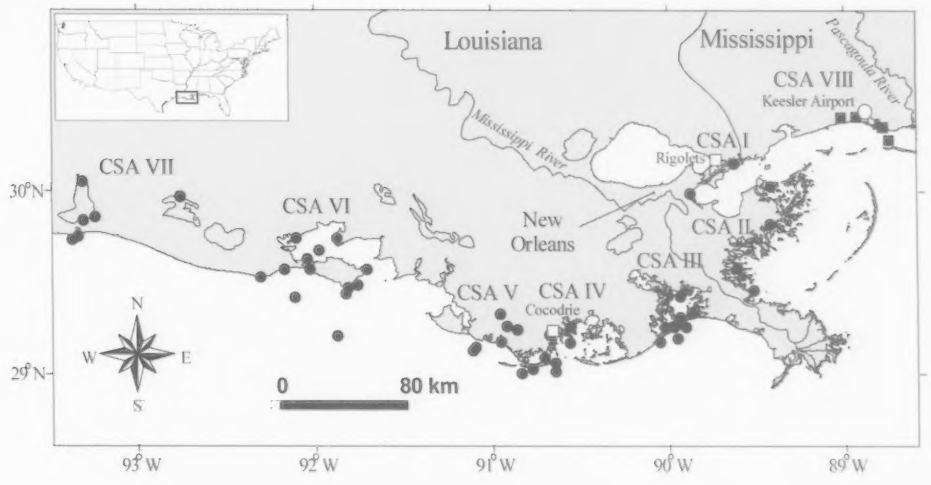

Figure 1

Trawl stations surveyed by Louisiana Department of Wildlife and Fisheries (47 solid circles) and Gulf Coast Research Laboratory (four solid squares), stations from the U.S. Army Corps of Engineers (two sea level gauges: open squares), and the wind station from the National Climatic Data Center (open circle). Coastal study areas (CSAs): I=Lake Borgne-Chandeleur Sound estuary; II=Breton Sound estuary; III=Barataria Bay estuary; IV=Terrebonne-Timbalier Bay estuary; V=Lake Mechant-Caillou Lake estuary; VI=Vermilion Bay estuary; VII=Calcasieu Lake estuary; and VIII=Biloxi estuary.

abundance, a wind momentum time series was formed by year from the difference between east and west and north and south winds. Two data sets were generated showing the east-west and north-south wind momentum values. To identify wind directions (angle with respect to the coast) influencing water level in the northcentral GOM, PV-Wave, vers. 6.21 (Visual Numerics Inc., Boulder, CO) software was used to correlate the Kessler Airport wind direction (vector) and water level from one gauge west (Cocodrie) and one gauge east (Rigolets) of the Mississippi River Delta.

Annual PDSI and precipitation values were calculated for each of the four divisions (southwest, southcentral, and southeast Louisiana, and coastal Mississippi) in the northcentral GOM. For each of the four divisions, an annual precipitation anomaly was calculated by subtracting the average value by year from the yearly values of precipitation. Annual PDSI (Pearson $r>0.649$, $P<0.001$) and precipitation (Pearson $r>0.646$, $P<0.001$) values were highly correlated among the four divisions and thus allowed calculation of regional annual (1967–2005) data for both variables.

Long-term, fishery-independent, biological data were acquired from 47 stations in Louisiana (Louisiana Department of Wildlife and Fisheries) and four stations in Mississippi (Gulf Coast Research Laboratory and Mississippi Department of Marine Resources). This region was divided into eight coastal study areas (CSAs): seven in Louisiana and one in Mississippi (Fig. 1). Louisiana data (CSAs I–VII) cover the period 1967 to 2005 and samples were collected weekly from March to October and biweekly from November to February. Mississippi data (CSA VIII) extended from 1973 to 2005 and samples were taken monthly. Both states, by agreement, use standard gear and sampling protocols: a 4.9-m otter trawl (1.9-cm bar mesh with a 6.35-mm mesh liner in the codend) pulled for 10 minutes. Crabs were counted and measured to the nearest carapace width (mm). Monthly surface salinities were calculated from trawl stations west (CSA III, V–VII) and east (CSA I and VIII) of the Mississippi River Delta. Monthly salinities were averaged to obtain single data sets of annual (1973–2004) salinity for each CSA. The annual salinity of each CSA was multiplied by the number of samples taken annually and the products for all CSAs were added and then divided by the total number of samples collected in the eight CSAs. The yearly regional salinity was a weighted average by sample size, which gives to the CSAs where few samples were collected less weight than those where large numbers of samples were taken in the calculation of the regional salinity data set. An annual weighted salinity anomaly was calculated by subtracting the average value by year from the yearly values of weighted salinity. The variability of salinity can be considered regionally, because two major rivers in the west (Mississippi and Atchafalaya rivers) and two in the east (Pearl and Pascagoula rivers) of the Mississippi River Delta are responsible for 90% of freshwater discharge to the northern GOM (Eleuterius, 1978; Perret et al., 1971).

Although the biological data for Louisiana cover the period 1967 to 2005, trawl sampling effort and areal

coverage among and within CSAs were variable from 1967 through 1981 and more equally distributed beginning in 1982. A regional data set of yearly overall abundance (all size classes) was constructed. The vast majority of the crabs collected were less than one year old. Crabs <50 mm CW represented 61.7% of the catch and crabs <90 mm CW represented 82%. To obtain a yearly catch per unit of effort (CPUE), the average catch by station in each study area was calculated by dividing the total catch by the total number of samples. The annual CPUE for each station within a study area was added and then divided by the number of stations to obtain a yearly CPUE for each of the eight CSAs. The annual CPUE of each CSA was multiplied by the number of samples taken annually and the products for all CSAs were added and then divided by the total number of samples collected in the eight CSAs. The yearly regional CPUE was a weighted average by sample size, which gives the CSAs with few collected samples less weight than those with a large number of samples in the calculation of the regional CPUE.

Climate-related hydrological regimes and crab abundance

Over the period of the biological surveys (1967–2005), two climate-related hydrological regimes (1973–94 and 1997–2005) were identified (Sanchez-Rubio et al., 2011). To evaluate the response of blue crab abundance to these hydrological regimes, a *t*-test was used. Relationships among crab abundance and oceanic-atmospheric oscillations and hydrological and meteorological parameters were determined by using correlation analysis. To identify models of oceanic-atmospheric oscillations and meteorological and hydrological parameters that contribute to the variability in blue crab abundance in the northcentral GOM, multiple linear regression analysis (Statistical Package R, vers. 2.7.0, http://www.r-project.org/) was used. To find the best-fitting model, an Akaike's information criterion (AIC; Akaike, 1981) and Bayesian information criterion (BIC; Raftery, 1996) were calculated for each model. To check model reliability, the models with the lowest BIC and AIC values were compared after having been corrected for small sample size (McQuarrie and Tsai, 1998). Multiple linear regression in SPSS (IBM, Somers, NY) was used on the selected models to determine their r^2 values.

Results

Climate-related hydrological regimes and crab abundance

Two long-term climate-influenced hydrological regimes were found to be related to two distinct periods of blue crab abundance in the northcentral GOM. Significance differences in blue crab mean abundance (t=3.196, P=0.003; Fig. 2) were found within regimes that were associated by Sanchez-Rubio et al. (2011) with wet and dry conditions. During regime I (wet), there were higher catches of juvenile crabs than during regime II (dry). The regime with the highest blue crab abundances had a significantly higher mean of the north-south wind momentum (t=2.187, P=0.038) and a lower mean of AMO (t=–7.276, P<0.001) than did the regime with low crab abundance (Table 2).

Correlation analysis showed that blue crab abundance was positively correlated with the north-south wind momentum (Pearson r=0.406, P=0.023) and PDSI (Pearson r=0.356, P=0.042) and was negatively related to salinity (Pearson r=0.345, P=0.053). According to the regression models developed from AIC and BIC, the north-south wind momentum in concert with either salinity, precipitation, or the Palmer drought severity index, or the combination of the NAO and precipitation were influential in determining 22% to 28% of the variability in blue crab abundance (Table 3). Figure 3 shows histograms of the variables that were associated with blue crab abundance by year.

Discussion

Early investigations into factors affecting population dynamics of blue crabs attempted to relate fluctuations in abundance to physiological tolerances to temperature and salinity. Livingston (1976) was among the first to

Table 2

Juvenile blue crab (*Callinectes sapidus*) weighted catch-per-unit-of-effort data and climatological factors showing significant differences in mean values during two hydrological regimes in the northcentral Gulf of Mexico. AMO: Atlantic Multidecadal Oscillation and NAO: North Atlantic Oscillation.

	Climate-related hydrological regimes	
Average values	AMO cold–NAO positive 1973–94	AMO warm–NAO negative 1997–2005
Weighted catch per unit of effort	7.207	4.395
AMO	–0.147	0.201
North–south wind momentum, (dynes/cm^2)h	0.083	–0.082

Table 3

Model results determined with Akaike's information criterion (AIC) and Bayesian information criterion (BIC) used to describe annual variability of the weighted catch per unit of effort (CPUE=average crab catch per ten minute trawl) of juvenile blue crabs (*Callinectes sapidus*) in the northcentral Gulf of Mexico.

Model	Response variables	Explanatory variables	df	Sum of squares	*F* value	*P*(>*F*)	Coeff.	AIC	BIC	r^2
1	Weighted CPUE	North–south wind momentum	1	32.261	6.8453	0.01438	5.477	51.8	0.38	0.28
		North Atlantic Oscillation	1	12.550	2.6629	0.11432	2.278			
		Precipitation	1	23.697	5.0282	0.03335	1.058			
		Intercept					5.616			
2		North–south wind momentum	1	32.261	6.3966	0.01735	5.049	53.0	0.18	0.23
		Weighted salinity	1	22.277	4.4169	0.04471	−0.3328			
		Intercept					6.0473			
3		North–south wind momentum	1	32.261	6.3389	0.01781	5.5061	53.3	0.46	0.22
		Precipitation	1	20.992	4.1248	0.05185	0.9928			
		Intercept					5.8755			
4		North–south wind momentum	1	32.261	6.3234	0.01794	4.7625	53.4	0.54	0.22
		Palmer drought severity index	1	20.642	4.0460	0.05399	0.5745			
		Intercept					5.8365			

suggest that the influence of salinity might be operating extrinsically by structuring the surrounding biotic community. Recent research indicates that predation affects abundance in the northern GOM. Studies on predator-prey interactions (Heck and Coen, 1995; Guillory and Prejean, 2001; Moksnes and Heck, 2006) and habitat selection and utilization (Williams et al., 1990; Morgan et al., 1996; Rakocinski et al., 2003) indicate that factors that increase or decrease refuge availability are also determinant in the establishment of population levels. Both inter- and intraspecific predation, operate to regulate abundance of juvenile blue crabs in the GOM (Guillory et al., 2001). A high diversity of predators, few predation-free refuges, and year round predation activity (i.e., a lack of seasonality in predation) all contribute to the high regional mortality of juvenile crabs (Heck and Coen, 1995). If predation is the primary determinant of population levels, then those factors that influence available refuge may ultimately control abundance.

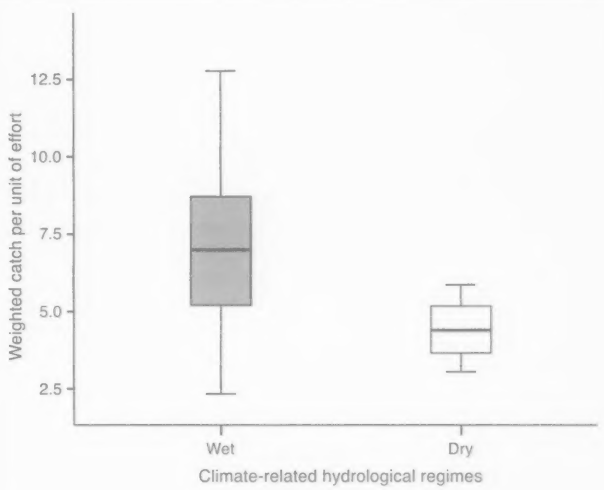

Figure 2

Weighted catch per unit of effort (CPUE=average crab catch per ten-minute trawl) of juvenile blue crabs (*Callinectes sapidus*) related to the two dominant climate-related hydrological regimes in the northcentral Gulf of Mexico between 1973 and 1994 (AMO cold–NAO positive: gray bar) and 1997–2005 (AMO warm–NAO negative: white bar). AMO=Atlantic Multidecadal Oscillation and NAO=North Atlantic Oscillation. Horizontal lines for each box plot indicate 5th, 25th, 50th (median), 75th, and 95th percentiles.

In the current study, the period of greatest crab abundance (climate-related hydrological regime I) was associated with a mean positive north–south wind momentum and a mean low value of AMO. Blue crab abundance was also positively correlated with the north–south component of wind momentum and PDSI and was negatively related to salinity. About 25% (22–28%) of the variability in blue crab abundance was explained by a north–south wind momentum in concert with either salinity, precipitation, or PDSI, or by the combination of NAO and precipitation. The AMO and NAO were found to be important drivers of climate-related features influencing long-term hydrological conditions across coastal Louisiana and Mississippi

(Sanchez-Rubio et al., 2011). Mississippi, Atchafalaya, Pearl, and Pascagoula river flows and blue crab abundance were higher during AMO cold and NAO positive phases than during AMO warm and NAO negative phases. Other studies have linked blue crab abundance to river flow and salinity. Guillory (2000) noted juvenile blue crab abundance was positively related to river flow and negatively related to salinity in fishery-independent (crabs <40 mm CW) trawl survey data for Louisiana. High commercial landings of blue crabs were associated with increased river flow by More (1969) in Texas bays, Wilber (1994) in Apalachicola Bay, Florida, and Guillory (2000) in Louisiana estuaries. Hydrological conditions associated with phases of AMO and NAO in conjunction with the north–south wind may influence blue crab predation dynamics through predator exclusion. Under an annual positive north–south wind regime with flooding rain events, greater availability of low-salinity habitats increases the survival of juvenile crabs by diminishing intra- and interspecific predation. Under an annual negative north–south wind regime (inshore water movement), low-salinity habitats are reduced and there is a greater suite of predators and an increased opportunity for predation.

Although long-term climatological patterns influence the abundance of estuarine organisms, there is also evidence that an interannual oceanic-atmospheric oscillation (ENSO) can affect population levels. In microtidal Louisiana estuaries, ENSO-related hydrological conditions were found to influence the abundance of estuarine organisms over limited time periods (Childers et al., 1990). High (or low) rates of local precipitation and Mississippi River discharge were generally associated with anomalously high (or low) marsh inundation, respectively, that coincided with ENSO warm (or ENSO cold) phases. The ENSO warm and cold phases generally coincided with the lowest abundance of organisms, and the ENSO neutral phase was related to high abundance. Sanchez-Rubio et al. (2011) found that the effect of ENSO phases on river discharge was most evident in the last climate-related hydrological regime (drought) in the Pascagoula River and flow from this river was significantly higher during ENSO warm and ENSO neutral phases than during the ENSO cold phase. Although the ENSO was found to affect river flow, the limited number of ENSO phases (warm, cold, neutral) occurring during the last hydrological regime precluded any meaningful analysis of the abundance of crabs in relation to ENSO events.

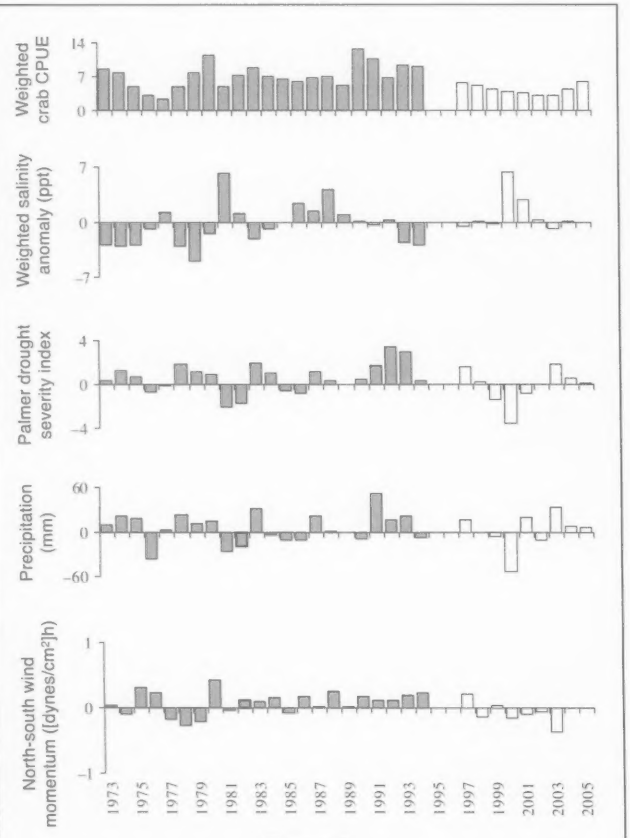

Figure 3

Weighted catch per unit of effort (CPUE=average crab catch per ten minute trawl) of juvenile blue crabs (*Callinectes sapidus*) related to highly influential hydrological and meteorological factors (salinity, PDSI, precipitation, and north–south wind momentum) in the northcentral Gulf of Mexico within two climate-related hydrological regimes (AMO cold–NAO positive: gray bars, and AMO warm–NAO negative: white bars). AMO=Atlantic Multidecadal Oscillation and NAO=North Atlantic Oscillation.

Implications for management

Management of any fishery requires some knowledge of the factors that contribute to year-class strength. Initial population levels are established by recruitment. In the northern GOM, recruitment success (measured as the number of megalopae at settlement) was found to be dependent on interannual variations in wind stress patterns coupled with basin-scale events, such as Loop Current spin-off eddies, generated during critical periods of larval development (Johnson and Perry, 1999; Perry et al., 2003). Seasonality of spawning coincided with climatological inner shelf water circulation patterns that transported larvae offshore initially but then acted to return them to shore at the appropriate developmental stage. Although annual temporal periodicity of settlement was similar, settlement was highly episodic and there were large annual variations in numbers of megalopae (Perry et al., 1995; Perry et al., 2003). Perry et al. (1998) noted that regard-

less of the level of recruitment, by the time crabs reach ~30 mm CW, population abundance begins to level off and then decreases at a gradual rate. In that study, high numbers of megalopae and early-stage crabs did not result in proportionally elevated numbers of late-stage juveniles; instead, high and low recruitment years had similar population levels. They concluded that the northcentral GOM blue crab fishery was not recruitment limited and that year-class strength was dependent on juvenile survival. In the northcentral GOM, there have been significant declines in numbers of later stage juveniles in trawl surveys; however, blue crabs at early life history stages collected in beam plankton trawls and seines do not exhibit similar trends (Riedel et al., 2010).

Climate interacts with an ever-changing physiographic landscape world-wide. Significant downward trends in abundance of juvenile blue crabs across the northern GOM have occurred over a period characterized by drought and unprecedented changes in habitat associated with catastrophic storms and the cumulative consequences of man-made alterations to coastal wetlands (Riedel et al., 2010). Recruitment has been adequate and numbers of megalopae and early juveniles do not exhibit declines. Unlike the fishery in Chesapeake Bay, the fishery in the GOM does not suffer from overharvesting (Riedel et al., 2010). There is strong evidence that fishery sustainability is dependent upon juvenile survival. In the northcentral GOM, climate and hydrological features operate to structure available habitat in ways that affect juvenile survival of blue crabs. Whether the shift to a more favorable climate phase would reverse declining trends is unknown because it is currently impossible to quantitatively account for the influence of changing habitats. The results of this work are a starting point toward understanding the complex relationship between climate, habitat, and fisheries productivity.

Acknowledgments

The authors would like to thank C. F. Rakocinski and R. P. Riedel for their expert advice. We are very grateful to V. Guillory, K. Ibos, J. Adriance, P. Cook, and M. Harbison from the Louisiana Department of Wildlife and Fisheries and the personnel from the University of Southern Mississippi, Gulf Coast Research Laboratory, Center for Fisheries Research and Development for providing us with the fishery independent data from the coastal study areas of Louisiana and Mississippi, respectively. Appreciation must also be expressed to M. G. Williams and C. A. Schloss of the University of Southern Mississippi, Gulf Coast Research Laboratory, Gunter Library.

Literature cited

Akaike, H.
1981. Likelihood of a model and information criteria. J. Econometrics 16:3–14.

Castellanos, D. L., and L. P. Rozas.
2001. Nekton use of submerged aquatic vegetation, marsh, and shallow unvegetated bottom in the Atchafalaya River Delta, a Louisiana tidal freshwater ecosystem. Estuaries 24:184–197.

Childers, D. L., J. W. Day Jr., and R. A. Muller.
1990. Relating climatological forcing to coastal water levels in Louisiana estuaries and the potential importance of El Niño-Southern Oscillation events. Clim. Res. 1:31–42.

Eleuterius, C. K.
1978. Classification of Mississippi Sound as to estuary hydrological type. Gulf Res. Rep. 6:185–187.

Guillory, V.
2000. Relationship of blue crab abundance to river discharge and salinity. Proc. Ann. Conf. SE Assoc. Fish Wildl. Agen. 54:213–220.

Guillory, V., H. Perry, and S. VanderKooy.
2001. The blue crab fishery of the Gulf of Mexico, United States: a regional management plan. Gulf States Mar. Fish. Comm. 96, 308 p. GSMFC, Ocean Springs, MS.

Guillory, V., and P. Prejean.
2001. Red drum predation on blue crabs (*Callinectes sapidus*). *In* Proceedings of the blue crab mortality symposium (V. Guillory, H. Perry, and S. Vanderkooy, eds.), p. 93–104. Gulf States Mar. Fish. Comm. 90, Ocean Springs, MS.

Heck, K. L. Jr., and L. D. Coen.
1995. Predation and the abundance of juvenile blue crabs: a comparison of selected East and Gulf Coast (USA) studies. Bull. Mar. Sci. 57:877–883.

Heck, K. L. Jr., L. D. Coen, and S. G. Morgan.
2001. Pre- and post-settlement factors as determinants of juvenile blue crab *Callinectes sapidus* abundance: results from the north-central Gulf of Mexico. Mar. Ecol. Prog. Ser. 222:163–176.

Johnson, D. R., and H. M. Perry.
1999. Blue crab larval dispersion and retention in the Mississippi Bight. Bull. Mar. Sci. 65:129–149.

Livingston, R. J.
1976. Diurnal and seasonal fluctuations of organisms in a North Florida estuary. Estuar. Coast. Mar. Sci. 4:373–400.

McQuarrie, A. D. R., and C. L. Tsai.
1998. Regression and time series model selection, 455 p. World Scientific Publ. Co., Singapore.

Minello, T. J., and J. W. Webb Jr.
1997. Use of natural and created *Spartina alterniflora* salt marshes by fishery species and other aquatic fauna in Galveston Bay, TX, USA. Mar. Ecol. Prog. Ser. 151:165–179.

Moksnes, P. O., and J. L. Heck Jr.
2006. Relative importance of habitat selection and predation for the distribution of blue crab megalopae and young juveniles. Mar. Ecol. Prog. Ser. 308:165–181.

More, W. R.
1969. A contribution to the biology of the blue crab (*Callinectes sapidus* Rathbun) in Texas, with a description of the fishery. TX Parks Wildl. Dep., Tech. Ser. 1:1–31.

Morgan, S. G., R. K. Zimmer-Faust, K. L. Heck Jr., and L. D. Coen.
1996. Population regulation of blue crabs *Callinectes sapidus* in the northern Gulf of Mexico: postlarval supply. Mar. Ecol. Prog. Ser. 133:73–88.

Perret, W. S., W. R. Latapie, J. F. Pollard, W. R. Mock, G. B. Adkins, W. J. Gaidry, and C. J. White.
1971. Fishes and invertebrates collected in trawl and

seine samples in Louisiana estuaries. *In* Cooperative Gulf of Mexico inventory and study phase IV, biology, section I, p. 39–105. LA Wildl. Fish. Comm., Baton Rouge, LA.

Perry, H. M., C. K. Eleuterius, C. B. Trigg, and J. R. Warren.
1995. Settlement patterns of *Callinectes sapidus* megalopae in Mississippi Sound: 1991, 1992. Bull. Mar. Sci. 57:821–833.

Perry, H. M., D. R. Johnson, K. M. Larsen, C. B. Trigg, and F. Vukovich.
1998. Blue crab larval dispersion and retention in the Mississippi Bight: testing the hypothesis. Bull. Mar. Sci. 72:331–346.

Perry, H. M., and K. C. Stuck.
1982. The life history of the blue crab in Mississippi with notes on larval distribution. Gulf States Mar. Fish. Comm. 7:17–22.

Perry, H., J. Warren, C. Trigg, and T. VanDevender.
1998. The blue crab fishery in Mississippi. J. Shellfish Res. 17:425–433.

Raftery, A. E.
1996. Approximate Bayes factors and accounting for model uncertainty in generalized linear models. Biometrika 83:251–266.

Rakocinski, C. F., H. M. Perry, M. A. Abney, and K. M. Larsen.
2003. Soft sediment recruitment dynamics of early blue crab stages in Mississippi Sound. Bull. Mar. Sci. 72:393–408.

Riedel, R., H. Perry, L. Hartman, and S. Heath.
2010. Population trends of demersal species from inshore waters of Mississippi and Alabama. Final Rep. MS-AL Sea Grant Consort, 89 p. [Available from Mississippi-Alabama Sea Grant, 703 East Beach Drive, Ocean Springs, MS.]

Rozas, L. P., and D. J. Reed.
1993. Nekton use of marsh-surface habitats in Louisiana (USA) deltaic salt marshes undergoing submergence. Mar. Ecol. Prog. Ser. 96:147–157.

Sanchez-Rubio, G., H. M. Perry, P. M. Biesiot, D. R. Johnson, and R. N. Lipcius.
2011. Oceanic-atmospheric modes of variability and their influence on Mississippi River and Pascagoula River flows. J. Hydrol. 396:72–81.

Wilber, D. H.
1994. The influence of Apalachicola River flows on blue crab, *Callinectes sapidus*, in north Florida. Fish. Bull. 92:180–188.

Williams, A. H., L. Coen, and M. Stoelting.
1900. Seasonal abundance, distribution, and habitat selection of juvenile *Callinectes sapidus* (Rathbun) in the northern Gulf of Mexico. J. Exp. Mar. Biol. Ecol. 137:165–183.

Mississippi River sustenance of brown shrimp (*Farfantepenaeus aztecus*) in Louisiana coastal waters

Brian Fry

Email address: bfry@lsu.edu

Department of Oceanography and Coastal Sciences
Louisiana State University
Baton Rouge, Louisiana 70803

Abstract—Brown shrimp (*Farfantepenaeus aztecus*) are abundant along the Louisiana coast, a coastline that is heavily influenced by one of the world's largest rivers, the Mississippi River. Stable carbon, nitrogen, and sulfur (CNS) isotopes of shrimp and their proventriculus (stomach) contents were assayed to trace riverine support of estuarine-dependent brown shrimp. Extensive inshore and offshore collections were made in the Louisiana coastal zone during 1999–2006 to document shrimp movement patterns across the bay and shelf region. Results showed an unexpectedly strong role for nursery areas in the river delta in supporting the offshore fishery, with about 46% of immigrants to offshore regions arriving from riverine marshes. Strong river influences also were evident offshore, where cluster analysis of combined CNS isotope data showed three regional station groups related to river inputs. Two nearer-river mid-shelf station groups showed isotope values indicating river fertilization and productivity responses in the benthic shrimp food web, and a deeper offshore station group to the south and west showed much less river influence. At several mid-shelf stations where hypoxia is common, shrimp were anomalously ^{15}N depleted versus their diets, and this $\delta^{15}N$ difference or mismatch may be useful in monitoring shrimp movement responses to hypoxia.

Manuscript submitted 10 July 2010.
Manuscript accepted 07 January 2011.
Fish. Bull. 109:147–161 (2011).

The views and opinions expressed or implied in this article are those of the author (or authors) and do not necessarily reflect the position of the National Marine Fisheries Service, NOAA.

Brown shrimp (*Farfantepenaeus aztecus*) have an estuarine-dependent life history that is well known (Gaidry and White[1]). Adults spawn offshore, and postlarvae enter bays to settle as benthic juveniles. The juveniles typically reside in bays for 1–3 months until they reach about 70–100 mm total length, then leave for offshore shelf areas where they may double in length before completing a largely annual life cycle. Both estuarine and offshore phases of this life cycle have been studied in detail; recent shrimp studies in estuaries have focused on loss of marsh nursery habitats (Peterson and Turner, 1994; Haas et al., 2004), and offshore studies have focused on bottom water hypoxia that can impede shrimp migrations and decrease overall habitat area for brown shrimp (Craig et al., 2005).

The brown shrimp fishery of Louisiana is one of the largest fisheries in the United States and occurs downstream of Mississippi River inflows that fertilize the Louisiana coastal zone (Moore et al., 1970). Nutrient loading from the Mississippi River has increased at least 2–4 times in recent decades in contrast to historical background levels (Turner and Rabalais, 1991; Turner et al., 2007), and this increase in fertilization of the coastal zone may be affecting offshore shrimp dynamics. In this study, stable isotopes were used to trace how the river currently supports brown shrimp populations because isotopes are increasingly used to trace linkages between riverine nutrients and coastal fisheries (Schlacher et al., 2005; Leaky et al., 2008).

The Mississippi River is one of the world's largest rivers in terms of catchment size, total discharge, and sediment load (Deegan et al., 1986; Rabalais et al., 1996). Most of the river flows into northern Gulf of Mexico in the Bird's Foot Delta south of New Orleans, and also into Fourleague Bay west of New Orleans where the Atchafalaya River carries 30% of the river flow into the Gulf of Mexico. During spring and early summer months when brown shrimp are found in coastal bays, most flow of the river is to the west along the coast and has typically high productivity and high chlorophyll levels in the shallow offshore waters within 5–10 km of the barrier islands (Walker and Rabalais, 2006). Eddies force some river water into bays where phytoplankton use nitrates from the river. Tides subsequently export productive phytoplankton to the Gulf of Mexico (Das et al., 2009). The high nutrients and strong water column mixing create conditions for high shrimp productivity that are similar to those observed in shrimp aquaculture ponds, but the coasts and bays are more open and allow extensive brown shrimp migrations at 10–100 km scales. In these open systems, it can be difficult to trace the connections between life history stages and populations that are important for managing fisheries.

[1] Gaidry, W. J., III, and C. J. White. 1973. Investigations of commercially important penaeid shrimp in Louisiana estuaries. LA Wildl. Fish. Comm. Tech. Bull. #8, 154 p. LA Wildl. Fish. Comm., New Orleans, LA.

Previous studies of stable isotopes for offshore brown shrimp were conducted mostly along the south Texas shelf, showing that isotope "tags" allow some estimates about those estuarine habitats that are most important in supporting offshore populations (Fry, 1981, 1983). In particular, seagrass meadows produced shrimp with high $\delta^{13}C$ values and small shrimp entering the offshore fishery often had these distinctive isotope tags, indicating a strong linkage between inshore seagrass meadows and offshore populations (Fry, 1981). Offshore shrimp populations in Texas waters and the deeper Gulf of Mexico had very uniform carbon isotope values within a 2‰ range, consistent with relatively uniform average isotopic compositions of phytoplankton and phytodetritus that support offshore benthic food webs (Fry, 1983; Fry et al., 1984). Estuarine shrimp had a much greater (>5×) diversity of isotope values, reflecting the much more diverse set of food types supporting benthic food webs in estuaries (Fry, 1981), but shrimp arriving offshore as immigrants gradually lost these divergent estuarine labels and their isotope values converged to relatively uniform offshore values. Experiments showed that this change in isotope label was due to shrimp replacing their old estuarine biomass during normal metabolism, while also acquiring new biomass from offshore foods (Fry and Arnold, 1982). Calculations indicated that a 2–4× increase in mass was generally sufficient to lose the estuarine isotope tags for rapidly growing shrimp that had switched to a new diet (Fry and Arnold, 1982; Fry, 2006). This tag loss could occur in 1–3 weeks for smaller-size (<125 mm) shrimp that grow at rates near 1 mm/day and occurs over a longer (3–8 week) period for any larger immigrant animals that grow more slowly offshore, but all immigrants gradually become residents as they acquire the distinctive offshore isotope tags. Experimental and field results thus both indicated that this type of food-related "disappearing" isotope tag had a relatively short life for rapidly growing brown shrimp, but work with the isotope tags was nonetheless interesting because shrimp acquire the isotope tags naturally without handling or stress, all shrimp are tagged instead of just a few, and the isotope tags provide information about origins that is very difficult to obtain otherwise (Fry 1981; 1983; 2008). These initial studies and much subsequent research has shown that isotopes can be used as tracers, tags, or labels for studying animal diets, origins, and movements (Hobson and Wassenaar, 2008; West et al., 2010).

Given that previous studies of shelf areas off Texas and deeper waters of the Gulf of Mexico show uniform carbon isotope values in areas that lack strong river inputs, a comparative examination of isotopes in Louisiana waters was undertaken in the present study to identify river impacts on brown shrimp origins and diets. A first goal was to test origins of shrimp along the Louisiana coast. Seagrass meadows that are hot spots of shrimp abundance in Texas waters are largely lacking along the Louisiana coastline owing to turbid waters, but Louisiana brown shrimp are nonetheless common in open bays and areas near salt marshes. Brown shrimp are especially abundant in Barataria and Terrebonne bays along the central Louisiana coast and these bays are sampled regularly by personnel of the Louisiana Department of Wildlife and Fisheries (LADWF) to help set various opening and closing dates for shrimp fishing seasons. These bays have relatively little input from the Mississippi River but are often considered the major estuarine source regions for Louisiana shrimp production (Gaidry and White[1]). However, during the course of this study brown shrimp were found to be also abundant in delta marshes in the Bird's Foot Delta around the mouth of the Mississippi River, just to the east of the central coast and Barataria and Terrebonne bays. To test whether bays of the central coast or riverine marshes were more important shrimp source areas for the offshore fishery, small shrimp were collected as they arrived as immigrants to the offshore system and tested for their isotope tags. A second goal of this study was to test for a distinctive riverprint or isotope landscape ("isoscape"; West et al., 2010) by mapping offshore shrimp isotopes to trace river subsidies to benthic food webs. The Mississippi River supplies most (>90%) of the freshwater in the Gulf of Mexico so that any river-related signals could be expected to be stronger in areas closer to the river.

Combinations of C, N, and S stable isotope measurements were investigated as possible tracers of river influences. Carbon isotopes were used to investigate bay origins and linkages to offshore productivity, with low $\delta^{13}C$ values (<–18‰) generally indicating estuarine origins, and highest offshore values (near –15‰) indicating higher phytoplankton productivity at the base of the food web (Fry, 1981; Fry and Wainright, 1991). For nitrogen isotopes, studies of nitrates in the Mississippi River show a relatively high average value near 8‰ (Fry and Allen, 2003), so that estuarine food webs incorporating nitrates became enriched in ^{15}N, a bottom-up labeling of whole food webs also observed in other human-impacted systems (Schlacher et al., 2005). Higher $\delta^{15}N$ was expected for shrimp from river-influenced delta marshes than for shrimp from Barataria and Terrebonne bays that have much smaller river inputs. Sulfur isotopes also can provide an interesting label when high productivity in the water column leads to more organic matter settling to the seafloor and more sulfate reduction in benthic sediments (Peterson and Howarth, 1987). Pelagic plants and animals have high $\delta^{34}S$ values near the +21‰ value of marine sulfate (Rees et al., 1978; Peterson et al., 1985), but sulfides that are produced in sediments from sulfate reduction have low $\delta^{34}S$ values and enter benthic food webs, resulting in lower $\delta^{34}S$ values of 5–15‰ for animals such as estuarine brown shrimp (Fry, 2008). Geochemical studies in the northern Gulf of Mexico indicate that most sedimentary sulfides are bound with iron (Lin and Morse, 1991), but it is still possible that some of these sulfides are used by benthic bacteria and enter the organic food web, so that lowest shrimp $\delta^{34}S$ values might be expected for eutrophic river-influenced areas.

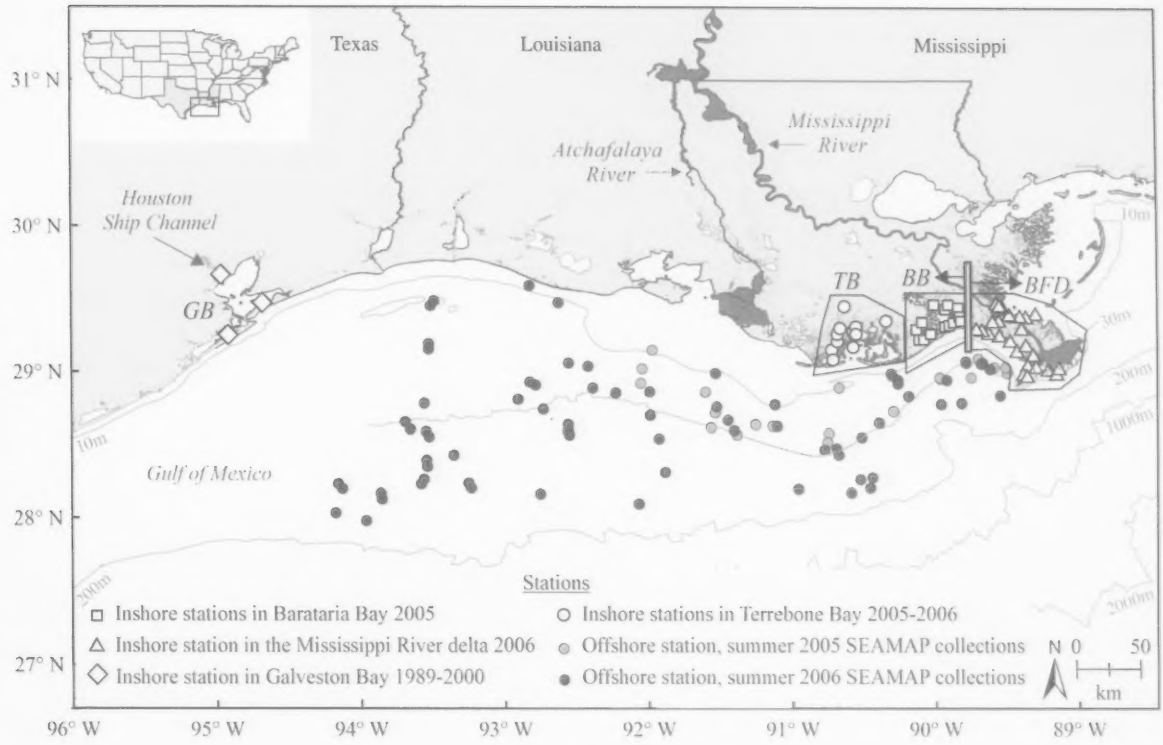

Figure 1

Study area along the Louisiana-Texas coast, northern Gulf of Mexico. River inflows important in this study are the Mississippi River at the Bird's Foot Delta, the Atchafalaya River along the central coast, and the Houston Ship Channel that flows into upper Galveston Bay. GB=Galveston Bay, TB=Terrebonne Bay, BB=Barataria Bay, BFD=Bird's Foot Delta. The north-south dividing line between BB and BFD marks the zero-km reference used in Figure 3. SEAMAP=Southeast Area Monitoring and Assessment Program.

Isotope studies are complementary to taxonomy-based studies of diets and generally show contributions from plants and bacteria in supporting food webs rather than details of predator-prey interactions (Fry, 2006). Taxonomic work was not part of this study but isotope data were collected for the proventriculus (stomach) contents of brown shrimp to help map river support of the benthic food web. The CNS isotope studies reported add to an extensive literature about shrimp isotopic variation in food webs of the Gulf of Mexico (Fry 1981, 1983, 2008; Fry et al., 1984, 2008) and also complement recent studies of stable isotope studies of fish in the northwestern Gulf of Mexico (Roelke and Cifuentes, 1997; Senn et al., 2010).

Materials and methods

Samples were collected from several locations in the northern Gulf of Mexico, from Galveston Bay in the west to the Bird's Foot Delta in the east (Fig. 1). Most samples from Louisiana bays were collected during spring (April and May) brown shrimp trawl surveys conducted by LADWF in 1999 and 2005 in Barataria and Terrebonne bays. Additional shrimp were collected with seines during June 2006 in Terrebonne Bay and in the Bird's Foot Delta. Offshore animals were collected during the National Marine Fisheries Service June–July summer SEAMAP (Southeast Area Monitoring and Assessment Program) surveys in 2005 and 2006. Offshore station depths declined gradually from 10 m inshore near barrier islands to the 200-m isobath at about 28°N (Fig. 1) and included intermediate mid-shelf areas regularly affected by summer hypoxia (Rabalais et al., 2002). Offshore isobaths run approximately parallel to the coast through most of the study region.

Shrimp were placed on ice and frozen soon after collection for 6–24 months until further processing. A few Galveston Bay samples were analyzed that were collected in previous studies in the 1990s and preserved in formalin (Rozas and Zimmerman, 2000). Preservation in formalin has been shown to influence C and N isotope composition, but not S isotope values (Edwards et al., 2002). Accordingly, isotope values reported here for the Galveston Bay samples have been adjusted by

+1.1‰ for $\delta^{13}C$ and −0.5‰ for $\delta^{15}N$ to account for the effects of formalin (Edwards et al., 2002).

In the laboratory, shrimp were thawed, total length and blotted wet mass were measured, and white muscle tissue was dissected from the tail area. Muscle tissue was cleaned by rinsing it under running tap water, then soaking the tissue in deionized water in glass vials for 15–60 minutes to remove saltwater. The water used for soaking was discarded, tissues were dried at 60°C, and then pulverized with a Wig-L-Bug automated grinder (Dentsply International, York, PA). Proventriculus contents were obtained by dissection, acidified with 10% HCl, centrifuged, and the stomach contents pellet was kept, and the acid was discarded. To further rinse and remove acid and traces of seawater, the pellet was resuspended with 20 mL of deionized water and then centrifuged again. This rinsing process was repeated three times before final drying of the pellet at 60°C. Shrimp were analyzed as individuals, but proventriculus contents were pooled by station to obtain enough material for analysis. Samples were analyzed according to established procedures for stable C, N, and S isotopic determinations (Fry, 2007, 2008). These procedures involve combustion of samples to CO_2, N_2, and SO_2 gases in an elemental analyzer, followed by chromatographic separation and measurement of these gases with an isotope ratio mass spectrometer. Results are reported in d notation as a ‰ difference from standards according to the formula

$$\delta \text{ (in ‰)} = (R_{SAMPLE}/R_{STANDARD} - 1)*1000,$$

where standards are PDB (PeeDee Belemnite) limestone for $\delta^{13}C$, nitrogen gas in air for $\delta^{15}N$, and CDT (Canyon Diable troilite) for $\delta^{34}S$, and corresponding R values are $^{13}C/^{12}C$, $^{15}N/^{14}N$, or $^{34}S/^{32}S$ (Fry, 2007).

Possible continued digestion during long-term storage in freezers and repeated washing of acidified proventriculus samples undoubtedly removed some labile organic matter from the proventriculus samples, but samples were treated similarly and used for between-sample and between-station comparisons. Shrimp tissues had low C/N ratios of 3.3–3.7 that were consistent with a mostly protein composition with little lipid content, and consequently no corrections were made to the carbon isotope data for lipid contributions (Fry and Allen, 2003; Post et al., 2007).

Mean values are given with standard errors of the mean (SE), unless otherwise stated. Statistical comparisons among multiple means were made by using Fisher's least significant difference method with significant differences indicated when $P<0.05$. Cluster analysis was done with the program Statgraphics Plus vers. 5.1 (Statpoint Technologies, Warrenton, VA).

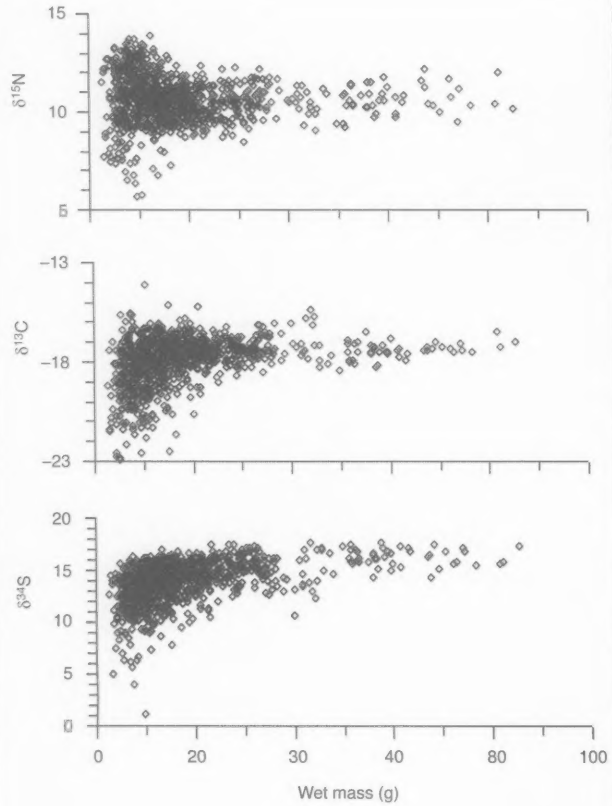

Figure 2

Stable isotope carbon, nitrogen, and sulfur (CNS) compositions ($\delta^{13}C$, $\delta^{15}N$, $\delta^{34}S$; in units of ‰) of brown shrimp (*Farfantepenaeus aztecus*) collected offshore in the Gulf of Mexico in summers of 2005 and 2006.

Results

Analysis of CNS isotope values for 969 offshore brown shrimp showed that isotope values of larger animals generally converged to a narrow range that was considered representative of offshore resident animals (Fig. 2). The number of samples was not equal for large and small shrimp (Fig. 2) because of the irregular availability of samples, but the pattern of convergence to much narrower isotope ranges for large animals was the expected pattern and the same as that observed in previous extensive studies of shrimp and fish in the northern Gulf of Mexico (Fry, 1981, 1983). In many cases, smaller shrimp had these same convergent isotope values likely due to early migration from estuaries and rapid growth on offshore diets (Fry, 1981). Divergent isotope values were more interesting, especially for $\delta^{15}N$, where small animals had values both above and below the values for larger shrimp

(Fig. 2). The spread in $\delta^{15}N$ values for small shrimp was an indication that different estuarine source regions might be involved, source regions with higher and lower $\delta^{15}N$ values than the offshore values. In contrast, smaller immigrant shrimp with $\delta^{13}C$ and $\delta^{34}S$ values divergent from those of the largest offshore animals had values mostly lower than the offshore values, so that estuarine source regions seemed likely to be similar in $\delta^{13}C$ and $\delta^{34}S$ values.

Shrimp were collected over several years to test these ideas about possible isotopic differences among estuarine source regions. Surveys of inshore Louisiana bays showed that shrimp from the Bird's Foot Delta had a combination of relatively high $\delta^{15}N$ values and low $\delta^{13}C$ values in contrast to shrimp from Terrebonne and Barataria bays (Fig. 3). Highest $\delta^{15}N$ values were reached in the central delta and extended along the eastern side of the delta. Stations along the northwest side of the delta at the margin of Barataria Bay showed the beginnings of an increase in $\delta^{15}N$, but the coordinated pattern of higher $\delta^{15}N$ and lower $\delta^{13}C$ developed about 20 km farther east of this margin (Fig. 3, Table 1). This same dual isotope pattern of high $\delta^{15}N$ and low $\delta^{13}C$ values was also found in another river-influenced bay system, at a station sampled in upper Galveston Bay near inflows from the Houston Ship Channel (Table 1, station Upper Galveston Bay vs. other Galveston Bay stations).

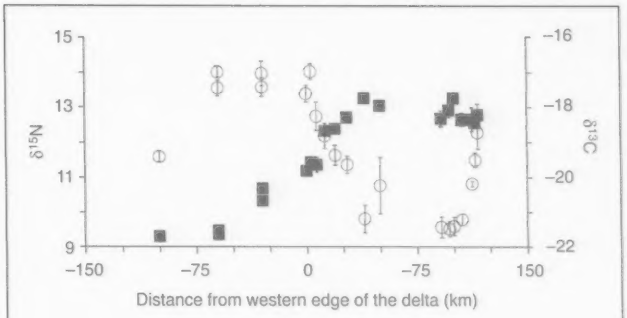

Figure 3

Average $\delta^{13}C$ and $\delta^{15}N$ values (in units of ‰) for inshore brown shrimp (*Farfantepenaeus aztecus*) collected in Terrebonne Bay (−100 km), three regions of Barataria Bay (west bay at −60 km, central bay at −30 km, and east bay at 0 km), and in the Bird's Foot Delta region (5–110 km). The north-south dividing line between Barataria Bay and Bird's Foot Delta shown in Figure 1 marks the zero-km reference used here. Values are means ±standard error from Table 1. Squares represent $\delta^{15}N$, circles $\delta^{13}C$.

Both shrimp size and isotope information were used to estimate immigrant origins in offshore populations. First, shrimp were selected that were relatively small (125 mm or less, 13 g wet mass or less). These shrimp were closest in size to shrimp collected in inshore bays, where the inshore shrimp averaged 85 mm and 4.7 g wet mass, whereas the <125 mm shrimp collected offshore averaged 109 mm and 9 g wet mass. It was the <125 mm offshore shrimp that were expected to have arrived most recently offshore and therefore best reflect prior feeding in inshore bays (Fry, 1981; Fry and Arnold, 1982), and it was these smaller animals that accounted for most of the variation in the offshore isotope values (Fig. 2). Secondly, the C and N isotope information for large offshore shrimp was used to set bounds or cut-off values expected for resident shrimp that had grown for longer periods of time offshore and had time to equilibrate with the offshore diets. As with approaches used earlier (Fry, 1981, 1983), data for largest shrimp were used as a second criterion to define isotope ranges characteristic for offshore residents, and shrimp >175 mm (>35 g wet mass) ranged from –15.3‰ to –18.4‰ for $\delta^{13}C$ and from 9.1‰ to 12.2‰ for $\delta^{15}N$. Overall, offshore residents were defined as >125 mm shrimp with isotope values between –15.3‰ to –18.4‰ for $\delta^{13}C$ and between 9.1‰ to 12.2‰ for $\delta^{15}N$. Isotope values for residents fell within the boxes in Figures 4 and 5.

Inshore studies showed that riverine shrimp from the Bird's Foot Delta generally had higher $\delta^{15}N$ and lower $\delta^{13}C$ than resident offshore animals (Fig. 4). Inshore shrimp from Barataria and Terrebonne bays had more diverse isotope values, but always had $\delta^{15}N$ values less than 11.6‰ (Fig. 4). Based on these isotope distributions, two types of immigrant shrimp to offshore systems were identified: riverine immigrants with high $\delta^{15}N$ and low $\delta^{13}C$ (>11.6‰ and <–18.4‰, respectively; solid squares in Fig. 5) and bay immigrants with lower $\delta^{15}N$ plus $\delta^{13}C$ values that were outside the range of offshore resident values (triangles in Fig. 5). A last group of shrimp was considered likely to resident (open diamonds in Fig. 5, see *Discussion* section).

Over the two years of summer collections, 406 shrimp were collected offshore that were <125 mm, and according to the above isotope-based criteria for distinguishing immigrants and residents, 185 of these shrimp were classified as residents at the time of collection and 221 were immigrants. About 46% of these immigrants had a riverine origin and 54% had a bay origin. The fraction of riverine immigrants was very similar in the two years, 48% in 2005 and 45% in 2006. The <125 mm immigrants were present mostly as mixed populations (bay+riverine+residents) along the inner and mid-shelf, and riverine shrimp were dominant (50% or greater of the <125 mm shrimp) at stations nearest the Bird's Foot Delta and along the central coast at stations to the south and west of the Atchafalaya River (Fig. 6).

The dual isotope label present in shrimp from the Bird's Foot Delta, as high $\delta^{15}N$ and low $\delta^{13}C$, was also present in proventriculus contents, i.e., both delta shrimp tissues (Fig. 4) and shrimp diets (Fig. 7) had relatively high $\delta^{15}N$ and low $\delta^{13}C$ values. The question was whether this riverine dual label would persist in offshore foods, so that animals feeding offshore might acquire this riverine dual label offshore and thus be

Table 1

Mean isotope values ±standard error (number of samples, *n*) for estuarine brown shrimp muscle tissue, 1999–2006, and isotope values for pooled, single samples of proventriculus (prov) contents for brown shrimp (*Farfantepenaeus aztecus*) in the Mississippi River delta. Distance in km is from the western edge of the delta (see Fig. 1).

km	Area	Site	Latitude (°N)	Longitude (°W)	$\delta^{13}C$‰ muscle	$\delta^{15}N$‰ muscle	$\delta^{34}S$‰ muscle	$\delta^{13}C$‰ prov	$\delta^{15}N$‰ prov	$\delta^{34}S$‰ prov
	Terrebonne Bay									
–100		2005–06 samples			–19.4 ±0.1(310)	9.3 ±0.1(310)	9.3 ±0.2(310)			
	Barataria Bay, western stations									
–60		1999, 4 western lower bay stations			–17.4 ±0.2(32)	9.5 ±0.1(32)	9.8 ±0.3(32)			
–60		2005, western bay stations			–17.0 ±0.2(112)	9.4 ±0.1(112)	9.9 ±0.1(112)			
	Barataria Bay, eastern stations									
–30		1999, 4 eastern lower bay stations			–17.0 ±0.3(39)	10.3 ±0.1(39)	10.4 ±0.2(39)			
–30		2005, eastern bay stations			–17.4 ±0.3(63)	10.7 ±0.1(63)	11.5 ±0.1(63)			
	western Delta				–19.6					
0		Lanaux Island Cut	29.30	89.71	–17.6 ±0.2(10)	11.2 ±0.1(10)	11.8 ±0.4(10)	–20.8	16.0	5.8
3		Shell Point	29.29	89.67	–17.0 ±0.2(10)	11.4 ±0.2(10)	12.5 ±0.3(10)	–20.1	13.7	2.1
7		Shell Island	29.27	89.63	–18.3 ±0.4(10)	11.4 ±0.1(10)	12.3 ±0.2(10)	–19.9	11.0	0.3
13		Scofield Pass Bay	29.25	89.55	–18.8 ±0.4(10)	12.3 ±0.1(10)	12.1 ±0.2(10)	–19.6	13.9	4.5
20		Red Pass	29.22	89.47	–19.4 ±0.3(10)	12.4 ±0.1(10)	9.7 ±0.4(10)	–20.8	16.2	7.5
28		Tiger Pass	29.15	89.43	–19.6 ±0.2(10)	12.7 ±0.1(10)	9.4 ±0.4(10)	–23.1	18.1	11.2
39		West Bay	29.05	89.35	–21.2 ±0.4(6)	13.3 ±0.3(6)	7.9 ±0.6(6)			
45		Tiger Pass	29.19	89.36	–20.9 ±0.3(5)	14.5 ±0.3(5)	3.4 ±0.9(5)			
	central and eastern delta									
50		Central East Bay	29.02	89.21	–20.2 ±0.8(5)	13.1 ±0.2(5)	9.6 ±0.4(5)	–24.2	15.0	12.2
92		Baptiste Collette	29.40	89.30	–21.4 ±0.3(10)	12.7 ±0.2(10)	10.3 ±0.4(10)			
97		Grand Bay	29.38	89.37	–21.5 ±0.2(10)	12.9 ±0.2(10)	11.0 ±0.3(10)	–21.5	15.2	4.6
100		Battledore Reef	29.39	89.41	–21.4 ±0.3(10)	13.3 ±0.2(10)	10.0 ±0.4(10)	–22.8	16.3	–0.7
106		Racoon Pass	29.40	89.48	–21.2 ±0.2(9)	12.7 ±0.3(9)	10.5 ±0.3(9)	–23.0	15.5	–1.6
113		California Point	29.45	89.53	–20.2 ±0.1(10)	12.7 ±0.1(10)	13.4 ±0.3(10)	–20.5	14.3	–5.5
115		Mangrove Point	29.30	89.55	–19.5 ±0.2(10)	12.6 ±0.3(10)	11.7 ±0.4(10)			
117		Sunrise Point	29.48	89.57	–18.7 ±0.5(10)	12.8 ±0.2(10)	11.6 ±0.5(10)			
	Galveston Bay									
		Upper Galveston Bay			–19.5 ±0.4(18)	13.9 ±0.2(18)	8.1 ±0.6(16)			
		Sportsmans Road			–15.8 ±0.2(9)	8.3 ±0.1(9)	5.9 ±0.4(9)			
		Oyster Drop			–15.0 ±0.3(18)	8.6 ±0.1(18)	6.9 ±0.3(18)			
		Elmgrove Point			–17.0 ±0.2(18)	9.3 ±0.2(18)	7.5 ±0.4(18)			

misclassified as immigrants from deltaic regions. In a test of this idea, proventriculus contents from near-delta offshore areas (open squares and open triangles in Fig. 7A) were sampled but generally did not show this riverine dual isotope label, i.e., 15 of 16 near-delta samples did not have the dual isotope delta label, but were relatively enriched in ^{13}C and followed the same isotope trend as that found for other samples collected from deeper offshore areas (Fig. 7B). Only one offshore proventriculus sample collected very close to the shore west of the Atchafalaya Delta had the dual-label riverine combination of low high $\delta^{15}N$ and low $\delta^{13}C$ (see open triangles with arrows, Fig. 7, A and B).

Because the inshore bay and delta regions contained geographic isoscape distinctions that were useful in following shrimp movements, the offshore data for residents also were examined for possible geographic patterns. Cluster analysis was used to identify separate groups by using multivariate data for 48 stations sampled in 2006 where measurements included CNS isotope values for proventriculus samples and parallel CNS isotope values for muscle samples. For the cluster analysis, the muscle averages were compiled by using only larger animals (>125 mm total length) that, as above, had C and N isotope values within the range of largest (>175 mm) resident animals, and therefore were classified as offshore residents. The resulting cluster analysis identified three general regional offshore groups of shrimp: two mid-shelf groups inshore and closer to the river, and one offshore group farther away from the river to the south and west (Fig. 8). The two mid-shelf groups were mostly in or near the area identified by Rabalais et al. (2002) as regularly affected by summer hypoxia and linked to inputs from the Mississippi River (Fig. 8, polygon), whereas the offshore group was largely on the southwest side of this region, away from river inputs (Fig. 8). The offshore group was significantly different in average isotope values from the inshore group in all cases for the mid-shelf transition group and in all but one case for the mid-shelf hypoxic group (Table 2).

Relative to this offshore group, the mid-shelf groups both showed significant enrichment in proventriculus ^{15}N and ^{13}C, and depletion in ^{34}S (Fig. 9,

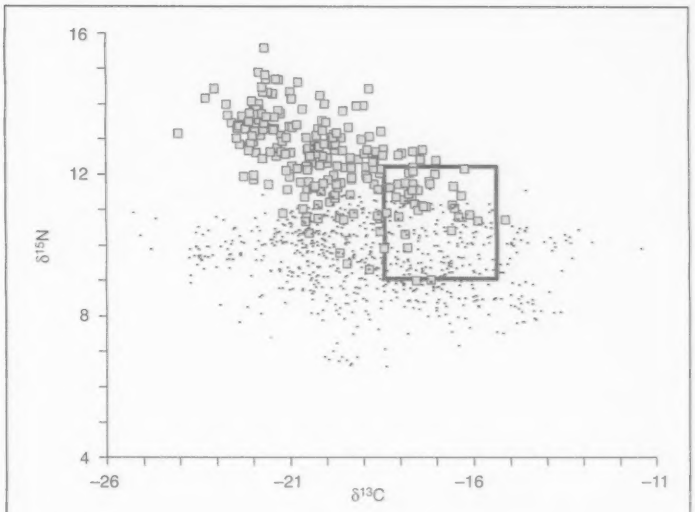

Figure 4

$\delta^{13}C$ and $\delta^{15}N$ values (in units of ‰) for inshore-collected brown shrimp (*Farfantepenaeus aztecus*). Shrimp collected in the delta (gray squares) had higher d^{15}N than shrimp collected from Barataria and Terrebonne bays (small bars). Box indicates range of values observed in the largest (>175 mm) offshore resident shrimp.

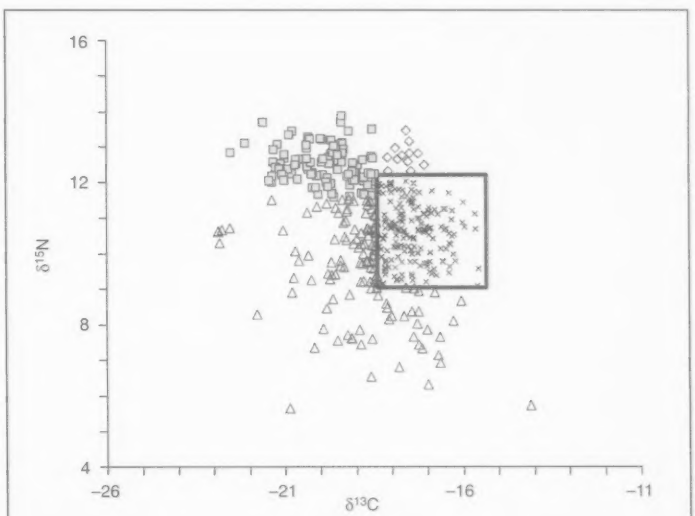

Figure 5

$\delta^{13}C$ and $\delta^{15}N$ values (in units of ‰) for smaller brown shrimp (*Farfantepenaeus aztecus*) (<125 mm total length) collected offshore and that had recently arrived from inshore estuaries. Shrimp were classified into three groups by considering the combined $\delta^{13}C$ and $\delta^{15}N$ data: riverine shrimp (gray squares), bay shrimp (triangles), residents (×'s and diamonds, with diamonds indicating likely residents of the hypoxic zone, see *Discussion* section). The boxed values indicate the range of values observed in largest (>175 mm) offshore resident shrimp.

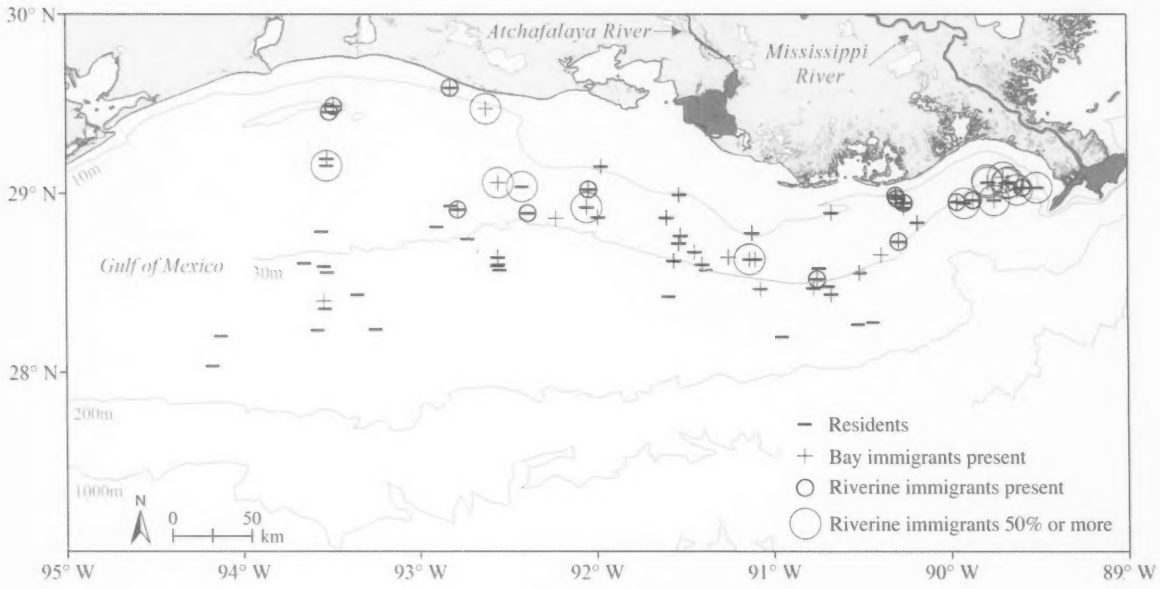

Figure 6

Offshore locations in the Gulf of Mexico where smaller (<125 mm) brown shrimp (*Farfantepenaeus aztecus*) were captured as immigrants from estuaries. Symbols indicate inferred origins of these shrimp.

Table 2), a triple isotope label associated with higher primary productivity (see *Discussion* section). These proventriculus isotope labels were strongest in the more inshore of the two groups (Fig. 9), namely the mid-shelf hypoxic group, and $\delta^{15}N$ values in the proventriculus contents were significantly higher in this group than in the offshore and mid-shelf transition group (Table 2). When all proventriculus samples were considered together, C and S isotopes were significantly ($P<0.01$) and linearly correlated with N isotopes (Fig. 10), consistent with mixing between two food sources across the shelf. The correlation of S and C isotopes for these samples also was significant ($P<0.01$, data not shown).

The mid-shelf and offshore station groups (Fig. 8) differed in their patterns of trophic enrichment factors (TEFs) (the difference between isotopes measured in consumers and their diets, i.e., TEF=muscle δ – proventriculus δ). Average TEFs for the most offshore group were close to expected (Peterson and Fry, 1987) at 2.8‰ and 0.2‰, respectively, for $\delta^{15}N$ and $\delta^{34}S$, but relatively high at 5.2‰ for $\delta^{13}C$ (Table 2). Inshore groups differed significantly from these offshore TEF values, notably with significantly lower nitrogen isotope TEF values for the mid-shelf groups (Table 2). For the more inshore of the two mid-shelf groups, average nitrogen isotope TEF values were unexpectedly negative (–2.2‰) because many proventriculus $\delta^{15}N$ values were >10.7‰ and therefore were higher than the average values for offshore resident shrimp (Table 2, Fig. 8, circled points).

Discussion

There are many reasons to expect strong river support of brown shrimp production, ranging from the riverine construction of inshore habitats by natural long-term delta-building processes to more recent river and nutrient-enhanced primary productivity of the offshore ecosystem (Deegan et al., 1986; Bierman et al., 1994; Green et al., 2008). Summer surface salinities are 20–33 psu across most of the study area owing to the enormous freshwater inputs from the Mississippi River, so that Louisiana brown shrimp exist in a river-influenced marine ecosystem. The river water affects the isotope biogeochemistry of receiving waters, adding nitrates with high $\delta^{15}N$ and dissolved inorganic carbon with low $\delta^{13}C$ (Fry and Allen, 2003). Primary productivity and the wider shrimp food webs seemed to respond to these basal isotope changes in a straightforward way, with shrimp having high $\delta^{15}N$ and low $\delta^{13}C$ in the Bird's Foot Delta region that was most influenced by the river. This same pattern of a riverine dual isotope label may be fairly general in human-influenced estuaries and was observed, for example, in shrimp from Galveston Bay at a low salinity station in the upper bay (Table 1) influenced by freshwater inflows from the urban Houston Ship Channel. The more negative average $\delta^{13}C$ values of –18.5‰ or less that characterize these systems seem to develop for brown shrimp in planktonic bays of the Gulf of Mexico when salinities are <20 psu (Fry, 1981, 1983). There is less local information for the Gulf of Mexico about the determinants of spatial $\delta^{15}N$

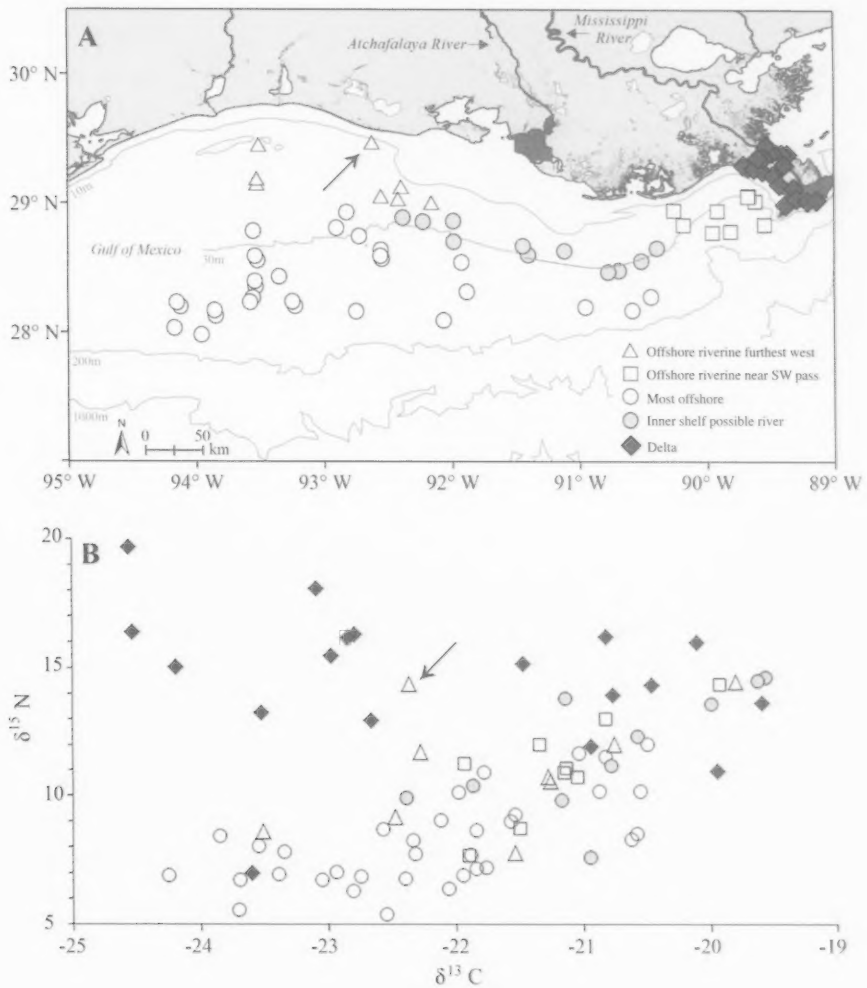

Figure 7

$\delta^{13}C$ and $\delta^{15}N$ values (in units of ‰) of proventriculus (gut content) samples collected in 2006. (**A**) Locations of sample collections. (**B**) Isotope values of samples. Arrows indicate the location (A) and isotope value (B) of the single offshore proventriculus sample that had isotope values similar to those of riverine samples (black diamonds) in the Bird's Foot Delta, as presented in the *Results* section.

patterns, but it is noteworthy that in the Bird's Foot Delta region, the high $\delta^{15}N$ values for brown shrimp extended over a greater distance than did the the low $\delta^{13}C$ values (Fig. 3). Stated another way, C isotope values returned to marine values more quickly than did N isotope values at both ends of the delta (Fig. 3). This difference between the N and C isotope patterns is expected because river N nutrient concentrations are very high and dominate freshwater-marine mixing dynamics (Fry, 2002). In contrast, river and marine sources have fairly similar inorganic carbon concentrations, so that riverine signals are diluted much more quickly for C than for N.

Riverine shrimp with the unique CN isotope tags of high $\delta^{15}N$ and low $\delta^{13}C$ accounted for about half of the recent immigrants arriving offshore. There is little independent tagging information that could validate this isotope estimate. LADWF does not sample low-salinity habitats in the Bird's Foot Delta and instead focuses on routine sampling of Barataria and Terrebonne bays of the central Louisiana coast to help set the periods for shrimp season openings and closings. River-influenced areas along the Bird's Foot Delta are not given a special focus by LADWF, but the isotope estimates from the present study may indicate that they deserve more focus in future work. This may be

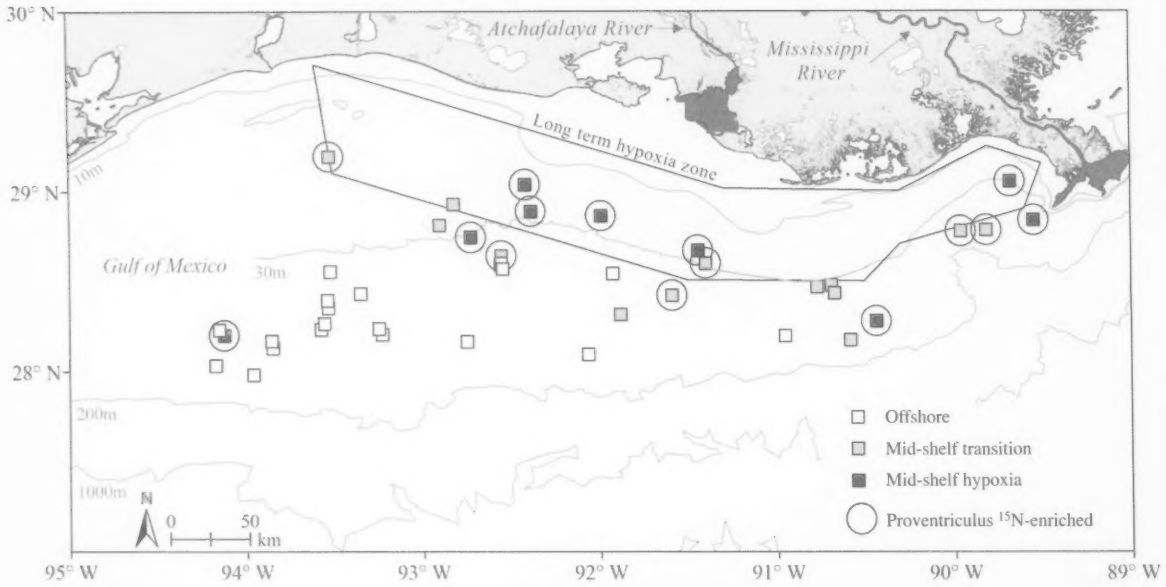

Figure 8

Station groupings from cluster analysis of samples from 2006. Circled points had ^{15}N-enriched proventriculus $\delta^{15}N$ >10.7‰, greater than average values for offshore resident brown shrimp (*Farfantepenaeus aztecus*). The polygon indicates the area of the long-term hypoxic zone documented by Rabalais et al. (2002), where hypoxia is present in >25% of summer surveys. Symbols indicate station groupings identified by cluster analysis.

especially true because of loss of inshore habitat in the Bird's Foot Delta (Britsch and Dunbar, 1993). Estimates for riverine shrimp contributions to offshore fisheries were very similar for 2005 and 2006, with 2005 having average river discharge and 2006 having about 60% average discharge (http://www.mvn.usace.army.mil/cgi-bin/watercontrol, accessed July 2010). The similar riverine contributions in the two different years may mean that it is the long-term structure of the deltaic marsh-bay platform rather than the annual river inputs that is more important for the shrimp supply to the offshore fishery.

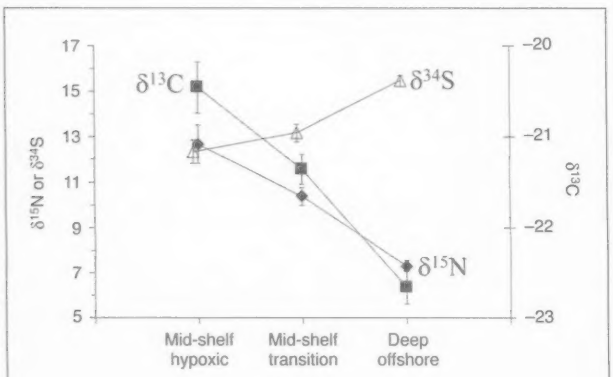

Figure 9

Trends in relation to depth for stable isotope averages (±1 standard error) in proventriculus contents of brown shrimp (*Farfantepenaeus aztecus*) collected from the Gulf of Mexico in 2006 (see also Table 2).

There are various reasons why the isotope estimates presented here could be overestimates for the contributions of riverine shrimp to offshore populations. For example, inshore sampling showed that both riverine and bay shrimp populations produce some shrimp that have the same isotope values as resident offshore shrimp (Fig. 4). The isotope accounting done here thus underestimates the contributions of the inshore populations, and if this underestimate is more severe for bay than riverine shrimp, this would lead to the apparent strong contribution of riverine shrimp. In the extreme, if all of the <125 mm offshore shrimp with isotope values inside the resident box of Figure 5 were actually misclassified and instead were all bay shrimp, the contribution of riverine shrimp would decline from 46% to 25%. Further research should include samples nearer the mouths of bays to check whether most animals leaving bays already have isotope values classified here as resident offshore shrimp, but in the end, even a 25% contribution of riverine shrimp is probably noteworthy for management purposes.

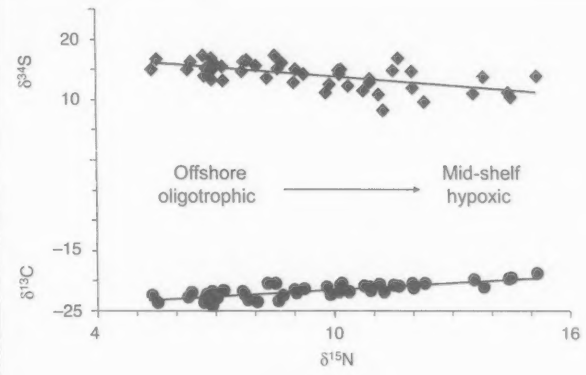

Figure 10

Covariation of proventriculus $\delta^{34}S$ and $\delta^{13}C$ with $d^{15}N$, from brown shrimp (*Farfantepenaeus aztecus*) samples collected from the Gulf of Mexico from 2006. Equations for top and bottom lines are respectively $\delta^{34}S=-0.5(\delta^{15}N)+18.8$ with $r^2=0.36$, and $\delta^{13}C=0.38(\delta^{15}N)-25.32$ with $r^2=0.64$. The relationship between $\delta^{34}S$ and $\delta^{13}C$ (not shown) was $\delta^{13}C=0.26(\delta^{34}S)-18.17$ with $r^2=0.21$. All isotope values have units of ‰.

Offshore phytoplankton productivity studies in Mississippi River plumes generally show ^{13}C-enriched values for particulate organic matter formed in inshore and mid-shelf regions (Fry and Wainright, 1991; Fry unpubl. data), so that the dual isotope tag of low $\delta^{13}C$ and high $\delta^{15}N$ used to source riverine shrimp seemed largely confined to estuaries and was only rarely present offshore (Fig. 7).

It is also possible that bays in adjacent Texas and other northern Gulf states supply some shrimp to the offshore Louisiana system. But those shrimp would likely have been offshore for extended periods of time and therefore would have been counted as residents in this study. Thus possible contributions from other states should have little effect on the estimates given above for bay and riverine contributions to Louisiana shrimp stocks.

It also was evident that estuarine conditions prevail offshore in this river-influenced shelf ecosystem that is often considered an offshore estuary. Isotopic compositions of shrimp and proventriculus contents followed the same triple isotope gradients involving high $\delta^{13}C$, high $\delta^{15}N$, and low $\delta^{34}S$ nearest the river, vs. low $\delta^{13}C$, low $\delta^{15}N$, and high $\delta^{34}S$ offshore. These gradients were largely aligned with other offshore features associated with the river, notably finfish biomass (Moore et al., 1970) and hypoxia (Rabalais et al., 2002). It is possible that some of these isotope gradients reflect normal depth-related onshore-offshore productivity gradients not associated with rivers, and this idea should be addressed in future comparative work involving continental shelf systems with little river influence. Initial data for the Texas shelf have shown some cases of onshore-

Table 2

Mean isotope values (‰ ±standard error of the mean) for brown shrimp (*Farfantepenaeus aztecus*) muscle tissue, proventriculus contents, and trophic enrichment factor at three offshore station groups in 2006. Muscle averages are for resident animals >125 mm and whose isotope values are within the isotope ranges set by animals >175 mm, as discussed in the text. Different superscript letters for mean values in a column indicate that values are significantly different ($P<0.05$). n=number of samples.

	Muscle tissue			Proventriculus contents			Trophic enrichment factor		
	$\delta^{13}C$	$\delta^{15}N$	$\delta^{34}S$	$\delta^{13}C$	$\delta^{15}N$	$\delta^{34}S$	$\delta^{13}C$	$\delta^{15}N$	$\delta^{34}S$
Offshore (n=22)	–17.43 ±0.04 ^{A}	10.15 ±0.06 ^{A}	15.7 ±0.2 ^{A}	–22.7 ±0.2 ^{A}	7.3 ±0.2 ^{A}	15.5 ±0.2 ^{A}	5.2 ±0.2 ^{A}	2.8 ±0.2 ^{A}	0.2 ±0.2 ^{A}
Mid-shelf transition (n=14)	–17.18 ±0.07 ^{B}	10.61 ±0.11 ^{B}	14.5 ±0.2 ^{B}	–21.4 ±0.2 ^{B}	10.4 ±0.4 ^{B}	13.2 ±0.4 ^{B}	4.2 ±0.1 ^{B}	0.2 ±0.4 ^{B}	1.3 ±0.4 ^{B}
Mid-shelf hypoxic (n=10)	–17.30 ±0.06 ^{AB}	10.53 ±0.13 ^{B}	14.0 ±0.5 ^{B}	–20.5 ±0.3 ^{C}	12.7 ±0.5 ^{C}	12.3 ±0.9 ^{B}	3.2 ±0.3 ^{C}	–2.2 ±0.5 ^{C}	1.7 ±0.7 ^{B}

offshore and seasonal C isotope changes in shrimp (Fry et al., 1984), but N and S isotope changes have not yet been systematically investigated. Comparative work might also focus on other river-influenced shelf systems and one recent study of the Thames River estuary (Leakey et al., 2008) has shown the same triple isotope riverine-offshore gradients observed in this study for the Mississippi River. Because of these similar results for the Thames River, and because the pattern of isotope signals is consistent with a riverine source with high $\delta^{15}N$, it seems likely that the Mississippi River is forcing many of the isotope signals observed on the Louisiana shelf.

The three regional shelf groups shown in Figures 8 and 9 were identified by cluster analysis by using three proventriculus isotope variables and three muscle isotope variables. These six variables were used in concert for two reasons. First, the separated proventriculus and muscle results each gave strong mid-shelf vs. offshore patterns (see significant differences among averages in Table 2), and therefore results could be legitimately combined for a stronger overall assessment. Second, the proventriculus and muscle samples show somewhat different aspects of shrimp biology and available diets, with proventriculus samples providing stronger local information and muscle samples providing stronger time-integrated samples. On the negative side, the proventriculus samples are often the leftovers after digestion and can include inorganic sediment grains with pyritic sulfides (Howarth, 1979, 1984), whereas muscle samples are taken from shrimp that are mobile and may reflect diets from another place. Because there were both positive and negative aspects to using the separated proventriculus and muscle isotope data, the combined data (Table 2) were used to reach a balanced overall assessment in the cluster analysis.

The offshore C isotopes showed a broad pattern of river influence across the inshore and middle shelf, consistent with wide dispersal of carbon from river-influenced planktonic primary producers. The riverine influence was expressed as higher $\delta^{13}C$ values in a mid-shelf maximum standing out against a background of lower $\delta^{13}C$ values both in shallower bays and in deeper offshore waters (Tables 1 and 2, Fig. 9). Higher $\delta^{13}C$ values are found associated especially with high productivity and diatom blooms (Fry and Wainright, 1991; Fry, 1996)—conditions that regularly occur on the Louisiana shelf that is affected by Mississippi River inputs (Rabalais et al., 1996; Dagg et al., 2007; Green et al., 2008). The deeper shelf to the south and west had lower $\delta^{13}C$ consistent with lower primary productivity (Fry and Boyd, 2010).

The offshore S isotopes were perhaps the most expected results, showing a consistent onshore-offshore gradient in both proventriculus and muscle $\delta^{34}S$ values (Table 2, Fig. 9). These gradients likely originate with river-induced organic carbon gradients in primary productivity that subsequently fuel benthic sulfate reduction and sulfide production in underlying sediments. The exact mechanism of sulfide incorporation into benthic food webs is still unknown but is likely the use of sulfides by bacteria growing in bottom sediments. Hypoxia may increase aspects of sulfide cycling, especially by decreasing the importance of oxygenic decomposition reactions while increasing the importance of anaerobic reactions such as sulfate reduction and sulfide production. Hypoxia also may decrease oxidation reactions that consume sulfide, and decreased infaunal activity and decreased bioirrigation in sediments may also occur when bottom waters become hypoxic (Eldridge and Morse, 2008). In sum, hypoxic conditions may promote more anaerobic conditions, more sulfide production and accumulation, and stronger bacterial uptake of sulfides into benthic food webs.

The N isotope results were quite surprising in the very high $\delta^{15}N$ values (up to 15.2‰) found for some proventriculus content samples in the mid-shelf hypoxic region—values that were higher than those for shrimp muscle. Ongoing studies show no large ^{15}N enrichment in particulate organic nitrogen samples collected in the water column in the offshore region, where values average 6–8‰ (Wissel et al., 2005; Fry, unpubl. data). In the absence of a planktonic origin, the source of the high $\delta^{15}N$ values likely is in the benthos. Brown shrimp are benthic carnivores that consume polychaetes and meiofauna (McTigue and Zimmerman, 1998; Fry et al., 2003), and offshore brown shrimp generally rely on a benthic food web with bacterial contributions. York et al. (2010) have speculated that nitrogen cycling in the benthos is leading to high $\delta^{15}N$ values of benthic bacteria, perhaps with some bacterial use of ^{15}N-enriched ammonium left over from nitrification or annamox reactions. Such processes are likely ubiquitous in shelf sediments, but details that are still to be elucidated could make these processes much more dominant in the low-oxygen mid-shelf hypoxic region. High $\delta^{15}N$ values were also found in inshore shrimp and proventriculus contents from the Bird's Foot Delta region (Table 2), and the common denominator leading to these high $\delta^{15}N$ values is likely eutrophic deposition of large amounts of organic phytodetritus to the benthos. $\delta^{15}N$ values >15‰ have also been observed in Mississippi River zebra mussels during summer, where high animal $\delta^{15}N$ values have been correlated with low ammonium concentrations in the river (Fry and Allen, 2003).

Whatever the mechanism underlying the high $\delta^{15}N$ values, it was evident that the proventriculus $\delta^{15}N$ values were often higher than those of offshore shrimp eating these foods (Table 2). Previous work with estuarine brown shrimp has shown that brown shrimp normally have positive trophic enrichment factors (TEFs) averaging about 2.3‰ higher than proventriculus contents $\delta^{15}N$ (Fry et al., 2003), and a similar average TEF of 2.8‰ was observed for the most offshore shrimp of the present study (Table 2). The observed opposite pattern of negative TEF values for some mid-shelf shrimp likely means that these shrimp have not spent the several weeks (that can be calculated from diet turnover dynamics) (Fry and Arnold, 1982) that they would need

in the hypoxic zone to come to equilibrium with the ^{15}N-enriched foods. This idea is reasonable given recent fisheries studies that show hypoxia is often displacing brown shrimp populations to areas of higher bottom-water oxygen (Craig and Crowder, 2005; Craig et al., 2005). In future studies, the disequilibrium or mismatch between shrimp and proventriculus $\delta^{15}N$ may help identify areas that do not continuously sustain brown shrimp populations. Areas where proventriculus $\delta^{15}N$ is higher than shrimp muscle $\delta^{15}N$ may be less suitable habitat that can be visited only briefly by brown shrimp. The isotope signals in diets of brown shrimp and their prey are built up over several weeks, so that the isotope measurements may provide longer-term information about shrimp use of hypoxic areas than do trawls that provide a more instantaneous snapshot of how brown shrimp are using an area (Craig et al., 2005).

However, occasional feeding in the hypoxic area should lead to somewhat elevated $\delta^{15}N$ values, so that higher $\delta^{15}N$ could develop in offshore resident shrimp. Several offshore shrimp were observed with high $\delta^{15}N$ that could indicate some feeding in the hypoxic zone. These animals also had high $\delta^{13}C$ values (less negative than –18‰; open diamonds in Fig. 5) expected for offshore residents rather than for migrants from inshore regions, and were accordingly classified as offshore residents for purposes of estimating movement and inshore contributions to offshore fisheries.

An interesting feature of this study was that offshore brown shrimp diets appeared to be linear mixtures between two sources, and variation in the source contributions accounted for most of the isotopic variation across the shelf (Fig. 10). The nature of these sources is not completely clear and may involve multiple factors. For example, high $\delta^{15}N$ values may reflect both a high value of Mississippi River nitrate at the base of coastal food webs (Fry and Allen, 2003; Wissel and Fry, 2005), and the presence of high trophic level consumers in the proventriculus contents. Conversely, low $\delta^{15}N$ may reflect relatively low values for offshore marine nitrate and prey from low trophic levels. Unfortunately, isotope values for specific prey taxa have not yet been measured for this shelf ecosystem, and therefore trophic-level effects for isotopes cannot be directly evaluated. Nonetheless, some inferences can be made from the measured isotope data for shrimp and their proventriculus contents, as follows.

The farthest offshore animals had high $\delta^{34}S$ values (Table 2) characteristic of mostly plankton-derived sulfur in the diet, with little contribution of benthic sulfides. These high $\delta^{34}S$ values are consistent with relatively oligotrophic conditions across the deeper shelf, and with lower $\delta^{34}S$ values indicating more eutrophic conditions inshore. Carbon isotope TEFs between offshore shrimp and proventriculus contents were surprisingly large at 3.2–5.2‰ (Table 2), especially compared to the general expectation that the carbon isotope TEF is near 0‰ for animals and their diets (Peterson and Fry, 1987) and compared to a measured carbon isotope TEF near 1‰ for estuarine Louisiana brown shrimp (Fry et al., 2003). The offshore shrimp muscle $\delta^{13}C$ values are fairly constant near –17.3‰, so that it is the very negative proventriculus values that lead to the large observed TEFs. Nonetheless, the proventriculus $\delta^{13}C$ values are near the long-term –22‰ value associated with offshore marine primary production (Fry and Sherr, 1984), and may represent a realistic marine background value. If this is the case, then mass balance calculations would indicate that the labile foods near –17.3‰ that are being assimilated out of the –22‰ marine background are likely a small part of the proventriculus contents. A consistent picture for the C and S results is that background, low-productivity pelagic conditions determine the food availability at the offshore stations, but labile fractions that are depleted in ^{34}S and enriched in ^{13}C are increasingly found in the proventriculus contents at the more eutrophic inshore stations (Fig. 10). These ideas need further study with taxonomic analyses of prey and with further studies on isotope changes during assimilation of offshore foods (Fry et al., 1984).

In conclusion, further studies of both CNS isotopes and proventriculus contents in offshore brown shrimp could supplement annual summer water quality assessments of hypoxia and help determine hypoxia effects on living resources. Brown shrimp transit the mid-shelf hypoxic areas and isotopes in shrimp caught offshore show strong spatial signals that likely vary between years with high and low river flow. Isotope signals have been used as early warning indicators of the effects of eutrophication in coastal bays (McClelland et al., 1997), and it is possible that monitoring shrimp isotopes may help assess the effects of hypoxia on Louisiana shrimp populations. Adding benthic shrimp isoscape monitoring to ongoing water quality monitoring programs generally may be helpful for understanding changes in fisheries productivity and animal movements in this and other river-influenced marine ecosystems (Leakey et al., 2008).

Acknowledgments

K. Johnson and B. Pellegrin of the NOAA Pascagoula Laboratory kindly provided the offshore shrimp samples from SEAMAP cruises. G. Peterson assisted in shrimp collections made in the Bird's Foot Delta region. LSU undergraduates E. Ecker, E. Gallagher, M. Grant, T. Pasqua, R. Sylvestri, and J. Wheatley helped with laboratory preparation of samples and data entry. J. Lentz drafted the maps used in this article. Brittany Graham read an initial draft of this manuscript and made helpful comments. This work was supported in part by Louisiana Sea Grant Projects R/CEH-13 and R-EFH-07, NOAA Multistress award NA 16OP2670, NOAA Coastal Ocean Program grant NA06NOS4780141, and NOAA grant 412 NA06OAR4320264 06111039 to the Northern Gulf Institute. This is N-GOMEX contribution 138.

Literature cited

Bierman, V. L., S. C. Hinz, D -W. Zhu, W. J. Wiseman, N. N. Rabalais, and R. E. Turner.
1994. A preliminary mass balance model of primary productivity and dissolved oxygen in the Mississippi River plume/inner Gulf shelf region. Estuaries 17:886–899.

Britsch, L. D., and J. B. Dunbar.
1993. Land loss rates: Louisiana coastal plain. J. Coastal Res. 9:324–338.

Craig, J. K., and L. B. Crowder.
2005. Hypoxia-induced habitat shifts and energetic consequences in Atlantic croaker and brown shrimp on the Gulf of Mexico shelf. Mar. Ecol. Progr. Ser. 294:79–94.

Craig, J. K., L. B. Crowder, and T. A. Henwood.
2005. Spatial distribution of brown shrimp (*Farfantepenaeus aztecus*) on the northwestern Gulf of Mexico shelf: effects of abundance and hypoxia. Can. J. Fish. Aquat. Sci. 62:1295–1308.

Das, A., D. Justic, and E. Swenson.
2009. Modeling estuarine-shelf exchanges in a deltaic estuary: Implications for coastal carbon budgets and hypoxia. Ecol. Model. 221:978–985.

Dagg M., J. Ammerman, R. Amon, W. Gardner, R. Green, and S. Lohrenz.
2007. A review of water column processes influencing hypoxia in the northern Gulf of Mexico. Estuaries Coasts 30:735–752.

Deegan, L. A., J. W. Day Jr., J. G. Gosselink, A. Yáñez-Arancibia, G. Soberon-Chavez, and P. Sanchez-Gil.
1986. Relationships among physical characteristics, vegetation distribution and fisheries yield in Gulf of Mexico estuaries. *In* Estuarine variability (D. A. Wolfe, ed.), p. 83–100. Academic Press, New York.

Edwards, M. S., T. F. Turner, and Z. D. Sharp.
2002. Short- and long term effects of fixation and preservation on stable isotope values ($\delta^{13}C$, $\delta^{15}N$, $\delta^{34}S$) of fluid-preserved museum specimens. Copeia 2002:1106–1112.

Eldridge, P. M., and J. W. Morse.
2008. Origins and temporal scales of hypoxia on the Louisiana shelf: Importance of benthic and subpycnocline water metabolism. Mar. Chem. 108:159–171.

Fry, B.
1981. Natural stable carbon isotope tag traces Texas shrimp migrations. Fish. Bull. 79:337–345.
1983. Fish and shrimp migrations in the northern Gulf of Mexico analyzed using stable C, N, and S isotope ratios. Fish. Bull. 81:789–801.
1996. $^{13}C/^{12}C$ fractionation by marine diatoms. Mar. Ecol. Progr. Ser. 134:283–294.
2002. Conservative mixing of stable isotopes across estuarine salinity gradients: A conceptual framework for monitoring watershed influences on downstream fisheries production. Estuaries 25:264–271.
2006. Stable isotope ecology, 308 p. Springer, New York.
2007. Coupled N, C, and S isotope measurements using a dual column GC system. Rapid Comm. Mass Spectr. 21:750–756.
2008. Importance of open bays as nurseries for Louisiana brown shrimp. Estuaries Coasts 31:776–789.

Fry, B., and Y. Allen.
2003. Stable isotopes in zebra mussels as bioindicators of river-watershed linkages. Rivers Res. Appl. 19:683–696.

Fry, B., R. K. Andersen, L. Entzeroth, J. L. Bird, and P. L. Parker.
1984. ^{13}C enrichment and oceanic food web structure in the northwestern Gulf of Mexico. Contrib. Mar. Sci. 27:49–63.

Fry, B., and C. K. Arnold.
1982. Rapid $^{13}C/^{12}C$ turnover during growth of brown shrimp (*Penaeus aztecus*). Oecologia (Berlin) 54:200–204.

Fry, B., D. Baltz, M. Benfield, J. Fleeger, A. Gace, H. A. Haas, and Z. Quinones.
2003. Chemical indicators of movement and residency for brown shrimp (*Farfantepenaeus aztecus*) in coastal Louisiana marshscapes. Estuaries 26:82–97.

Fry, B., and B. Boyd.
2010. Oxygen concentration and isotope studies of productivity and respiration on the Louisiana continental shelf, July 2007. *In* Earth, life, and isotopes (N. Ohkouchi, I. Tayasu, and K. Koba, eds.), p. 223–247. Kyoto University Press, Japan.

Fry, B., and E. Sherr.
1984. $\delta^{13}C$ measurements as indicators of carbon flow in marine and freshwater ecosystems. Contrib. Mar. Sci. 27:13–47.

Fry, B., and S. C. Wainright.
1991. Diatom sources of 13C-rich carbon in marine food webs. Mar. Ecol. Progr. Ser. 76:149–157.

Green, R. E., G. A. Breed, M. J. Dagg, and S. E. Lohrenz.
2008. Modeling the response of primary production and sedimentation to variable nitrate loading in the Mississippi River plume. Cont. Shelf Res. 28:1451–1465.

Haas, H. L, K. A. Rose, B. Fry, T. J. Minello, and L. Rozas.
2004. Brown shrimp on the edge: linking habitat to survival using an individual-based simulation model. Ecol. Appl. 14:1232–1247.

Hobson, K. A., and L. I. Wassenaar, eds.
2008. Tracking animal migrations with stable isotopes. Terrestrial Ecology Series, vol. 1, 160 p. Elsevier Science, Maryland, MO.

Howarth, R. W.
1979. Pyrite—its rapid formation in a salt marsh and its importance in ecosystem metabolism. Science 203:49–51.
1984. The ecological significance of sulfur in the energy dynamics of salt marsh and coastal marine sediments. Biogeochem. 1:5–27.

Leakey, C. D. B., M. J. Attrill, S. Jennings, and M. F. Fitzsimons.
2008. Stable isotopes in juvenile marine fishes and their invertebrate prey from the Thames Estuary, UK, and adjacent coastal regions. Estuar. Coast. Shelf Sci. 77:513–522.

Lin, S., and J. W. Morse.
1991. Sulfate reduction and iron sulphide mineral formation in Gulf of Mexico anoxic sediments. Am. J. Sci. 291:55–89.

McClelland, J. W., I. Valiela, and B. Michener.
1997. Nitrogen-stable isotope signatures in estuarine food webs: A record of increasing urbanization in coastal watersheds. Limnol. Oceanogr. 42:930–937.

McTigue, T. A., and R. J. Zimmerman.
1998. The use of infauna by juvenile *Penaeus aztecus* Ives and *Penaeus setiferus* (Linnaeus). Estuaries 21:160–175.

Moore, D., H. A. Brusher, and L. Trent.
1970. Relative abundance, seasonal distribution, and species composition of demersal fishes off Louisiana and Texas, 1962–1963. Contrib. Mar. Sci. 15:45–70.

Peterson, B. J., and B. Fry.
1987. Stable isotopes in ecosystem studies. Ann. Rev. Ecol. System. 18:293–320.

Peterson, B. J., and R. W. Howarth.
1987. Sulfur, carbon, and nitrogen isotopes used to trace organic matter flow in the salt-marsh estuaries of Sapelo Island, Georgia. Limnol. Oceanogr. 32:1195–1213.

Peterson, B. J., R. W. Howarth, and R. H. Garritt.
1985. Multiple stable isotopes used to trace the flow of organic matter in estuarine food webs. Science 227:1361–1363.

Peterson, G. W., and R. E. Turner.
1994. The value of salt marsh edge vs. interior as a habitat for fish and decapod crustaceans in a Louisiana tidal marsh. Estuaries 17:235–262.

Post, D. M., C. A Layman, D. A., Arrington, G. Takimoto, J. Quattrochi, and C. G. Montana.
2007. Getting to the fat of the matter: models, methods and assumptions for dealing with lipids in stable isotope analysis. Oecologia 152:179–189.

Rabalais, N. N., R. E. Turner, and W. J. Wiseman, Jr.
2002. Hypoxia in the Gulf of Mexico, a.k.a. "The Dead Zone". Annu. Rev. Ecol. Syst. 33:235–263.

Rabalais, N. N., W. J. Wiseman, R. E. Turner, B. K. SenGupta, and Q. Dortch.
1996. Nutrient changes in the Mississippi River and system responses on the adjacent continental shelf. Estuaries 19:386–407.

Rees, C. E., W. J. Jenkins, and J. Monster.
1978. Sulfur isotopic composition of ocean water sulfate. Geochim. Cosmochim. Acta 42:377–381.

Roelke, L. A., and L. A. Cifuentes.
1997. Use of stable isotopes to assess groups of king mackerel, *Scomberomorus cavalla*, in the Gulf of Mexico and southeastern Florida. Fish. Bull. 95:540–551.

Rozas, L. P., and R. J. Zimmerman.
2000. Small-scale patterns of nekton use among marsh and adjacent shallow nonvegetated areas of the Galveston Bay Estuary, Texas (USA). Mar. Ecol. Progr. Ser. 193: 217–239.

Schlacher, T. A., B. Liddell, T. F. Gaston, and M. Schlacher-Hoenlinger.
2005. Fish track wastewater pollution to estuaries. Oecologia 144:570–584.

Senn, D. B., E. J. Chesney, J. D. Blum, M. S. Bank, A. Age, and J. P. Shine.
2010. Stable isotope (N, C, Hg) study of methylmercury sources and trophic transfer in the Northern Gulf of Mexico. Environ. Sci. Tech. 44:1630–1637.

Turner, R. E., and N. N. Rabalais.
1991. Changes in Mississippi River water quality this century and implications for coastal food webs. BioScience 41:140–147.

Turner, R. E., N. N. Rabalais, R. B. Alexander, G. McIsaac, and R. W. Howarth.
2007. Characterization of nutrient, organic carbon, and sediment loads and concentrations from the Mississippi River into the Northern Gulf of Mexico. Estuaries Coasts 30:773–790.

Walker, N., and N. N. Rabalais.
2006. Relationships among satellite chlorophyll a, river inputs, and hypoxia on the Louisiana continental shelf, Gulf of Mexico. Estuaries Coasts 29:1081–1093.

West, J. B., G. J. Bowen, T. E. Dawson, and K. P. Tu, eds.
2010. Isoscapes: Understanding movement, pattern, and process on Earth through isotope mapping, 487p. Springer Science+Business Media B.V., New York and Dordrecht, The Netherlands.

Wissel, B., and B. Fry.
2005. Tracing Mississippi River influences in estuarine food webs of coastal Louisiana. Oecologia 144:659–672.

Wissel, B., A. Gaçe, and B. Fry.
2005. Tracing river influences on phytoplankton dynamics in two Louisiana estuaries. Ecology 86:2251–2762.

York, J. K., G. Tomasky, I. Valiela, and A. E. Giblin.
2010. Isotopic approach to determining the fate of ammonium regenerated from sediments in a eutrophic sub-estuary of Waquoit Bay, MA. Estuaries Coasts 33:1069–1079.

Stage-specific vertical distribution of Alaska plaice (*Pleuronectes quadrituberculatus*) eggs in the eastern Bering Sea

Janet T. Duffy-Anderson (contact author)
Deborah M. Blood
Kathryn L. Mier

Email address for contact author Janet.Duffy-Anderson@noaa.gov

Resource Assessment and Conservation Engineering Division
Recruitment Processes Program
Alaska Fisheries Science Center
National Marine Fisheries Service
National Oceanic and Atmospheric Administration
7600 Sand Point Way NE
Seattle, Washington 98115-6349

Abstract—The stage-specific distribution of Alaska plaice (*Pleuronectes quadrituberculatus*) eggs in the southeastern Bering Sea was examined with collections made in mid-May in 2002, 2003, 2005, and 2006. Eggs in the early stages of development were found primarily offshore of the 40-m isobath. Eggs in the middle and late stages of development were found inshore and offshore of the 40-m isobath. There was some evidence that early-stage eggs occur deeper in the water column than late-stage eggs, although year-to-year variability in that trend was observed. Most eggs were in the later stages of development; therefore the majority of spawning is estimated to have occurred a few weeks before collection—probably April—and may be highly synchronized among local spawning areas. Results indicate that sampling with continuous underway fish egg collectors (CUFES) should be supplemented with sampling of the entire water column to ensure adequate samples of all egg stages of Alaska plaice. Data presented offer new information on the stage-dependent horizontal and vertical distribution of Alaska plaice eggs in the Bering Sea and provide further evidence that the early life history stages of this species are vulnerable to near-surface variations in hydrographical conditions and climate forcing.

Manuscript submitted 6 July 2010.
Manuscript accepted 19 January 2011.
Fish. Bull 109:162–169 (2011).

The views and opinions expressed or implied in this article are those of the author (or authors) and do not necessarily reflect the position of the National Marine Fisheries Service, NOAA.

Knowledge of the vertical distributions of fish eggs and larvae is important to understanding how wind and currents may affect early life stages. The eggs of several pleuronectid species in the North Pacific are positively buoyant (Pearcy, 1962; Bailey et al., 2005). Retention of pelagic eggs at the top of the water column exposes them to wind mixing that ensures an adequate oxygen supply for the developing egg, but also increases susceptibility of the eggs to stochastic wind events and adverse advection. Consistent baroclinic flows below the wind-mixed layer facilitate retention of developing eggs, but also could expose eggs to anoxia and increased predation. Vertical position often changes with development, and stage-dependent ascension can occur slowly throughout the developmental period, or quickly once eggs reach a critical stage.

Alaska plaice (*Pleuronectes quadrituberculatus*) is one of the major shallow water flatfishes in the Bering Sea; however, there is not a significant fishery for the species. Alaska plaice are primarily harvested as bycatch in fisheries targeting other, more lucrative groundfishes, and a large portion of the Alaska plaice biomass is discarded. Adult Alaska plaice spawn in spring over the middle Bering Sea shelf at depths of 50–100 m, and egg and larval stages are pelagic (Bailey et al., 2003). Previous work (Duffy-Anderson et al., 2010) has shown that Alaska plaice larvae occur in the upper 20 m of the water column, but vertical patterns of egg distribution have not been determined.

The continuous underway fish egg sampler (CUFES; Checkley et al., 1997) is a tested collection system used in sampling near-surface eggs from a fixed depth (3 m) and has the advantage of being able to sample eggs in adverse weather conditions when tows with nets are not possible (Checkley et al., 2000; Lo et al., 2001). The CUFES has been used in other regions to sample and estimate the densities of marine fish eggs in the water column (Dopolo et al., 2005; Pepin et al., 2005). Accurate derivation of depth-integrated egg densities from near-surface estimates requires a complete understanding of patterns of vertical egg distribution with depth and development, but this information is not available for a number of fish species in the Bering Sea, including Alaska plaice.

The goals of the present study were 1) to determine the developmental stage of Alaska plaice eggs collected from depth-discrete tows conducted in the eastern Bering Sea; 2) to examine the vertical distribution of staged eggs; and 3) to determine whether the CUFES could be a suitable sampler of Alaska plaice eggs in the Bering Sea.

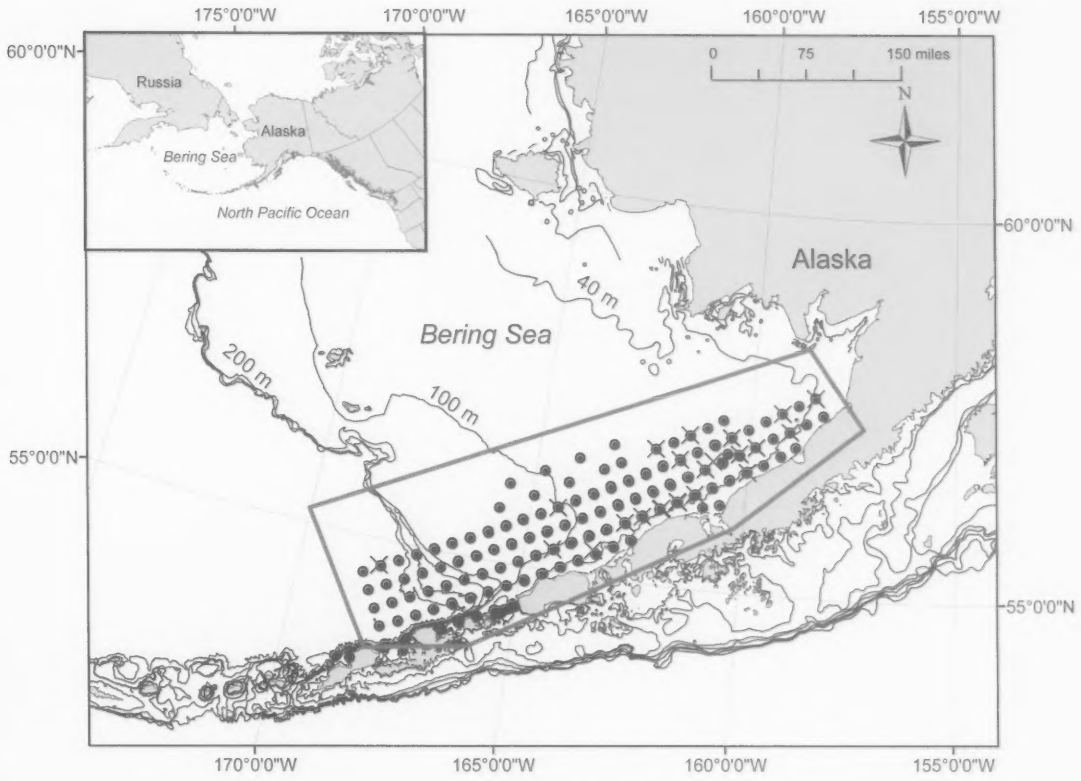

Figure 1

Map of study region (inset) and stations where eggs of Alaska plaice (*Pleuronectes quadrituberculatus*) were collected with the multiple opening and closing net and environmental sampling system (X) and neuston net (●) tows in the eastern Bering Sea during 2002–06. The polygon delineates the sampling area.

Materials and methods

Alaska plaice eggs were obtained from a series of fisheries research cruises conducted by the Alaska Fisheries Science Center (AFSC) along the Alaska Peninsula in the eastern Bering Sea in 2002, 2003, 2005, and 2006 (Fig. 1, Table 1). Eggs were collected from surface waters (<0.5 m depth) with a Sameoto neuston net with 505-µm mesh (Sameoto and Jaroszynski, 1969; Jump et al., 2008). Depth-discrete sampling was conducted by using a 1-m^2 multiple opening and closing net and environmental sampling system (MOCNESS; Wiebe et al., 1976) with 505-µm mesh nets in 2003 and 2005. Depth intervals sampled were 0–10 m, 10–20 m, 20–30 m, 30–40 m, 40–50 m, and >60 m. Oceanographic variables were collected simultaneously with all sampling, and these data have been published elsewhere (Duffy-Anderson et al., 2010).

All eggs were fixed in 5% formalin, sorted, identified, and enumerated at the Plankton Sorting and Identification Center in Szczecin, Poland. Egg identifications were verified, and Alaska plaice eggs were measured and staged at the Alaska Fisheries Science Center in Seattle, WA.

Table 1

Number of Alaska plaice (*Pleuronectes quadrituberculatus*) eggs collected and staged by year and gear type. MOCNESS=multiple opening and closing net and environmental sampling system.

Year	Cruise dates	Gears used	Number of eggs collected and staged
2002	12–21 May	Neuston net	16
		MOCNESS	2
2003	17–24 May	Neuston net	26
		MOCNESS	353
2005	10–20 May	Neuston net	295
		MOCNESS	867
2006	8–19 May	Neuston net	615

Developmental stages of eggs

Stages of Alaska plaice eggs were determined according to developmental criteria standardized and described by Blood et al. (1994) for walleye pollock (*Theragra chalcogramma*). Staging criteria for walleye pollock are the standard criteria used to determine northern marine teleost egg development and were easily adapted to egg development in Alaska plaice. Modifications were made to the protocol in order to accommodate additional embryonic growth in Alaska plaice. For the present study, the last stage (21) in the egg development schedule for walleye pollock is defined as that stage when the tail tip reaches the back of the embryo's head and two stages are added: stage 22, when the tail tip extends to ¼ of the circumference of the egg beyond the snout; and stage 23, when the tail tip extends to ½ of the circumference of the egg beyond the snout.

Eggs were then binned into three broader categories that comprised 1) early-stage eggs (E: stages 1–12), which includes all stages before the closing of the blastopore; 2) middle-stage eggs (M: stages 13–15), when the blastopore is closed, the margin of the tail is defined, and the tail bud is thick, but the margin remains attached to the yolk; and 3) late-stage eggs (L: 16–23), when the tail lifts away from yolk and lengthens and encircles the top half of the yolk to extend just beyond the head of the embryo. The late-stage period was further subdivided into three stages after determining that the majority of eggs were in one of the following stages of development; early-late stage (EL: stages 16–18); middle-late stage (ML: 19–21); and late-late stage (LL: 22–23).

Collections with the neuston net

Eggs were collected from surface waters (<1 m depth) across the southern Bering Sea shelf in the vicinity of the Alaska Peninsula. Collections were made over the basin, outer, middle, and inner shelves. Eggs from each tow were staged and the hypothesis that there were differences in geographic (horizontal) distribution with stage of development was examined by using Cramer-von Mises tests.

Vertical distributions of eggs determined with MOCNESS tows

The hypothesis that vertical patterns in egg abundance vary with depth and developmental stage was evaluated by using data collected from MOCNESS tows. A fourth root transformation was used to improve the normality of the data. In 2003, a series of MOCNESS tows were conducted at a single station, whereas in 2005, MOCNESS tows were conducted at multiple stations over the Bering Sea shelf. A general linear model ANOVA was used for each cruise by using haul as a blocking factor in 2003, and station as a blocking factor in 2005. If significant differences with depth were found, the analysis was followed with Fisher's least significant difference comparisons (Milliken and Johnson, 1992). We also checked for autocorrelation in 2003 (Durbin Watson statistic) because in that year samples were taken over time at a single station.

Results

Stages of developing eggs

More than 2100 eggs were examined for this work (Table 1), of which more than 950 eggs were collected from neuston nets and the remainder from MOCNESS tows. The earliest developmental stage observed was stage 5 (32 cells) (Table 2); we estimated these eggs would be about 1 day old at *in situ* temperatures (4°C). Egg development studies of walleye pollock and arrowtooth flounder (*Atheresthes stomias*) have established that the time required to reach stage 5 is 18–28 hours at about 3°C (Blood, 2002; Blood et al., 2007), and we assumed similar rates for Alaska plaice eggs. The presence of stage-5 eggs indicates that residual spawning occurred in mid-May; however, the vast majority of the eggs were late-stage eggs (Table 2), indicating that most spawning occurred a few weeks before sampling (Pertseva-Ostroumova, 1961). Most eggs collected were at stage 22. Hatching occurs at stage 23; the eyes of embryos are fully pigmented and numbers of eggs are greatly reduced in contrast to stage 22.

Collections with the neuston net

Eggs collected from neustonic surface collections represented all stages of development (Fig. 2). Results of all pairwise Cramer-von Mises tests for differences in spatial distributions showed that there were no significant differences between the geographic distributions of any stages of larvae, except between the geographic distributions of EL and ML (P=0.002). However, there were some trends that could be discerned. Earliest stage eggs collected in the neuston layer appeared to concentrate offshore of the 40-m isobath, over bottom depths ranging from 40 to 75 m. Eggs in middle stages of development appeared to spread shoreward toward shallower depths, but catches of eggs in both the early and middle stages of development were comparatively low. Late-stage eggs occurred over depths ranging from 40 to 100 m.

Vertical distributions of eggs determined with MOCNESS tows

Vertical distributions of Alaska plaice eggs showed differences in depth distribution with ontogenetic stage (Fig. 3), and differences between years. In 2003, there was no significant effect of haul and therefore no autocorrelation (Durbin Watson statistic=1.91; effect of haul), and eggs were generally distributed throughout the water column. There was only one egg collected in the early stage and it was located in the deepest depth stratum (40–50 m). There were no collections of eggs

Table 2

Results of staging Alaska plaice (*Pleuronectes quadrituberculatus)* eggs and the percentage of eggs in each developmental stage bin by gear type (early: stages 1–12; middle: stages 13–15; late: stages 16–23). The late stage was subdivided into three categories (early late: stages 16–18; middle late: stages 19–21; and late late: stages 22–23). Stages were adapted from Blood et al. (1994) and two developmental stages were added for this study. MOCNESS=multiple opening and closing net and environmental sampling system.

	Developmental stage	Number of eggs/stage (neuston net and MOCNESS)	Percentage of total eggs/stage (neuston net and MOCNESS)		Neuston net (percentage of eggs collected)	MOCNESS (percentage of eggs collected)
Early	1	0	0			
	2	0	0			
	3	0	0			
	4	0	0			
	5	3	0.14			
	6	7	0.32			
	7	20	0.92			
	8	2	0.09			
	9	20	0.92			
	10	7	0.32			
	11	14	0.64			
	12	10	0.46			
				Total	8.1	0.5
Middle	13	10	0.46			
	14	23	1.06			
	15	51	2.35			
				Total	8.4	0.4
Early late	16	58	2.67			
	17	158	7.27			
	18	67	3.08			
				Total	23.0	5.2
Middle late	19	209	9.61			
	20	230	10.58			
	21	285	13.11			
				Total	30.2	35.7
Late late	22	727	33.44			
	23	272	12.51			
				Total	30.3	58.2

in the middle stages of development (stages 13–15). Among late-stage eggs in 2003, the densities of egg abundances were depressed in the near surface waters (0–10 m) and significantly so for ML and LL stages (Table 3). In general however, most eggs were collected from above the mixed layer (<30 m). In 2005, a different pattern emerged; late-stage eggs consistently occurred at shallower depths than did earlier stages (Fig. 3), and the majority were collected in near-surface waters. Statistical examination revealed that more eggs were collected from depths 0–10 m and 10–20 m than in any of the deeper depths.

Considered collectively, approximately 34% of the catch in the two years occurred in the top 10 m of the water column, 24% occurred between 10 and 20 m, 18% between 20 and 30 m, 11% between 30 and 40 m, 8% between 40 and 50 m, and 5% between 50 and 60 m depth.

Discussion

This is the first study to describe stage-dependent vertical and horizontal distribution of Alaska plaice eggs. Our data indicate that spawning occurs offshore of the 40-m isobath, and likely near-bottom, confirming hypotheses outlined in Bailey et al. (2003). Eggs occur throughout the water column, but many eggs occur in the upper water column (<30 m depth). The vast majority of eggs collected in the present study were in the later stages of development, and we estimate that the majority of spawning occurred a few weeks before collection. Maxi-

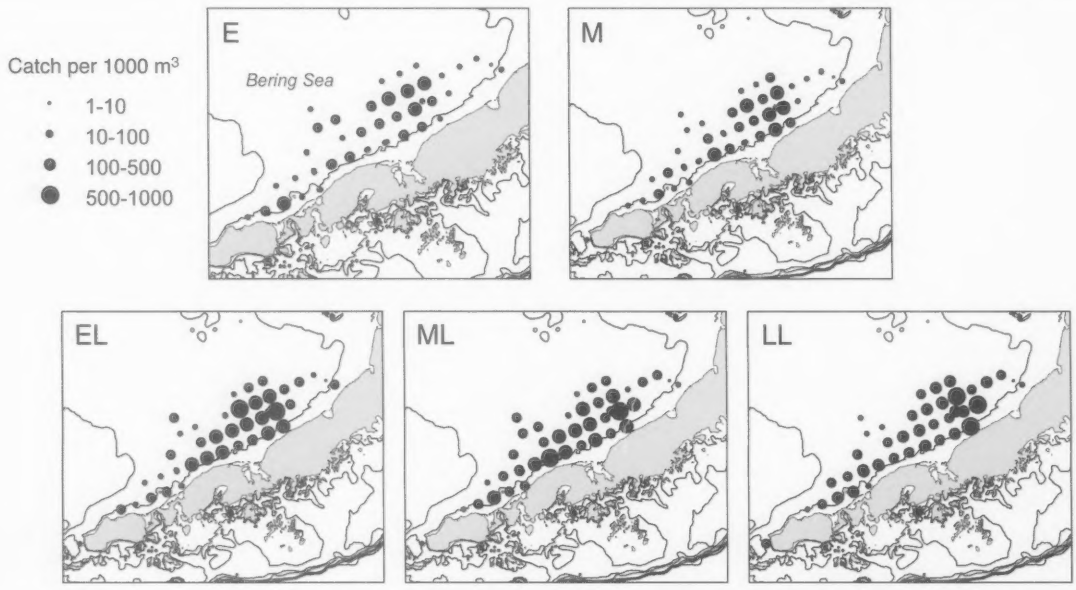

Figure 2

Abundance and geographic distribution of Alaska plaice (*Pleuronectes quadrituberculatus*) eggs (at different stages: early [E] and middle [M]; and at three stages within the late stage: early late [EL], middle late [ML], late late [LL]) collected in the neuston layer over the middle Bering Sea shelf. Catch is expressed as eggs/1000 m^3. The period of early-stage (E) eggs comprises stages 1–12, the period of middle-stage (M) eggs comprises stages 13–15, and the period of late-stage (L) eggs comprises stages 16–23.

mum larval abundance in the Bering Sea occurs in May (Duffy-Anderson et al., 2010) and probably reflects peak hatching of eggs spawned in April and a relatively high degree of spawning synchrony.

The geographic sampling area over which these eggs were collected was small compared to the potential spawning area over the Bering Sea continental shelf, and available evidence indicates that Alaska plaice do spawn over a large portion of the middle domain of the continental shelf (Zhang et al., 1998). The wind-mixed layer in the Bering Sea generally extends to 25–30 m in spring (Stabeno et al., 2001), and our data reveal that Alaska plaice eggs primarily occur above or within this layer. As such, the eggs are vulnerable to the stochastic effects of wind activity, which could disperse them widely over the shelf, especially in early spring months (March–April) when the likelihood of storm events is high. However, prevailing winds over the shelf in late spring–summer are southwesterly and would therefore transport late-stage eggs and newly hatched larvae from the middle shelf toward nursery areas along the Alaska mainland coast. Indeed, previous work has shown that Alaska plaice larvae are relatively rare over the continental shelf (Bailey et al., 2003), lending credence to the idea of shoreward transport of older egg stages and hatched larvae. It should be noted that retention in near-surface layers is also likely to promote faster rates of egg development because temperatures in the upper water column are 1–3°C warmer than those at depth over the middle shelf during spring.

Alaska plaice eggs do occur in near-surface waters, making them accessible to CUFES system, but many eggs also occur below the depths sampled with the CUFES. Therefore, abundance determined from eggs caught with the CUFES system may be underestimated—particularly the abundance of early stages that might be deeper in the water column. This observation has been made elsewhere (Lo et al., 2001; Dopolo et al., 2005), and at least in the case of Alaska plaice, we recommend that sampling with the CUFES system be supplemented with sampling of the entire water column to ensure adequate sampling of eggs at all stages of development. Moreover, sampling earlier in the spring, in March–April, for earlier stages is encouraged.

Acknowledgments

Thanks to the officers and crew of the NOAA ship RV *Miller Freeman*. Comments by T. Smart, C. Jump, J. Napp, and three anonymous reviewers improved the manuscript. Funds were provided by the North Pacific

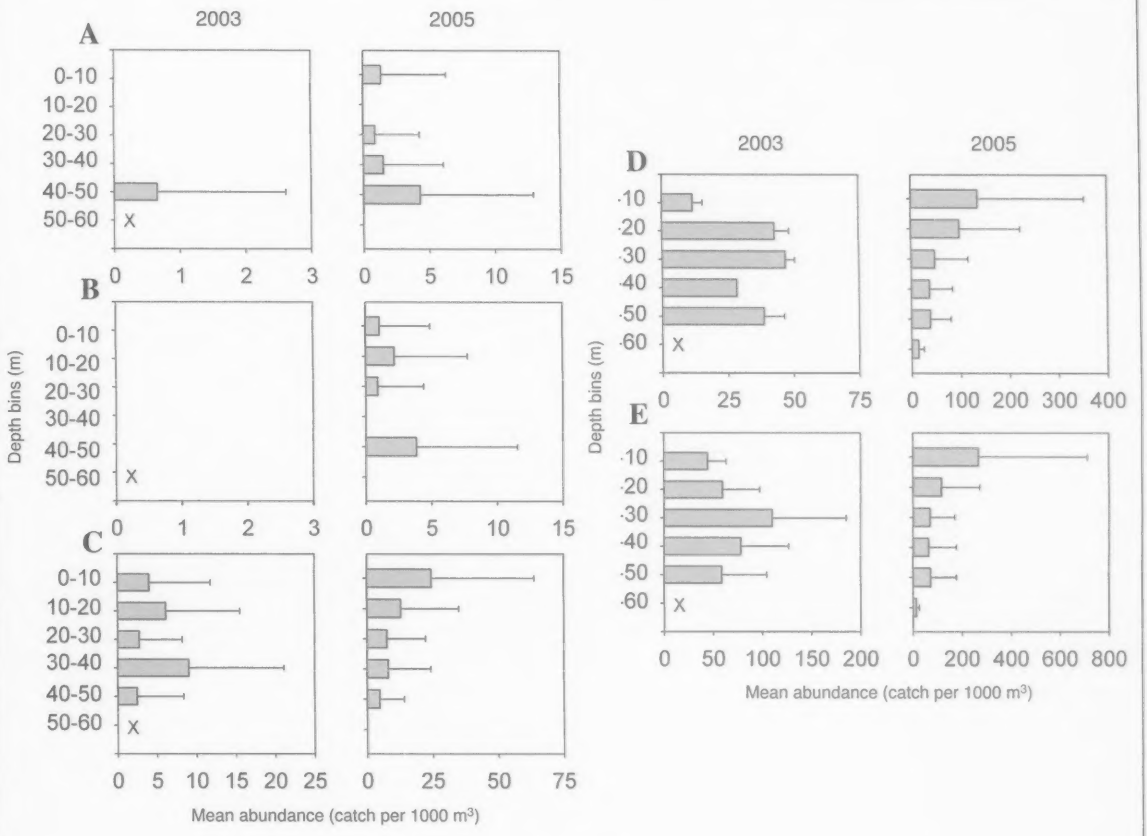

Figure 3

Mean abundance (± standard deviation) of Alaska plaice (*Pleuronectes quadrituberculatus*) eggs by developmental stage and depth. The symbol × indicates that no sample was taken at that depth. Data are derived from catches with the multiple opening and closing net and environmental sampling system in 2003 and 2005. (**A**) Early stage, (**B**) middle stage, (**C**) early-late stage, (**D**) middle-late stage, (**E**) late-late stage.

Table 3

Statistical comparisons Off differences in abundances of Alaska plaice (*Pleuronectes quadrituberculatus*) eggs in 2003 and 2005 by depth bin. Significance is noted at $P<0.05$. ns=not significant. ML=middle late stage. LL=late late stage.

ML 2003	0–10 m	10–20 m	20–30 m	30–40 m	40–50 m	50–60 m	60+ m
0–10 m	ns						
10–20 m	0.004	ns					
20–30 m	<0.001	ns	ns				
30–40 m	0.035	ns	ns	ns			
40–50 m	0.001	ns	ns	ns	ns		
50–60 m	ns	ns	ns	ns	ns	ns	
60+ m	ns	ns	ns	ns	ns	ns	ns

continued

Table 3 (continued)

LL 2003	0–10 m	10–20 m	20–30 m	30–40 m	40–50 m	50–60 m	60+ m
0–10 m	ns						
10–20 m	ns	ns					
20–30 m	0.002	0.017	ns				
30–40 m	ns	ns	ns	ns			
40–50 m	0.041	ns	ns	ns	ns		
50–60 m	ns	ns	ns	ns	ns	ns	
60+ m	ns	ns	ns	ns	ns	ns	ns
ML 2005	**0–10 m**	**10–20 m**	**20–30 m**	**30–40 m**	**40–50 m**	**50–60 m**	**60+ m**
0–10 m	ns						
10–20 m	ns	ns					
20–30 m	ns	0.009	ns				
30–40 m	ns	0.017	ns	ns			
40–50 m	0.005	0.001	ns	ns	ns		
50–60 m	ns	0.022	ns	ns	ns	ns	
60+ m	ns	0.032	ns	ns	ns	ns	ns
LL 2005	**0–10 m**	**10–20 m**	**20–30 m**	**30–40 m**	**40–50 m**	**50–60 m**	**60+ m**
0–10 m	ns						
10–20 m	ns	ns					
20–30 m	0.013	ns	ns				
30–40 m	0.003	0.022	ns	ns			
40–50 m	<0.001	<0.001	0.017	ns	ns		
50–60 m	ns	ns	ns	ns	ns	ns	
60+ m	.007	0.03	ns	ns	ns	ns	ns

and Climate Regimes and Ecosystem Productivity (NPCREP) program and the Alaska Fisheries Science Center's Resource Assessment Conservation and Engineering Division (NOAA). This research is contribution EcoFOCI-N736 to NOAA's Ecosystems and Fisheries-Oceanography Coordinated Investigations program.

Literature cited

Bailey, K. M., E. Brown, and J. T. Duffy-Anderson.
2003. Aspects of distribution, transport, and recruitment of Alaska plaice (*Pleuronectes quadrituberculatus*) in the Gulf of Alaska and eastern Bering Sea: comparison of marginal and central populations. J. Sea Res. 50:87–95.

Bailey, K. M., H. Nakata, and H. W. Van der Veer.
2005. The planktonic stages of flatfishes: physical and biological interactions in transport processes. *In* Flatfishes: biology and exploitation (R. N. Gibson, ed.), p. 94–119. Blackwell Science Publ., Oxford, U.K.

Blood, D. M.
2002. Low temperature incubation of walleye pollock (*Theragra chalcogramma*) from the southeast Bering Sea and Shelikof Strait, Gulf of Alaska. Deep Sea Res. II 49:6095–6108.

Blood, D. M., A. C. Matarese, and M. S. Busby.
2007. Spawning, egg development, and early life history dynamics of arrowtooth flounder (*Atheresthes stomias*) in the Gulf of Alaska. NOAA Prof. Paper NMFS 7, 28 p.

Blood, D. M., A. C. Matarese, and M. M. Yoklavich.
1994. Embryonic development of walleye pollock, *Theragra chalcogramma*, from Shelikof Strait, Gulf of Alaska. Fish. Bull. 92:207–222.

Checkley, D. M., Jr, J. R. Hunter, L. Motos, and C.D. van der Lingen.
2000. Report of a workshop on the use of the continuous underway fish egg sampler (CUFES) for mapping spawning habitats of pelagic fish. GLOBEC Rep. 14:1–65.

Checkley, D. M., P. B. Ortner, L. R. Settle, and S. R. Cummings.
1997. A continuous, underway fish egg sampler. Fish. Oceanogr. 6:58–73.

Dopolo, M. T., C. D. van der Lingen, and C. L. Moloney.
2005. Stage-dependent vertical distribution of pelagic fish eggs on the western Agulhas Bank, South Africa. Afr. J. Mar. Sci. 27:249–256.

Duffy-Anderson, J. T., M. Doyle, K. L. Mier, P. Stabeno, and T. Wilderbuer.
2010. Early life ecology of Alaska plaice (*Pleuronectes quadrituberculatus*) in the eastern Bering Sea: distribution, transport pathways, and effects of hydrography. J. Sea Res. 64:3–14.

Jump, C. M., J. T. Duffy-Anderson, and K. L. Mier.
2008. Comparison of neustonic ichthyoplankton samplers in the Gulf of Alaska. Fish. Res. 89:222–229.
Lo, N. C. H., J. R. Hunter, and R. Charter.
2001. Use of a continuous egg sampler for ichthyoplankton surveys: application to estimation of daily egg production of Pacific sardine (*Sardinops sagax*) off California. Fish Bull. 99:554–571.
Milliken, G. A. and D. E. Johnson.
1992. Analysis of messy data. Vol. I: design experiments, 473 p. Chapman and Hall, London.
Pearcy, W. G.
1962. Distribution and origin of demersal eggs within the order Pleuronectiformes. J. Conseil 27:232–235.
Pepin, P., P. V. R. Snelgrove, and K. P. Carter.
2005. Accuracy and precision of the continuous underway fish egg sampler (CUFES) and bongo nets: a comparison of three species of temperate fish. Fish. Oceanogr. 14:432–447.
Pertseva-Ostroumova, T. A.
1961. The reproduction and development of far eastern flounders. Akad. Nauk SSSR Inst. Okeanol., 484 p. [Transl. by Fish. Res. Board Can., 1967, Transl. Ser. 856.]
Sameoto, D. D., and L. O. Jaroszynski.
1969. Otter surface trawl: a new neuston net. J. Fish. Res. Board Can. 26:2240–2244.
Stabeno, P. J., N. A. Bond, N. B. Kachel, S. A. Salo, and J. D. Schumacher.
2001. On the temporal variability of the physical environment over the south-eastern Bering Sea. Fish. Oceanogr. 10:81–98.
Wiebe, P. H., K. H. Burt, S. H. Boyd, and A. W. Morton.
1976. A multiple opening/closing net and environmental sensing system for sampling zooplankton. J. Mar. Res. 34:313–326.
Zhang, C. I., T. K. Wilderbuer, and G. E. Walters.
1998. Biological characteristics and fishery assessment of Alaska plaice, *Pleuronectes quadrituberculatus*, in the eastern Bering Sea. Mar. Fish. Rev. 60:16–27.

Use of SARIMA models to assess data-poor fisheries: a case study with a sciaenid fishery off Portugal

Nuno Prista (contact author)[1,2]
Norou Diawara[3]
Maria José Costa[1,2]
Cynthia Jones[4]

Email address for contact author: nmprista@ipimar.pt

[1] Centro de Oceanografia
Faculdade de Ciências da Universidade de Lisboa
Campo Grande, 1749-016
Lisboa, Portugal
Present address for contact author: Unidade de Recursos Marinhos e Sustentabilidade
Instituto Nacional de Recursos Biológicos (INRB, I.P./IPIMAR)
Avenida de Brasília, 1449-006
Lisboa, Portugal

[2] Departamento de Biologia Animal
Faculdade de Ciências da Universidade de Lisboa
Campo Grande, 1749-016
Lisboa, Portugal

[3] Department of Mathematics and Statistics
Old Dominion University
Norfolk, Virginia 23529-0077

[4] Center for Quantitative Fisheries Ecology
Old Dominion University
800W 46th Street
Norfolk, Virginia 23508-2099

Abstract—Research on assessment and monitoring methods has primarily focused on fisheries with long multivariate data sets. Less research exists on methods applicable to data-poor fisheries with univariate data sets with a small sample size. In this study, we examine the capabilities of seasonal autoregressive integrated moving average (SARIMA) models to fit, forecast, and monitor the landings of such data-poor fisheries. We use a European fishery on meagre (Sciaenidae: *Argyrosomus regius*), where only a short time series of landings was available to model (n=60 months), as our case-study. We show that despite the limited sample size, a SARIMA model could be found that adequately fitted and forecasted the time series of meagre landings (12-month forecasts; mean error: 3.5 tons (t); annual absolute percentage error: 15.4%). We derive model-based prediction intervals and show how they can be used to detect problematic situations in the fishery. Our results indicate that over the course of one year the meagre landings remained within the prediction limits of the model and therefore indicated no need for urgent management intervention. We discuss the information that SARIMA model structure conveys on the meagre life-cycle and fishery, the methodological requirements of SARIMA forecasting of data-poor fisheries landings, and the capabilities SARIMA models present within current efforts to monitor the world's data-poorest resources.

Manuscript submitted 8 March 2010.
Manuscript accepted 20 January 2011.
Fish. Bull. 109:170–185 (2011).

The views and opinions expressed or implied in this article are those of the author (or authors) and do not necessarily reflect the position of the National Marine Fisheries Service, NOAA.

Research, assessment, and management have traditionally focused on fisheries with the greatest landings and revenues (Scandol, 2005; Vasconcellos and Cochrane, 2005). Such fisheries are generally data-rich and have available the funds and expertise required to complete stock assessments and provide state-of-the-art advice to management. However, that is not the case for the vast majority of fisheries worldwide, which remain subjected to limited (if any) assessment and management (Vasconcellos and Cochrane, 2005). The latter have been collectively termed "data-poor fisheries" and are characterized by a low diversity and quantity of data, limitations in funding and expertise, and an overall shortage of assessment methods (Mahon, 1997; Scandol, 2005). Among the world's data-poorest fisheries are nearly all fisheries in developing countries, but also most fisheries in developed countries, namely the smaller-scale or less valuable commercial and recreational ones (NRC, 1998; Berkes et al., 2001; EEA, 2005; Vasconcellos and Cochrane, 2005; Worm et al., 2009; OSPAR, 2010; ICES[1]).

Assessment of data-poor fisheries requires a significantly different approach from their data-rich counterparts. For data-poor fisheries, many deterministic multivariate stock assessment models cannot be used (e.g., NRC, 1998) and more pragmatic assessment methods must be put in place, particularly when fishery-independent data are not available and fishing effort cannot be quantified (Berkes et al., 2001; Scandol, 2003; ICES[1]). In many countries, the most readily available fisheries data are commercial landings because of their

[1] ICES (International Council for the Exploration of the Sea). 2008. Report of the study group on management strategies (SGMAS), 74 p. ICES CM 2008/ACOM:24, Copenhagen, Denmark.

connection to the economy and business (Vasconcellos and Cochrane, 2005). Commercial landings result from complex interactions between the environment, the fishing fleet, and the stocks, and therefore do not directly reflect the status of exploited populations. However, landing records contain valuable information that can be useful to managers if routine monitoring, rather than stock assessment, is established as a management objective (Scandol, 2003). In fact, even if they provide suboptimal indications on the status of the stocks, statistical analyses of landings can lead to the timely detection of phenomena such as sudden increases in fishing effort or marked population declines that could otherwise remain undetected (Caddy, 1999). Such detection is important—particularly within multispecies, budget-limited, management contexts—because it allows the prioritization of research and management actions toward the subset of fisheries and stocks most likely to be depleted (Scandol, 2003).

Autoregressive integrated moving-average (ARIMA) models are simple time series models that can be used to fit and forecast univariate data such as fisheries landings. With ARIMA models data are assumed to be the output of a stochastic process, generated by unknown causes, from which future values can be predicted as a linear combination of past observations and estimates of current and past random shocks to the system (Box et al., 2008). In fisheries, ARIMA models (and their seasonal multiplicative version, SARIMA) have a long record of successful application that extends from modeling (e.g., Hare and Francis, 1994; Fogarty and Miller, 2004) to short-term forecasting of a variety of variables and resources for both data-rich and data-poor fisheries (Table 1). Specifically, SARIMA models, which are applicable to many already-available landings data sets, have been found to provide both annual and monthly forecasts that are comparable to, or even better than forecasts from many multivariate models, including some with fishing effort among the predictors (Stergiou et al., 1997).

The good record, flexibility, and simplicity of SARIMA models have made them natural candidates for the modeling of data-poor fisheries (Rothschild et al., 1996). However, to date, SARIMA models in fisheries have only been applied in detail on relatively long time series (≥120 months) (Table 1), and a single study has provided a few (but not detailed) results from shorter series (Lloret et al., 2000). Such emphasis of previous SARIMA modeling on long time series finds little support in statistical literature where 50 months is generally regarded as the minimum sample size for model application (e.g., Pankratz, 1983; Chatfield, 1996a). Additionally, most literature to date has focused on SARIMA models as tools to generate accurate forecasts of future landings. However, in addition to good forecasting, these models also possess significant capabilities for monitoring landings that have remained unexplored. These capabilities become apparent when SARIMA models are approached from a statistical process-control perspective and it is made known that SARIMA model forecasts include the assumption of persistence (through time) of the process that generated the data (Box et al., 2008; Mesnil and Petitgas, 2009). Briefly, good landing forecasts are only attainable as long as significant changes do not take place in the fishery; therefore large forecast errors can be regarded as indications that can be changes in the fishery process took place that may require management intervention (Pajuelo and Lorenzo, 1995; Georgakarakos et al., 2006; Box et al., 2008).

In this study, we report the first detailed application of SARIMA models for monitoring of data-poor fisheries landings. We use data from a previously unassessed Portuguese fishery on meagre (Sciaenidae: *Argyrosomus regius*) as our example. The meagre is a valuable top predator from European coastal waters but its stocks have not been analytically assessed because of limitations in data, personnel, and funding existing at the national level. At the time of our analysis only a short time series of monthly landings (60 months) was available for this fishery, a situation that replicates conditions found in many other data-poor fisheries worldwide. We show that the short time series was not a problem for SARIMA modeling and forecasting and that prediction intervals from SARIMA models can be used to provide this fishery with basic monitoring. We suggest that SARIMA models should be more widely considered to extend the coverage of monitoring to all exploited marine resources.

Materials and methods

Meagre (*Argyrosomus regius*) and its fisheries

Meagre is one of the world's largest and most valuable sciaenids (up to 180 cm, 50 kg, and with a US$ 15 per kg exvessel price). It ranges from France to Senegal, and the largest fisheries take place off Mauritania, Morocco, and Egypt. In Europe, the meagre constitutes a prized trophy-fish for anglers and an important income for small-scale commercial fishermen along the Atlantic shores of France, Spain, and Portugal. Its biology and life cycle remain scarcely documented, but recent concerns about the overexploitation of juveniles and interests in aquaculture production have sparked some research. Currently, the fish is known to be fairly long-lived (up to 44 yr) (Prista et al., 2009), to present fast juvenile growth (Morales-Nin et al., 2010) and to spawn at 3–4 yr old (N. Prista, unpubl. data). Data on adult growth and reproduction have not been published, but preliminary reports indicate a life-cycle characterized by fast growth, high fecundity, and a long reproductive span, and that the estuaries of the Gironde (France), Tagus (Portugal), and Guadalquivir (SW Spain) rivers constitute the main spawning habitats (Quéméner, 2002; Prista et al.[2]; N.

[2] Prista, N., C. M. Jones, J. L. Costa, and M. J. Costa. 2008. Inferring fish movements from small-scale fisheries data: the case of *Argyrosomus regius* (Sciaenidae) in Portugal, 19 p. ICES CM 2008/K-19, Copenhagen, Denmark.

Prista, unpubl. data). Marked seasonal variations in landings linked to juvenile and adult migrations have been identified in local fisheries (Quéro and Vayne, 1987; Prista et al.[2]). Overall, adults are thought to come inshore from spring to early summer to spawn but their overwintering grounds are still unknown; juveniles are thought

Table 1

Primary fisheries literature that present seasonal autoregressive integrated moving-average models. Only studies with quantitative forecast results are displayed. "No."=the number of series, "Freq"=the sampling frequency (W=weekly, M=monthly, A=annual), "*n*" is the sample size of the fitting period, "F"=number of forecasts, "models" indicates the type of models compared, and "PI" indicates if prediction intervals were presented (yes, no). "/" separates annual and monthly data sets when both were analyzed. "sp" = species, "nsp groups" = nonspecific groups, "rel." = relative, "CPUE"=catch per unit of effort, "LPUE"=landings per unit of effort.

Reference	Species	Variable	No.	Freq	*n*	F	Models[a]	PI
Saila et al. (1980)	*Jasus edwardsii*	CPUE	1	M	144	12	1,5	n
Mendelssohn (1981)	*Katsuwonus pelamis*	catch/effort	1	M	180	12	12	n
Fogarty (1988)	*Homarus americanus*	catch/CPUE	3/1	A/M	41–58/216	1/12	12	n
Jeffries et al. (1989)	*Pseudopleuronectes americanus*	rel. abundance	2/3	A/M	27/156;324	2/12	—	y
Stergiou (1989)	*Sardina pilchardus*	catch	1	M	204	12	—	n
Noakes et al. (1990)	*Oncorhynchus nerka*	total returns	2	A	24	8	1,10,12,19,20	n
Stergiou (1990a)	*Engraulis encrasicolus*	catch	1	M	252	24	—	n
Stergiou (1990b)	Mullidae	catch	1	M	252	24	—	n
Campbell et al. (1991)	*Homarus americanus*	catch	4	A	61–97	10	12	n
Molinet et al. (1991)	*Penaeus* spp., *Lutjanus synagris*	landings/LPUE	2	M	132;180	24	—	n
Stergiou (1991)	*Trachurus* sp.	catch	1	M	252	12	1,8	n
Tsai and Chai (1992)	*Morone saxatilis*	harvest	1	A	27	4	3,4,12	n
Pajuelo and Lorenzo (1995)	1 nsp group	catch	1	M	131	24	—	y
Stergiou and Christou (1996)	4 sp; 12 nsp groups	catch	16	A	24	2	1–9	n
Stergiou et al. (1997)	4 sp; 12 nsp groups	catch	16	M	288	24	1–5,7–9	n
Park (1998)	*Theragra chalcogramma*	landings	1	M	264	24	—	n
Lloret et al. (2000)[6]	30 sp; 36 nsp groups	catch	66	M	51–200	12	—	y
Georgakarakos et al. (2002, 2006)	*Loligo vulgaris*, *Todarodes sagittatus*	landings	2	M	174	12	11,15,16	y
Pierce and Boyle (2003)	*Loligo forbesi*	LPUE	1	A/M	27/324	3/36	3, 12	y
Stergiou et al. (2003)	*Xiphias gladius*	catch	1	M	180	12	8,13	n
Zhou (2003)	*Oncorhynchus tshawytscha*	spawner density	2	A	11	4	1, 15	n
Hanson et al. (2006)	*Brevoortia tyrannus*, *B. patronus*	landings	2	A	57;63	10	3,14,15	n
Koutroumanidis et al. (2006)	*E. encrasicolus*, *Merluccius merluccius*, *Sarda sarda*	landings	3	M	216;252	12	17,18	n
Czerwinski et al. (2007)	*Hippoglossus stenolepis*	CPUE	1	W	107	31	15	n
Tsitsika et al. (2007)	Total pelagic production *E. encrasicolus*, *S. pilchardus*, *T. trachurus*	CPUE	4	M	180	12	11	y

[a] Models compared: 1=naïve, 2=linear regression (LR), 3=multiple LR, 4=multiple LR with correlated errors, 5=harmonic LR, 6=Fox surplus-yield, 7=model combination, 8=exponential, 9=vector autoregressive, 10=periodic autoregressive, 11=multivariate ARIMA, 12= transfer function noise, 13=census method II (X-11), U.S. Dep. Commer., 14=state space models, 15=artificial neural networks, 16=Bayesian dynamic modeling, 17=genetic modeling for optimal forecasting, 18=fuzzy expected intervals, 19=stock-recruitment, 20=sibling.

[b] The Lloret et al. (2000) study includes 12 series with 51–64 months.

to use estuaries as nursery areas during the warmer months and overwinter in adjoining coastal grounds (Quéro and Vayne, 1987; Quéméner, 2002; Prista et al.[2]; N. Prista, unpubl. data).

Recently, substantial conservation risks have been identified in European meagre fisheries that are related to the overexploitation of juvenile and adults schools in estuaries and nearby coastal areas (Quéméner, 2002; Prista et al.[2]). To protect juveniles, precautionary management measures have been put in place (namely minimum landing size regulations) but the actual status of the meagre stocks was never assessed. This lack of assessment mainly results from a lack of sufficient multivariate time-series data and because national assessment priorities, funding, and expertise are generally allocated to the largest national and transnational fisheries instead of the less-significant, albeit numerous and regionally important, ones. The fish being largely absent from routine fishery-independent surveys (Quéro and Vayne, 1987; F. Cardador, personal commun.[3]) and difficulties related to its sampling at port and the estimation of fishing effort (Prista et al.[2,4]) further contribute to its unassessed status. In this type of setting, if simple methods are not put in place that can, at least, detect the most alarming signals in the landings data it is likely that stock collapses can occur without being detected.

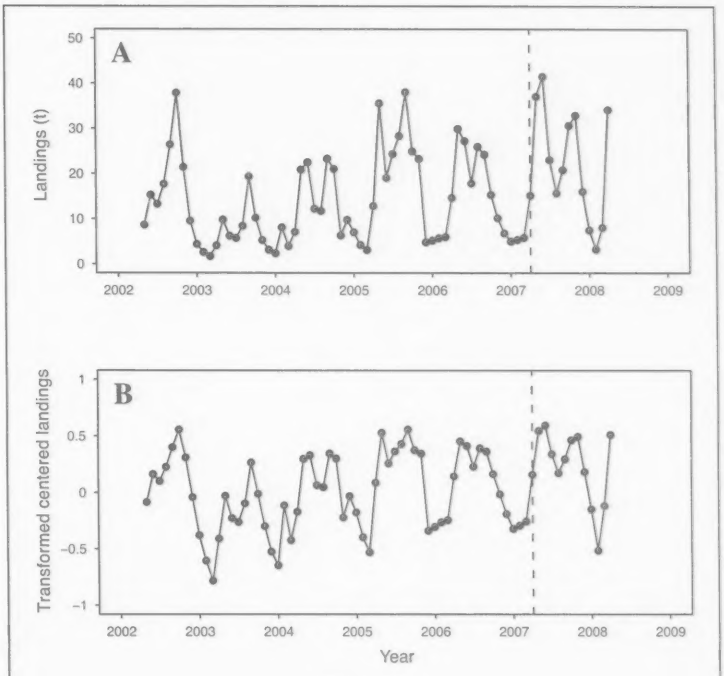

Figure 1

Time series of monthly meagre (*Argyrosomus regius*) landings, in tons, in the Lisboa region of the Portuguese coast (May 2002 to April 2008). The dashed vertical line is the forecast origin (April 2007) and separates the fitting period (May 2002 to April 2007, left) from the hold-out period (May 2007 to April 2008, right). (A) Raw data. (B) Log_{10}-transformed mean-centered data.

Data set and data transformations

The Lisboa region in Central West Portugal (henceforth termed "Lisboa region") (38°25′N to 38°59′N lat., ~9°15′W long.) is the main fishing area for meagre off the Iberian Peninsula (between 29% and 45% of annual landings of meagre, all gears combined, in 2001–05). In this region, most of the catch is associated with the Tagus estuary and its adjoining coastal area. The catch derives essentially from a small-scale artisanal fleet in which gillnets, trammel nets, and longlines are used to catch meagre during its spawning and nursery season (Prista et al.[2]). To minimize overfishing of juvenile fish, a minimum landing size of 42 cm was established in 2002 that complements an array of other gear-related and effort-related management regulations that are not specific to meagre.

To test SARIMA models in the monitoring of the Lisboa meagre landings, we obtained a time series of meagre monthly landings from the Portuguese General-Directorate for Fisheries and Aquaculture (DGPA). The landings data resulted from mandatory reports of fish sales obtained at all ports of the Lisboa region (N=14) from May 2002 to April 2008 (i.e., 72 monthly values) as part of a routine data collection program (Fig. 1). We used the first 60 months to fit the SARIMA models and the last 12 months as a hold-out period to evaluate forecasting performance and to monitor the fishery. Some previous data were available on this fishery, but those data were found to be unreliable because of contamination with landings from Portuguese vessels operating off North African waters. No significant management interventions occurred on the fishery during the course of our study.

Before fitting a SARIMA model, the time series must be checked for violations of the weak stationarity assumption of the models (Brockwell and Davis, 2002; Box et al., 2008). In SARIMA models, trend and seasonal nonstationarities are handled directly by the model

[3] Cardador, Fátima. 2008. INRB, I.P./IPIMAR, Av. Brasília, 1449-006 Lisboa, Portugal.

[4] Prista, N., J. L. Costa, M. J. Costa, and C. M. Jones. 2007. New methodology for studying large valuable fish in data poor situations: commercial mark-recapture of meagre *Argyrosomus regius* in the southern coast of Portugal, 18 p.

Table 2

Candidate set of seasonal autoregressive integrated moving-average models. The "rule" column displays the mathematical expression used to determine the autoregressive components (p) and moving-average components (q) of the candidate models. "Max AR term" and "Max MA term" columns display the maximum autoregressive (AR) and moving-average (MA) lags included in the model equations, with respect to the original (x_t) and 12-month differenced $\log_{10}$-transformed mean-centered data ($w_t=\nabla_{12}^1 y_t=\nabla_{12}^1(\log_{10}x_t-4.022)$), respectively.

Model structure	No. of models	Rule	Max AR term	Max MA term
$(p,0,q)\times(0,1,0)_{12}$	325	$q<25-p; p\leq 24$	$w_{t-24}; x_{t-36}$	z_{t-12}
$(p,0,q)\times(1,1,0)_{12}$	91	$q<13-p; p\leq 12$	$w_{t-24}; x_{t-36}$	z_{t-12}
$(p,0,q)\times(0,1,1)_{12}$	91	$q<13-p; p\leq 12$	$w_{t-12}; x_{t-24}$	z_{t-24}
$(p,0,q)\times(1,1,1)_{12}$	1	$q=0; p=0$	$w_{t-12}; x_{t-24}$	z_{t-12}

structure so that only the nonstationarity of variance needs to be addressed before model fitting. The meagre time series (x_t, t=1, ... ,60) was seasonal and exhibited no trend (Fig. 1A), but annual variance-mean plots indicated an increase in variance with the series mean. To correct this, we evaluated Box-Cox transformations (Box and Cox, 1964) and found that a $\log_{10}$ transformation successfully stabilized the variance of the series. Accordingly, we log-transformed the data, subtracted its mean, and then used the mean-centered log-transformed data set (y_t, t=1, ... ,60) as input to the SARIMA analyses (Fig. 1B).

Data modeling

We fitted SARIMA models to the meagre data using a semi-automated approach based on a combination of the Box-Jenkins method with small-sample, bias-corrected Akaike information criteria (AIC_c) model selection (Rothschild et al., 1996; Brockwell and Davis, 2002). This approach involved three major steps: 1) selection of the candidate model set; 2) estimation of the model and determination of AIC_c; and 3) a diagnostic check. Details on the notation and model selection procedures used to fit SARIMA models to short time series are given in Appendices 1 and 2.

Selection of the candidate model set was carried out by first analyzing sample estimates of the autocorrelation function (ACF) and partial autocorrelation function (PACF) in order to select the three major orders of the SARIMA models: d, D, and S. In the meagre case, we concluded that a configuration with d=0, D=1, and S=12 should be adopted (see *Results* section). Consequently, a SARIMA$(p,0,q)\times(P,1,Q)_{12}$ was selected as the basic model structure of the candidate set, with p, q, P, and Q left to vary. There is no *a priori* method to determine the maximum value that p, q, P, and Q can take, but the maximum orders of the models are obviously restricted by sample size. In our analysis, we conditioned p, q, P, and Q to the upper boundary $max(p+q+SP+SQ)=24$ and $p+q\leq 12$ (Table 2), which caused the maximum possible term of any SARIMA model to be x_{t-36} and the maximum possible number of parameters to be 13. We found this procedure to provide a good compromise between model complexity and the convergence of estimation algorithms.

Model estimation was carried out by using maximum likelihood methods, after conditional sum of squares estimation of the starting values (Brockwell and Davis, 2002). Given the large number of models requiring estimation (Table 2), we developed a semi-automated software routine in R, vers. 2.5.1 (R Development Core Team, 2007) that estimated the models and output their AIC_c values. This routine used several functions incorporated in the R packages "stats" (R Development Core Team, 2007), "tseries" (Trapletti and Hornik, 2007), and "FinTS" (Graves, 2008). After estimation, the model with the minimum AIC_c was selected for further analysis.

Diagnostic checks on the AIC_c-selected model involved the following steps: 1) verification of the resemblance of residuals to white noise (ACF plots, Ljung-Box test, cumulative periodogram test); 2) tests on the normality of residuals (Jarque-Bera and Shapiro-Wilks tests); and 3) confirmation of model stationarity, invertibility, and parameter redundancy (Shapiro et al., 1968; Ljung and Box, 1978; Jarque and Bera, 1987; Box et al., 2008). All tests were carried out at a significance level of α=0.05. The variance explained by the model was determined as $1-\hat{\sigma}^2/\sigma_{y_t}^2$ (Stergiou, 1990a).

Forecasts and model performance

We evaluated 12 months of model forecasts, using the last month of the fitting data set as the forecast origin (i.e., April 2007). Forecasts were obtained in the mean-centered transformed scale ($\hat{y}_h$, h=1,...,12) and in the original scale of the data ($\hat{x}_h$, h=1,...,12), after correcting for back-transformation bias (Pankratz, 1983). SARIMA model performance was assessed by comparing h-step forecasts ($\hat{x}_h$ and $\hat{y}_h$) with monthly landings observed between May 2007 and April 2008 (x_h and y_h). This was done by evaluating monthly forecast errors (e.g., $e_h=\hat{x}_h-x_h$) and then considering a set of accuracy measures: 1) annual root mean-square error (RMSE); 2) mean error (ME); 3) absolute percent error (APE_h); 4) mean absolute percent error (MAPE); and 5) annual percent

error (PE) (Mendelssohn, 1981; Hyndman and Koehler, 2006). From these, RMSE was evaluated in the transformed scale to allow its comparison to $\hat{\sigma}$, and all others were computed in the more user-friendly original scale of the data. Additionally, we compared the forecasting performance of the SARIMA model against two simple naïve forecasting models (naïve model 1 or NM1, and naïve model 2 or NM2) (Noakes et al., 1990; Stergiou et al., 1997). The latter represented *ad hoc* forecasting models likely to be used in data-poor fisheries with short time series of landings: with NM1, future landings were assumed to be equal to the landings registered in the previous year; and with NM2, future landings were assumed to be equal to the average monthly landings registered in the fitting period. We also evaluated the Kitanidis and Bras (1980) coefficient of persistence (P) that summarizes forecasting results by comparing them with those of a naïve model where landings at time t+1 are assumed equal to landings at time t. This coefficient takes values smaller than or equal to 1, with P=1 representing perfect model forecasts.

Monitoring of fisheries

SARIMA models predict the future on the assumption that the statistical properties of the process generating the data remain the same over time (Box et al., 2008). When framed within the perspective of statistical process control (e.g., Scandol, 2005; Box et al., 2008; Mesnil and Petitgas, 2009), this characteristic allows the predictions of well-developed SARIMA models to be used as "guidelines" to monitor future observations. When a SARIMA model is found that appropriately fits the landings data, a significant departure of its forecasts from future observations can be seen as an indication that changes in the underlying fishery process have occurred (=out-of-control situation). In contrast, if such a significant departure does not take place, then there is no indication for such changes (= in-control situation). From a data-poor fisheries perspective, such a distinction means that if funding is limited and multiple fisheries require assessment, research and management efforts should be allocated to fisheries displaying out-of-control decreasing trends in production rather than to fisheries that remain stable or display in-control increasing trends (Scandol, 2003, 2005).

The distinction between in-control and out-of-control landings requires a set of detection limits. To date, process-control detection limits for fisheries indicators have been derived mostly from historical reference data (Scandol, 2003; Mesnil and Petitgas 2009; Petitgas, 2009). However, most fisheries have only a few years of collected data and consequently historical limits are difficult to estimate. In such situations, model-based detection limits like the prediction intervals (PIs) of SARIMA models (Chatfield, 1993; Box et al., 2008) provide easy-to-compute detection limits that explicitly take into account the correlation structure of the data. SARIMA PIs resemble confidence intervals for model forecasts and consist of upper and lower boundaries that encompass a 1–α probability region for future forecasts (Chatfield, 1993). Their main use is to convey the uncertainty around forecasts (De Gooijer and Hyndman, 2006). However, because prediction intervals encompass only future observations, as long as no structural changes take place in the underlying process (Chatfield, 1993), their boundaries can be used to monitor univariate data such as fisheries landings.

To date, the prediction intervals (PIs) from SARIMA models have seldom been reported in fisheries literature and, when they have, with little detail and discussion (Table 1). To monitor the landings of the meagre fishery we used two types of PIs: single step PIs ($PI_{ss,h}$) and multistep PIs ($PI_{ms,h}$). Single step PIs refer to a single monthly forecast (e.g., h=3) and are useful for determining whether a specific monthly observation is an outlier at a given significance level α. Multistep PIs encompass a 1–α prediction region that is a simultaneous PI for all observations registered up to a certain h-step and are useful in detecting systematic departures from historical patterns. We calculated $PI_{ss,h}$ as $\hat{y}_h \pm t_{df,\alpha/2}\sqrt{PMSE_h}$ where $PMSE_h$ is the expected mean squared prediction error at step h and df=N–DS–d–r (Chatfield, 1993; Harvey, 1989). In the calculation of multistep PIs, we used a conservative approach based on a first-order Bonferroni inequality, whereby $PI_{ms,h}$ is given as $\hat{y}_h \pm t_{df,\alpha/2h}\sqrt{PMSE_h}$ and joint prediction intervals of, at least, 1–α around the point forecasts are obtained (Chan et al., 2004).

Results

Data modeling

Large autocorrelations were recorded for lags 1, 2, 11, 12, 23, and 24 with values 0.68, 0.32, 0.44, 0.46, 0.28 and 0.31, respectively (Fig. 2). The sharp decrease in autocorrelation values after lag 2 (0.07 at lag 3) indicated no evidence of a long-term trend; consequently, there was no need to include a first-lag difference term in the SARIMA model structure (d=0). In contrast, large autocorrelation values were registered at annual lags (and its multiples) which indicated the need to include a 12-month difference term in the models (S=12, D=1) (Fig. 2). The ACF and PACF plots of the differenced series provided further support for these conclusions (Fig. 2). Accordingly, a SARIMA$(p,0,q)\times(P,1,Q)_{12}$ was selected as the basic structure of the SARIMA candidate set.

Out of all models in the candidate set, a SARIMA$(0,0,5)\times(1,1,0)_{12}$ was selected as the best model for the meagre data (−2 ln (L)=−26.32, n=48, r=7, AIC_c=−9.52). This model had the following equation:

$$(1+0.65_{[.10]}B^{12})\ \nabla^1_{12}y_t = (1+0.63_{[.19]}B+0.56_{[.15]}B^2 + 0.51_{[.17]}B^3 + 0.93_{[.18]}B^4 + 0.60_{[.21]}B^5)z_t\ ,$$

with a noise variance estimate of $\hat{\sigma}$=0.025 and

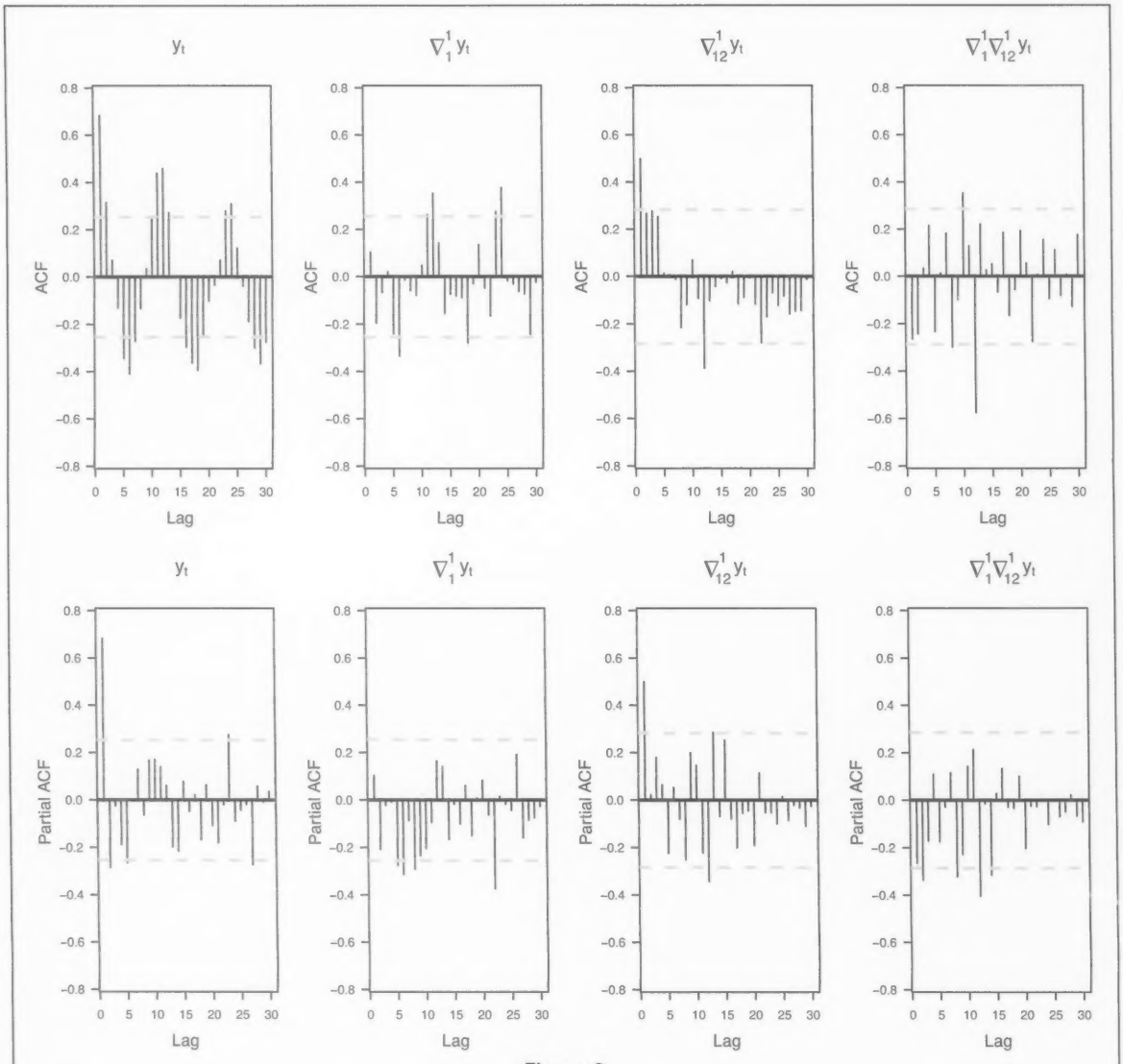

Figure 2

Sample autocorrelation function (ACF) and partial autocorrelation function (PACF) of the transformed meagre (*Argyrosomus regius*) landings. ACF/PACF plots for $\log_{10}$-transformed mean-centered data (y_t, far left), lag-1 differenced series ($\nabla_1^1 y_t$), lag-12 differenced series ($\nabla_{12}^1 y_t$), and lag-1 and lag-12 differenced series ($\nabla_1^1\nabla_{12}^1 y_t$, far right) are displayed. Horizontal dashed lines represent the 95% confidence limits valid under the null hypothesis of white noise error structure.

where y_t = the mean-centered log-transformed meagre series (i.e., $y_t = \log_{10} x_t - 4.022$) and the values in {} are the standard errors of the estimates.

Diagnostic checks indicated that the SARIMA model was stationary and invertible and did not have redundant parameters. The residuals were white noise (Ljung-Box Q=3.35, P-value>0.05) and passed asymptotic normality tests (Shapiro-Wilk W=0.97, P-value >0.05; Jarque-Bera LM=4.91, P-value >0.05) indicating the model fitted the data and errors were normally distributed. The model explained 78.2% of the variance of the series.

The final process equation selected for the meagre data was

$$\log_{10}X_t = 0.35\log_{10}X_{t-12} + 0.65\log_{10}X_{t-24} + Z_t + 0.63Z_{t-1} + 0.56Z_{t-2} + 0.51Z_{t-3} + 0.93Z_{t-4} + 0.60Z_{t-5},$$

where $Z_t \sim N(0, 0.025)$.

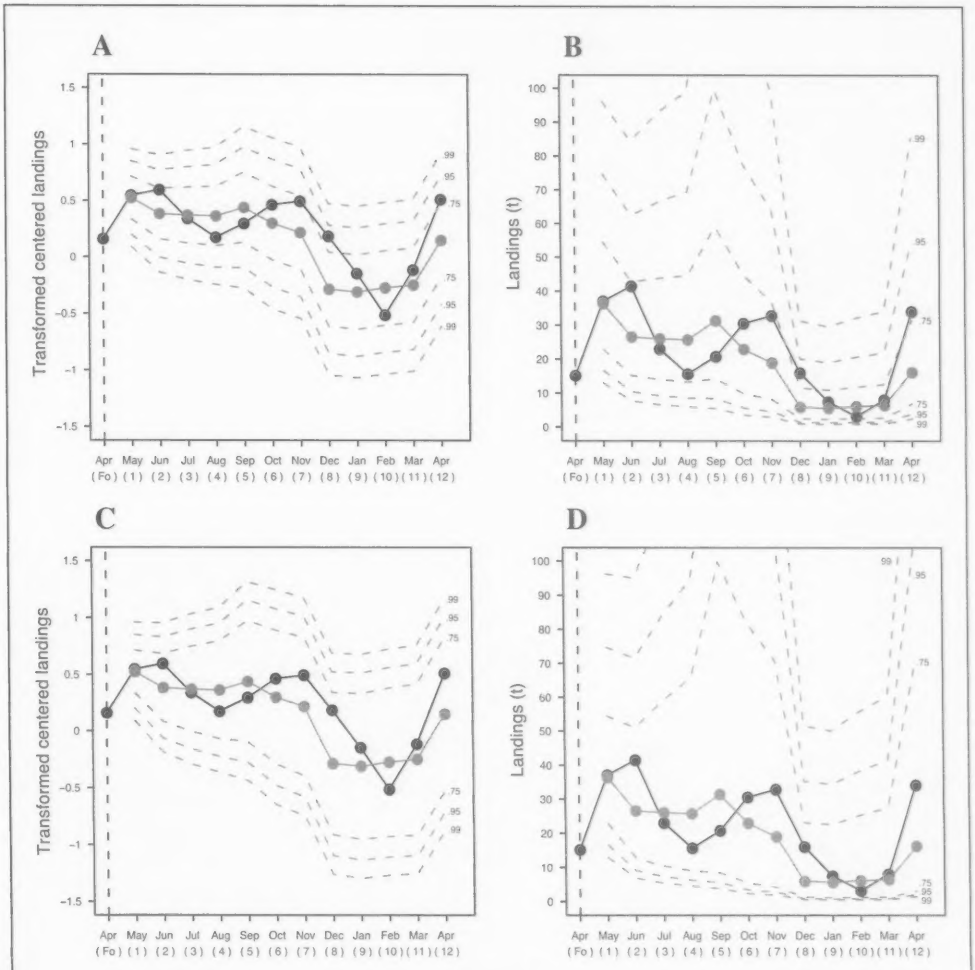

Figure 3

Forecasts and forecast prediction intervals (PIs) of meagre (*Argyrosomus regius*) landings. The dashed vertical line is the forecast origin ("Fo", April 2007). The gray circles and line represent the monthly forecasts. The black circles and line represent observed monthly landings. The dashed gray lines represent the upper and lower 75%, 95%, and 99% prediction intervals. (**A** and **B**) Single step prediction intervals ($PI_{ss,h}$) of transformed centered landings and back-transformed landings, respectively in C and D. Multistep prediction intervals ($PI_{ms,h}$) of transformed centered landings and back-transformed landings, respectively.

Model forecasts and performance

The model forecasts presented two local maxima (May 2007 and September 2007) followed by a four-month period of low landings (December 2007 through March 2008) and an increase in the last month (April 2008) (Fig. 3, Table 3). This pattern in forecasts matched the one in observed landings and the only deviations were that the actual maxima took place one to two months later and the winter trough was sharper than that predicted by the model (Fig. 3). RMSE during the hold-out period (0.234) was ≈1.5 times the RMSE of the fitting period. Eight of the 12 forecasts registered negative errors, but the low ME and PE indicated that underestimation was minor in global terms. APE was large in August, September, December, and April, reflecting the delay in cessation of the 2007 fishing season and the hastening of the 2008 fishing season. Maximum APE coincided with the lowest landings (February), and the minimum APE with the first month forecasted (May) (Table 3). MAPE was 40.3%, reflecting the lagged seasonality and the low landings observed during the winter period.

Table 3

Forecasts of meagre (*Argyrosomus regius*) landings (May 2007 to April 2008). Observed landings (x_h), forecasted landings ($\hat{x}_h$), monthly forecast errors (e_h), monthly absolute percent error (APE_h), mean error (ME), and mean absolute percent error (MAPE) are displayed for the two naïve models (NM1 and NM2) and the seasonal autoregressive integrated moving-average model (SAR). Annual root mean-square error of the mean-centered transformed data (RMSE) and annual percent error (PE) for NM1, NM2 and SAR were 0.261 and 30.2%, 0.285 and 38.9%, and 0.234 and 15.4%, respectively.

			Forecasts ($\hat{x}_h$)			Forecast errors (e_h)			APE_h		
Month	Step (h)	Obs (x_h)	NM1	NM2	SAR	NM1	NM2	SAR	NM1	NM2	SAR
May-07	1	37.1	29.9	21.0	36.4	–7.2	–16.1	–0.7	19.4	43.5	1.8
Jun-07	2	41.5	27.2	18.1	26.6	–14.3	–23.4	–14.9	34.4	56.5	35.8
Jul-07	3	23.0	17.9	14.7	26.1	–5.2	–8.3	+3.1	22.4	36.2	13.3
Aug-07	4	15.7	25.9	18.4	25.8	+10.2	+2.8	+10.1	65.3	17.6	64.7
Sep-07	5	20.8	24.2	26.3	31.4	+3.4	+5.5	+10.6	16.3	26.2	51.1
Oct-07	6	30.6	15.3	21.9	23.0	–15.2	–8.7	–7.6	49.8	28.5	24.9
Nov-07	7	32.9	10.2	13.3	19.0	–22.7	–19.6	–13.9	69.0	59.5	42.2
Dec-07	8	16.1	6.8	6.8	6.0	–9.3	–9.2	–10.1	57.7	57.5	62.8
Jan-08	9	7.5	5.0	4.8	5.7	–2.5	–2.7	–1.8	32.8	35.7	24.5
Feb-08	10	3.2	5.4	5.2	6.1	+2.1	+2.0	+2.9	66.6	61.9	90.7
Mar-08	11	8.0	5.8	4.1	6.5	–2.2	–3.9	–1.5	27.3	48.6	19.0
Apr-08	12	34.1	15.2	10.8	16.3	–18.9	–23.4	–17.9	55.5	68.4	52.4
Mean	1:12	22.5	15.7	13.8	19.1	–6.8	–8.8	–3.5	43.1	45.0	40.3
Sum	1:12	270.5	188.8	165.4	228.9	–81.7	–105.1	–41.6	—	—	—

As with SARIMA forecasts, naïve model predictions also lagged observed values by one or two months. However, the SARIMA forecasts registered the best performance in all accuracy measures, resulting in a 10% to 18% reduction in RMSE, 49% to 60% reduction in ME, 6% to 10% reduction in MAPE, and ≈15% reduction in PE (Table 3). The coefficient of persistence of the SARIMA model was also better (P=0.46) than the one registered by NM1 (P=0.23) and NM2 (P=0.03).

Monitoring of fisheries

During the hold-out period, observed landings remained entirely within the 95% prediction intervals of the SARIMA forecasts (Fig. 3), indicating that the observed forecast errors were within the range of values expected from random variability. Consequently the time series for meagre landings may be described as having remained in-control during the forecasting period. The PIs were symmetrical in the log-transformed scale (Fig. 3, A and C), but asymmetrical in the original scale of the data (Fig. 3, B and D). This pattern was expected from predictions of log-transformed data and indicates that sudden increases in monthly landings (positive forecast errors) are considered "more acceptable" than sudden decreases (negative forecast errors). Individual forecast errors that could have signaled an alarm ranged from 4.3 to 23.0 t (negative errors) to 13.5–68.3 t (positive errors). In relative terms, alarms would have been triggered by a higher than 54–75% drop, or by a higher than 105–238% increase, in monthly landings (Table 4). Compared to monthly PIs, multistep PIs were wider as a result of the increasing number of comparisons performed (Table 4). Even so, it is noticeable that such widening took place mainly on their upper boundary, and only a 12% increase was observed on their lower boundary.

Discussion

Interpretation of the models

Univariate SARIMA models based on landings do not have explanatory variables, but several studies have found the mathematical formulation in the models to correlate well with fish life history and fleet dynamics (Stergiou, 1990b; Stergiou et al., 1997; Lloret et al., 2000). In Europe, adult and juvenile meagre are thought to perform spring–summer migrations to major estuaries, remaining there until mid-summer (adults) and autumn (juveniles). These migrations are well known to local fishermen that actively target the meagre schools while they reside in estuarine grounds (Quéro and Vayne, 1987; Prista et al.[2]). Such interactions between fish migrations and directed fishing effort are likely the cause of the strong seasonal component of the SARIMA model because target effort tends to intensify the natural seasonal signal generated by fish migrating through a fishery (Lloret et al., 2000; Prista et al. 2008). In the case of central Portugal, such intensification is likely modulated at an interannual level by the expectations created for local fishermen by catches obtained in pre-

Table 4

Prediction intervals of meagre (*Argyrosomus regius*) landings (May 2007 to April 2008). Point forecasts ($\hat{x}_h$) and 95% boundaries of the single step ($PI_{ss,h}$) and multistep ($PI_{ms,h}$) prediction intervals are displayed. The prediction boundaries are given as absolute errors ($|e_h|$) and absolute percent errors (APE_h) in each monthly forecast step (h). In each cell, the left and right values represent the lower and upper boundaries, respectively.

			$PI_{ss,h}$		$PI_{ms,h}$	
Month	Step (h)	$\hat{x}_h$	$\|e_h\|$	APE_h	$\|e_h\|$	APE_h
May-07	1	36.4	19.7–38.4	54–105	19.7–38.4	54–105
Jun-07	2	26.6	16.2–35.8	61–135	17.5–45.0	66–169
Jul-07	3	26.1	16.9–40.5	65–155	18.8–58.0	72–222
Aug-07	4	25.8	17.3–43.7	67–169	19.6–68.8	76–266
Sep-07	5	31.4	23.0–68.3	73–217	25.9–120.0	82–382
Oct-07	6	23.0	17.3–54.7	75–238	19.5–103.6	85–451
Nov-07	7	19.0	14.3–45.2	75–238	16.2–89.7	85–472
Dec-07	8	6.0	4.5–14.2	75–238	5.1–29.4	86–491
Jan-08	9	5.7	4.3–13.5	75–238	4.9–28.8	86–509
Feb-08	10	6.1	4.6–14.6	75–238	5.3–32.2	87–525
Mar-08	11	6.5	4.9–15.5	75–238	5.7–35.1	87–539
Apr-08	12	16.3	12.3–38.7	75–238	14.2–89.9	87–553

ceding years (represented in the seasonal autoregressive term) and, at an intra-annual level, by random environmental and anthropogenic perturbations occurring on the fishery system (represented in the set of nonseasonal moving-average terms).

Model fit and forecast performance

The univariate SARIMA model presented a good fit to the short time series of meagre landings, explaining most of its variance and adequately modeling the seasonality and correlation structure of the data. Similar results were obtained in other studies of short and long time series: up to 68% (Lloret et al., 2000, series ≤64 months), 75% (Saila et al., 1980), 77% (Stergiou et al., 2003), 84–96% (Stergiou, 1989, 1991; Stergiou et al., 1997), and 93% (Pajuelo and Lorenzo, 1995). Taken together, these results indicate that SARIMA models should be adequate for data sets of monthly landings in general, and not just those with larger sample sizes. Bearing in mind that the minimum series length usually stated for SARIMA model fitting is 50 (Pankratz, 1983; Chatfield, 1996b), such generalized applicability may make SARIMA models particularly useful for fisheries with less reliable historical records or where only recently landings have been sampled.

In addition to a good fit, the SARIMA model also provided good short-term forecasts of meagre landings. The fact that all observed values were located within the predicted intervals of the model, and that naïve forecasts presented similarly lagged seasonality, indicates that the main forecast errors more likely resulted from natural variations in the timing of fish migrations and fishing seasons (Quéro and Vayne, 1987; Prista et al.[2]) or from specifics of SARIMA forecasts and accuracy measures (namely, correlation and APE sensitivity to near-zero observations) (Hyndman and Koehler, 2006; Box et al., 2008) than from model misspecification. At the annual level, the 15% error achieved is comparable to results previously obtained in larger data sets and well within the 10–20% range considered acceptable for market-planning and fisheries management (e.g., Mendelssohn, 1981; Pajuelo and Lorenzo, 1995; Hanson et al., 2006). Additionally, SARIMA forecasts clearly outperformed naïve forcasting in all accuracy metrics, underscoring the large benefits of using these models instead of simpler alternatives (Saila et al., 1980; Stergiou, 1991; Stergiou et al., 1997). Considered together with the overall good forecasting performance reported by Lloret et al. (2000) in their shorter series, these results build confidence that SARIMA models are useful for forecasting short time series of landings and thus can substantially contribute to the planning and management of many data-poor fisheries.

Use of SARIMA models to forecast landings of data-poor fisheries

SARIMA models forecast future landings by directly handling the seasonality and autocorrelation structure of the data and assuming the continuity over time of past time series behavior (Box et al., 2008). These models are known to be well adapted to forecast highly seasonal and autocorrelated data (Stergiou et al., 1997; Georgakarakos et al., 2006). Additionally, some authors have reported better SARIMA forecasting performances in fisheries with lower interannual variability, namely those that target benthic and demersal long-lived spe-

cies (Lloret et al., 2000). The data for meagre are autocorrelated and present a relatively stable seasonal pattern. Also, the meagre is long-lived and a targeted fish in central Portugal (Prista et al., 2009; Prista et al.[2]). Therefore, it is possible such features contributed to the good forecasts obtained from the SARIMA model. However, we note that the landings of many short-lived pelagic species and species with variable seasonal patterns have also been well forecasted with SARIMA models (Stergiou, 1990a; Stergiou et al., 1997; Georgakarakos et al., 2006; Tsitsika et al., 2007) and that the meagre landings also display substantial annual and monthly stochasticity Therefore, such general patterns should not be considered as strict limitations to SARIMA forecasting. More importantly, we note that SARIMA models can forecast well only if they have been adequately identified and estimated, and always under the assumption that the future is behaving like the past (Chatfield, 1993). Consequently, factors like data quality, presence of outliers, and model selection criteria are also very important for model performance. We discuss these next.

The quality of the input data for SARIMA models is determined mainly by the temporal stability of the statistical properties of the fisheries process and the consistency of its sampling over time. Consequently, although accuracy is required for some model applications (e.g., Zhou, 2003), data inaccuracies do not necessarily undermine SARIMA forecasts as long as factors such as fishing practices, regulatory measures, or data collection practices can be assumed to remain constant. When dealing with shorter series, a careful check whether these assumptions hold becomes particularly important because model identification and estimation are very dependent on the few observations available (Hyndman and Kostenko, 2007) and statistical techniques used to incorporate the effects of process changes in the models (e.g., Fogarty and Miller, 2004) are difficult to implement. In the case of meagre, the use of a short and recent time series better supported the assumption that data collection procedures, fishing techniques, fishery regulations, unreported landings, discards, and law enforcement practices did not change over time. In contrast, it is probable that these assumptions were not met in some less successful applications of the model to longer time series (e.g., Park, 1998).

Outliers are known to cause trouble in time series model identification, estimation, and forecasts—an effect that is amplified in shorter time series (Chatfield, 1993; Trívez and Nievas, 1998). The effects of outliers on forecasting performance are most disastrous when they occur near the forecasting origin because there they not only condition model structure and parameter estimates but are directly incorporated into the forecasts (Chatfield, 1993). The meagre data set presented no apparent outliers and this likely contributed to the good fit and forecasting performance achieved. If outliers were present, specific modeling techniques could have been used to estimate their influence, smooth them, or incorporate them into the model (e.g., Chen and Liu, 1993; Lloret et al., 2000). We note, however, that any outlier during the hold-out period could still have changed our perception of model performance, even if it did not compromise the overall adequacy of the SARIMA model to forecast the landings.

In time series analysis, adequate model specification is considered the most important driver of forecasting accuracy (Chatfield, 1996b). The difficulties of specifying an appropriate model increase for data sets with lower information content, such as those of highly variable short time series from more complex processes (Hyndman and Kostenko, 2007; Appendix 2). To date, fisheries applications of SARIMA models have essentially relied on Box-Jenkins (BJ) model selection procedures to specify a model, and models with $p \leq 2$ and $q \leq 2$ have generally been selected (e.g., Mendelssohn, 1981; Pajuelo and Lorenzo, 1995; Lloret et al., 2000). Compared to these, the model for meagre seems overparameterized, but we note that all of its parameters are statistically significant and that the low $RMSE_{forec.}$ to $RMSE_{fit}$ ratio indicates an excellent correspondence between fit and forecasting performances (Chatfield, 1996b). In fact, although reduced model parameterization is considered beneficial to accuracy in forecasting, the most important aspect of time series analysis is not the number of parameters, but the degree to which the model approximates the statistical process underlying the data and whether or not it achieves the forecasting objectives (Chatfield, 1996b; Burnham and Anderson, 2002). In the case of meagre, had Box-Jenkins procedures been used, the selected models would be simpler and would still adequately fit the data: $(1,0,0)\times(1,1,0)_{12}$ or $(0,0,1)\times(0,1,1)_{12}$. However, they would have performed worse than our AIC_c-selected model in most performance metrics (RMSE: 0.245 and 0.302, APE: 1.7–92.7% and 20.6–72.4%, MAPE: 44.1% and 44.0%, PE: 13.7% and 31.7%, respectively). These results show the impact that different model selection techniques may have on forecasting performance with SARIMA models and stress the importance of considering objective data-driven criteria like AIC_c for circumventing the subjectivities of model selection in smaller data sets (Hurvich and Tsai, 1989; Burnham and Anderson, 2002).

Conclusions

Use of SARIMA models in monitoring fisheries

From a strictly forecasting perspective, SARIMA models have often been criticized for the excessive reliance on past time series behavior and their difficulty in predicting future structural changes (Georgakarakos et al., 2002; Koutroumanidis et al., 2006). Our results show that these drawbacks can become major advantages when SARIMA models are used for monitoring fisheries. At present, none of the European meagre fisheries is subjected to routine analytical assessment. By fitting

SARIMA models to already available landings data we were able to carry out a first baseline evaluation of one such fishery, using limited funds and minimal time.

Our study provides a first example of how SARIMA models can be used to monitor data-poor fisheries. In the case of meagre, the data displayed no trend and the 95% SARIMA prediction intervals fully encompassed all monthly landings, thus indicating a stable "in-control" fishery. Note that by stating this, at no point do we suggest that the meagre fishery is sustainable long-term because landings do not necessarily reflect stock abundance and our study was limited in time. We suggest only that, since no motive for alarm exists in landings data, and because funds, personnel, and expertise are limited at the national level, attention should be allocated to fisheries that, contrary to the meagre, display decreasing trends or out-of-control situations. Similar types of pragmatic reasoning are generally of great help to fisheries managers handling multiple data-poor fishery scenarios because they help them prioritize management actions for the subset of "problematic" resources in a statistically sound way (Scandol, 2003, 2005).

Underlying the usefulness of SARIMA models in monitoring the meagre fishery and other data-poor fisheries is the use of prediction intervals as reference points to signal alarming trends or sudden level shifts in the fisheries process (Caddy, 1999; Scandol, 2003; Mesnil and Petitgas, 2009). SARIMA PIs have been previously reported in the literature (Table 1), but their use in monitoring was not explored or formalized. These intervals are currently the focus of much statistical research on how to deal with their tendency toward "over-optimism," i.e., the fact that nominal 95% prediction intervals generally contain less than 95% of future observations (Chatfield, 1993). Fortunately, from a fisheries conservation perspective such over-optimism does not constitute a major problem because narrower PIs will be more sensitive to changes in the fisheries process.

Statistical process control (SPC) monitoring of univariate fisheries indicators has become the focus of increased research attention (Scandol, 2003, 2005; Mesnil and Petitgas, 2009; Petitgas, 2009; ICES[1]). The use of SARIMA PIs is similar to that of SPC control-charts, which makes them interesting candidates for the simultaneous monitoring of multiple fisheries and fisheries indicators (Caddy, 1999; Scandol, 2005; Petitgas, 2009). For such cases, SARIMA PIs offer the advantage of being model-based and do not require extensive historical reference data. They are also free from the assumption of statistical independence that frequently troubles the estimation of SPC detection limits (Mesnil and Petitgas, 2009). The simulation framework proposed by Scandol (2003, 2005) for SPC charts provides a means whereby SARIMA PIs can be calibrated toward specific detection rates and management goals. Such calibration was beyond the objectives our study but constitutes an interesting research route for those in charge of more holistic fisheries management.

SARIMA models in assessments of data-poor fisheries

Formal stock assessment has traditionally been considered as the starting point of any fisheries assessment (Mahon, 1997; Berkes et al., 2001). Such an approach is highly desirable but will not be implemented easily, nor quickly, in the many existing data-poor fisheries (Vasconcellos and Cochrane, 2005). In fact, NRC (1998) estimated that 16% of U.S. stocks are not subjected to assessment; and the European Environmental Agency (EEA, 2005) estimated that, depending on the region considered, 20–90% of commercial stocks exploited in the Northeast Atlantic and Mediterranean are not routinely assessed. These figures are much worse in developing countries and when discard and bycatch species are included in the estimates (Vasconcellos and Cochrane, 2005). Addressing such situations requires increased focus on alternative stock indicators and assessment methods that can be used to monitor more fisheries by using available (or easily obtainable) data, funds, and human resources (e.g., Caddy, 1999; Scandol, 2005; Mesnil and Petitgas, 2009; OSPAR, 2010; ICES[1]). Univariate time series models fitted to landings data may be, for some time longer, the best possible approach to extend assessment and management coverage to many of these unassessed resources.

SARIMA modeling and process-control schemes do not constitute alternatives to analytical stock assessment models. Rather, whenever possible, they should be seen as statistical tools to support expert judgment, funding allocation, and management decisions in the most data-limited and assessment-limited settings (Scandol, 2003; 2005). SARIMA modeling and model-based monitoring have a range of characteristics that make them worthy of future exploration in data-poor contexts. Among these are their appropriateness to numerous resources and variables, their strong statistical background and ecological plausibility, their good forecasting performance and easy-to-estimate detection limits, and their applicability to both long and short time series. Furthermore, SARIMA models can also be used to model the nonspecific groupings that dominate many landings data sets, or can be upgraded if multivariate data become available (Stergiou et al., 1997; Vasconcellos and Cochrane, 2005). Finally, the availability of SARIMA models in open-source software packages and their routine use in sectors other than fisheries (e.g., sales, economics, engineering) (Brockwell and Davis, 2002; Box et al., 2008) may be decisive advantages in budget-limited and expertise-limited countries.

Acknowledgments

Funding for this work was provided by a "Fundação para a Ciência e a Tecnologia" (FCT) grant BD/12550/2003 to N. Prista and by research project CORV (DGPA–Mare: FEDER–22–05–01–FDR–00036). We thank Direcção Geral das Pescas e Aquicultura (DGPA) for providing the meagre data set. We thank D. S. Stoffer and D. R.

Anderson for suggestions on the use of the "arima" function and AIC_c model selection, respectively. We further thank M. F. Lane, J. L. Costa, J. J. Schaffler, and J. R. Ashford for commenting on earlier drafts of this manuscript. We thank the three anonymous reviewers for their constructive comments on this manuscript.

Literature cited

Akaike, H.
1974. A new look at the statistical model identification. IEEE T. Autom. Contr. 19:716–723.

Berkes, F., R. Mahon, P. McConney, R. Pollnac, and R. Pomeroy.
2001. Managing small-scale fisheries: alternative directions and methods, 320 p. IDRC Books, Ottawa, Canada.

Box, G., and D. Cox.
1964. An analysis of transformations. J. R. Stat. Soc. Ser. B 26:211–243.

Box, G. E. P., G. M. Jenkins, and G. C. Reinsel.
2008. Time series: forecasting and control, 4th ed., 784 p. John Wiley & Sons, Hoboken, NJ.

Brockwell, P., and R. Davis.
2002. Introduction to time series and forecasting, 2nd ed., 469 p. Springer, New York.

Burnham, K. P., and D. R. Anderson.
2002. Model selection and multi-model inference: a practical information-theoretic approach, 2nd ed., 488 p. Springer, New York.

Caddy, J. F.
1999. Deciding on precautionary management measures for a stock based on a suite of limit reference points (LRPs) as a basis for a multi-LRP harvest law. Northwest Atl. Fish. Org. Sci. Counc. Stud. 32:55–68.

Campbell, A., D. J. Noakes, and R. W. Elner.
1991. Temperature and lobster, *Homarus americanus*, yield relationships. Can. J. Fish. Aquat. Sci. 48:2073–2082.

Chan, W., S. Cheung, and K. Wu.
2004. Multiple forecasts with autoregressive time series models: case studies. Math. Comput. Simul. 64:421–430.

Chatfield, C.
1993. Calculating interval forecasts. J. Bus. Econ. Stat. 11:121–135.
1996a. The analysis of time series: an introduction, 5th ed., 283 p. Chapman & Hall/CRC, Boca Raton, FL.
1996b. Model uncertainty and forecast accuracy. J. Forecast. 15:495–508.

Chen, C., and L. -M. Liu.
1993. Joint estimation of model parameters and outlier effects in time series. J. Am. Stat. Assoc. 88:284–297.

Czerwinski, I. A., J. C. Gutiérrez-Estrada, and J. A. Hernando-Casal.
2007. Short-term forecasting of halibut CPUE: linear and non-linear univariate approaches. Fish. Res. 86:120–128.

De Gooijer, J. G., B. Abraham, A. Gould, and L. Robinson.
1985. Methods for determining the order of an autoregressive-moving average process: a survey. Int. Stat. Rev. 53:301–329.

De Gooijer, J. G., and R. J. Hyndman.
2006. 25 years of time series forecasting. Int. J. Forecast. 22:442–473.

EEA (European Environmental Agency).
2005. The European environment—state and outlook 2005, 570 p. European Environmental Agency, Copenhagen, Denmark.

Fogarty, M. J.
1988. Time series models of the Maine lobster fishery: the effect of temperature. Can. J. Fish. Aquat. Sci. 45:1145–1153.

Fogarty, M. J., and T. J. Miller.
2004. Impact of a change in reporting systems in the Maryland blue crab fishery. Fish. Res. 68:37–43.

Georgakarakos, S., J. Haralabous, V. Valavanis, C. Arvanitidis, D. Koutsoubas, and A. Kapantagakis.
2002. Loliginid and ommastrephid stock prediction in Greek waters using time series analysis techniques. Bull. Mar. Sci. 71:269–287.

Georgakarakos, S., D. Koutsoubas, and V. Valavanis.
2006. Time series analysis and forecasting techniques applied on loliginid and ommastrephid landings in Greek waters. Fish. Res. 78:55–71.

Graves, S.
2008. Companion to Tsay (2005) analysis of financial time series. R package vers. 0.10-12. URL: http://CRAN.R-project.org., accessed October 2008.

Hanson, P. J., D. S. Vaughan, and S. Narayan.
2006. Forecasting annual harvests of Atlantic and Gulf menhaden. N. Am. J. Fish. Manag. 26:753–764.

Hare, S. R., and R. C. Francis.
1994. Climate change and salmon production in the Northeast Pacific Ocean. *In* Climate change and northern fish populations (R. J. Beamish, ed.). Can. Spec. Publ. Fish. Aquat. Sci. 121:357–372.

Harvey, A. C.
1989. Forecasting, structural time series models and the Kalman filter, 572 p. Cambridge Univ. Press, Cambridge.

Hurvich, C. M., and C. -L. Tsai.
1989. Regression and time series model selection in small samples. Biometrika 76:297–307.

Hyndman, R. J., and A. B. Koehler.
2006. Another look at measures of forecast accuracy. Int. J. Forecast. 22:679–688.

Hyndman, R. J., and A. V. Kostenko.
2007. Minimum sample size requirements for seasonal forecasting models. Foresight 6:12–15.

Jarque, C., and A. Bera.
1987. Efficient tests for normality, homoscedascity and serial independence of regression residuals. Econ. Lett. 6:255–259.

Jeffries, P., A. Keller, and S. Hale.
1989. Predicting winter flounder (*Pseudopleuronectes americanus*) catches by time series analysis. Can. J. Fish. Aquat. Sci. 46:650–659.

Kitanidis, P. K., and R. L. Bras.
1980. Real-time forecasting with a conceptual hydrologic model 2: applications and results. Water Resour. Res. 16:1034–1044.

Koutroumanidis, T., L. Iliadis, and G. K. Sylaios.
2006. Time-series modeling of fishery landings using ARIMA models and fuzzy expected intervals software. Environ. Model. Softw. 21:1711–1721.

Ljung, G., and G. Box.
1978. On a measure of lack of fit in time series models. Biometrika 65:297–303.

Lloret, J., J. Lleonart, and I. Solé.
2000. Time series modeling of landings in Northwest Mediterranean Sea. ICES J. Mar. Sci. 57:171–184.

Mahon, R.
1997. Does fisheries science serve the needs of managers of small stocks in developing countries? Can. J. Fish. Aquat. Sci. 54:2207–2213.
Mendelssohn, R.
1981. Using Box-Jenkins models to forecast fishery dynamics: identification, estimation, and checking. Fish. Bull. 78:887–896.
Mesnil, B., and P. Petitgas.
2009. Detection of changes in time-series of indicators using CUSUM control charts. Aquat. Living Resour. 22:187–192.
Molinet, R., M. T. Badaracco, and J. J. Salaya.
1991. Time series analysis for the shrimp and snapper fisheries in Golfo Triste, Venezuela. Sci. Mar. 55:427–437.
Morales-Nin, B., A. Grau, S. Pérez-Mayol, and M. M. Gil.
2010. Marking otoliths, age validation and growth of *Argyrosomus regius* juveniles (Sciaenidae). Fish. Res, 106:76–80.
Noakes, D. J., D. W. Welch, M. Henderson, and E. Mansfield.
1990. A comparison of preseason forecasting methods for returns of two British Columbia sockeye salmon stocks. N. Am. J. Fish. Manag. 10:46–57.
NRC (National Research Council).
1998. Improving fish stock assessments, 177 p. National Academy Press, Washington, D.C.
OSPAR (Oslo and Paris Commission).
2010. Quality status report 2010, 176 p. OSPAR Commission, London, UK.
Pajuelo, J. G., and J. M. Lorenzo.
1995. Analysis and forecasting of the demersal fishery of the Canary Islands using an ARIMA model. Sci. Mar. 59:155–164.
Pankratz, A.
1983. Forecasting with univariate Box-Jenkins models: concepts and cases, 576 p. John Wiley & Sons, Hoboken, NJ.
Park, H. -H.
1998. Analysis and prediction of walleye pollock (*Theragra chalcogramma*) landings in Korea by time series analysis. Fish. Res. 38:1–7.
Petitgas, P.
2009. The CUSUM out-of-control table to monitor changes in fish stock status using many indicators. Aquat. Living Resour. 22:201–206.
Pierce, G. J., and P. R. Boyle.
2003. Empirical modelling of interannual trends in abundance of squid (*Loligo forbesi* in Scottish waters. Fish. Res. 59:305–326.
Prista, N., J. L. Costa, M. J. Costa, and C. M. Jones.
2009. Age determination in meagre *Argyrosomus regius*. Relat. Ciênt. Téc. Inst. Invest. Pescas Mar: Série Digital 49:1–54. URL: http://ipimar-inrb.ipimar.pt/pdf/Reln49.pdf, accessed September 2010.
Quéméner, L.
2002. Le maigre commun (*Argyrosomus regius*)—biologie, pêche, marché et potentiel aquacole, 32 p. IFREMER, Plouzané, France. [In French.]
Quéro, J.-C., and J. -J. Vayne.
1987. Le maigre, *Argyrosomus regius* (Asso, 1801) (Pisces, Perciformes, Sciaenidae) du Golfe de Gascogne et des eaux plus septentrionales. Rev. Trav. Inst. Pêches Marit. 49:35–66 [In French.]
R Development Core Team.
2007. R: A language and environment for statistical computing. R Foundation for Statistical Computing. URL: http://www.R-project.org, accessed August 2007.
Rothschild, B. J., S. G. Smith, and H. Li.
1996. The application of time series analysis to fisheries population assessment and modeling. *In* Stock assessment: quantitative methods and applications for small-scale fisheries (V. F. Gallucci, S. B. Saila, D. J. Gustafson, and B. J. Rothschild, eds), p. 354–402. CRC Press, Boca Raton, FL.
Saila, S. B., M. Wigbout, and R. J. Lermit.
1980. Comparison of some time series models for the analysis of fisheries data. ICES J. Mar. Sci. 39:44–52.
Scandol, J.
2003. Use of cumulative sum (CUSUM) control charts of landed catch in the management of fisheries. Fish. Res. 64:19–36.
2005. Use of quality control methods to monitor the status of fish stocks. *In* Fisheries assessment and management in data-limited situations (G. H. Kruse, V. F. Gallucci, D. E. Hay, R. I. Perry, R. M. Peterman, T. C. Shirley, P. D. Spencer, B. Wilson, and D. Woodby, eds.), p. 213–233. Alaska Sea Grant College Program, Univ. Alaska, Fairbanks, AK.
Shapiro, S., M. Wilk, and H. Chen.
1968. A comparative study of various tests for normality. J. Am. Stat. Assoc. 63:1343–1372.
Shumway, R. H., and D. S. Stoffer.
2006. Time series analysis and its applications: with R examples, 2nd ed., 575 p. Springer, New York.
Stergiou, K. I.
1989. Modelling and forecasting the fishery for pilchard *Sardina pilchardus* in Greek waters using ARIMA time-series models. ICES J. Mar. Sci. 46:16–23.
1990a. A seasonal autoregressive model of the anchovy *Engraulis encrasicolus* fishery in the eastern Mediterranean. Fish. Bull. 88:411–414.
1990b. Prediction of the Mullidae fishery in the eastern Mediterranean 24 months in advance. Fish. Res. 9:67–74.
1991. Short-term fisheries forecasting: a comparison of smoothing, ARIMA and regression techniques. J. Appl. Ichthyol. 7:193–204.
Stergiou, K. I., and E. D. Christou.
1996. Modelling and forecasting annual fisheries catches: comparison of regression, univariate and multivariate time series methods. Fish. Res. 25:105–138.
Stergiou, K. I., E. D. Christou, and G. Petrakis.
1997. Modelling and forecasting monthly fisheries catches: comparison of regression, univariate and multivariate time series methods. Fish. Res. 29:55–95.
Stergiou, K. I., G. Tserpes, and P. Peristeraki.
2003. Modelling and forecasting monthly swordfish catches in the Eastern Mediterranean. Sci. Mar. 67:283–290.
Trapletti, A., and K. Hornik.
2007. Tseries: time series analysis and computational finance. R package vers. 0.10-12. URL: http://CRAN.R-project.org, accessed December 2007.
Trívez, F. J., and J. Nievas.
1998. Analyzing the effects of level shifts and temporary changes on the identification of ARIMA models. J. Appl. Stat. 25:409–424.
Tsai, C. -F., and A. -L. Chai.
1992. Short-term forecasting of the striped bass *Morone saxatilis* commercial harvest in the Maryland portion of Chesapeake Bay. Fish. Res. 15:67–82.

Tsitsika, E. V., C. D. Maravelias, and J. Haralabous.
2007. Modeling and forecasting pelagic fish production using univariate and multivariate ARIMA models. Fish. Sci. 73:979–988.

Vasconcellos, M., and K. Cochrane.
2005. Overview of world status of data-limited fisheries: inferences from landing statistics. *In* Fisheries assessment and management in data-limited situations (G. H. Kruse, V. F. Gallucci, D. E. Hay, R. I. Perry, R. M. Peterman, T. C. Shirley, P. D. Spencer, B. Wilson, and D. Woodby, eds.), p. 1–20. Alaska Sea Grant College Program, Univ. Alaska, Fairbanks, AK.

Worm, K., R. Hilborn, J. K. Baum, T. A. Branch, J. S. Collie, C. Costello, M. J. Fogarty, E. A. Fulton, J. A. Hutchings, S. Jennings, O. P. Jensen, H. K. Lotze, P. M. Mace, T. R. McClanahan, C. Minto, S. R. Palumbi, A. M. Parma, D. Ricard, A. A. Rosenberg, R. Watson, and D. Zeller.
2009. Rebuilding global fisheries. Science 325:578–585.

Zhou, S.
2003. Application of artificial neural networks for forecasting salmon escapement. N. Am. J. Fish. Manag. 23:48–59.

Appendix 1

ARIMA and SARIMA models

An extensive review of ARIMA and SARIMA models can be found in, e.g., Box et al. (2008) and Brockwell and Davis (2002). A mean-centered time series x_t can be modeled as an ARIMA(p,d,q), where p, d, q are nonnegative integers, if it can be adequately fitted with the process equation

$$\phi(B)(1-B)^d X_t = \theta(B) Z_t ,$$

where for a time interval T, $(X_t)_{t\in T}$ is a sequence of random variables, B is a backshift differencing operator $B^h X_t = X_{t-h}$ (h nonnegative integer), $(1-B)^d X_t = \nabla_1^d X_t$ is stationary, $\phi(B)$ and $\theta(B)$ are linear filters defined as $\phi(B)=1-\phi_1 B-\phi_2 B^2-\ldots-\phi_p B^p$ and $\theta(B)=1+\theta_1 B+\theta_2 B^2+\ldots+\theta_q B^q$ and $(Z_t)_{t\in T}$ is a sequence of uncorrelated random variables with zero mean and variance σ^2 (termed white noise). In ARIMA models the orders p, q, and d define the structure of the model, by specifying the autoregressive (AR) and moving average (MA) components of an autoregressive–moving average process (ARMA[p,q]). d is the degree of differencing ($d \geq 1$) required for X_t to become stationary. This differencing involves the loss of d observations in the series.

The SARIMA $(p,d,q)\times(P,D,Q)_S$ models, where P, D, Q, and S are nonnegative integers, extend the modeling capabilities of ARIMA(p,d,q) models to seasonal processes. The SARIMA process equation is given by

$$\phi(B)\Phi(B^S)(1-B)^d(1-B^S)^D X_t = \theta(B)\Theta(B^S) Z_t ,$$

where X_t, Z_t, $\phi(B)$ and $\theta(B)$ are defined as above, $(1-B)^d (1-B^S)^D X_t = \nabla_1^d \nabla_S^D X_t$ is stationary, and $\Phi(B^S)$ and $\Theta(B^S)$ are seasonal linear filters defined as $\Phi(B^S)=1-\Phi_1 B^S-\Phi_2 B^{2S}-\ldots-\Phi_P B^{PS}$ and $\Theta(B^S)=1+\Theta_1 B^S+\Theta_2 B^{2S}+\ldots+\Theta_Q B^{QS}$. In SARIMA, P defines the seasonal autoregressive component of the model (SAR) and Q the seasonal moving average component of the model (SMA). S represents the seasonal period (e.g., 12 months) and D is the degree of seasonal differencing. Together, S and D account for seasonal nonstationarity in X_t through a data transformation that involves the loss of DS observations in the series.

Appendix 2

Selection of ARIMA and SARIMA models

Box-Jenkins approach ARIMA and SARIMA models are usually fitted by using a sequence of three general steps collectively known as the Box-Jenkins (BJ) method: 1) identification of the model; 2) estimation of the model; and 3) a diagnostic check of the model (Box et al., 2008). In the identification stage, a model structure $(p,d,q)\times(P,D,Q)_S$ is selected by comparisons of sample ACF and PACF with theoretical ACF/PACF profiles of AR, MA and ARMA processes. In the estimation stage, the model structure is fitted to the data and its parameters are estimated, generally by using conditional sum of squares or maximum likelihood methods. In the diagnostic check stage, the goodness-of-fit and assumptions for the model are evaluated and, if necessary, the BJ procedure is repeated until a suitable model is found. This model is then used to forecast future values (Box et al., 2008). In-depth theoretical coverage of the BJ method is given in Box et al. (2008) and extensive practical applications are provided in Pankratz (1983) and Brockwell and Davis (2002).

The model identification stage of the BJ method is widely considered its most subjective step because it relies primarily on graphical interpretations of ACF/PACF estimates obtained from a single sample. This interpretation requires substantial analytical expertise and knowledge of the time series (both of which are problematic in data-poor scenarios) and is troublesome when complex ARMA processes have generated the data (Harvey, 1989; Shumway and Stoffer, 2006). Furthermore, it can also be confounded by existing correlations among ACF/PACF estimates (Box et al., 2008). The minimum sample size generally advised for SARIMA model fitting is 50 observations (Pankratz, 1983; Chatfield, 1996b), but see Hyndman and Kostenko (2007) for an absolute lower limit. When sample size is large (e.g., $n \geq 100$), ACF/PACF estimates have lower variability and are more likely to approximate the theoretical ACF/PACF estimates of the underlying process. In such cases, less subjectivity exists in identification of the model. However, when sample size is small, the interpretation of ACF/PACF patterns becomes increasingly confounded by the large variance of the sample estimates, particularly at larger lags ($\geq n/4$) (Box et al., 2008). This variability substantially increases the subjectivity of the model identification

stage of the BJ method and is the main issue to be dealt with when analyzing shorter time series.

AIC approach To circumvent the subjectivity of the identification of the model with the BJ method and to aid in the determination of the final orders of the ARMA processes a wide variety of model selection criteria have been developed (De Gooijer et al., 1985). The most frequently used are the Akaike information criteria (AIC) (Akaike, 1974) and the small-sample, bias-corrected equivalent, AIC_c (Hurvich and Tsai, 1989). Contrary to the Box-Jenkins method, AIC/AIC_c selection of a model involves the a priori estimation by maximum likelihood methods of a set of model structures (here termed the candidate set). This estimation is followed by the determination of the AIC/AIC_c values for each individual model. The model with minimum AIC/AIC_c is then selected as the model that is closest to the statistical process "generating" the data. In SARIMA models, AIC is calculated as

$$AIC=-2\ln(L)+2r\ ,$$

where $\ln(L)$ is the log-likelihood of the model, $r=p+q+P+Q+1$, and the AIC_c is given by

$$AIC_c=-2\ln(L)+2r+2r(r+1)/(n-r-1)\ ,$$

where $n=N-DS-d$ is the number observations used to fit the model. AIC/AIC_c constitute objective methods to achieve model parsimony through a trade-off between the variance explained by the model and penalty terms caused by excessive model parameters. Both of them are well founded in the principles of information and likelihood theory and have been applied extensively in time series, fisheries, and ecological literature (e.g., Brockwell and Davis, 2002; Burnham and Anderson, 2002; Hanson et al., 2006). Burnham and Anderson (2002) suggest AIC_c is used when $n/r \leq 40$, which prompts the consideration of this small-sample, bias-corrected version of AIC in studies of short time series.

Season- and depth-dependent variability of a demersal fish assemblage in a large fjord estuary (Puget Sound, Washington)

Jonathan C. P. Reum (contact author)

Timothy E. Essington

Email address for contact author: reumj@u.washington.edu

School of Aquatic and Fishery Sciences
Box 355020
University of Washington
Seattle, Washington 98195

Abstract—Fjord estuaries are common along the northeast Pacific coastline, but little information is available on fish assemblage structure and its spatiotemporal variability. Here, we examined changes in diversity metrics, species biomasses, and biomass spectra (the distribution of biomass across body size classes) over three seasons (fall, winter, summer) and at multiple depths (20 to 160 m) in Puget Sound, Washington, a deep and highly urbanized fjord estuary on the U.S. west coast. Our results indicate that this fish assemblage is dominated by cartilaginous species (spotted ratfish [*Hydrolagus colliei*] and spiny dogfish [*Squalus acanthias*]) and therefore differs fundamentally from fish assemblages found in shallower estuaries in the northeast Pacific. Diversity was greatest in shallow waters (<40 m), where the assemblage was composed primarily of flatfishes and sculpins, and lowest in deep waters (>80 m) that are more common in Puget Sound and that are dominated by spotted ratfish and seasonally (fall and summer) by spiny dogfish. Strong depth-dependent variation in the demersal fish assemblage may be a general feature of deep fjord estuaries and indicates pronounced spatial variability in the food web. Future comparisons with less impacted fjords may offer insight into whether cartilaginous species naturally dominate these systems or only do so under conditions related to human-caused ecosystem degradation. Information on species distributions is critical for marine spatial planning and for modeling energy flows in coastal food webs. The data presented here will aid these endeavors and highlight areas for future research in this important yet understudied system.

Manuscript submitted 6 July 2010.
Manuscript accepted 3 February 2011.
Fish. Bull. 109:186–197 (2011).

The views and opinions expressed or implied in this article are those of the author (or authors) and do not necessarily reflect the position of the National Marine Fisheries Service, NOAA.

Estuaries are highly productive habitats that support a diversity of species, but have suffered because of growing human demands (Kennish, 2002; Lotze et al., 2006). Recognition of declining fish, marine mammal, and seabird populations and the need to consider the multiplicity of causative agents for these declines and their ecological consequences have prompted an interest in adopting ecosystem-based approaches for management, whereby knowledge of ecological interactions, such as trophodynamic control and competition is used to inform policy decisions (Pikitch et al., 2004). Our ability to implement more holistic management approaches, however, can be limited by a lack of basic information on the distribution and abundance of species that a system comprises and how these vary over time and space. This information is particularly lacking for fjord estuaries that are common features along the northeast Pacific coastline. Fjord estuaries differ from other estuaries by possessing a deep inner basin that is separated from continental shelf waters by a shallow sill near the mouth of the estuary. Although some of these ecosystems are remote and show little sign of degradation, commercial and recreational fishing, aquaculture, shoreline development, pollution, and logging are degrading a growing number of them.

Puget Sound, WA, is the southernmost fjord estuary in the northeast Pacific and supports major urban centers with a combined human population of 4 million (PSAT[1]). Over the past 150 years Puget Sound has been commercially fished and subject to increasing rates of habitat loss, eutrophication, pollution, and, more recently, acidification. Presently, commercial fishing for groundfish is not permitted, but some species (e.g., *Sebastes* spp., lingcod [*Ophiodon elongates*]) are targeted by recreational fishermen. Although an ecosystem-based approach is clearly relevant for Puget Sound, there is a paucity of published information on how the demersal fishes of Puget Sound use different habitats, and thus a need for studies on assemblage structure. Identifying major patterns of assemblage variability along different habitat gradients has practical implications not only for modeling energy flows, but for devising monitoring schemes that can adequately quantify interannual changes in population abundance (Greenstreet et al., 1997; Thompson and Mapstone, 2002). Although project and agency reports provide some descriptive analyses on Puget Sound fish communities, peer-reviewed literature on demersal fish distributions from other deep fjords in the northeastern Pacific are rare.

[1] PSAT (Puget Sound Action Team). 2007. State of the Sound. 2007. Publication no. PSAT 07-01, 96 p. Office of the Governor, Olympia, State of Washington. [Available at: http://www.psp.wa.gov/documents.php, accessed February 2011.)

Here we evaluated depth- and season-related changes in the demersal fish assemblage structure over a 10-month period in the Central Basin—the largest and deepest of four subbasins within Puget Sound. We anticipated strong spatial gradients in community composition on the basis of typical patterns of demersal fish assemblages in other ecosystems (e.g., Mueter and Norcross, 1999) and also hypothesized that species might exhibit seasonal patterns of habitat use that would be reflected in community structure. First, we evaluated differences in assemblage diversity metrics across depths and seasons. Second, we performed taxon-based multivariate analyses on the fish assemblage and explicitly tested whether assemblage structure was related to season and depth. Finally, we performed a size-based analysis, examining variability in the distribution of biomass across body size classes (biomass spectra) to identify whether the prevalence of small-body or large-body individuals also changed with depth and season. The value of examining biomass spectra is grounded in the observation that trophic level generally increases with body size in aquatic systems (Kerr, 1974; Jennings et al., 2001), and the relative importance of different body size classes to the overall flow of energy in the food web can be revealed by biomass spectra (Haedrich and Merrett, 1992). The patterns revealed by each of these approaches were subsequently compared.

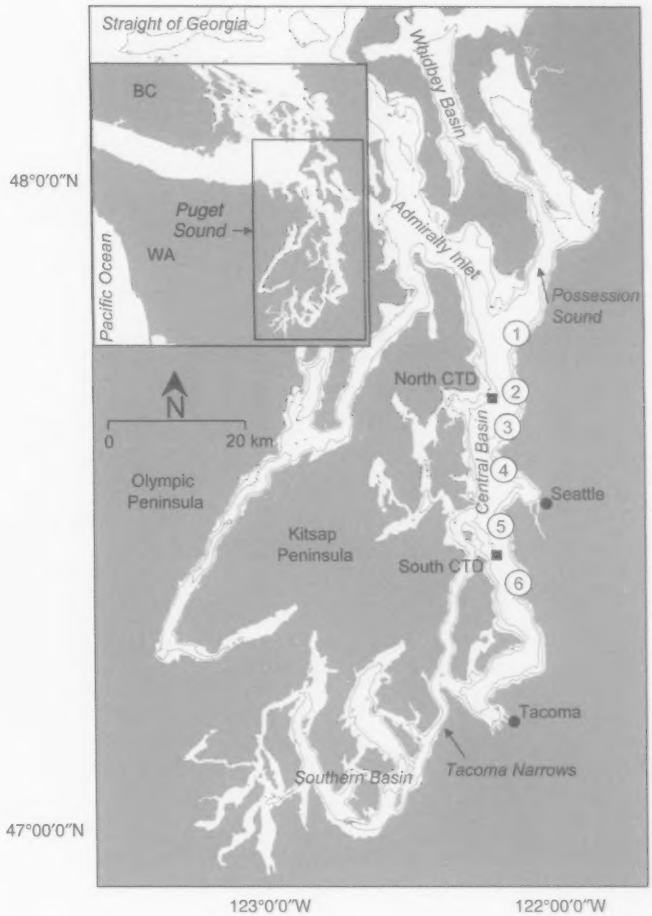

Figure 1

Demersal fish assemblages were sampled with bottom trawls at six stations (indicated by the circled numbers) in the Central Basin of Puget Sound, WA. At each station, depths at 20, 40, 80, and 160 m were sampled. Sampling occurred in October 2004 and March and July 2005. Isobaths at 40 and 160 m are indicated. Sampling sites where conductivity-temperature-density instruments (CTDs) were deployed by the King County Puget Sound Marine Monitoring Program to determine temperature and salinity are denoted by square symbols.

Materials and methods

Data collection

The demersal fish assemblage was sampled by bottom trawl during 18–22 October 2004, 10–14 March, and 7–11 July 2005 along the eastern coastline of the largest subbasin within Puget Sound, the Central Basin (Fig. 1). The Central Basin is separated from the Strait of Georgia and Whidbey Basin by a sill (~60 m depth) at Admiralty Inlet and by Possession Sound to the north, respectively, and from Southern Basin by a sill at Tacoma Narrows (Fig. 1). We identified six sampling stations located in low-relief regions and amenable to bottom trawls spaced 5–10 km apart (high relief, hard bottom habitats are not common in this region of Puget Sound). At each station, we sampled four sites at depths of 20, 40, 80, and 160 m. In October we sampled stations 1–4, sampling all four depths. To increase the spatial coverage of the survey in March, we visited stations 1, and 3–6, but only sampled at 40 and 160 m. Lastly, in July we visited stations 1, 3, 4, 5, and 6, and sampled all four depths. In this manner we were able to increase the spatial coverage of the survey while maintaining overlap with the previous season. We modified our survey when necessary because of limitations in boat and crew time and because of the absence of prior information on which we could base our survey.

Sampling was performed during daylight hours with a 400-mesh Eastern otter bottom trawl lined with 3.2-cm mesh in the codend. The net had a head rope and foot rope of 21.4 m and 28.7 m, respectively, and the gear was towed across the seafloor for 400—500 m at 2.5 knots. Catch was sorted to species, weighed, enumerated, and subsampled for length composition of fish. Catch was standardized to biomass density (g/m^2) by using measurements of the area swept by the net. The area

swept was calculated by multiplying the tow distance by the net opening width, the latter calculated from an empirical relationship between depth and net width.

To compare differences in salinity and temperature among depths, months, and latitude we obtained data from the King County Puget Sound Marine Monitoring Program which monthly monitors water quality at two stations in the northern and southern regions of the survey area (Fig. 1). Data were collected with a conductivity-temperature-density instrument (CTD) consisting of an SBE 3 temperature sensor, SBE 4 conductivity sensor, and SBE 29 pressure sensor (SeaBird Electroics Inc., Bellevue, WA) and were binned at 0.5-m intervals. CTD sampling occurred within 10 days of trawl sampling.

Statistical analysis

More than 200 species of fish have been documented in Puget Sound, but many of these are rare or sparsely distributed such that an intensive sampling effort would be required to sufficiently describe the distribution patterns of all species. Instead, we focused our research on the commonly occurring species that accounted for the bulk of the demersal fish biomass and therefore represent the most significant fish in the food web. To calculate diversity metrics for comparisons, rare species that occurred in fewer than 10% of the sampled trawls were removed from the data set; the exclusion of rare species permitted a coarse-scale evaluation of differences in the common components of the assemblage. Differences in species richness (N) and diversity (Shannon-Wiener diversity index, H'; Krebs, 1989) across depths and among months were examined by using two-way analysis of variance (ANOVA). Standard two-way ANOVA requires that treatment levels be fully replicated across both main factors (in this case, depth and month). Because we lacked samples from depths of 20 m and 40 m in March, we performed two sets of tests. In the first set we included samples from all four depths, but only from October and July. In the second, we included samples from all three months, but only from 40 and 160 m. Initial examination of the data indicated normal or near-normal distributions, therefore data transformations were not called for because ANOVA is robust to minor departures from normality (Zar, 1984). In instances where either of the main factors was significant, Tukey's honestly significant difference (HSD) tests were used to identify which depth and month levels differed.

In the above analysis, both N and H' are simple and widely used measures of diversity that describe the number or relative biomass of species at each sample but ignore similarity in species composition among samples. In contrast, canonical correspondence analyses (CCA) are used to explicitly evaluate multivariate patterns of species biomass among sample sites. Essentially, CCA is a multivariate extension of multiple regression where species and sites are simultaneously ordinated in a manner that maximizes the variance related to a set of explanatory (constraining) variables (ter Braak, 1986). As with multiple regression, the inertia, or variance explained, by a given model can be determined and the significance of the explanatory variable tested (Legendre and Legendre, 1998). In instances where two or more sets of explanatory variables are of interest (in this case, month and depth), partial CCA can be employed to isolate the effect of each variable (Legendre and Legendre, 1998). The technique is analogous to partial regression, where the response variable (species biomass) is first constrained by one of the explanatory variables (either month or depth, expressed as factors with dummy variable coding). The resulting residuals are then constrained by the second explanatory variable. Effectively, the first explanatory variable is treated as a confounding variable and its effect is "cleansed" from the data set. The assemblage pattern related solely to the second explanatory variable can then be isolated and explored (Legendre and Legendre, 1998). An advantage of CCA over standard univariate tests of species biomass (e.g., ANOVA) is that the method simultaneously depicts the strength and direction of species responses to predictor variables by the position and spread of species in ordinate space. The approach therefore offers insights into species associations that are not readily obtained by univariate methods (Legendre and Legendre, 1998).

We applied partial CCA to the data set alternating depth and month as the confounding and explicit explanatory variables, respectively. We recognized that the habitat of most fishes changes with body size (Werner and Gilliam, 1984) and therefore we divided species with abundant, small size classes (individuals less than 30% of maximum recorded total length [TL] that occurred in at least 10% of the sites sampled) into small and large size classes (greater than 30% of maximum recorded TL were categorized as large) and we treated them as distinct species in the analysis. An exception was made for spiny dogfish, which possessed a bimodal size distribution that separated at approximately 500 mm or 47% of the maximum recorded TL.

Owing to the lack of samples from 20- and 80-m depths in March, we performed partial CCA (one each for depth and month), using 1) samples collected from all three months, but from 40 and 160 m only; and 2) for all four depths from October and July only for a total of four partial CCA tests. We identify the data included in each univariate and multivariate analysis by labeling tests as "all-months" or "October+July," respectively. The analysis was split to avoid ambiguity that may have arisen from performing partial CCA on data lacking full treatment replication across factor levels (Anderson and Gribble, 1998).

To increase the robustness of each CCA only species that occurred in at least 20% of the sites sampled were included. The variance explained by a global CCA model (month+depth) was used in conjunction with results from the partial CCA to identify variance components that were uniquely and jointly explained by each predictor (Borcard et al., 1992; Anderson and Gribble, 1998). The significance of each predictor in the global and

partial CCA models was tested by comparing a pseudo F statistic to a null distribution generated by permuting the species-site matrix 5000 times (Legendre and Legendre, 1998).

The analysis of biomass spectra paralleled our analyses of the biomass of assemblage species. Length-frequency information for each species was used to divide species biomass into $\log_2$ body size classes. The total sum of biomass (all species) in each size class was then normalized by dividing the biomass by the antilog body size interval of each respective size class, as is commonly done in analyses of biomass spectra (Kerr, 1974; Sprules et al., 1983). In subsequent partial CCA, the size class biomass×site matrix was treated as the response variable.

To determine whether the analyses should account for spatial autocorrelation, we tested residuals resulting from the global species biomass and biomass spectra CCA models for spatial dependence, using a multiscale direct ordination technique. The method entails performing a constrained ordination on the global model CCA residuals with an explanatory matrix that is coded for geographic distance (Wagner, 2004). We used a grain-size equivalent to 0.1° latitude that resuled in four distance classes. Results were nonsignificant for species biomass and biomass spectra models, indicating that spatial structure at the assemblage level was not detectable. We therefore disregarded spatial dimensions and pooled samples by depth and season in subsequent analyses. During the exploratory stage of our analysis, univariate and multivariate tests that were performed with biomass densities resulted in conclusions similar to those obtained with numerical densities. We chose to limit our analyses to biomass densities to avoid redundancy and because the importance of a species to energy flow in a food web is more readily (although not perfectly) approximated by information on its biomass. We considered all statistical tests significant at the $P=0.05$ level.

Results

We captured 23,100 individual fish in our survey that represented 62 species from 23 different families. Of these, 32 species occurred in more than 10% of the trawls. In general, small size classes (<30% of maximum recorded length) for individual species were rare and only English sole (*Parophrys vetulus*), and spiny dogfish (*Squalus acanthias*) were abundant enough for inclusion in the analysis as separate size classes. Water conditions were relatively homogenous throughout the area surveyed. Temperature and salinity values differed by less than 1°C and 0.2, respectively, between the northern and southern CTD stations for each depth and month combination (Table 1). Differences in temperature and salinity among depths were small in October and March but were more evident in July; waters 20 m deep were warmer and fresher by 1.3° and 0.8°C, respectively (Table 1).

Table 1

Temperature (°C) and salinity measurements obtained with conductivity-temperature-density (CTD) casts from the northern (N) and southern (S) regions of the area surveyed in Central Basin, Puget Sound. Data were obtained within ten days of trawl sampling. Although stations at 20 and 80 m were not sampled in March, water properties are provided to aid comparisons among sampling months.

		Temperature		Salinity	
Month	Depth (m)	N	S	N	S
October	20	12.1	12.1	30.3	30.5
	40	11.9	12.0	30.5	30.6
	80	11.7	11.8	30.6	30.7
	160	11.4	11.5	30.7	30.8
March	20	8.7	8.5	29.6	29.5
	40	8.7	8.5	29.7	29.6
	80	8.7	8.4	29.9	29.9
	160	8.8	8.3	30.1	29.8
July	20	12.8	13.0	29.6	29.6
	40	12.1	12.1	29.8	29.8
	80	11.5	11.4	30.0	30.0
	160	11.5	11.4	30.4	30.4

Overall, spotted ratfish (*Hydrolagus colliei*), spiny dogfish, and flatfish were the dominant taxonomic groups in the survey. Biomass patterns observed at each depth and month combination are depicted in Figure 2. Shallow waters (20 and 40 m) were dominated by flatfishes, which composed between 64% and 83% of the fish assemblage biomass in all three months. In deep water. assemblage biomass was nearly double that found in shallow waters (80 and 160 m; Fig. 2). In total, spotted ratfish composed approximately 80% of the fish assemblage at 160 m in all three months (Fig. 2). Spiny dogfish were found primarily at depths of 80 and 160 in October, were nearly absent from the survey in March (two individuals were captured), and present at all depths in July, with the highest biomasses occurring at depths of 80 and 160 m (Fig. 2).

Diversity metrics

Variation in species richness (N) was observed across depths in both October+July (ANOVA, $F_{[3,32]}=3.9$, $P=0.01$) and all-months tests (ANOVA, $F_{[1,26]}=103.7$, $P<0.001$) where N at 40 m was higher than at 160 m (Fig. 3). *Post hoc* analyses of the October+July test indicated that N at 160 m was significantly lower than at 80 m, but that both of these depths did not differ from N at 20 and 40 m (Fig. 3). Similar patterns were observed for species diversity (H'), with significant differences across depth for both the October+July and all-months tests (ANOVA, $F_{[1,32]}=18.4$, $P<0.001$ and $F_{[1,26]}=137.3$, $P<0.001$, respectively; Fig. 3). In both all-months and

October+July tests H' at 160 m was significantly lower than that observed at shallower depths (Fig. 3).

N did not differ significantly across months (ANOVA, $F_{[1,32]}$=1.7, P=0.18 and $F_{[1,26]}$=0.3847, P=0.68 in October+July and all-months tests, respectively) and there was no significant interaction between depth and month (ANOVA, $F_{[3,32]}$=2.3, P=0.08 and $F_{[2,26]}$=1.4, P=0.26 in October+July and all-months tests, respectively). In contrast, H' in the October+July test differed significantly by month (ANOVA, $F_{[1,32]}$=13.4, P<0.001), as well as the interaction between depth and month (ANOVA, $F_{[3,32]}$=8.3275, P<0.001). Overall, H' was higher in October than in July and the interaction term appears to be related to a strong seasonal change in H' at 80 m (Fig. 3). Month and the interaction between month and depth were not significant in the test for all-months (ANOVA, $F_{[1,26]}$=2.0, P=0.15 and $F_{[1,26]}$=1.7, P=0.2, respectively).

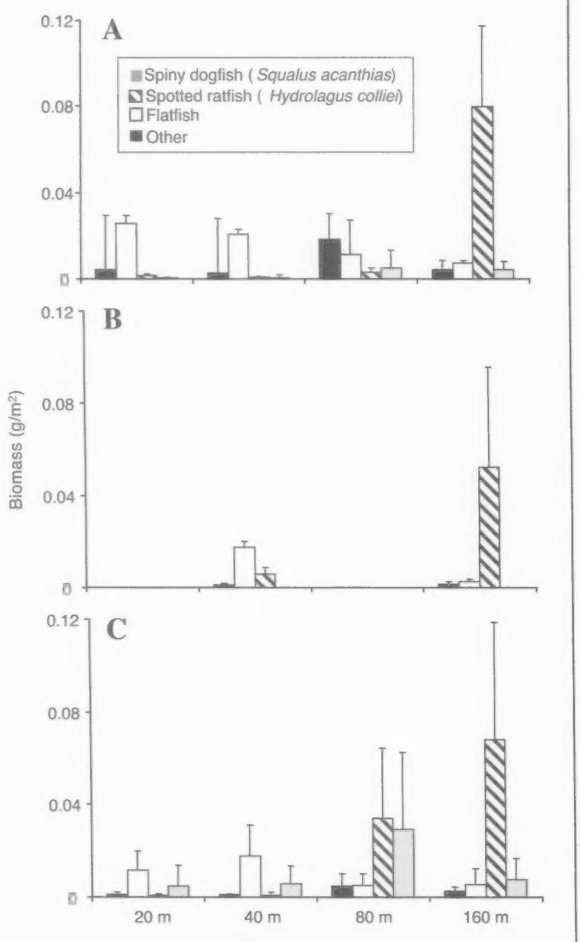

Figure 2

Average biomass of the major fish groups in the demersal fish assemblage observed at different depths from the Central Basin, Puget Sound in (**A**) October 2004, (**B**) March 2005, and (**C**) July 2005. Error bars indicate standard deviation. For October, March, and July, 4, 4, and 5 sites were sampled at each depth, respectively.

Taxon-based analysis

Depth was a significant predictor of assemblage structure in all-months and in October+July CCA tests, and explained 44% ($F_{[1,27]}$=19.1, P<0.001) and 34% ($F_{[3,33]}$=6.1, P<0.001) of the variances, respectively. Season explained a smaller proportion of the variance (5%) in the October+July CCA test ($F_{[1,33]}$=2.7, P<0.05) and was not a significant predictor in the all-months test ($F_{[1,27]}$=1.9, P<0.18). Temporal shifts in depth distributions were negligible at the assemblage level; the joint variance explained by season and depth was zero for October+July and all-months analyses.

The resulting tri-plots for each partial CCA (based on weighted averages of the species scores) simultaneously depict the centroid of the sites coded for the constraining variables and the position (eigenvectors) of the species forming the response matrix. Examination of the depth partial CCA tri-plots for October+July and all-months analyses, indicated that the first CCA axis primarily separated shallow (20 and 40 m) and deep (80 and 160 m) fish communities (Fig. 4). The spread of the variable centroids indicates the relative differences in species composition among the respective depth and month factors (distant centroids are more dissimilar in species composition than close centroids). Species centered near the origin of the tri-plot have little to no association with the predictor variables included in the analyses, but those furthest from the origin have higher loadings, the strongest associations with the CCA axis, and contribute the most to differentiating sites that separate along the same axis. For the October+July samples, the second CCA axis also separated the 80- and 160-m fish assemblages (Fig. 4). Partial CCA results for the October+July and all-months samples confirmed that 160 m was dominated by spotted ratfish and small spiny dogfish, but that Pacific hake (*Merluccius productus*), rex sole (*Glyptocephalus zachirus*), and dover sole (*Microstomus pacificus*) also typified that depth (Fig. 4). Furthermore, species that were associated with both 80 and 160 m included large spiny dogfish, and quillback rockfish (*Sebastes maliger*), brown rockfish (*Sebastes auriculatus*), blackbelly eelpout (*Lycodes pacificus*), Pacific tomcod (*Microgadus proximus*), walleye pollock (*Theragra chalcogramma*), shiner perch (*Cymatogaster aggregate*), pile perch (*Rhacochilus vacca*), black tip poacher (*Xeneretmus latifrons*), slender sole (*Lyopsetta exilis*), and plainfin midshipman (*Porichthys*

notatus; Fig. 4). In shallow waters (20 and 40 m) several flatfishes dominated including small and large English sole, rock sole (*Lepidopsetta bilineata*), C-O sole (*Pleuronichthys coenosus*), Pacific sanddab (*Citharichthys sordidus*), and sand sole (*Psettichthys melanostictus*) among other species (Fig. 4).

In the October+July analyses, temporal changes in assemblage structure were largely driven by species that were found primarily at depths of 80 m. The biomass of shiner perch, pile perch, walleye pollock, and Pacific tomcod was highest in October and the biomass of large spiny dogfish and slender sole was highest in July (Fig. 4). At depths of 20 and 40 m, the biomass of small English sole and C-O sole was highest in October and the biomass of staghorn sculpin (*Leptocottus armatus*) and sand sole was highest in July. The biomass of species that typified the 160-m depths changed little between October and July (e.g., spotted ratfish, dover sole, rex sole, and Pacific hake; Fig. 4). In the all-months analysis, species with higher biomass in March included C-O sole, sand sole, great sculpin, and rock sole (Fig. 4).

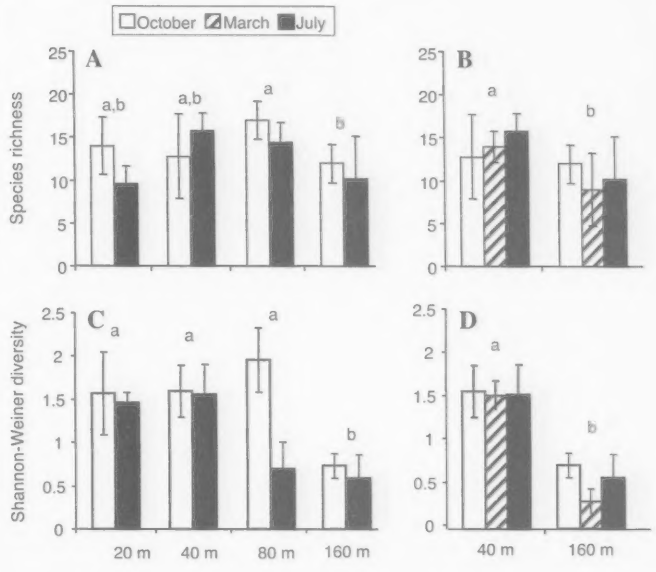

Figure 3

Average species richness (N; upper panel) for (**A**) October and July samples and (**B**) October, March, and July (all-months) by depth sampled. Average species diversity (H'; lower panel) for October and July samples (**C**) and October, March and July (**D**). Lower case letters above each depth category denote depths that do not differ on the basis of *post hoc* Tukey honestly significant difference tests. (A) and (C) correspond to October+July two-way ANOVA tests and (B) and (D) correspond to all-months two-way ANOVA tests. H' differed by month only for the October+July. Note: depths at 20 and 80 m were not sampled in March. Error bars indicate standard deviation. For October, March, and July, 4, 4, and 5 sites were sampled at each depth, respectively.

Size-based analysis

Body sizes encountered in the survey spanned eleven size classes, ranging from 2 to 2048 g. Overall, biomass spectra were nonlinear in appearance and approximately parabolic for most depth and season combinations (Fig. 5). For that reason metrics describing linear biomass size spectra (intercept, slope) were not estimated. Deep waters were dominated by individuals larger than 32 g, whereas shallow waters contained relatively more individuals that were less than 128 g (Fig. 5). Temporal differences were most apparent at depths of 80 m where biomass was concentrated in body size classes greater than 128 g in July and at 40 m that contained peak biomass levels in the 16-g body size class in March. Overall, 28% and 29% of the biomass spectra variance was associated with depth in both all-months ($F_{[1,10]}$=5.4, P<0.001) and October+July tests ($F_{[3,10]}$=2.3, P<0.001), respectively. Month explained a smaller but significant proportion of variance in the October+July test (11%; $F_{[1,10]}$=2.1, P<0.001) and was not a significant predictor in the all seasons test ($F_{[1,33]}$=2.1, P=0.09). Variance explained jointly by season and depth was again zero.

In the October+July analyses, the first CCA axis accounted for 20.9% of the total variation and separated the shallow (20 and 40 m) and deep assemblages (160 m). The second axis accounted for 10.3% of the variance and distinguished 80 m from the other depths. The largest size class (2048 g) was associated with depths of 80 m, and the next three largest size classes (256, 512, and 1024 g) were associated with depths of 160 m (Fig. 6). In contrast, the smallest size classes (4, 8, and 16 g) were affiliated with depths of 20 and 40 m. The remaining intermediate body size classes were near the origin of the ordination plot and not closely associated with any of the depths. The analysis of all-months tests reiterated these patterns (Fig. 6). Tracking the arrival of dogfish, the size classes with the strongest temporal responses were also the largest size classes (1024 and 2048 g) which exhibited higher abundances in July (Fig. 6). In October, biomass in the smallest size classes (2, 8, and 16 g) was relatively higher.

Discussion

Fjord systems such as Puget Sound typically possess steep bathymetries and deep basins that result in deep-water habitat relatively close to shore. As expected, the demersal fish assemblage in Puget Sound varied

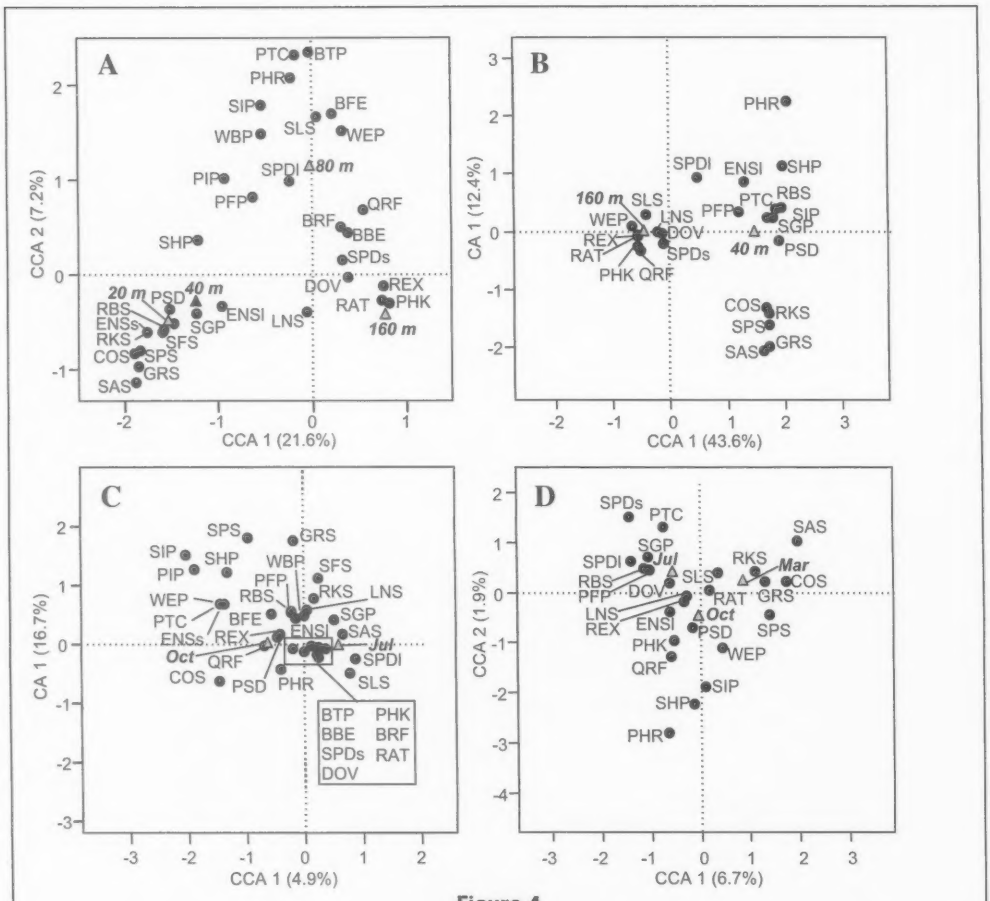

Figure 4

Species-based partial canonical correspondence analysis (CCA) tri-plots for fall+summer and all-seasons analyses in which depth (**A**, **B**) and season (**C**, **D**) are the constraining variables, respectively. In the tri-plots, the site centroids coded for each constraining factor are indicated by triangles. The proximity of factor centroids in ordination space to one another corresponds to their respective similarity in average species composition. Species that have strong loadings (large eigenvectors) are distant from the tri-plot origin and contribute the most to differentiating factor centroids that separate along the same axis. The eigenvalue or variance associated with each axis is indicated by parentheses. In cases were the constraining factor consisted of only two groups as in (B) and (C) only one CCA axis was generated. To aid interpretation two dimensional plots were generated by plotting the CCA (*x*-axis) against the residual axis (*y*-axis) derived from standard correspondence analysis (CA) performed on the remaining community variance. Species codes: BFE=bigfin eelpout (*Lycodes cortezianus*); BBE=blackbelly eelpout (*Lycodes pacificus*); BTP=blacktip poacher (*Xeneretmus latifrons*); BRF=brown rockfish (*Sebastes auriculatus*); COS=C-O sole (*Pleuronichthys coenosus*); DOV=Dover sole (*Microstomus pacificus*); ENSl and ENSs for English sole (*Parophrys vetulus*) large and small, respectively; GRS=breat sculpin (*Myoxocephalus polyacanthocephalus*); LNS=longnose skate (*Raja rhina*); PHK=Pacific hake (*Merluccius productus*); PHR=Pacific herring (*Clupea pallasii pallasii*); PSD=Pacific sanddab (*Citharichthys sordidus*); PTC=Pacific tomcod (*Microgadus proximus*); PIP=pile perch (*Rhacochilus vacca*); PFP=plainfin midshipman (*Porichthys notatus*); QRF=quillback rockfish (*Sebastes maliger*); REX=rex sole (*Glyptocephalus zachirus*); RKS=rock sole (*Lepidopsetta bilineata*); RBS=roughback sculpin (*Chitonotus pugetensis*); SAS=sand sole (*Psettichthys melanostictus*); RAT=spotted ratfish (*Hydrolagus colliei*); SGP=sturgeon poacher (*Podothecus accipenserinus*); SFS=sailfin sculpin (*Nautichthys oculofasciatus*); SIP=shiner perch (*Cymatogaster aggregata*); SLS=slender sole (*Lyopsetta exilis*); SPS=speckled sanddab (*Citharichthys stigmaeus*); SPDl and SPDs=spiny dogfish (*Squalus acanthias*) large and small, respectively; SHP=staghorn sculpin (*Leptocottus armatus*); WEP=walleye pollock (*Theragra chalcogramma*); WBP=whitebarred prickleback (*Poroclinus rothrocki*).

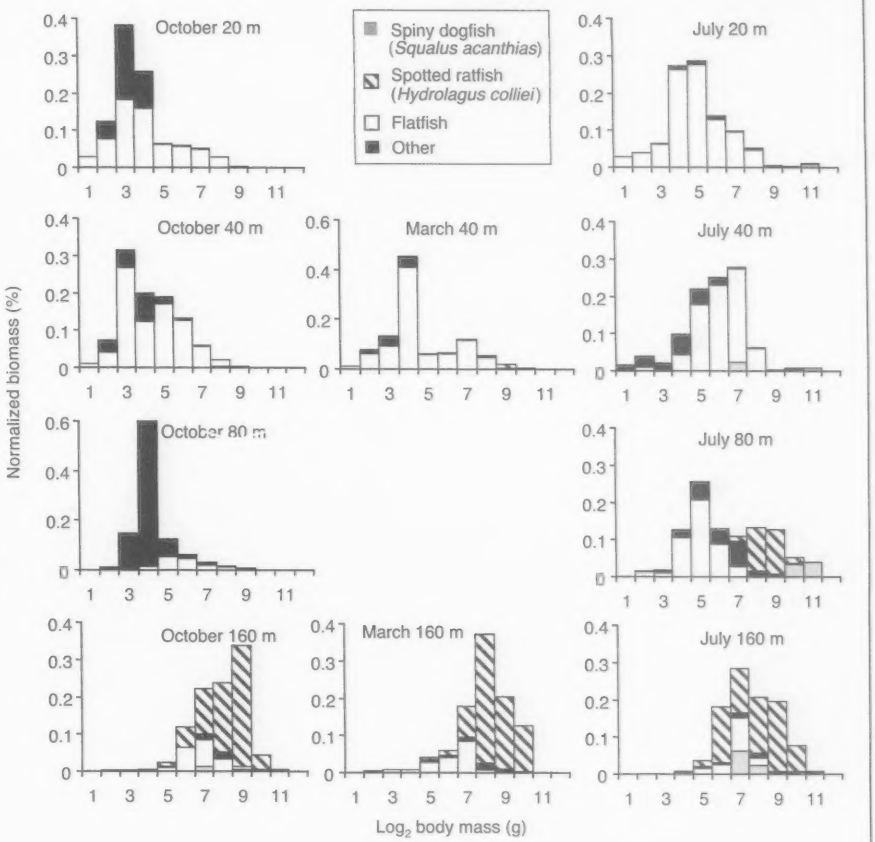

Figure 5

Average normalized biomass spectra of the demersal fish assemblage from the Central Basin of Puget Sound sampled with bottom trawl at different depths from October 2004 and March and July 2005.

substantially across depths and among seasons, but was unusual in that chondrichthyans (spotted ratfish and spiny dogfish) made up a majority of the fish biomass. Fish assemblages in estuaries on the outer coast of Washington, Oregon, and California are dominated by teleosts (e.g., Armor and Herrgesell, 1985; Bottom and Jones, 1990; De Ben et al., 1990), and this finding shows that demersal fish assemblages in Puget Sound differ fundamentally from shallower estuarine systems.

Total assemblage biomass at depths of 80 and 160 m principally comprised spotted ratfish year round and spiny dogfish seasonally. Deepwater habitat is widespread in the Central Basin (average depth: 120 m; Burns, 1985), making these two species the dominant species, in biomass, in the area surveyed. An abundance of spotted ratfish has also been noted in deep waters immediately adjoining Puget Sound (Palsson et al.[2]), but what remains poorly understood is whether spotted ratfish are common in northeastern Pacific fjords or whether they are superabundant only in Puget Sound. Spotted ratfish are primarily benthic feeders, feeding on polychaetes and bivalves and occasionally on small fishes (Quinn et al., 1980), which indicates that they potentially are competitors to benthic feeding flatfishes (Reum and Essington, 2008). In addition, they are preyed upon by large elasmobranchs (e.g., sixgill sharks [*Hexanchus griseus*], spiny dogfish). There is presently insufficient information to evaluate whether the high abundance of spotted ratfish is a secondary effect of shifts in food web structure, or whether other envi-

[2] Palsson, W. A., S. Hoffmann, P. Clarke, and J. Beam. 2003. Results from the 2001 transboundary trawl survey of the southern Strait of Georgia, San Juan Archipelago and adjacent waters, 117 p. Washington State Dept. Fish and Wildlife, Olympia, WA.

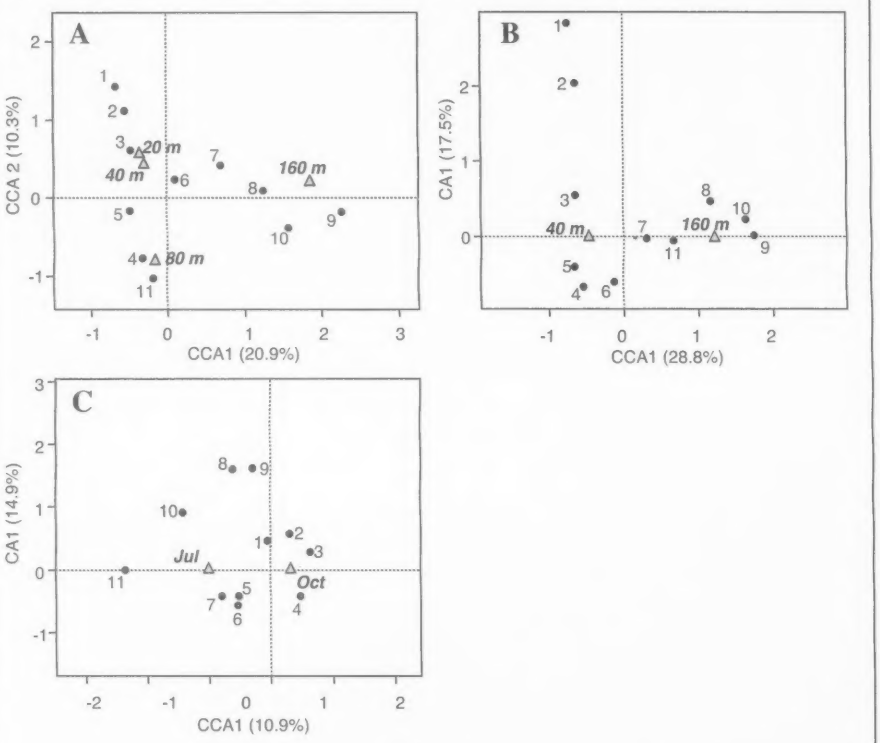

Figure 6

Partial canonical correspondence analysis (CCA) tri-plots of biomass spectra of fall+summer and all seasons analyses in which depth is the constraining variable for (**A**) and (**B**), respectively. For all seasons, only depth was significantly related to variation in the biomass spectra (**C**). In the tri-plots, the site centroids coded for each constraining factor are indicated by triangles. The proximity of factor centroids in ordination space to one another corresponds to their respective similarity in distribution of biomass across body size classes. Body size classes are indicated by circles. Those that have strong loadings (large eigenvectors) are distant from the tri-plot origin and contribute the most to differentiating factor centroids that separate along the same axis. The eigenvalue or variance associated with each axis is indicated within parentheses. In cases were the constraining factor consisted of only two groups, as in (B) and (C), only one CCA axis was generated. To aid interpretation two-dimensional plots were generated by plotting the CCA (*x*-axis) against the residual axis (*y*-axis) derived from standard correspondence analysis (CA) performed on the remaining community variance.

ronmental features of Puget Sound promote their high abundance. Historical abundance records of spotted ratfish in Puget Sound are available in agency and project reports and indicate that they have been a common component of the food web at least since the 1930s, but it is difficult to extract trends from these data because of the lack of standardization of sample sites and gears. Future comparisons with less impacted fjords may offer insight into whether cartilaginous species naturally dominate in these systems or do so only under conditions related to human-caused ecosystem degradation. Despite our poor understanding of long-term changes in the Puget Sound fish community, the high abundance of ratfish in the area surveyed indicate that they likely constitute a significant node in the Puget Sound food web and are therefore deserving of further study.

Spiny dogfish was the most abundant demersal piscivore and may have a particularly important influence on assemblage structure in Puget Sound and other coastal ecosystems. Spiny dogfish have a diverse diet, feeding on Pacific herring, flatfish, spotted ratfish, salmonids, as wells as a wide range of benthic and pelagic invertebrates (Reum and Essington, 2008; Beamish and Sweeting, 2009). Large mobile predators such as spiny dogfish play an important role by linking different communities through predation and may stabilize

communities by dampening oscillations in prey populations through behavioral mechanisms such as switching prey (McCann et al., 2005). Moreover, understanding how large predators use different habitats is important for estimating prey mortality rates and system energy flows (Bax, 1998). Information on spiny dogfish movement patterns in Puget Sound is limited to tagging studies from the 1940s and 1970s. Results from these studies indicate that approximately 70% of the spiny dogfish population resides in the Sound and the adjoining Strait of Georgia for multiple years, while the remaining dogfish are transient (McFarlane and King, 2003). Spiny dogfish on the outer Washington and British Columbia coasts are known to exhibit seasonal latitudinal migrations, but seasonal movements of dogfish tagged within Puget Sound and the Strait of Georgia are less clear (McFarlane and King, 2009; Taylor and Gallucci, 2009) and remain the subject of ongoing research. It is unknown whether spiny dogfish migrate in the winter to other subbasins within Puget Sound, to habitats shallower than 20 m, or whether they simply feed higher in the water column, disassociating with the benthos. There is evidence that catch rates of spiny dogfish in monitoring surveys have declined since the mid 1980s (Palsson, 2009) and that growth and size-at-maturity have also undergone substantial shifts (Taylor and Galluci, 2009). Characterizing movement patterns and population dynamics will clarify the impact of spiny dogfish on nearshore food webs.

As demonstrated in Puget Sound, fjordal fish assemblages vary markedly in space and time, and this variation has practical implications for modeling energy flows and interspecific interactions such as predation and competition. Food web models can foster ecosystem based management because they offer a framework for summarizing system knowledge and permit the simulation of alternative management scenarios. However, food web models for Puget Sound (as well as any other temperate system) parameterized by using fish abundances from one season alone may misrepresent the importance of different feeding modes and mischaracterize patterns of trophic links in the fish assemblage (Greenstreet et al., 1997). In addition, stark differences between deep and shallow assemblages in terms of total biomass and species composition indicate strong spatial structuring in the likelihood and intensity of interactions among species, which may be a more general feature of fjord estuaries with similar deep basin bathymetrics. The data presented here, when coupled with diet information, provide a basis for determining the parameters of trophodynamic models that account for spatial and temporal variability in the fish assemblage (e.g., Pauly et al., 2000).

The use of three separate methods for analyzing differences in the demersal fish assemblage allowed us to investigate whether our interpretation of assemblage variation differed depending on the method. All three methods indicated significant differences between shallow (20, 40, and 80 m) and deep waters (160 m) across seasons, with the exception of N, where values from 20 and 40 m waters did not differ from values in 160 m waters. We note however, that variation in N may have been artificially reduced by our exclusion of rare species from the analysis. In contrast, species diversity, H', which takes into account the relative biomass of each species, should be more robust to the exclusion of rare species. Results from taxon-based CCA complemented results from the diversity metrics by highlighting those species that co-varied with depth and simultaneously depicted site similarity in ordination space. Lastly, size-based analyses revealed differences in assemblage structure based on biomass spectra, a macroecological descriptor of assemblage structure (Jennings, 2005). Because body size is correlated with trophic level in aquatic systems (Kerr 1974; Jennings et al., 2001), differences in biomass spectra among assemblages may reveal fundamental differences in trophic structure (Rice, 2000; Sweeting et al., 2009). Significant depth related differences in the biomass spectra paralleled results from our taxon-based analyses and offer evidence that food web structure likely varies with depth. Combined, these approaches offer alternative prisms through which to view the demersal fish assemblage and mutually confirm important differences in assemblage structure.

As with other marine fish surveys, our results are partly contingent on the effectiveness of the sampling gear and are premised on the assumption that catchability varies little among species. To maintain comparability with past demersal fish studies in Puget Sound we intentionally sampled using trawl equipment with specifications nearly identical to those used in previous agency surveys in the region. The use of bottom trawls, however, also meant that species associated with rocky reef habitats would be excluded from our survey because the gear was suitable only for trawling in soft-bottom habitats. Moreover, large species such as six gill shark, which typically exceed 2 m in length in Puget Sound, were missed from the survey altogether. For future comparisons with other fjord systems, an effort should be made to sample regions with similar soft bottom habitats. We note that the data presented here reflect daytime distribution patterns, and diel movements of species may potentially connect deep and shallow communities. Another limitation of the present study is that our results span only a single time period and cover only a single basin in Puget Sound. Thus, we do not presume that the patterns described here will necessarily hold for all regions and be stable across time. Indeed, ample evidence from marine ecosystems points to the dynamic nature of community structure (Anderson and Piatt, 1999). Future research may very well improve our estimates of diversity and increase our understanding of temporal shifts in the Puget Sound fish assemblage.

Although depth and season were clearly important in explaining community structure and species abundances, roughly one-half of the variation in these metrics was not related to depth or season. Differences in temperature and salinity between the northern and southern CTD stations were relatively slight and differ-

ences among other parameters, such as oxygen concentration and turbidity (data not shown), showed similar patterns. Because water conditions vary little in the region surveyed they are unlikely to explain site-specific variability. Other unmeasured variables, however, such as substrate composition, sediment contamination, or shoreline and land cover characteristics in regions adjoining each sample site may potentially explain additional variance in the assemblage. We note, however, that spatial autocorrelation was not detected in the data set and indicates that spatially structured environmental variables, such as those that covary with coastal urbanization, are unlikely to explain much additional variation at least at the spatial scales embraced by our survey (Borcard et al., 1992).

Our research provides the first published assessment of seasonal variability in assemblage structure across multiple depths in the Puget Sound demersal fish assemblage and offers insight into general features of deep fjord systems. We found strong structuring of the assemblage by depth and smaller, although important, differences across seasons. These shifts were manifest in simple assemblage metrics and in multivariate taxon-based and size-based analyses. The identification of these patterns, in turn, identifies priorities for future investigators that will further our understanding of the demersal assemblage and the forces that act to shape it. Notably, we identified species that may seasonally modify the Puget Sound food web in significant ways (e.g., spiny dogfish) and we confirmed the findings of other researchers who have identified spotted ratfish as one of the most abundant fishes in the Puget Sound region (Quinnel and Schmitt[3]). Remarkably, research directed toward uncovering the life history and ecology of spotted ratfish has been limited (but see Quinn et al., 1980; Barnett et al. 2009). Furthermore, key species in the Puget Sound food web may be those that link habitats through movement and foraging activities. Understanding diel and seasonal-scale movement patterns will greatly improve our understanding of the Puget Sound fish assemblage.

Acknowledgments

Financial support was provided for J. Reum by the Vincet Liguori Fellowship and funding for boat time was provided by the University of Washington Research Royalties Fund. We are grateful to A. Beaubreaux, M. Hunsicker, J. Murphy, K. Marshall, M. Anderson, and D. English for assistance with field work. Comments from M. Hunsicker, C. Harvey, G. Williams, and three anonymous reviewers greatly improved earlier versions of this article.

[3] Quinnell, S., and C. Schmitt. 1991. Abundance of Puget Sound demersal fishes: 1987 research trawl survey results, 240 p. Washington State Dept. Fish and Wildlife, Olympia, WA.

Literature cited

Armor, C. and P. L. Herrgesell.
1985. Distribution and abundance of fishes in the San Francisco Bay estuary between 1980 and 1982. Hydrobiol. 129:211–227

Anderson, M. J., and N. A. Gribble.
1998. Partitioning the variation among spatial, temporal and environmental components in a multivariate data set. Aust. J. Ecol. 23:158–167

Anderson, P. J., and J. F. Piatt.
1999. Community reorganization in the Gulf of Alaska following ocean climate regime shift. Mar. Ecol. Prog. Ser. 189:117–123.

Barnett, L. A. K, R. L. Earley, D. A. Ebert, and G. M. Cailliet.
2009. Maturity, fecundity, and reproductive cycle of the spotted ratfish, *Hydrolagus colliei*. Mar. Biol. 156:301–316

Bax, N. J.
1998. The significance and prediction of predation in marine fisheries. ICES J. Mar. Sci. 55:997–1030

Beamish R. J., and R. M. Sweeting.
2009. Spiny dogfish in the pelagic waters of the Strait of Georgia and Puget Sound. *In* Biology and management of dogfish sharks (V. F. Gallucci, G. A. McFarlane, and G. G. Bargmann, eds.), p. 101–118. Am. Fish. Soc., Bethesda, MD.

Borcard, D., P. Legendre, and P. Drapeau.
1992. Partialling out the spatial component of ecological variation. Ecology 73:1045–1055.

Bottom, D. L. and K. K. Jones.
1990. Species composition, distribution, and invertebrate prey of fish assemblages in the Columbia River Estuary. Prog. Oceanog. 25:243–270.

Burns, R.
1985. The shape and form of Puget Sound, 100 p. Washington Sea Grant Program, Seattle, WA.

De Ben, W. A., W. D. Clothier, G. R. Ditsworth, and D. J. Baumgartner.
1990. Spatiotemporal fluctuations in the distribution and abundance of demersal fish and epibenthic crustaceans in Yaquina Bay, Oregon. Estuaries 13:469–478.

Greenstreet, S. P. R., A. D. Bryant, N. Broekhuizen, S. J. Hall, and M. R. Heath.
1997. Seasonal variation in the consumption of food by fish in the North Sea and implications for food web dynamics. ICES J. Mar. Sci. 54:243–266.

Haedrich, R. L., and N. R. Merrett.
1992. Production/biomass ratios, size frequencies, and biomass spectra in deep-sea demersal fishes. *In* Deep-sea food chains and the global carbon cycle (G. T. Rowe and V. Pariente, eds.), p. 157–182. Kluwer Academic Publ., Amsterdam.

Jennings, S.
2005. Size-based analyses of aquatic food webs. *In* Aquatic Food Webs: An Ecosystems Approach (A. Belgrano, A., U. M, Scharler, J. Dunne, and R. E. Ulanowicz, eds.), p. 86–97. Oxford Univ. Press, New York.

Jennings, S., J. K. Pinnegar, N. V. C. Polunin, and T. W. Boon.
2001. Weak cross-species relationships between body size and trophic level belie powerful size-based trophic structuring in fish communities. J Anim. Ecol. 70:934–944.

Kennish, M. J.
2002. Environmental threats and environmental future of estuaries. Environ. Conserv. 29:78–107.

Kerr, S. R.
1974. Theory of size distribution in ecological communities. J. Fish. Res. Board Can. 31:1859–1862.
Krebs, C. J.
1989. Ecological methodology, 654 p. Harper Collins Publishers, Inc., New York.
Legendre, P., and L. Legendre.
1998. Numerical ecology, 2nd ed., 853 p. Elsevier Science, Amsterdam.
Lotze, H. K., H. S. Lenihan, B. J. Bourque, R. H. Bradbury, R. G. Cooke, M. C. Kay, S. M. McCann, K. S., J. B. Rasmussen, and J. Umbanhowar.
2005. The dynamics of spatially coupled food webs. Ecol. Lett. 8:513–523.
McFarlane, G. A., and J. R. King.
2003. Migration patterns of spiny dogfish (*Squalus acanthias*) in the North Pacific Ocean. Fish. Bull. 101:358–367.
2009. Movement patterns of spiny dogfish within the Strait of Georgia. *In* Biology and management of dogfish sharks (V. F. Gallucci, G. A. McFarlane, and G. G. Bargmann, eds.), p. 77–88. Am. Fish. Soc., Bethesda, MD.
Mueter, F. J. and B. L. Norcross.
1999. Linking community structure of small demersal fishes around Kodiak Island, Alaska, to environmental variables. Mar. Ecol. Prog. Ser. 190:37–51.
Palsson W. A.
2009. The status of spiny dogfish in Puget Sound. *In* Biology and management of dogfish sharks (V. F. Gallucci, G. A. McFarlane, and G. G. Bargmann, eds.), p. 53–66. Am. Fish. Soc., Bethesda, MD.
Pauly, D., V. Christensen, S., and C. J. Walters.
2000. Ecopath, Ecosim and Ecospace as tools for evaluating ecosystem impact of fisheries. ICES J. Mar. Sci. 57:697–706.
Pikitch, E. K., C. Santora, E. A. Babcock, A. Bakun, R. Bonfil, D. O. Conover, P. Dayton, P. Doukakis, D. Fluharty, B. Heneman, E. D. Houde, J. Link, P. A. Livingston, M. Mangel, M. K. McAllister, J. Pope, and K. J. Sainsbury.
2004. Ecosystem-based fishery management. Science 305:346–347.
Quinn, T. P., B. C. Miller, and C. Wingert.
1980. Depth distribution and seasonal and diel movements of ratfish, *Hydrolagus colliei*, in Puget Sound, Washington. Fish. Bull. 78: 816–821.
Reum, J. C. P., and T. E. Essington.
2008. Seasonal variation in guild structure of the Puget Sound demersal fish community. Estuar. Coasts 31:790–801.
Rice, J. C.
2000. Evaluating fishery impacts using metrics of community structure. ICES J. Mar. Sci. 57:682–688.
Sprules, W. G., J. M. Casselman, and B. J. Shuter.
1983. Size distribution of pelagic particles in lakes. Can. J. Fish. Aquat. Sci. 40:1761–1769.
Sweeting, C. J., F. Badalamenti, G. D'Anna, C. Pipitone, and N. V. C. Polunin.
2009. Steeper biomass spectra of demersal fish communities after trawler exclusion in Sicily. ICES J. Mar. Sci. 66:195–202.
Taylor, I. G. and V. F. Gallucci.
2009. Unconfounding the effects of climate and density- dependence using 60 years of data on spiny dogfish. Can. J. Fish. Aquat. Sci. 66:351–366.
ter Braak, C. J. F.
1986. Canonical correspondence analysis: a new eigenvector technique for multivariate direct gradient analysis. Ecology 67:1167–1179.
Thompson, A. A., and B. D. Mapstone.
2002. Intra- versus inter-annual variation in counts of reef fishes and interpretations of long-term monitoring studies. Mar. Ecol. Prog. Ser. 232:247–257.
Wagner, H. H.
2004. Direct multi-scale ordination with canonical correspondence analysis. Ecology 85:342–351.
Werner, E. E., and J. F. Gilliam.
1984. The ontogenetic niche and species interactions in size structured populations. Ann. Rev. Ecol. Syst. 15:393–425.
Zar, J. H.
1984. Biostatistical analysis, 2nd ed., 718 p. Prentice Hall, Inc., Englewood Cliffs, NJ.

Interactions of age-dependent mortality and selectivity functions in age-based stock assessment models

Xi He (contact author)
Stephen Ralston
Alec D. MacCall

Email address for contact author: xi.he@noaa.gov

Fisheries Ecology Division
Southwest Fisheries Science Center
National Marine Fisheries Service
National Oceanic and Atmospheric Administration
110 Shaffer Road
Santa Cruz, California 95060

Abstract—The natural mortality rate (M) of fish varies with size and age, although it is often assumed to be constant in stock assessments. Misspecification of M may bias important assessment quantities. We simulated fishery data, using an age-based population model, and then conducted stock assessments on the simulated data. Results were compared to known values. Misspecification of M had a negligible effect on the estimation of relative stock depletion; however, misspecification of M had a large effect on the estimation of parameters describing the stock recruitment relationship, age-specific selectivity, and catchability. If high M occurs in juvenile and old fish, but is misspecified in the assessment model, virgin biomass and catchability are often poorly estimated. In addition, stock recruitment relationships are often very difficult to estimate, and steepness values are commonly estimated at the upper bound (1.0) and overfishing limits tend to be biased low. Natural mortality can be estimated in assessment models if M is constant across ages or if selectivity is asymptotic. However if M is higher in old fish and selectivity is dome-shaped, M and the selectivity cannot both be adequately estimated because of strong interactions between M and selectivity.

Manuscript submitted 18 August 2010.
Manuscript accepted 17 February 2011.
Fish. Bull. 109:198–216 (2011).

The views and opinions expressed or implied in this article are those of the author (or authors) and do not necessarily reflect the position of the National Marine Fisheries Service, NOAA.

Correctly specifying the instantaneous rate of natural mortality (M) in stock assessment models is important because misspecification may lead to over- or underestimates of critical assessment quantities, including stock depletion, maximum sustainable yield (MSY), virgin biomass, and density dependence (Lapointe et al., 1989; Thompson, 1994; Mertz and Myers, 1997; Punt and Walker, 1998; Clark, 1999; Wang et al., 2006). It is widely believed that natural mortality varies with age or size; young (small) fish have higher natural mortality rates due to higher predation risks, disease, or starvation (Lorenzen, 1996), whereas older (larger) fish may have increased natural mortality with senescence or because of cumulative reproductive stress (Mangel, 2003; Moustahfid et al., 2009).

In spite of the widely held perception that natural mortality varies considerably with age, most stock assessment models assume that M is constant for all ages, mainly because there are insufficient data with which to estimate natural mortality on an age-specific basis. Another reason for assuming constant M in stock assessment models is that natural mortality is typically highly correlated with other key parameters, including stock recruitment and selectivity parameters (Lapointe et al., 1992; Thompson, 1994; Schnute and Richards, 1995; Fu and Quinn, 2000), quantities that are often quite difficult to estimate with accuracy (Maunder et al.[1]).

In previous studies a variety of approaches have been developed to estimate natural mortality, including the use of maximum observed age (Hoenig, 1983) and life-history parameters (Alverson and Carney, 1975; Gunderson, 1980; Myers and Doyle, 1983; Roff, 1992; Jensen, 1996; Gunderson, 1997). In other studies, life-history data and environmental variables have been combined to establish empirical relationships to predict natural mortality (Pauly, 1980; Gislason et al., 2010). These studies have provided estimates of natural mortality that can be useful for stock assessments but these estimates may not be sufficient for species-specific stock assessment because of bias (e.g., only a subset of possible life histories was considered). Other studies have shown that unless species-specific data were collected before exploitation of the species, estimates of

[1] Maunder, M. N., H. H. Lee, and K. R. Piner. 2010. A review of natural mortality, its estimation, and use in fisheries stock assessment. Unpubl. manuscr, 35 p. Inter-American Tropical Tuna Commission, 8604 La Jolla Shores Drive, La Jolla, CA.

natural mortality are impractical, if not impossible, to derive from fishery or survey data, because of the interaction between fishing and natural mortality (Vetter, 1988; Quinn and Deriso, 1999). Clark (1999) examined the effects of incorrectly specifying M for a simple age-structured stock assessment and concluded that errors in M mainly affect estimates of fishing mortality and abundance, but not estimates of age-specific selectivity.

In most regions of the world, where statistical stock assessments of single species provide the basis for management advice (Worm et al., 2009), it is commonplace to assume a constant natural mortality rate for all exploitable ages or sizes (or for both). Moreover, natural mortality is also typically assumed to be constant over time and identical among regions (Punt, 2003; Yin and Sampson, 2004; PFMC, 2008). Uncertainty in the use of constant natural mortality in these assessment models is usually evaluated by an approach that is similar to likelihood profiles, where M values are changed and other parameters are fixed. However, this approach is highly dependent on the specific model structure and parameter settings being evaluated. For example, if stock recruitment relationships or selectivity functions are fixed in an assessment model, likelihood profile methods on natural mortality can provide only the validity of the model fitted to fixed values of natural mortality and not the validity of the model for its interactions with other model parameters.

In this study, we compare stock assessment results among simulated populations with different natural mortality schedules. The simulation data were generated with an age-based population model characterized by exploitation from a single fishery with a constant selectivity pattern over an extended period of time, representing somewhat ideal conditions. Simulations were crafted to reflect conditions in the U.S. west coast groundfish fishery—the source of most available fishery data for the last 40 years, a period when fishing intensity was high in the early years and has been low in recent years. In the simulation operating model, two different natural mortality patterns were used: 1) constant natural mortality for all ages; and 2) elevated values of M in both juvenile and old fish. The data, along with sampling errors, were input into the assessment models. In the assessment model, natural mortality was assumed to be known and constant for all ages, estimated to be constant for all ages, or was estimated to follow an age-specific pattern. Estimated quantities from the assessments were then compared with the simulation models that generated the data. Important assessment results, e.g., stock depletion and stock-recruit relationships, were then compared to evaluate the effect of misspecification of natural mortality and selectivity on stock assessment estimates. In addition, results from the assessment models were compared with and without an informative parameter prior for spawner-recruit steepness parameters.

Methods

Simulation model

The simulation or operating model in this study was an age-structured population model with a max age of 30 years. The last age was an age plus group. The Beverton-Holt stock-recruitment function was used to model stock recruitment. In particular, the "steepness" parameterization of Mace and Doonan[2] with h=0.6 was used (see also Dorn, 2002). Recruitment variability was lognormal with σ_R set equal to 0.5 and lognormal survey variability set to equal 0.25. Specifics of the simulated population dynamics are presented in the Appendix. Base values for biological, fishery, and modeling parameters are presented in Table 1. Because of variability in recruitment and catchability, the model was run for 260 years, with the first 200 years as a "burn-in" period with no fishing to minimize the effect of initial conditions in the model. Only the last 40 years of data were provided for the assessment model.

Biological parameters, including growth, fecundity, and the length-weight relationship were patterned after widow rockfish (*Sebastes entomelas*) off the U.S. west coast (He et al., 2009). Although widow rockfish shows differences between the sexes in biological parameters, the same values were used for both sexes to simplify the model.

We modeled two different functional types of age-dependent natural mortality (M) in the simulations including 1) constant natural mortality for all ages (0.15/yr); and 2) high M in both juvenile and old fish (Table 2; Fig. 1). The annual sample size for age compositions was 500 for all simulations—a size that ensured that informative age composition data were available to the assessment models.

We used only one fishery in the operating model, and catches began in the last 40 years of the simulations. Fishing mortalities (F) were modeled as proportions of F_{MSY}, which varied over time. During the first 20 years, fishing at F_{MSY} occurred, and in the last 20 years fishing mortality was 10% of F_{MSY}. Two types of fishery selectivity patterns were simulated, i.e., simple asymptotic logistic and double normal curves (Fig. 2). The later was moderately dome-shaped and is implemented in the stock synthesis model (Methot, 2009a), a widely used stock assessment model. In all simulations the ascending limbs of the two selectivity curves were constrained to be similar, i.e., 50% of individuals were selected at age 8. The above specific values and patterns in M, F, and selectivity were based on typical life history patterns of fish, and fishing patterns, off the U.S. west coast (e.g., those of widow rockfish).

[2] Mace, P. M., and I. J. Doonan. 1988. A generalized bioeconomic simulation model for fish population dynamics. New Zealand Fishery Assessment Res. Doc., 88/4, 21 p. MAF Fisheries, Greta Point, Wellington, New Zealand.

Table 1

Biological, fishery, and modeling parameters used in the simulation model to evaluate interactions between mortality and selectivity. See Appendix for equations, definitions of parameters, and symbols. Parameters are the same for both sexes. True values are the base parameter values used in the simulation models. Lower and upper bounds are boundary limits used in the stock assessment program. NA=not applicable.

Parameter	Symbol	True value	Estimated in assessment model	Lower and upper bounds	Unit and note
Minimum age	a_{min}	0	No	NA	Year
Maximum age	a_{max}	30	No	NA	Age plus group
Virgin recruitment	R_0	10	Yes	0.1, 30	Log scale
Recruitment steepness	h	0.6	Yes	0.2, 1.0	
Annual recruit deviation	R_y^{δ}	0	Yes	–5, 5	Log scale, 76 years
Growth	K	0.14	No	NA	Per year
Growth	L_{∞}	50.54	No	NA	cm
Growth	t_0	–2.68	No	NA	Year
Length–weight	τ_1	5.45e-6	No	NA	
Length–weight	τ_2	3.2878	No	NA	Kg/cm
Natural mortality	M	0.15	Yes or no	0.01, 1	Per year, varied, see text
Logistic selectivity	η_1	8	Yes	0, 50	50% selectivity at age 8
Logistic selectivity	η_2	5	Yes	0, 50	Width for 95% selection
Double normal selectivity	η_1	13	Yes	–507, 533	See Appendix
Double normal selectivity	η_2	–2	Yes	–82, 80	See Appendix
Double normal selectivity	η_3	3.5	Yes	–136, 143	See Appendix
Double normal selectivity	η_4	2.6	Yes	–101,106	See Appendix
Double normal selectivity	η_5	–5	Yes	–205, 195	See Appendix
Double normal selectivity	η_6	0.65	Yes	–25, 26	See Appendix
Catchability—survey of juveniles	q_1	0	Yes	–5, 5	Log scale
Catchability—survey of adults	q_2	0	Yes	–5, 5	Log scale
Recruitment variability	σ_R	0.6	No	NA	
Catch variability	σ_{ψ}	0.05	No	NA	
Variability—survey of adults	$\sigma_{i,1}$	0.25	No	NA	
Variability—survey of adults	$\sigma_{i,2}$	0.25	No	NA	
Annual age sample size	n	500	No	NA	

Stock assessment model

The simulation data were fitted to the stock assessment model by using stock synthesis (SS3, vers. 3.04b) software (Methot, 2009a, 2009b). Other than patterns in natural mortality and selectivity, a correct population structure was assumed in the assessment model, and likewise for the growth, fecundity, and the length-weight relationship. There were three ways in which natural mortality (M) was treated in the assessment models. First, M was assumed to be constant and was fixed at the same value of M=0.15/yr as in the simulation model (Fig. 1; Table 2, runs 1–12). Second, a single M was estimated (runs 13 and 15). Third, four values of M were estimated (runs 14 and 16). In the third case, we used the breakpoint method in the SS3 program, and the four breakpoints (M_1, M_2, M_3, and M_4) were defined for ages 2, 3, 24, and 25. In this case, M_1 was used for ages 0 to 2, M_2 was used for age 3, M_3 was used for age 24, M_4 for ages 25 to 30, and M values for ages between 4 and 23 were linearly interpolated between M_3 and M_4.

Fishery data from the simulation model consisted of annual catches, annual age composition data, and survey indices. Fishing mortality was estimated by using the hybrid method in the SS3 program. The hybrid method in the SS3 program is a simplified parameterization method (see Methot, 2009a). Because of relatively small variations of catch data generated in the simulation models (coefficient of variation [CV]=0.05), this method produces nearly identical fishing mortality estimates as in fully parameterized fishing mortality (see Methot, 2009a). Other estimated parameters in the assessment model included the stock-recruit relationship, selectivity, catchability coefficients, and annual recruitment deviations from the stock-recruit curve (Table 1). Initial values for all estimated parameters were set to be the same as those in the simulation models. Noninformative priors were used in parameter

Table 2

Model and parameter specifications in simulation and assessment models used to evaluate interactions between mortality and selectivity. Constant natural mortality (M=0.15) is used in all runs except runs 14 and 16. A normal prior is used as h prior.

Run no.	No. of simulations	True selectivity	Selectivity function used in assessment	h prior in assessment	True M in simulation	M estimated in assessment model
1	3000	Logistic	Logistic	Yes	Constant	No
2	500	Logistic	Logistic	Yes	High M in juvenile and old fish	No
3	500	Double normal	Double normal	Yes	Constant	No
4	500	Double normal	Double normal	Yes	High M in juvenile and old fish	No
5	500	Logistic	Double normal	Yes	Constant	No
6	500	Logistic	Double normal	Yes	High M in juvenile and old fish	No
7	500	Double normal	Logistic	Yes	Constant	No
8	500	Double normal	Logistic	Yes	High M in juvenile and old fish	No
9	500	Logistic	Logistic	No	Constant	No
10	500	Logistic	Logistic	No	High M in juvenile and old fish	No
11	500	Double normal	Double normal	No	Constant	No
12	500	Double normal	Double normal	No	High M in juvenile and old fish	No
13	500	Logistic	Logistic	No	Constant	Yes (1 parameter)
14	500	Logistic	Logistic	No	High M in juvenile and old fish	Yes (4 parameters)
15	500	Double normal	Double normal	No	Constant	Yes (1 parameter)
16	500	Double normal	Double normal	No	High M in juvenile and old fish	Yes (4 parameters)

estimation except for spawner-recruit steepness (h), in which case h=0.6 and a normal prior with standard deviation (SD)=0.1 was either used (runs 1–8), or not used (runs 9–16) in the assessment models.

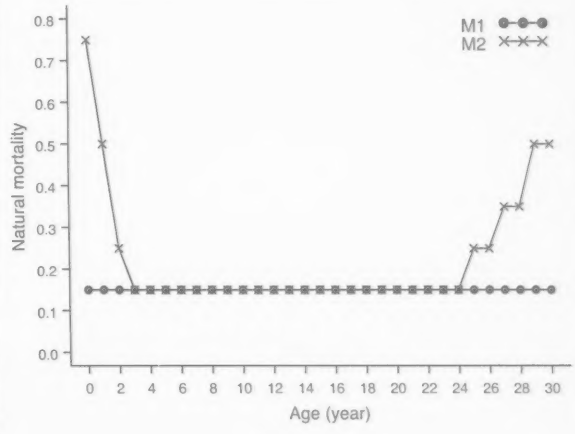

Figure 1

Patterns of natural mortality by age used in simulation models to evaluate interactions between mortality and selectivity. M1 has constant M by age, and M2 has higher M values in juvenile and old fish.

Comparisons of simulation and assessment results

For evaluating each simulation scenario (Table 2), the simulation was repeated 500 times and the simulated data from each run were inputted into the SS3 model. A successful assessment model run was then achieved if the value of the maximum gradient component was less than 0.05. If an assessment model run did not converge, that realization was flagged as a failed run and a new set of data was generated from the operating model.

Assessment model outputs were compared with known quantities from the simulation model for a subset of key assessment results. These included 1) a time series of spawning output; 2) estimated stock-recruitment parameters; 3) terminal stock depletion; 4) the overfishing limit (OFL); and 5) catchability coefficients. The OFL is a recently developed reference point used in the United States and is defined as the catch available from the estimated terminal biomass if fished at F_{MSY}. For each comparison between the simulation and assessment models, a discrepancy statistic was computed. For four quantities, i.e., virgin spawning output (B_0), virgin recruitment (R_0), stock depletion, and OFL, the relative discrepancy ($S_{\%}$) was computed as a percent deviation from the simulation model:

$$S_{\%} = 100 \frac{X_a - X_s}{X_s}, \quad (1)$$

where X_a and X_S are quantities from the assessment and simulation, respectively.

In contrast, for steepness (h) and catchability (q_i) the absolute discrepancy (S_{abs}) between the assessment and simulation models was computed by using absolute differences according to the following equation:

$$S_{abs} = X_a - X_s. \quad (2)$$

To test the congruence of the simulation and assessment models, 3000 runs were conducted by using the default setup between the simulation and assessment models (Table 2). Note that in the default setup (run 1), simple logistic selectivity was used in both the simulation and assessment models. Likewise, M was constant and correctly specified in both models. Thus, no model specification errors existed in fits of the default model. For all other simulation scenarios, 500 simulations were conducted. Early testing runs indicated that 500 simulations were sufficient to capture the range of outputs. Median values from the simulation-assessment runs were then computed along with 2.5% and 97.5% of percentiles.

Performance of the assessment models was also measured by using two performance statistics. The first statistic measured the percentage of SS3 runs that were completed (% run completed). Runs were considered completed whenever the program finished estimation, regardless of how or if the assessment model produced sensible results. Incomplete runs were those when the program stopped in the middle of the procedure without producing any SS3 outputs. The second performance statistics (% maximum gradient component [MGC] satisfied) measured the percentage of runs that not only were completed, but also satisfied the convergence criteria with MGC less than 0.05 and a positive-definite Hessian matrix. It should be noted that even when MGC was <0.05 there was no assurance that the model had reached a global optimum. The threshold value for the MGC was set to be 0.05. The choice of this value was based on earlier testing runs, in which the default setup (run 1) was used and the result with the MGC of 0.05 was the same as that from other testing runs with smaller MGC values (e.g., 0.001).

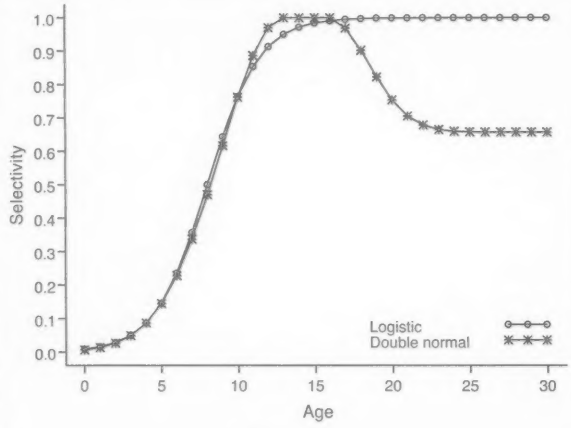

Figure 2

Two selectivity functions (logistic and double normal) used in simulation models to evaluate interactions between mortality and selectivity.

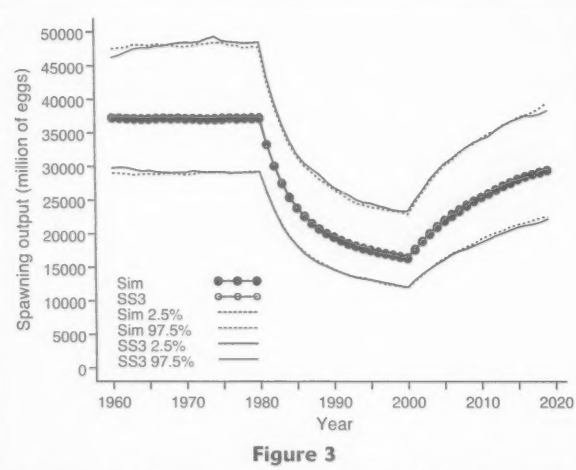

Figure 3

Time series of spawning outputs from simulation (Sim) and stock synthesis (SS3) assessment models from run 1. Closed circles are median simulation outputs and open circles are median assessment outputs. Assessment outputs are barely visible because most of them overlap simulation outputs. Lines are 2.5% and 97.5% of quantiles from simulation (dashed lines) and assessment (solid lines) model outputs.

Results

Testing simulation models

Simulation models were tested by using the default setup in the operating model and the assessment model (run 1). As expected, the time series of median spawning output, as well as their 2.5% and 97.5% percentiles, between the simulation and assessment models matched very well (Table 3; Fig. 3). Frequency plots of the estimated differences in virgin spawning output (B_0), depletion, and OFL between simulation and assessment models showed that the differences were very

Table 3

Key assessment model estimates on biological, fishery, and management parameters and their comparisons with their correct values. For virgin spawning output, depletion, and overfishing limit (OFL, in metric tons [t]), the statistics are expressed as the percent difference of medians between simulations and assessments with 2.5% and 95% percentiles seen in parentheses. Values equal to zero indicate no difference between the simulation and assessment models. For steepness and catchability, the estimated values and their ranges are used. The true value of steepness (h) is 0.6 and the true values of two survey catchabilities (q_2 and q_2) are 1.0. Selectivity fits are indicated by three categories: good, fair, or bad.

Run no.	Virgin spawning output (B_0)	Steepness (h)	Adult survey catchability (q_1)	Juvenile survey catchability (q_2)	Selectivity fit	Depletion	OFL (t)
1	0.5	0.59	0.98	0.99	Good	−2.0	−2.2
	(−19.9, 26.8)	(0.35, 0.75)	(0.84, 1.14)	(0.84, 1.19)		(−27.0, 31.1)	(−22.3, 18.2)
2	−21.3	0.76	1.35	3.62	Fair	−6.3	−32.4
	(−41.9, 2.5)	(0.61, 0.87)	(1.16, 1.56)	(3.03, 4.28)		(−32.9, 37.0)	(−48.3, 11.7)
3	1.0	0.59	0.97	0.99	Good	−2.1	−1.7
	(−20.3, 32.3)	(0.35, 0.74)	(0.82, 1.17)	(0.83, 1.18)		(−27.7, 27.2)	(−21.4, 19.5)
4	7.5	0.60	0.95	2.80	Bad	−4.3	−9.7
	(−21.1, 42.0)	(0.36, 0.74)	(0.81, 1.21)	(2.36, 3.39)		(−30.7, 31.8)	(−26.2, 9.4)
5	5.3	0.59	0.88	0.96	Fair	−2.7	−0.1
	(−17.7, 32.6)	(0.36, 0.73)	(0.77, 1.04)	(0.81, 1.14)		(−28.3, 29.6)	(−20.9, 20.6)
6	9.2	0.61	0.87	2.72	Bad	−3.9	−10.1
	(−20.9, 47.4)	(0.35, 0.73)	(0.73, 1.02)	(2.32, 3.16)		(−30.6, 31.7)	(−24.9, 9.3)
7	−11.6	0.63	1.13	1.11	Bad	0.8	−6.6
	(−30.0, 13.2)	(0.40, 0.78)	(1.00, 1.32)	(0.95, 1.32)		(−25.8, 31.3)	(−27.9, 11.6)
8	−29.6	0.78	1.55	3.96	Bad	−5.1	−35.8
	(−47.4, −6.4)	(0.64, 0.90)	(1.36, 1.78)	(3.36, 4.76)		(−32.9, 33.0)	(−51.6, −19.1)
9	1.6	0.57	0.99	1.00	Good	−2.0	−3.4
	(−18.7, 25.0)	(0.31, 1.00)	(0.84, 1.13)	(0.84, 1.17)		(−26.1, 30.4)	(−20.5, 15.9)
10	−24.1	1.00	1.33	3.50	Fair	2.1	−29.6
	(−43.2, −0.5)	(0.63, 1.00)	(1.13, 1.52)	(2.93, 4.22)		(−29.8, 46.6)	(−46.5, −9.7)
11	1.8	0.58	0.97	0.99	Good	−1.8	−2.3
	(−19.8, 33.0)	(0.32, 1.00)	(0.83, 1.14)	(0.84, 1.17)		(−27.5, 31.8)	(−20.5, 16.6)
12	9.5	0.60	0.95	2.80	Fair	−6.9	−10.1
	(−18.9, 45.8)	(0.34, 1.00)	(0.81, 1.17)	(2.37, 3.32)		(−31.1, 24.2)	(−25.8, 6.1)
13	0.3	0.62	0.98	1.00	Good	−1.5	−2.4
	(−26.1, 37.8)	(0.32, 1.00)	(0.82, 1.15)	(0.77, 1.30)		(−29.0, 33.8)	(−21.4, 22.7)
14	−0.4	0.58	0.98	1.19	Good	−0.9	−3.7
	(−24.1, −32.6)	(0.33, 1.00)	(0.82, 1.16)	(0.79, 1.79)		(−27.5, 36.9)	(−24.0, 21.0)
15	−1.1	0.61	0.98	1.03	Good	0.0	−4.1
	(−24.4, 35.6)	(0.33, 1.00)	(0.83, 1.16)	(0.78, 1.29)		(−28.0, 31.7)	(−22.31, 21.1)
16	22.9	0.55	0.96	1.67	Fair	−6.0	−19.7
	(−1.9, 110.4)	(0.21, 1.00)	(0.80, 1.13)	(0.68, 4.33)		(−33.2, 34.0)	(−52.2, 20.3)

small (Tables 3 and 4), and their distributions were centered near zero and symmetrical (Fig. 4). Other key assessment outputs, such as steepness (h) and the two catchability coefficients (q_1 and q_2), in comparisons between the simulation and assessment models also matched very well (Table 3). Selectivity was also estimated well in the stock assessment models (Fig. 5). In this setting, with no model specification error, the estimation model performed very well; 100% of runs finished and 100% MGC values were smaller than specified critical values (Table 5).

Effects of misspecified *M* on assessment results

If selectivity functions were asymptotic and correctly specified in the assessment models (runs 1 and 2), population depletion was generally well estimated, even when natural mortality was misspecified in assessment models (Table 3). However, the OFL estimates were lower by more than 32% than the true values if young and old fish were characterized by increasing natural mortality, but M was assumed to be constant in the assessment (Table 3, run 2). The estimated

Table 4

Performance and convergences of assessment models. Percentages of runs finished indicate that the assessment models finished stock synthesis (SS3) runs but maximum gradient component (MGC) statistics did not satisfy convergence criteria. Percentages of MGC satisfied indicate that the assessment models finished SS3 runs and MGC statistics satisfied convergence criteria (MGC<0.05).

Run no.	No. of simulations	% of runs finished	% MGC satisfied	No. of parameters
1	3000	100.0	100.0	82
2	500	100.0	100.0	82
3	500	86.2	81.3	86
4	500	78.6	48.2	86
5	500	83.3	81.0	86
6	500	70.2	53.0	86
7	500	100.0	100.0	82
8	500	100.0	100.0	82
9	500	100.0	100.0	82
10	500	100.0	100.0	82
11	500	84.5	80.1	86
12	500	77.4	45.7	86
13	500	100.0	100.0	83
14	500	100.0	100.0	86
15	500	83.8	79.5	87
16	500	75.1	48.4	90

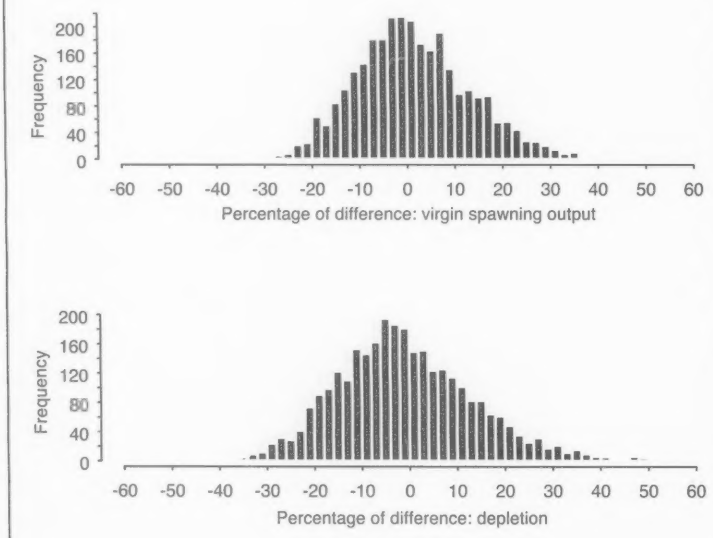

Figure 4

Frequency plots of estimated differences of virgin spawning outputs (B_0) and depletions between simulation and stock synthesis (SS3) assessment models from run 1. The differences are percentages of differences between simulation and assessment divided by true simulation values. Values equaled to zero indicate no differences between simulation and assessment models.

population trajectories were very different between the simulation and assessment models for run 2 (top right panel, Fig. 6), and stock recruitment parameters (B_0, h) were poorly estimated, with B_0 being lower and h being higher in the assessment models than those in the simulation models. The estimated catchability coefficients in the assessment models were higher than those in the simulation models. Estimated catchability coefficients for juvenile fish (q_2) were especially high (>3.6 versus the correct value of 1.0) for run 2. This result occurred also for all other scenarios in which juvenile natural mortalities were misspecified in assessment models (Table 3). However, estimated selectivity functions matched fairly well between the simulation and estimation models (top row, Fig. 7). Performance of the stock assessment models in this setting was very good; 100% of the runs finished successfully and MGC values were satisfied (Table 4).

Similar results were obtained if selectivity functions were double normal and were correctly specified in the

Table 5

Estimated natural mortalities (M) with 2.5% and 97.5% quantiles in parentheses for runs 13 to 16. A single M for all ages is estimated in runs 13 and 15, and four M values (break points) are estimated in runs 14 and 16. See the *Methods* section for how these four M values were assigned to each age group.

Run no.	M_1	M_2	M_3	M_4
13	0.150 (0.139, 0.161)			
14	0.448 (0.377, 0.513)	0.148 (0.108, 0.193)	0.147 (0.119, 0.169)	0.359 (0.321, 0.404)
15	0.148 (0.138, 0.163)			
16	0.285 (0.131, 0.450)	0.169 (0.068, 0.258)	0.139 (0.080, 0.225)	0.074 (0.010, 0.389)

assessment models (runs 3 and 4). Population depletion, as well as other stock assessment parameters, was well estimated if M was constant in both simulation and assessment models (run 3, second row in Fig. 6 and Table 3). The estimated double normal selectivity functions in the assessment model also matched well with that in the simulation model (run 3 in Fig. 7). Estimated population depletions were also matched reasonably well, even with misspecified natural mortalities, but the estimated OFL statistics were about 10% negatively biased (run 4, Table 3). However, if natural mortality was higher for younger and older age classes in the simulation models but was constant in the assessment models, the estimated population trajectories were different, with the estimated B_0 biased high (run 4 in Fig. 6; Table 3). Selectivity functions matched fairly well in the ascending limb between the simulation and assessment models but failed to match the descending limb of the selectivity curve (run 4, Fig. 7). Convergence of the estimation model was poor in this setting. In runs 3 and 4, 86.2% and 78.6% of 500 SS3 runs finished successfully, respectively, whereas only 81.3% and 48.2% of 500 SS3 runs produced satisfactory MGC values (Table 4).

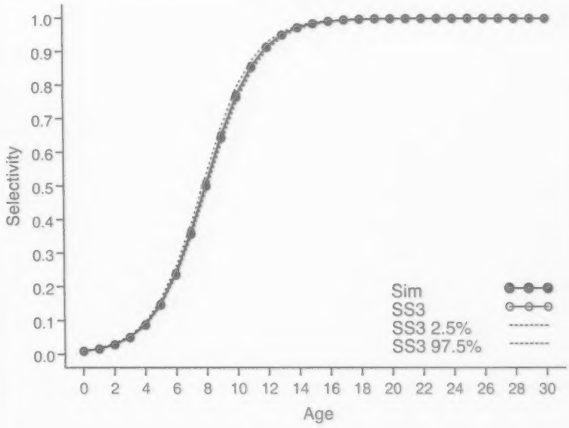

Figure 5

Estimated selectivity functions from simulation (Sim) and stock synthesis (SS3) assessment models for run 1. Dashed lines are 2.5% and 97.5% quantiles from assessment model outputs.

If selectivity functions were logistic in the simulation models but were double normal in the assessment models and M was correctly specified (runs 5 and 6, Table 2), most of the estimated parameters from the stock assessment models were close to those in the simulation models, generally less than 10% of differences (Table 3). However, when natural mortality in the simulation model varied, but was assumed constant in the assessment model, the estimated catchability coefficient for the juvenile survey (q_2) was positively biased (run 6, Table 3). Time series of estimated spawning output matched reasonably well (runs 5 and 6, Fig. 6), and the estimated selectivity function showed a negative bias for old fish (runs 5 and 6, Fig. 7). Convergence performance was poor (Table 4); less than 83.3% of runs finished and only 53.0% of runs satisfied the MGC criterion (Table 5).

If selectivity functions were double normal in the simulation model but were misspecified as logistic functions in the estimation model (runs 7 and 8, Table 2), the curves fits were very poor, as expected (last row in Fig. 7 and Table 3). Spawning output was poorly estimated; all estimated spawning outputs were lower than those in the simulation models in the early years (last row in Fig. 6). If natural mortality was incorrectly specified in the assessment models (run 8), estimated parameters from the stock assessment models were strongly biased (Table 3). This bias included high correlations between the two stock recruitment parameters (B_0 and h), and positive biases in both catchability coefficients (q_1 and q_2) (Table 3). Convergence of the assessment models, however, was very good. The percentages of runs finishing successfully and satisfying the MGC criterion were 100% (Table 4).

If no prior for h was used in the assessment models and natural mortality was assumed to be constant (runs 9 to12), the results in general were very similar to those from runs 1 to 4, where a prior on h was used (Figs. 8 and 9; Table 3). However, an important ex-

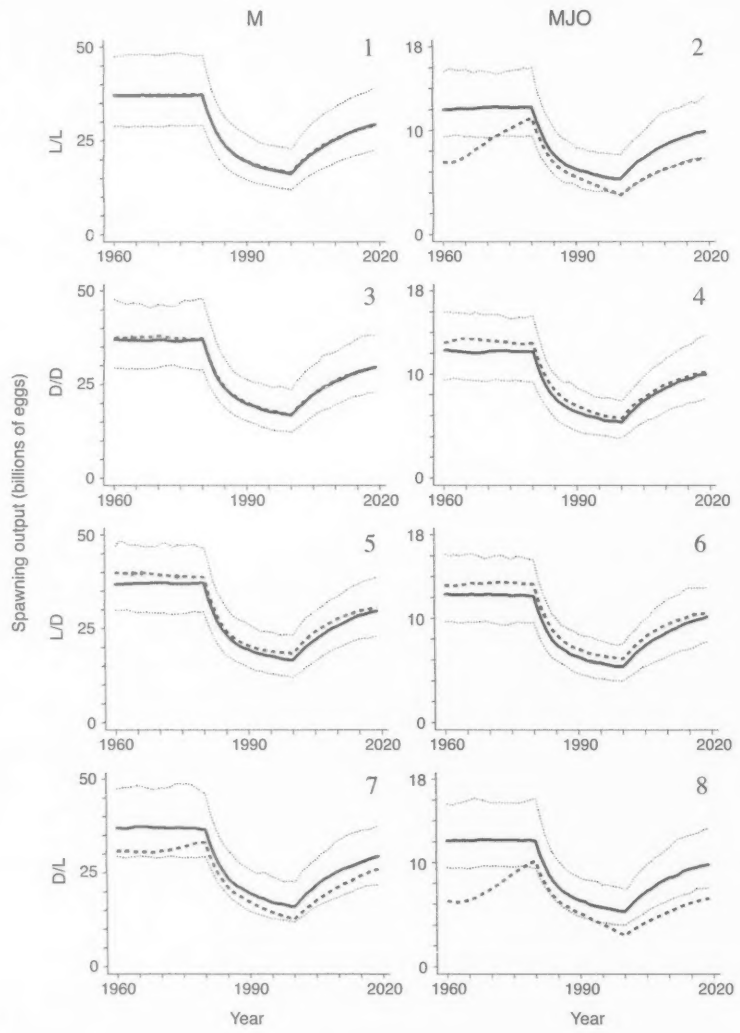

Figure 6

Time series of spawning outputs from simulation and stock synthesis assessment models (runs 1 to 8). The run number is shown in the upper right of each graph. See Table 2 for model and parameter setup for all runs. Solid lines are median simulation outputs and thick dashed lines are median assessment outputs. Thin dashed lines are 2.5% and 97.5% of quantiles from simulation outputs. Specifications for each panel are: M=constant M and MJO=high M in juvenile and old fish; L/L=logistic selectivity in both simulation and assessment models; D/D=double normal selectivity in both simulation and assessment models; D/L=double normal selectivity in simulation model, but logistic selectivity in assessment model; and L/D=logistic selectivity in simulation model, but double normal selectivity in assessment model.

ception was that a high percentage of runs estimated steepness at the upper bound of (h=1.0). If logistic selectivity functions were used and natural mortalities were correctly specified in both simulation and assessment models (run 9), there were still 16% of runs with h at the upper bound (Fig. 10). If logistic selectivity functions were used but natural mortality was incorrectly specified assessment models (run 10),

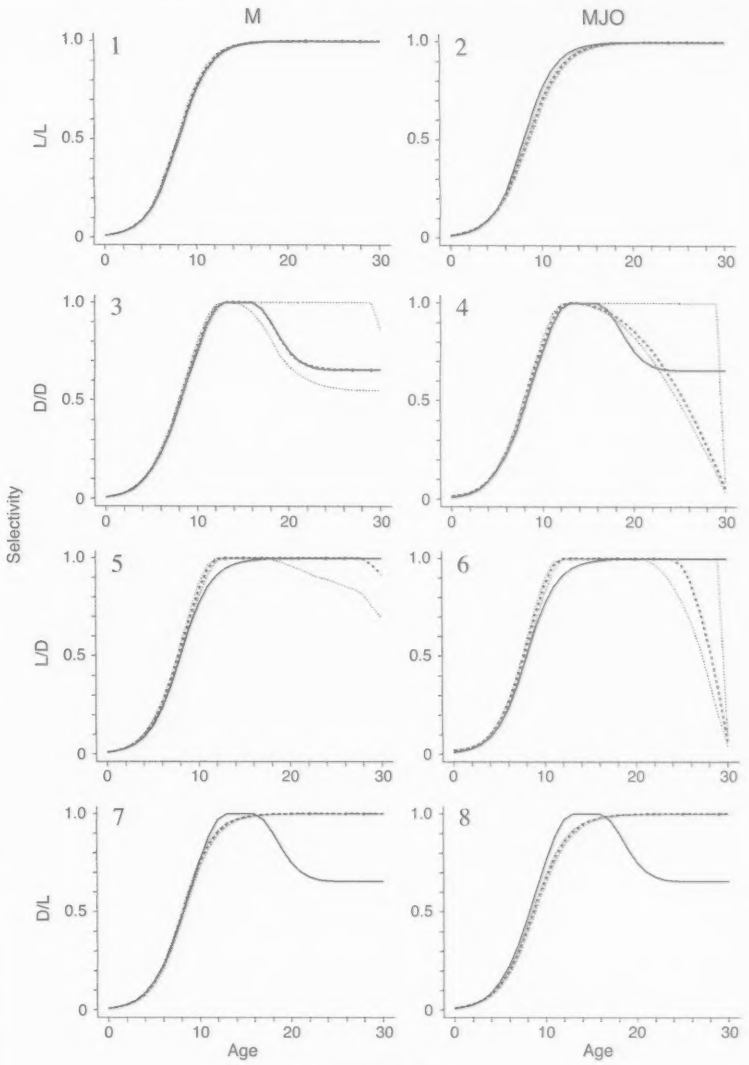

Figure 7

True selectivity from simulation models and estimated selectivity from stock synthesis assessment models (run 1 to run 8). The run number are shown in the upper left of each graph. Solid lines are true selectivity and thick dashed lines are median selectivity from assessment models. Thin dashed lines are 2.5% and 97.5% quantiles from assessment outputs. Specifications for each panel are: M=constant M and MJO=high M in juvenile and old fish; L/L=logistic selectivity in both simulation and assessment models; D/D=double normal selectivity in both simulation and assessment models; D/L=double normal selectivity in simulation model, but logistic selectivity in assessment model; and L/D=logistic selectivity in simulation model, but double normal selectivity in assessment model.

there were close to 90% of runs with h=1.0 (Fig. 10). If double normal selectivity functions were used and natural mortality was constant in both simulation and assessment models (run 11), 17% of runs settled on the upper bound (h=1.0) (Fig. 10). Results were similar even when natural mortality was high for both juvenile and old fish in the simulation model but was assumed to be constant in the assessment model

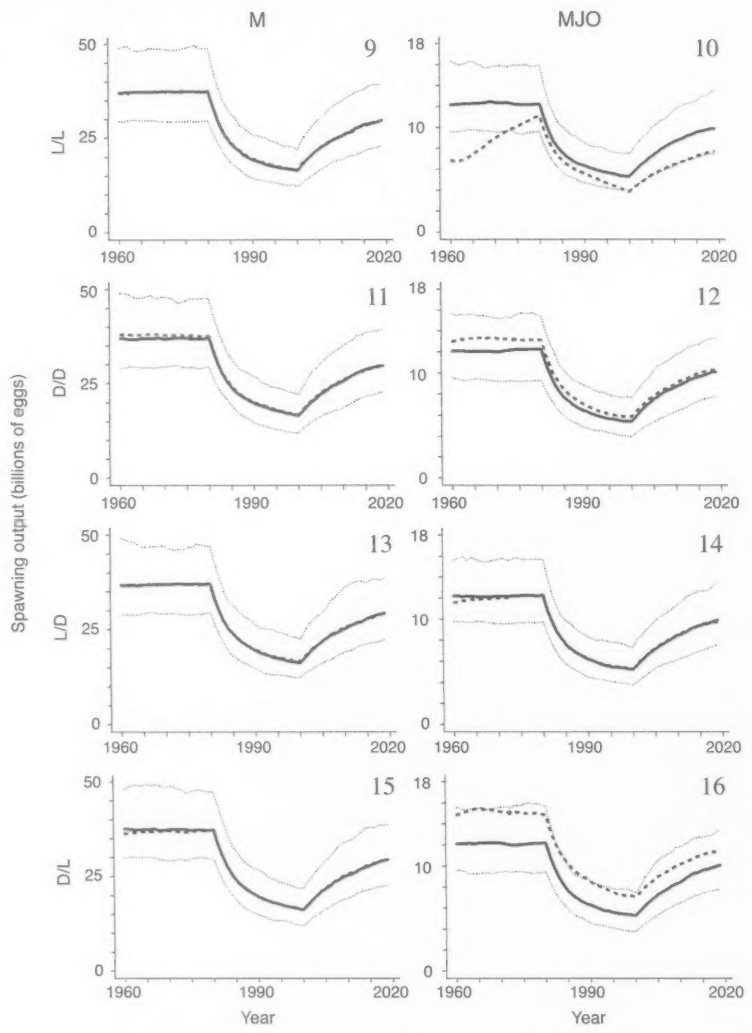

Figure 8

Time series of spawning outputs from simulation and stock synthesis assessment models (runs 9 to 16). The run number is shown in the upper right of each graph. See Table 2 for model and parameter setup for all runs Solid lines are median simulation outputs and thick dashed lines are median assessment outputs. Thin dashed lines are 2.5% and 97.5% of quantiles from simulation outputs. Specifications for each panel are: M=constant M and MJO=high M in juvenile and old fish; L/L=logistic selectivity in both simulation and assessment models; D/D=double normal selectivity in both simulation and assessment models; D/L=double normal selectivity in simulation model, but logistic selectivity in assessment model; and L/D=logistic selectivity in simulation model, but double normal selectivity in assessment model.

(Fig. 10). However, selectivity was poorly fitted for old fish (panel 12, Fig. 9). Percentages of runs that finished and that had satisfactory MGC rates were similar to those runs (runs 1 to 4) with the same selectivity and M specifications but with h priors included (Table 4).

If no priors for h were used and natural mortality was estimated in the assessment models (runs 13 to

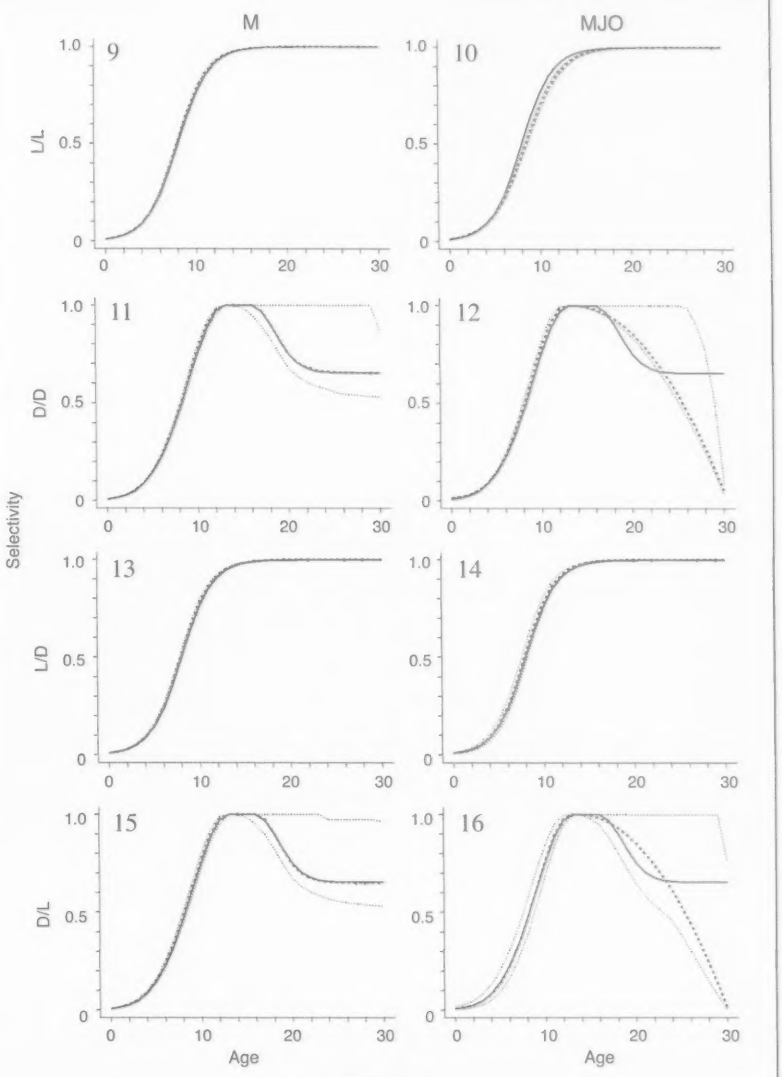

Figure 9

True selectivity from simulation models and estimated selectivity from stock synthesis assessment models (run 9 to run 16). The run number is shown in the upper left of each graph. Solid lines are true selectivity and thick dashed lines are median selectivity from assessment models. Thin dashed lines are 2.5% and 97.5% quantiles from assessment outputs. Specifications for each panel are: M=constant M and MJO=high M in juvenile and old fish; L/L=logistic selectivity in both simulation and assessment models; D/D=double normal selectivity in both simulation and assessment models; D/L=double normal selectivity in simulation model, but logistic selectivity in assessment model; and L/D=logistic selectivity in simulation model, but double normal selectivity in assessment model.

16), the results varied. For runs 13 and 15, in which a single natural mortality was used for all ages and was estimated in the assessment models, key assessment outputs, including spawning outputs, selectivity, and distributions of estimated h values, were very similar to runs 9 and 11 (Tables 3 and 4; Figs. 8–10). Estimated values of natural mortality (M) were also very close to the true underlying M values (Table 5).

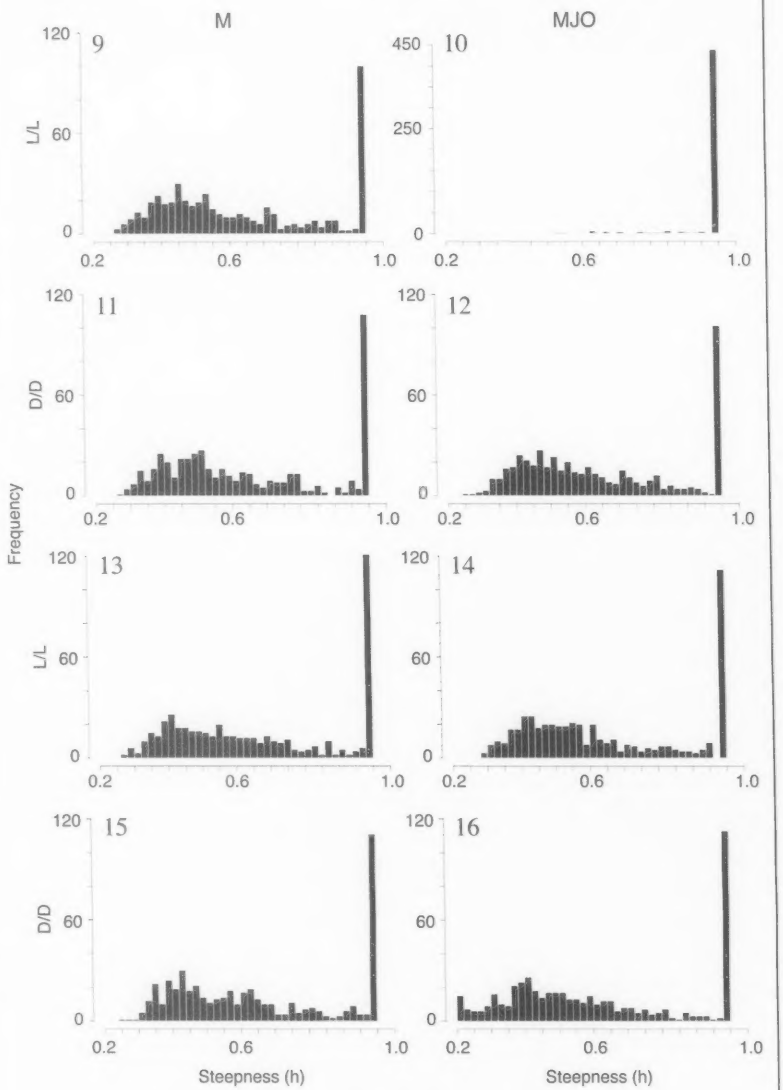

Figure 10

Frequency plots of estimated steepness (h) in stock synthesis assessment model for runs 9 to 16. The run number is shown in the upper left of each graph. True steepness value is 0.6. No prior for h was used in the assessment models. Specifications for each panel are: M=constant M and MJO=high M in juvenile and old fish; L/L=logistic selectivity in both simulation and assessment models; D/D=double normal selectivity in both simulation and assessment models; D/L=double normal selectivity in simulation model but logistic selectivity in assessment model; and L/D=logistic selectivity in simulation model, but double normal selectivity in assessment model.

For run 14, which had the same model configuration as run 10, except that four natural mortality values were used in both the simulation and estimation models, the assessment outputs matched well with those in the simulation model (Table 3; Figs. 8 and 9). Estimated natural mortalities also matched reasonably well with

the true values (Table 5). For run 16, which had the same model configuration as run 12 except that four natural mortalities were used in both models, the assessment outputs matched very poorly with those in the simulation model (Table 3; Figs. 8 and 9). Spawning outputs of all years, including B_0, estimated by the assessment model were much higher than those in the simulation model (Table 3; panel 16 in Fig. 8), and selectivity was poorly fitted for old fish (panel 16, Fig. 9). Estimated natural mortalities for old fish (M_4) showed a bi-modal distribution (Fig. 11), and there were strong interactions between estimated M_4 and selectivity for old fish (e.g., fish at age 30) (Fig. 12). There was a high proportion of cases (394 out of 500, Fig. 12) where M was estimated to be very small (mean=0.03).

Patterns of convergence performance, between runs 9 to 12 and between runs 13 to 16, were very similar to those runs between runs 1 to 4 because these runs had the same setup for selectivities (Table 4).

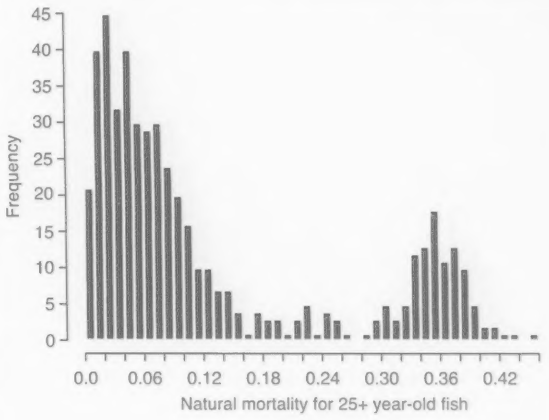

Figure 11

Frequency plots of estimated natural mortality for 25+ year-old fish (M_4) from run 16. True M_4 values ranged from 0.25 to 0.5, and no prior for steepness (h) was used in the assessment models.

Discussion

Our research has shown that the assumption of a constant natural mortality for all ages when natural mortality is actually elevated in young and old fish can lead to inaccurate estimates of many important population and management quantities. The manner in which selectivity is modeled is also very important in determining which assessment parameters are poorly estimated and how these interact with one another in the model.

In general, population depletion was well estimated, even when mortality and selectivity were incorrectly specified in assessment models because population depletion is a robust indicator of population status. This is mainly because depletion is estimated as the ratio of two quantities (terminal spawning output divided by virgin spawning output), both of which exhibit similar relative biases. Estimates of another management variable, i.e., the OFL, were consistently biased, although 95% quantile intervals overlapped zero for some runs. These results indicate that OFL may be a more precautionary management indicator than population depletion. However, more research is needed to compare these two indicators because OFL depends on F_{MSY} and biomass in the terminal year and estimates of these two quantities were strongly influenced by how natural mortality, selectivity and other population parameters were modeled in the assessment.

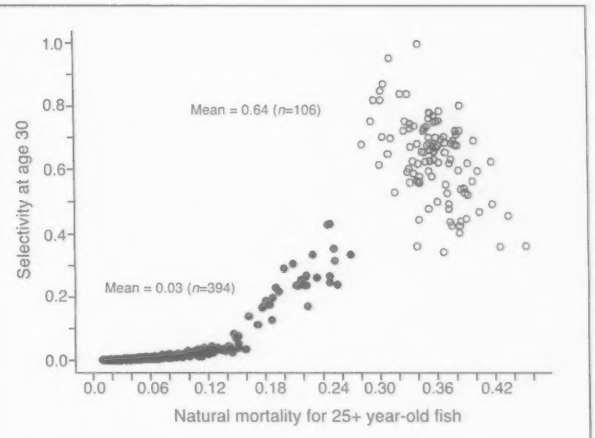

Figure 12

Estimated selectivity at age 30 versus natural mortality for 25+ year-old fish (M_4) from run 16. True M_4 values ranged from 0.25 to 0.5 and no prior for steepness (h) was used in the assessment models. Outputs were plotted in two separated groups based on the estimated M_4 values. The first group had estimated M_4 values ≤0.28 (solid dots) and the second had estimated M_4 values >0.28. Means on the graph are mean selectivities for age-30 fish.

Our results show that catchability coefficients for juvenile and adult surveys can be strongly positively biased if natural mortalities are higher in young and old fish but are misspecified in the estimation model, even when selectivity is correctly specified. If juvenile natural mortality is higher than that for adult fish, but is assumed to be the same as that for adult fish, catchability coefficients for juveniles from surveys of prerecruits are poorly estimated. In many stock assessments, these coefficients are unknown and are often very small numbers because relative abundance is measured in

surveys. In this case there is no logical way within the estimation model to identify these poorly estimated parameters. In cases where survey indices are derived to measure absolute population abundances, catchability coefficients for these survey indices could be estimated to be greater than unity because of misspecified natural mortality.

The best to model selectivity in stock assessment models poses great challenges. This is especially true in modeling the selectivity of old fish. That is, one must decide if asymptotic (i.e., logistic) or dome-shaped (i.e., double normal) selectivity should be used. In most cases, no field or experimental data exist to support the choice of which form of selectivity is appropriate. As shown in this study, decreased selectivity in old fish can erroneously be attributed to increased natural mortality in old fish, and stock assessment models cannot resolve this error. In addition, the available sampling data for old fish in either age or length compositions are typically rare and render the estimation of the descending portions of selectivity curves imprecise and uncertain. Moreover, misspecifications of selectivity for old fish can still lead to moderately incorrect estimates of population status and management parameters (runs 7, 8, 11, and 12). Such incorrect estimates can have a greater effect on population status if old fish have higher weight-specific fecundity than young spawners, as is the case in many rockfish species along the U.S. west coast (Dick, 2009).

Double normal selectivity has been widely used in recent stock assessments where the SS3 program was used. It has six parameters and is a very flexible selectivity function that can model a wide range of shapes for fishery selectivity (Methot, 2009a). Our study shows that double normal selectivity can sometimes lead to "unstable" estimations in stock assessment models. That is, the model may fail to converge properly, even in the absence of model specification error (runs 3 to 6, and runs 11 and 12). In the case of run 3, in which double normal selectivity is used in both the simulation and the assessment model, and natural mortality is also correctly specified, model runs succeeded only 86% of the time and the MGC criterion was satisfied only 81% of the time. This finding further highlights the difficulty in estimating the descending portion of a dome-shaped selectivity curve and the uncertainty in estimating selectivity parameters. Unstable descending curves have also been observed in some recent west coast groundfish assessments, where selectivities for the last age (length) group drops to a very small value (He et al., 2009). Further study on the stability of double normal selectivity may be needed to address this issue.

We also conducted additional runs, in which high natural mortalities were simulated only for juvenile fish, and only for old fish, but were assumed to be constant in assessment models. The results showed that if high natural mortalities in juvenile fish existed but were misspecified in the assessment model, catchability coefficients for surveys of juveniles would be estimated to be much higher in assessment models (from 2.5 to 3.6 as compared to the true value of 1.0). Other assessment results for runs with high natural mortalities in juvenile fish, however, were very similar to runs presented in this paper. If only high natural mortalities for old fish existed but were misspecified in the assessment model, assessment results would also be very similar to those of runs presented in this study with no biases in estimates for catchability coefficients for surveys of juveniles. This conclusion would indicate that effects of misspecifications of natural mortalities for juvenile and old fish on assessment results are mostly independent of each other.

Natural mortality has rarely been treated as an estimable parameter and has often been set as a constant in stock assessment models. Our study shows that, given informative age composition data, natural mortality can be estimated if M is constant across ages or selectivity is asymptotic. However, if M is high in both juvenile and old fish, and selectivity is dome-shaped, estimates of M for old fish are very unreliable because that parameter strongly interacts with selectivity. Because we examined only limited scenarios of data and model configurations, further and more detailed studies are needed to fully explore the feasibility and benefits of estimating natural mortality for fishery stock assessments.

Stock assessment models in this study were fitted to data from simulation models with known model structure and error variance. In all simulation runs, the stock-recruitment function variability parameter was fixed (S_R=0.5) and is relatively small compared to that of some stock assessments of the U.S. westcoast groundfish (Field et al., 2009; He et al., 2009; Wallace and Hamel, 2009). Given that the simulation data were much "better" than those available for most stock assessments, we found that it is still difficult to estimate the stock-recruitment relationship. As shown in runs 9 to 12, in which no priors for steepness (h) were given to the model, steepness was often estimated to be near or at the upper bound of 1.0 (Fig. 10), as has been found in other studies (Magnusson and Hilborn, 2007; Haltuch et al., 2008). This finding indicates that it is very difficult, if not impossible, to accurately estimate stock productivity in practice, where other uncertainties, such as model structures or lack of recruitment surveys, may further confound this issue (Haltuch et al., 2009). Test runs on the simulation and assessment models with much longer time periods (300-year runs with 200 years of fishing down and data outputs to assessment models) show that estimates of stock recruitment relationships were reasonably close to true values. But this long period of data collection is generally not available for stock assessments. In many previous studies, the difficulty in estimating stock recruitment relationships has been emphasized, and sufficient biological information and fisheries data, which are lacking in many fisheries, are required to achieve reasonable estimation for stock recruitment relationships (Myers et al., 1995; Rose et al., 2001; Magnusson and Hilborn, 2007; Conn et al., 2010). Further studies on how or if

stock-recruitment relationships can be estimated at given levels of recruitment variability, data availability, and stock contracts are needed to provide general guidelines for estimating stock-recruitment relationship in assessment models.

We believe that even with informative data and a correctly specified estimation model, there are strong interactions between natural mortality and fishery selectivity in stock assessment models. Misspecification of both parameters can lead to poor estimates of important population and fishery parameters, which in turn can produce under- or over-estimates of important management quantities, such as stock depletion and OFL. Improvement in the assessment modeling approach itself may not resolve these problems because of the interdependence of mortality, selectivity, and stock recruitment functions within the models. Uncertainty analysis of stock assessment models on age- or length-specific mortality and selectivity is also needed and should be included for assessments of model performance and for management of assessed stocks.

Acknowledgments

We thank E. Dick and J. Field for helpful comments on earlier versions of the manuscript. We also thank three anonymous reviewers for very helpful and constructive comments on earlier versions of the manuscript.

Literature cited

Alverson, D. L., and M. J. Carney.
1975. A graphic review of the growth and decay of population cohorts. J. Cons. Int. Explor. Mer 36:133–143.

Clark, W. G.
1999. Effects of an erroneous natural mortality rate on a simple age-structured stock assessment. Can. J. Fish. Aquat. Sci. 56:1721–1731.

Conn, P. B, E. H. Williams, and K. W. Shertzer.
2010. When can we reliably estimate the productivity of fish stocks. Can. J. Fish. Aquat. Sci. 67:511–523.

Dick, E. J.
2009. Modeling the reproductive potential of rockfishes (*Sebastes* spp.). Ph.D. diss., 353 p. Univ. California, Santa Cruz, CA.

Dorn, M. W.
2002. Advice on west coast rockfish harvest rates from Bayesian meta-analysis of stock-recruit relationships. N. Am. J. Fish. Manag. 22:280–300.

Field, C. F., D. J. Dick, D. Pearson, and A. D. MacCall.
2009. Status of bocaccio, *Sebastes paucispinis*, in the Conception, Monterey and Eureka INPFC area for 2009. Status of the Pacific coast groundfish through 2009, stock assessment and fishery evaluation: stock assessment, STAR panel report, and rebuilding analysis, 255 p. [Available from Pacific Fishery Management Council, 7700 NE Ambassador Place, Suite 101, Portland, OR 97220-1384.]

Fu, C., and T. J. Quinn II.
2000. Estimability of natural mortality and other population parameters in a length based model: *Pandalus borealis* in Kachemak Bay, Alaska. Can. J. Fish. Aquat. Sci. 39:1195–1207.

Gislason, H., N. Daan, J. C. Rice, and J. G. Pope.
2010. Size, growth, temperature and the natural mortality of marine fish. Fish Fish. 11:149–158.

Gunderson, D. R.
1980. Using r-K selection theory to predict natural mortality. Can. J. Fish. Aquat. Sci. 37:2266–2271.
1997. Trade-off between reproductive effort and adult survival in oviparous and viviparous fishes. Can. J. Fish. Aquat. Sci. 54:990–998.

Haltuch, M. A., A. E. Punt, and M. W. Dorn.
2008. Evaluating alternative estimators of fishery management reference points. Fish. Res. 94:290–303.
2009. Evaluating the estimation of fishery management reference points in a variable environment. Fish. Res. 100:42–56.

He, X, D. E. Pearson, D. J. Dick, J. C. Field, S. Ralston, and A. D. MacCall.
2009. Status of the widow rockfish resource in 2009. Status of the Pacific coast groundfish through 2009, stock assessment and fishery evaluation: stock assessment, STAR panel report, and rebuilding analysis, 187 p. [Available from Pacific Fishery Management Council, 7700 NE Ambassador Place, Suite 101, Portland, OR 97220-1384.]

Hoening, J. M.
1983. Empirical use of longevity data to estimate total mortality rates. Fish. Bull. 82:898–903.

Jensen, A. L.
1996. Beverton and Holt life history invariants result from optimal trade-off of reproduction and survival. Can. J. Fish. Aquat. Sci. 53:820–822.

Lapointe, M. F., R. M. Peterman, and A. D. MacCall.
1989. Trends in fishing mortality rate along with errors in natural mortality rate can cause spurious time trends in fish stock abundances estimated by virtual population analysis (VPA). Can. J. Fish. Aquat. Sci. 46:2129–2139.

Lapointe, M. F., R. M. Peterman, and B. J. Rothschild.
1992. Variable natural mortality rates inflate variance of recruitments estimated from virtual population analysis (VPA). Can. J. Fish. Aquat. Sci. 49:2020–2027.

Lorenzen, K.
1996. The relationship between body weight and natural mortality in juvenile and adult fish: a comparison of natural ecosystems and aquaculture. J. Fish Biol. 49:627–647.

Magnusson, A., and R. Hilborn.
2007. What makes fisheries data informative? Fish Fish. 8:337–358.

Mangel, M.
2003. Environment and longevity: the demography of the growth rate. *In* Life span: evolutionary, ecological, and demographic perspectives, Supplement to population and development review (J. R. Carey and S. Tuljapurkar, eds.), p. 57–70. Population Council, New York.

Mertz, G., and R. A. Myers.
1997. Influence of errors in natural mortality estimates in cohort analysis. Can. J. Fish. Aquat. Sci. 54:1608–1612.

Methot, R. D.
2009a. User manual for stock synthesis, model vers. 3.04b, 143 p. Northwest Fisheries Science Center, NOAA Fisheries, 2725 Montlake Boulevard East, Seattle, WA.
2009b. Stock assessment: operational models in support of fisheries management. *In* The future of fisheries

science in North America, vol. 31 (R. J. Beamish and B. J. Rothschild, eds.), p. 137–165. Fish & Fisheries Series, Springer Science, Hoboken, NJ.

Moustahfid, H., J. S. Link, W. J. Overholtz, and M. C Tyrrell.
2009. The advantage of explicitly incorporating predation mortality into age-structured stock assessment models: an application for Atlantic mackerel. ICES J. Mar. Sci. 66:445–454.

Myers, R. A., N. J. Barrowman, J. A. Hutchings, and A. A. Rosenberg.
1995. Population dynamics of exploited fish stocks at low population levels. Science 269:1106–1108.

Myers, R. A., and R. W. Doyle.
1983. Predicting natural mortality rates and reproduction-mortality trade-offs from fish life history data. Can. J. Fish. Aquat. Sci. 40:612–620.

PFMC (Pacific Fishery Management Council).
2008. Status of the Pacific coast groundfish fishery through 2008, stock assessment and fishery evaluation: stock assessments, STAR panel reports, and rebuilding analyses, 13 p. [Available from Pacific Fishery Management Council, 7700 NE Ambassador Place, Suite 101, Portland, OR 97220-1384.]

Punt, A. E.
2003. Evaluating the efficacy of managing west coast groundfish resources through simulation. Fish. Bull. 101:860–873.

Punt, A. E. and T. I. Walker.
1998. Stock assessment and risk analysis for the school shark (*Galeorhinus galeus*) off southern Australia. Mar. Freshw. Res. 49:719–731.

Pauly, D.
1980. On the interrelationships between natural mortality, growth parameters, and mean environmental temperature in 175 stocks. J. Cons. Int. Explor. Mer 39:175–192.

Quinn, T. J., II, and R. B. Deriso.
1999. Quantitative fish dynamics, 542 p. Oxford Univ. Press. New York.

Roff. D. A.
1992. The evolution of life histories, 535 p. Chapman and Hall, New York.

Rose, K. A., J. H. Cowan, K. O. Winemiller, R. A. Myers, and R. Hilborn.
2001. Compensatory density dependence in fish populations: importance, controversy, understanding and prognosis. Fish Fish. 2:293–327.

Schnute, J. T. and L. J. Richards.
1995. The influence of error on population estimates from catch-age models. Can. J. Fish. Aquat. Sci. 52:2063–2077.

Thompson, G. G.
1994. Confounding of gear selectivity and the natural mortality rate in cases where the former is a nonmonotone function of age. Can. J. Fish. Aquat. Sci. 51:2654–2664.

Vetter, E. F.
1988. Estimation of natural mortality in fish stocks: a review. Fish. Bull. 86:25–43.

Wallace, J. R., and O. S. Hamel.
2009. Status and future prospects for the darkblotched rockfish resources in waters off Washington, Oregon, and California as updated in 2009. Status of the Pacific coast groundfish through 2009, stock assessment and fishery evaluation: stock assessment, STAR panel report, and rebuilding analysis, 179 p. [Available from Pacific Fishery Management Council, 7700 NE Ambassador Place, Suite 101, Portland, OR 97220-1384.]

Wang, S. P., C. L. Sun, A. E. Punt, and S. Z. Yeh.
2006. Application of the sex-specific age-structured assessment method for swordfish, *Xiphias gladius*, in the North Pacific Ocean. Fish. Res. 84:282–300.

Worm, B., R. Hilborn, J. K. Baum, T. A. Branch, J. S. Collie, C. Costello, M. J. Fogarty, E. A. Fulton, J. A. Hutchings, S. Jennings, O. P. Jensen, H. K. Lotze, P. M. Mace, T. R. McClanahan, C. Minto, S. R. Palumbi, A. M. Parma, D. Ricard, A. A. Rosenberg, R. Watson, and D. Zeller.
2009. Rebuilding global fisheries. Science 325:578–585.

Yin, Y., and D. B. Sampson.
2004. Bias and precision of estimates from an age-structured stock assessment program in relation to stock and data characteristics. N. Am. J. Fish. Manag. 24: 865–879.

Appendix: Description of simulation model and data errors

The population is age-structured and is assumed to be subject to one fishery with constant selectivity over years. There are two survey indices. Recruits vary over years and there are sampling errors in surveys, catches, and age-composition data.

Initial condition and cohort growth

Initial conditions of the population are numbers of fish at sex x, at age a, and at the first model year (y=0), which is given by the equation

$$N_{x,0,a} = \begin{cases} 0.5R_0 & \text{if } a = a_{\min} \\ N_{x,0,a-1}e^{-M_{x,a}} & \text{if } a_{\min} < a < 3 * a_{\max} \end{cases}, \quad (1)$$

where R_0 = initial (virgin) recruitment;
a_{min} = age of recruitment (minimum age in model);
a_{max} = maximum age, including age-plus groups; and
$M_{x,a}$ = natural mortality for sex x, at age a, which is constant across years, and can be constant or vary by age, depending on the model setup.

Population dynamics

The numbers of fish in subsequent years are given by the equations

$$N_{x,y,a} = \begin{cases} 0.5R_y & \text{if } a = a_{\min} \\ N_{x,y-1,a-1}e^{-\left(M_{x,a}+F_{x,y-1,a}\right)} & \text{if } a_{\min} < a < a_{\max} \\ N_{x,y-1,a-1}e^{-\left(M_{x,a}+F_{x,y-1,a_{\max}}\right)} + N_{x,y-1,a_{\max}}e^{-\left(M_{x,a}+F_{x,y-1,a_{\max}}\right)} & \text{if } a = a_{\max} \end{cases}, \quad (2)$$

where R_y = expected recruitment at year y and is modeled by the Beverton-Holt stock recruit relationship:

$$R_y = \frac{SO_y}{\alpha + \beta SO_y}, \quad (3)$$

where R_y = recruitment at year y;
SO_y = spawning output at year y; and
α and β are recruitment parameters.

The relationship can be reparameterized by using a steepness parameter (h):

$$\alpha = \frac{\frac{B_0}{R_0}(1-h)}{4h}, \quad (4)$$

and

$$\beta = \frac{5h-1}{4hR_0}, \quad (5)$$

where B_0 is virgin spawning output (B_0=SO_0), and
R_0 is defined previously.

The "steepness" is the expected fraction of R_0 at 0.2 B_0 and is set to range from 0.2 to 1.0. When h=0.2, recruits are a linear function of spawning output (β=0, and $R_y = \frac{1}{\alpha} SO_y$). When h=1, recruits are constant and independent of spawning output (α=0, and $R_y = \frac{1}{\beta}$). In the simulation, R_y is replaced by actual annual recruitment (R_y^1, see Eq. 15) which includes annual recruitment deviation (R_y^δ).

Selectivity, fishing mortality, and catch

Selectivity is same for both sexes. Logistic selectivity is given by the equation

$$S_a = \frac{1}{1 + e^{-\ln(19)(a-\eta_2)/\eta_1}}, \quad (6)$$

where η_1, and η_2 are selectivity parameters.

Double normal selectivity is a special function for selectivity used by the SS3 program with two normal functions jointed by smooth functions. Details of this special function are given in Methot (2009a). There are six parameters in this selectivity function: (η_1) ascending inflection age; (η_2) width of plateau expressed as logistic between maximum selectivity and maximum age; (η_3) logarithm of ascending width; (η_4) logarithm of descending width; (η_5) selectivity at age 0 expressed as logistic between 0 and 1; and (η_6) selectivity at maximum age expressed as logistic between 0 and 1.

Fishing mortality is given by

$$F_{x,y,a} = FF_y S_a, \quad (7)$$

where FF_y = full fishing mortality for year y; and
S_a = selectivity at age at.

Annual catch by fishery at sex x, and age a is given by

$$C_{x,y,a} = N_{x,y,a} \frac{F_{x,y,a}}{M_x + F_{x,y,a}} \left(1 - e^{-(M_{x,a} + F_{x,y,a})}\right). \quad (8)$$

Landing by fishery f at year y, ψ_y, is given by

$$\Psi_y = \sum_x \sum_a C_{x,y,a} W_{x,a}, \quad (9)$$

where $W_{x,a}$ = weight of fish at sex x an age a, which is assumed to be constant for all years.

Growth, weight and spawning output

Growth and length-weight relationship are given by

$$L_{x,a} = L_x^\infty \left(1 - e^{-K_x(a - t_x^0)}\right) \quad (10)$$

$$W_{x,a} = \tau_1 L_a^{\tau_2}, \quad (11)$$

where $L_{x,a}$ = length at sex x and age a;
L_x^∞, K_x, and t_x^0 = growth parameters for sex x; and
$\tau_1$and τ_1 = length-weight parameters.

Annual biomass B_y is given by

$$B_y = \sum_x \sum_a N_{x,y,a} W_{x,a}. \quad (12)$$

Annual spawning output is given by

$$SO_y = \sum_a P_a N_{1,y,a} G_a, \quad (13)$$

where P_a = proportion of mature females at age a; and
G_a = fecundity for female at age a.

Abundance index

The abundance index (I) for year y and survey i has the following relationship:

$$I_{y,i} = q_i \sum_x \sum_a N_{y,x,a} S_{x,a}, \quad (14)$$

where q_i = catchability coefficient for survey i;
$N_{y,x,a}$ = population abundance; and
$S_{x,a}$ = selectivity for sex x and age a.

When the abundance index ($I_{y,s}$) is outputted to the assessment model, a new index ($I'_{y,s}$) is created by adding sampling error to $I_{y,s}$ (see Eq. 16).

Recruit variability and sampling errors:

Estimated annual recruitment (R'_y), annual survey indices ($I'_{y,s}$), and annual landings (ψ'_y) are all subject to log-normal errors with zero means and their respective standard deviations:

$$R'_y = R_y e^{R''_y} \quad (15)$$

$$I'_{y,i} = I_{y,i} e^{I^{\delta}_{y,i}} \tag{16}$$

$$\Psi'_{y} = \Psi_{y} e^{\Psi^{\delta}_{y}} \tag{17}$$

where $R^{\delta}_{y} \sim N(0,\sigma^2_R)$, $I^{\delta}_{i,y} \sim N(0,\sigma^2_i)$, and $\Psi^{\delta}_{y} \sim N(0,\sigma^2_{\Psi})$.

Age-composition data are subject to multinomial sampling errors with a fixed number of aged fish (n) for all years:

$$X_{y,x,a} \in \{0,\ldots,n\} \tag{18}$$

$$\sum_{x}\sum_{a} X_{x,a} = n. \tag{19}$$

A meta-analytic approach to quantifying scientific uncertainty in stock assessments

Stephen Ralston (contact author)[1]

André E. Punt[2]

Owen S. Hamel[3]

John D. DeVore[4]

Ramon J. Conser[5]

Email address for contact author: Steve.Ralston@noaa.gov

[1] National Marine Fisheries Service
Southwest Fisheries Science Center
Fisheries Ecology Division
110 Shaffer Road
Santa Cruz, California 95060

[2] University of Washington
School of Aquatic and Fishery Science
1122 NE Boat Street
Seattle, Washington 98195

[3] National Marine Fisheries Service
Fishery Resource Analysis and Monitoring Division
2725 Montlake Blvd. East
Seattle, Washington 98112

[4] Pacific Fishery Management Council
7700 NE Ambassador Place, Suite 101
Portland, Oregon 97220

[5] National Marine Fisheries Service
Southwest Fisheries Science Center
Fisheries Resource Division
8604 La Jolla Shores Drive
La Jolla, California 92037

Abstract—Quantifying scientific uncertainty when setting total allowable catch limits for fish stocks is a major challenge, but it is a requirement in the United States since changes to national fisheries legislation. Multiple sources of error are readily identifiable, including estimation error, model specification error, forecast error, and errors associated with the definition and estimation of reference points. Our focus here, however, is to quantify the influence of estimation error and model specification error on assessment outcomes. These are fundamental sources of uncertainty in developing scientific advice concerning appropriate catch levels and although a study of these two factors may not be inclusive, it is feasible with available information. For data-rich stock assessments conducted on the U.S. west coast we report approximate coefficients of variation in terminal biomass estimates from assessments based on inversion of the assessment of the model's Hessian matrix (i.e., the asymptotic standard error). To summarize variation "among" stock assessments, as a proxy for model specification error, we characterize variation among multiple historical assessments of the same stock. Results indicate that for 17 groundfish and coastal pelagic species, the mean coefficient of variation of terminal biomass is 18%. In contrast, the coefficient of variation ascribable to model specification error (i.e., pooled among-assessment variation) is 37%. We show that if a precautionary probability of overfishing equal to 0.40 is adopted by managers, and only model specification error is considered, a 9% reduction in the overfishing catch level is indicated.

Manuscript submitted 20 September 2010.
Manuscript accepted 23 February 2011.
Fish. Bull. 109:217–231 (2011).

The views and opinions expressed or implied in this article are those of the author (or authors) and do not necessarily reflect the position of the National Marine Fisheries Service, NOAA.

It has long been recognized that precautionary measures in fisheries management should be related to the amount of uncertainty in the science that is used to evaluate stock status (Caddy and McGarvey, 1996; FAO, 1996). However, few fisheries jurisdictions have adopted precautionary harvest control rules that are designed to reduce "risk-neutral" point estimates of catch based on the amount of uncertainty in the estimates, although at least two examples of this type of precautionary approach exist in the management of marine mammal populations. The International Whaling Commission has adopted a management procedure for baleen whales where, for example, a posterior distribution for the output of a harvest control rule is computed, and the catch limit is set close to the 40th percentile of the distribution (IWC, 1999; Punt and Donovan, 2007). Likewise, with the potential biological removals method (Wade, 1998), the level of marine mammal take at which management action must occur is based on the 20th percentile of the most recent estimate of abundance.

The reauthorization of the Magnuson-Stevens Fishery Conservation and Management Act (MSA) in 2006 changed the requirements for how management actions are developed for U.S. fisheries. The eight Regional Fishery Management Councils are now required to set annual catch limits (ACLs) for all managed stocks that are "in the fishery." National Standard Guidelines have now been developed to assist in the implementation of the reauthorized act (Federal Register, 2009), which defines two sources of uncertainty that must be considered when establishing ACLs: 1) scientific uncertainty, including error pertaining to both the data and to parameter estimation; and 2) management uncertainty, which represents uncertainty in the efficacy of management practices that are designed to ensure that harvest limits are not exceeded. The focus of this study is on the first of these two sources of uncertainty.

Defining "scientific uncertainty" is not trivial. It is therefore not surprising that a variety of approaches have been taken to quantifying un-

certainty in fisheries assessments. Methods that aim to quantify the variance of assessment model outputs, given an assumed model structure, include asymptotic statistics, bootstrapping, and the use of Bayesian methods (Hilborn and Walters, 1992; Quinn and Deriso, 1999; Punt and Hilborn, 1997). These techniques are commonly applied in stock assessments, although they all are conditioned on some combination of 1) an assumed model structure; 2) prespecified parameters (e.g., natural mortality); 3) the particular data sets the analyst uses, which may be a subset of those available; and 4) the statistical weights that are assigned to the data elements. Moreover, it is often true that in assessments of data-poor species, more parameters are fixed than in those of data-rich species—a situation that leads to the paradoxical situation where estimates of uncertainty are frequently greater for assessments where more is known (e.g., Pribac et al., 2005). It is also not uncommon that estimated confidence intervals are later shown to have been unrealistically narrow (Stewart and Hamel, 2010).

Uncertainty associated with having selected a particular model from a set of competing models can be assessed by using sensitivity tests, and, in a few cases, model averaging has been used to account for uncertainty due to model structure (e.g., Brandon and Wade, 2006; Brodziak and Piner, 2010). Model averaging is only effective, however, when all selected models are fitted to the same data sets. In principle, Monte Carlo methods can be used to quantify model uncertainty if probabilities can be assigned to the various models and data sets under consideration (e.g., Restrepo et al., 1992). However, these methods are not without their limitations (Poole et al., 1997), and assigning probabilities to, for example, alternative values of a prespecified parameter can be difficult (e.g., Kolody et al., 2008).

The reauthorized MSA and National Standard Guidelines define the overfishing limit (OFL) as the current catch that results from fishing at a rate (F_{MSY}) that is expected to produce the long-term maximum sustainable yield (MSY); catches in excess of the OFL, or fishing mortalities in excess of F_{MSY}, constitute overfishing. Furthermore, the acceptable biological catch (ABC) is the maximum allowable ACL and is defined as a catch which is lower than the OFL to account for scientific uncertainty. On the U.S. west coast, the Pacific Fishery Management Council (PFMC) has adopted a policy of defining the ABC as the product of the OFL and a fractional factor or "buffer" that is based on the probability that the ABC exceeds the true (but unknown) OFL, a value termed P^* (Shertzer et al., 2008; PFMC, 2010). A P^*=0.5 is equivalent to fishing at F_{MSY}, with no precautionary reduction to account for scientific uncertainty. Thus, the approach adopted by the PFMC requires the development of an ABC control rule that maps a policy decision (P^*<0.5) to a buffer that is used to reduce the OFL to an ABC.

We outline and apply the approach developed by members of the Scientific and Statistical Committee of the PFMC to calculate these factors for groundfish and coastal pelagic species on the basis of results from historical analyses. With a historical analysis, we summarize the results of all the assessments that have been conducted for a particular stock. Importantly, repeat assessments conducted for the PMFC often incorporate a variety of changes that include many of the model specification problems identified above. Although our approach is purely empirical and somewhat *ad hoc*, it is a pragmatic way to address the new legislative requirement to account for scientific uncertainty and to set precautionary catch limits. It was formally adopted by the PFMC for use in setting total allowable groundfish catches for the 2011–12 biennium (PFMC, 2010).

Materials and methods

Sources of uncertainty

Calculation of an OFL typically involves three steps: 1) estimation of current exploitable biomass (B_t); 2) projection of the population biomass into the future for some number of years; and 3) application of an estimate of F_{MSY} to the forecasts of future biomass. Although there are clear uncertainties associated with each step, the Scientific and Statistical Committee elected to focus first and foremost on variation in the estimation of the biomass in the terminal year of groundfish and coastal pelagic species stock assessments. That biomass is a significant source of uncertainty is aptly illustrated in Figure 1, which shows the results of the 15 Pacific whiting (*Merluccius productus*) stock assessments that have been conducted for the PFMC over the last 18 years (Stewart and Hamel, 2010). It is instructive to examine this species because it is one of the most data-rich[1] stocks managed by the PFMC, is of substantial economic importance, and has been assessed largely on an annual basis for many years. However, estimates of biomass have been highly variable from a historical perspective, in spite of considerable scientific resources having been devoted to evaluating the status of this stock. Note, for example, that estimated spawning biomasses in 1985 ranged from 1.2 to 5.9×10^6 metric tons (t) over the 15 stock assessments, representing a 5-fold range in abundance.

There are many reasons for this type of "among" assessment variability in stock size estimates, including differences in 1) overall model structure; 2) altered fixed values and prior distributions for important parameters; 3) changes in the availability of data; 4) the composition of the review panel; 5) the makeup of the analytical team that conducted the assessment; and 6) the modeling software that was used. Impor-

[1] Data-rich stock assessments contain many informative data elements, which typically would include catch (landings+discards), life history information (growth, natural mortality, and reproductive parameters), annual age or length compositions sampled from the fishery, and trend indices.

tantly, these factors contribute to variation in all groundfish and coastal pelagic species stock assessments at the PFMC, collectively exhibit considerable variation among historical assessments. Moreover, it is unsettling to managers when stock size estimates fluctuate greatly from one assessment to the next because this fluctuation undermines confidence for scientific advice. Hence, we assert that quantifying and accounting for this source of uncertainty is the first and most important factor to consider when establishing a buffer between the OFL and the ABC. We recognize, however, that as the quantification of scientific uncertainty develops in the future it will be important to expand consideration to other sources of errors, including forecast uncertainty (Shertzer et al., 2008) and uncertainty in estimating optimal harvest rates (e.g., Dorn, 2002; Prager et al., 2003; Punt et al., 2008). Hence, quantification of variation as revealed here should be considered only a lower bound on total uncertainty. Moreover, even if both forecast and harvest rate uncertainty were incorporated into our analysis, we note that many other factors exist that would be difficult to quantify, including the effects of climate and ecosystem interactions on the estimation of OFLs.

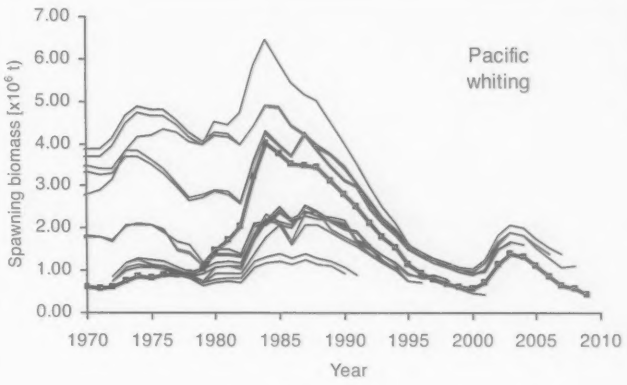

Figure 1

Biomass time series for Pacific whiting (*Merluccius productus*) based on 15 historical stock assessments conducted for the Pacific Fishery Management Council. The bold line with square symbols represents the most recent stock assessment used in the meta-analysis; the other lines represent time series of abundance developed from earlier assessments.

Quantifying biomass uncertainty

We initially consider two types of uncertainty in biomass estimation. The first is due to estimation error, also termed stochastic uncertainty (Pawitan, 2001). We quantify this type of uncertainty using the estimated coefficient of variation (CV) for the terminal-year biomass taken from the most recent stock assessment conducted. In a very limited number of studies (e.g., Pacific ocean perch [*Sebastes alutus*]), full Bayesian integration of uncertainty with Monte Carlo Markov Chain analysis has been achieved. However, on the U.S. west coast such cases are the exception. Hence, we report the asymptotic standard error for the estimate of terminal biomass developed by inverting the model's Hessian matrix as a first-order approximation of variation, i.e., the observed Fisher information statistic (Pawitan, 2001). The accuracy of this approximation depends on how well the log-likelihood surface at its maximum can be approximated by quadratic curvature, and on proper specification of the likelihood components, including appropriate error distributions and variance weightings.

We view this error estimate as a measure of statistical uncertainty within a stock assessment model that is conditioned on all the structural assumptions embedded within the model. We convert the asymptotic standard error to a CV by simple division using the terminal biomass estimate as the denominator. It is important to note that we limit our consideration to terminal-year biomass because under the reauthorized MSA, quantification of scientific uncertainty is used to prevent "overfishing," which occurs when 1) the current year catch exceeds the OFL; or 2) an updated assessment retrospectively indicates that fishing mortality exceeded F_{MSY}. Overfishing *per se* occurs only on an annual basis, although the chronic effect of overfishing results in stocks becoming depleted, and if fishing mortality is substantially greater than F_{MSY}, a stock will eventually become overfished.

The second type of uncertainty can be thought of as among-assessment variation, which is attributable to a wide variety of factors, many of which represent a significant form of model or inductive uncertainty (Pawitan, 2001). Assertion of asymptotic or dome-shaped selectivity patterns is one example, as is incorporation of age-dependent natural mortality. Assumptions regarding such structural issues will often change from one assessment to the next. Likewise, values for biologically important parameters (e.g., natural mortality or spawner-recruit productivity), which are prespecified when using auxiliary information (or expert judgment), may change, or an entire new data series may be incorporated into the assessment as new data become available. Beyond such changes in model specification, among-assessment variation includes other sources of variability due to, for example, differences in the reviewers who evaluated, suggested changes to, and ultimately approved an assessment model.

To quantify among-assessment variability we assembled time series of biomass from historical assessments of groundfish and coastal pelagic species

stocks. We excluded updated assessments, where data were simply refreshed and not extensively reviewed, because of strong constraints imposed on how much they could change from the last comprehensive assessment (PFMC[2]). When the definition of biomass changed among the available assessments (e.g., mid-year biomass in one assessment and beginning-year biomass in another), we used ratio estimation (Cochran, 1977) over a common time period to standardize to a common metric across all assessments that were conducted for that stock. We also limited the data points under consideration to no more than those that represent the last 20 years reported in the most recent assessment to focus attention on variation associated with the estimation of terminal year biomass. Finally, we trimmed the time series to include only the most recent 15, 10, and 5 years to evaluate the stability of the estimates of among-assessment uncertainty in relation to time interval selection criteria.

Variation in biomass estimates among a set of stock assessments can be quantified in a number of ways. We evaluated three approaches to calculating variation around a point of central tendency:

1 Consider all biomass estimates for a year as equally plausible representations of reality. Biomass variation between two stock assessments was quantified by forming all possible ratios of estimated biomasses in common years. Specifically, if there was an estimate of biomass (B) for year t from assessments i and j, we calculated: $R_{i|j,t} = B_{i,t}/B_{j,t}$, i.e., the proportional deviation of assessment i using assessment j as a standard. Based on a symmetry argument, we also calculated $R_{j|i,t}$ and all the ratios were $\log_e$-transformed. Note that because $\ln(R_{i|j,t})=-\ln(R_{j|i,t})$, the distributions were perfectly symmetrical. For each stock under consideration the standard deviation (σ^*) of the ratios was calculated. This statistic is positively biased, however, because it is based on the ratio of two lognormal random variables ($B_{i,t}$ and $B_{j,t}$). The appropriate bias correction term ($\sqrt{2}$) was derived (Mohr[3]) and applied so that the corrected estimator is $\sigma=\sigma^*/\sqrt{2}$. Thus, in the first approach we used the bias-adjusted estimate of the standard deviation of the $\ln(R_i|_{j,t})$ as a quantitative measure of among-assessment variation.
2 Consider the mean of biomass estimates in a year as the best estimate of central tendency. In this approach, variation in biomass was measured as squared deviations from the annual mean in log-space. Specifically, we calculated the mean log-biomass in year t as:

$$\overline{\ln[B_t]} = \frac{1}{n_t}\sum_i \ln[B_{i,t}],$$

where n_t is the number of available assessments in year t($n_t \geq 2$). The standard deviation (σ) is then calculated as follows:

$$\sigma = \sqrt{\frac{1}{\sum_t n_t - 1}\sum_t \sum_i (\ln[B_{i,t}] - \overline{\ln[B_t]})^2}.$$

3 Consider the most recent stock assessment as the best estimate of central tendency. This approach is the same as the second, except that the mean ($\overline{\ln[B_t]}$) is replaced by the logarithms of the biomass estimates from the most recent stock assessment, and the most recent year is excluded from the summations and the calculation of the n_t. With this approach, the most current information is assumed to represent the best estimate of the population mean.

For lognormally distributed random variables, the CV on the arithmetic scale is equal to

$$CV = \sqrt{\exp(\sigma^2) - 1},$$

where σ^2 is the variance on the logarithmic scale (Johnson and Kotz, 1970). We used this relationship to convert variances on the logarithmic scale to the arithmetic scale for comparison.

Meta-analytic inference for management

The PFMC groundfish fishery management plan includes approximately 90 species and, with the exception of "ecosystem component" species and stock complexes, OFLs, ABCs, and ACLs need to be developed for them all. However, less than 30% of the stocks listed in the fishery management plan have been assessed. Even among stocks that have been assessed, several have been studied only once. Therefore, historical biomass variation among assessments cannot routinely be estimated on a stock-specific basis. Thus, there is some merit in pooling results from well-studied species to develop estimates of meta-analytic proxy variance for all groundfish and coastal pelagic species stocks, and potentially even for those that have been assessed multiple times.

Based on management practices at the PFMC there are four natural groupings of species to consider, i.e., rockfish, roundfish, flatfish, and coastal pelagic species. The first three are groundfish categories that have group-specific proxy F_{MSY} harvest rates (Dorn, 2002; Ralston, 2002), whereas coastal pelagic species are managed in a separate fishery management plan. We considered two methods of pooling stock-specific variances: 1) take the square root of the average of the stock-specific variances; and 2) aggregate all the

[2] PFMC. 2008. Terms of reference for the groundfish stock assessment and review process for 2009_2010, 35 p. Pacific Fishery Management Council, 7700 NE Ambassador Place, Suite 101, Portland, Oregon 97220-1384. [Available at: http://www.pcouncil.org/wp-content/uploads/GF_Stock_Assessment_TOR_2009-102.pdf.]

[3] Mohr, Michael S. 2009. Groundfish ABC accounting for scientific uncertainty derivation of biomass scalar, 4 p. Unpubl. document submitted to Pacific Fishery Management Council Scientific and Statistical Committee. Author's address: NMFS, SWFSC, 110 Shaffer Rd., Santa Cruz, CA 95060.

residuals and calculate the standard deviation of the pooled set. The first method gives each species equal weight and does not overemphasize stocks that have been assessed many times (e.g., Pacific whiting). Conversely, the second method treats each data point as an independent observation. Neither approach is ideal given the lack of independence in the data.

Results

Most of the groundfish and coastal pelagic species stock assessments that have been conducted for the PFMC have employed the stock synthesis framework (Methot, 2000), which provides a very flexible, integrated modeling environment. For our analysis we considered only data-rich stocks that have been assessed more than once (15 groundfish and two coastal pelagic species stocks)—an approach that excluded many species from consideration. Owing to the large number of citations (81) needed to fully document the assessment literature of these stocks, all of which appear in the stock assessment and fishery evaluation documents produced by the PFMC, we present only summary information for each assessment that includes the stock, year, and authorship (Table 1)[4].

There is a preponderance of rockfish among the 17 species analyzed. The number of assessments included in the meta-analysis ranged from two (chilipepper [*Sebastes goodei*]) to a high of fifteen (Pacific whiting) (Table 2). Results presented in Figure 2 (A and B) show biomass trajectories from 1970 through 2009 for the 16 stocks that were not whiting stocks. Note that there is good correspondence among assessments for some species (e.g., darkblotched rockfish [*Sebastes crameri*]) and poor correspondence for others (e.g., shortspine thornyhead [*Sebastolobus alascanus*]). One should be cautious in interpreting this correspondence to indicate the degree of uncertainty in stock biomass because random variation in correspondence between species is to be expected. In the case of shortspine thornyhead, new information indicating dome-shaped selectivity was largely responsible for the large change in the biomass estimates for the 2005 assessment.

Comparisons of methods

When the assessment data were restricted to the last twenty years, the three approaches (all ratio combinations, deviations from the mean, and deviations from the most recent assessment) yielded average estimates of σ over all stocks equal to 0.382, 0.337, and 0.307, respectively. Approach two (i.e., squared deviations from the mean in log-space) was selected as the preferred method for calculating uncertainty by the Scientific and Statistical Committee because it had two desirable features, i.e., deviations were calculated from the best estimate of central tendency and estimated values of σ were unlikely to change markedly with new assessments (unlike approach three, which relies on the most recent assessment as the reference). Coincidently the calculation produced an intermediate result among the three approaches.

Similarly, a sensitivity test of the results to the number of years included in the calculation revealed that estimates of σ were robust to the time period used in the calculation. For example, when only the last 15 years of data were used, σ was 0.338 (compared with 0.337 for 20 years). Likewise, when the final 10 and 5 years of data were used, estimates of σ were 0.371 and 0.344, respectively. Note that in these latter two cases some species were excluded because of sparseness of data for these species. Hence, a standard temporal window equal to the last 20 years of assessment data was adopted as the basis for quantifying variation among stock assessments.

Stock-specific results

Figure 3 shows the distributions of residuals for the 17 stocks based on the selected approach. Note that some species (e.g., chilipepper and shortspine thornyhead) show a strongly bimodal distribution—a pattern that results when few assessments are available and biomass trajectories do not intersect. However, most of the distributions are unimodal, generally symmetric, and centered on or near zero.

Table 2 presents the number of deviations and the estimated log-scale standard deviation (σ) for each of the stocks, which collectively ranged from 0.103 (darkblotched rockfish) to 0.923 (shortspine thornyhead) with an average of 0.337. Also presented in the table are the estimated asymptotic coefficients of variation (CVs) for terminal biomass from the most recently completed stock assessment. These CVs, which approximate within-assessment estimation error, ranged from 9% (shortspine thornyhead and Dover sole [*Microstomus pacificus*]) to 41% (Pacific sardine [*Sardinops sagax*]), with a mean of 18%. This is undoubtedly an underestimate, however, because of the presence of key fixed parameters (e.g., natural mortality) in almost all the assessments we reviewed.

To compare among-assessment variation to within-assessment variation, the log-scale standard deviation estimates were expressed as CVs on the arithmetic scale (Johnson and Kotz, 1970), and the two statistics were plotted against one another (Figure 4). It is evident that shortspine thornyhead is an outlier, with the lowest "within" CV (stochastic uncertainty) and the highest "among" CV (inductive uncertainty). As a rule, among-assessment CVs (mean=36%) were greater than within-assessment CVs, as evidenced by the preponderance of points falling to the right side of the line of equality.

[4] Individuals should contact the PFMC (John.DeVore@noaa.gov) or visit http://www.pcouncil.org/groundfish/stock-assessments/ or http://www.pcouncil.org/coastal-pelagic-species/stock-assessment-and-fishery-evaluation-safe-documents/ for copies of specific assessment documents.

Table 1

Groundfish and coastal pelagic species stock assessments used in quantifying historical retrospective biomass variation.

Stock group	Species	Year	Author(s)[1]
Rockfish	bocaccio (*Sebastes paucisipinis*)	1996	Ralston et al.
		1999	MacCall et al.
		2002	MacCall
		2003	MacCall
		2009	Field et al.
	canary rockfish (*Sebastes pinniger*)	1994	Sampson and Stewart
		1996	Sampson
		1999	Crone et al.
		1999	Williams et al.
		2002	Methot and Piner
		2005	Methot and Stewart
		2008	Stewart
		2009	Stewart
	chilipepper (*Sebastes goodei*)	1998	Ralston et al.
		2008	Field
	darkblotched rockfish (*Sebastes crameri*)	2003	Rogers
		2005	Rogers
		2009	Wallace and Hamel
	Pacific ocean perch (*Sebastes alutus*)	1992	Ianelli et al.
		1998	Ianelli and Zimmerman
		2009	Hamel
	widow rockfish (*Sebastes entomelas*)	1997	Ralston and Pearson
		2000	Williams et al.
		2003	He et al.
		2006	He et al.
		2009	He et al.
	yelloweye rockfish (*Sebastes ruberrimus*)	2001	Wallace
		2002	Methot et al.
		2006	Wallace et al.
		2009	Stewart et al.
	yellowtail rockfish (*Sebastes flavidus*)	1991	Tagart
		1993	Tagart
		1996	Tagart and Wallace
		1997	Tagart et al.
		2000	Tagart et al.
		2005	Wallace and Lai
	shortspine thornyhead (*Sebastolobus alascanus*)	1994	Ianelli et al.
		2001	Piner and Methot
		2005	Hamel
Roundfish	cabezon (*Scorpaenichthys marmoratus*)	2004	Cope et al.
		2006	Cope and Punt
		2009	Cope and Key
	Pacific whiting (*Merluccius productus*)	1991	Dorn and Methot
		1992	Dorn and Methot
		1993	Dorn et al.
		1994	Dorn
		1995	Dorn
		1996	Dorn
		1997	Dorn and Saunders
		1999	Dorn et al.
		2002	Helser et al.

continued

Table 1 (continued)

Stock group	Species	Year	Author(s)[1]
Roundfish *(continued)*	Pacific whiting (*Merluccius productus*)	2004	Helser et al.
		2005	Helser et al.
		2006	Helser et al.
		2007	Helser and Martell
		2008	Helser et al.
		2009	Hamel and Stewart
	lingcod (*Ophiodon elongatus*)	2000	Jagielo et al.
		2003	Jagielo et al.
		2005	Jagielo and Wallace
		2009	Hamel et al.
	sablefish (*Anoplopoma fimbria*)	1992	Methot
		1994	Methot et al.
		1997	Crone et al.
		1998	Methot et al.
		2001	Schirripa and Methot
		2005	Schirripa and Colbert
		2007	Schirripa
Flatfish	Dover sole (*Microstomus pacificus*)	1997	Brodziak
		2001	Sampson and Wood
		2005	Sampson
	petrale sole (*Eopsetta jordani*)	1999	Sampson and Lee
		2005	Lai et al.
		2009	Haltuch and Hicks
Coastal pelagic	Pacific mackerel (*Scomber japonicus*)	2004	Hill and Crone
		2005	Hill and Crone
		2007	Dorval et al.
		2009	Crone et al.
	Pacific sardine (*Sardinops sagax*)	2004	Conser et al.
		2007	Hill et al.
		2009	Hill et al.

[1] Individuals should contact the PFMC (John.DeVore@noaa.gov) for copies of specific assessment documents or visit "http://www.pcouncil.org/groundfish/stock-assessments/" or "http://www.pcouncil.org/coastal-pelagic-species/stock-assessment-and-fishery-evaluation-safe-documents/".

Pooled results

Figure 5 shows the unweighted, pooled distributions of residuals for the four groupings of stocks. The distribution for rockfish is close to normal, whereas those for roundfish and flatfish exhibit some non-normal features. For example, the distribution for coastal pelagic species exhibits a tail to the left. However, the pooled estimates of σ are all rather similar, regardless of the method used to aggregate the data (Table 3). Although to some degree the point estimates of σ differ among groups, the sample sizes are also rather small. To explore whether the data provide support for treating each group separately, estimates of σ^2 were fitted by using a linear mixed model with group as a random effect. That analysis provided no support for stratification by group; the point estimate of the between-group variance was essentially zero ($<10^{-5}$).

Given the lack of support for among-group variation in σ, we combined the data over all stocks. In this instance, because the need to treat each species as a replicate is not required, method 2 (simple pooling of all residuals) is most justified. Aggregating the deviations over all stocks (Fig. 6) led to a point estimate of σ=0.358. If the residuals are assumed to be independent, an approximate 95% confidence interval for the statistic is $0.342 \leq \sigma \leq 0.374$.

Discussion

We evaluated three approaches for quantifying scientific uncertainty in the groundfish and coastal pelagic stock assessments that have been conducted over the last 20 years for the PFMC. We conclude that measurement of log-scale variability as deviations from the mean is a suitable analytical approach for measuring uncertainty in biomass estimates. Moreover, a comparison of stock- and group-specific estimates indicated that a single value of σ=0.36, which is equivalent to a CV of 37% on the arithmetic scale, is a reasonable lower-bound

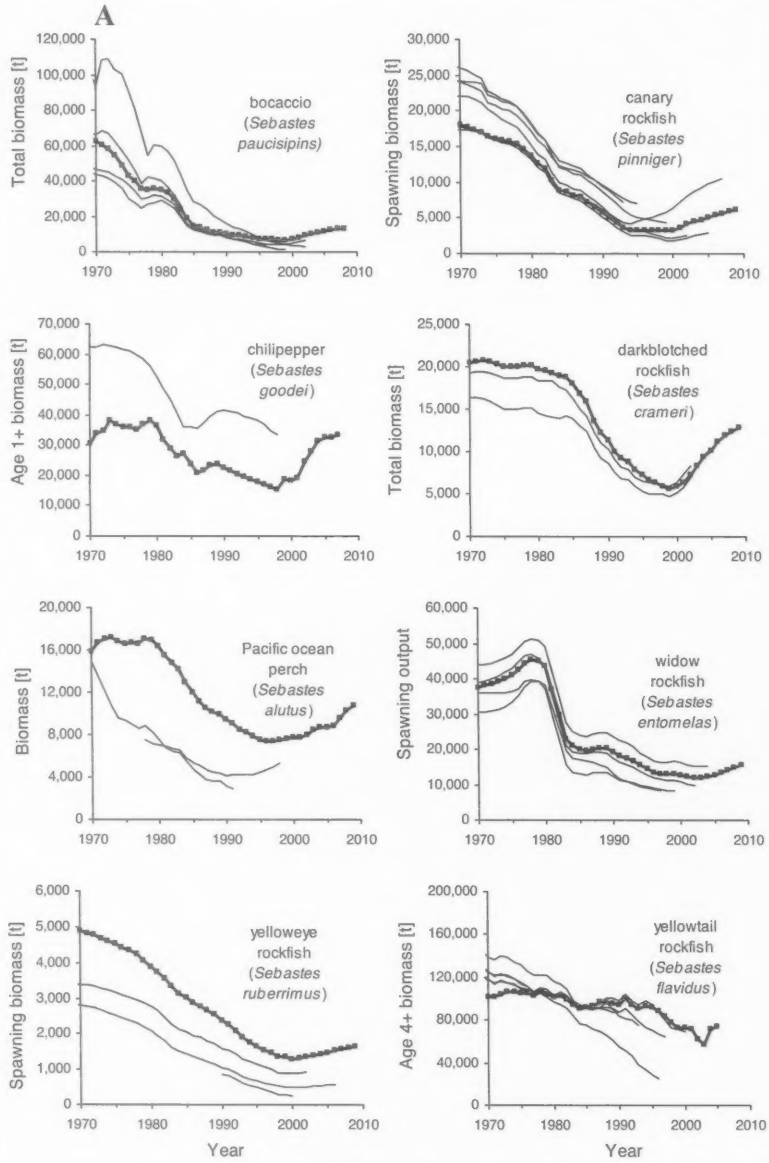

Figure 2

(**A** and **B**) Biomass time series for 16 selected groundfish and coastal pelagic species from stock assessments conducted for the Pacific Fishery Management Council on the west coast of the United States. In each panel the bold line with square symbols represents the most recent stock assessment that was completed, whereas the lighter lines represent biomass time series from earlier assessments.

proxy for all groundfish and coastal pelagic species stocks. Among all the 17 stocks listed in Table 2, only Pacific sardine yielded a Hessian-based "within" CV that is greater (41%). On average, variation among stock assessments was about twice that of the estimation error within assessments (18%).

Our approach is empirical and we simply strive to quantify variation in biomass estimates from repeats

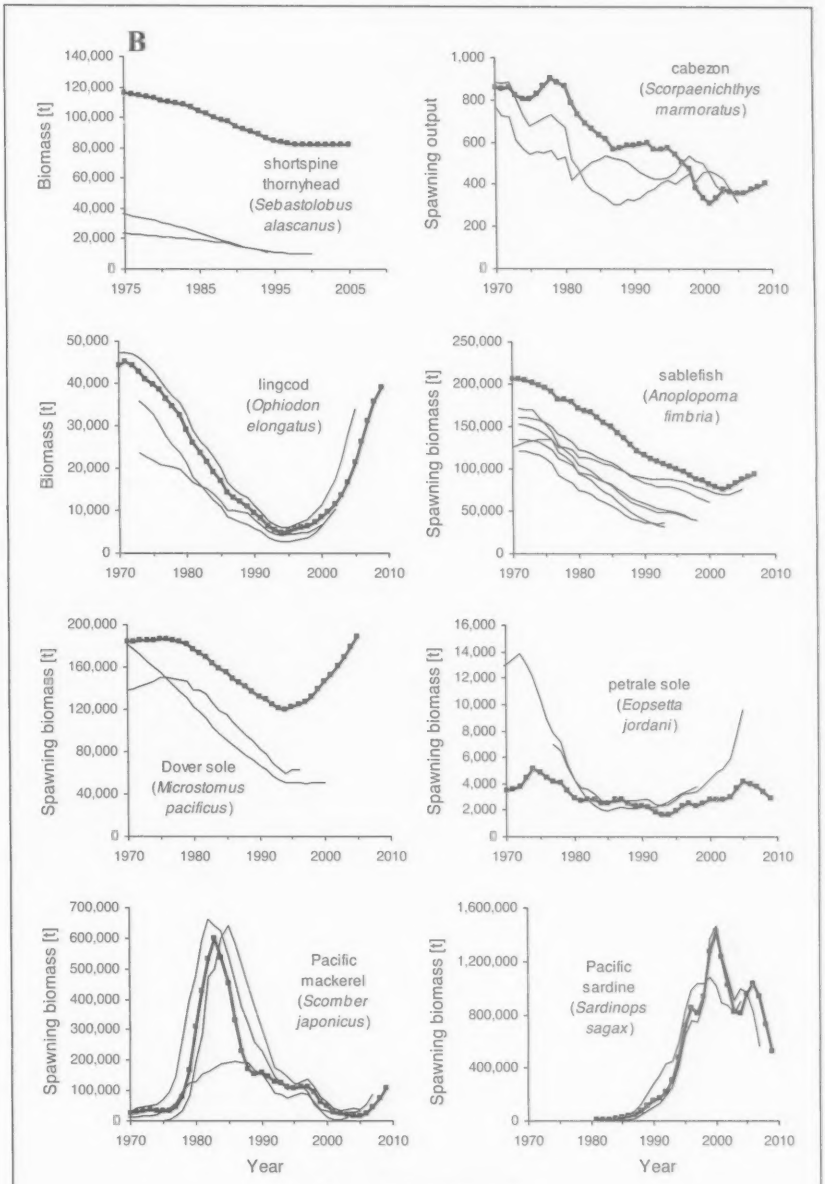

Figure 2 (continued)

of data-rich stock assessments that have been conducted for the PFMC. Although the approach lacks a theoretical basis, the method incorporates many of the factors that lead to model uncertainty, which we have shown is much greater than within-model estimation errors. One concern with the analysis is that calculation of uncertainty as squared deviations from the mean (approach 2) includes the assumption of the independence of the residuals, which is surely violated given that repeats of an assessment provide much the same data. Likewise, our findings pertain strictly to groundfish and coastal pelagic species found off the U.S. west coast. To the extent that the availability of data and the assessment "culture" in that region is distinctive (e.g., the use of the Stock Synthesis modeling platform and a willingness to adopt meta-analytic results as proxy metrics), our specific findings may not be of general use elsewhere. Even so, our general

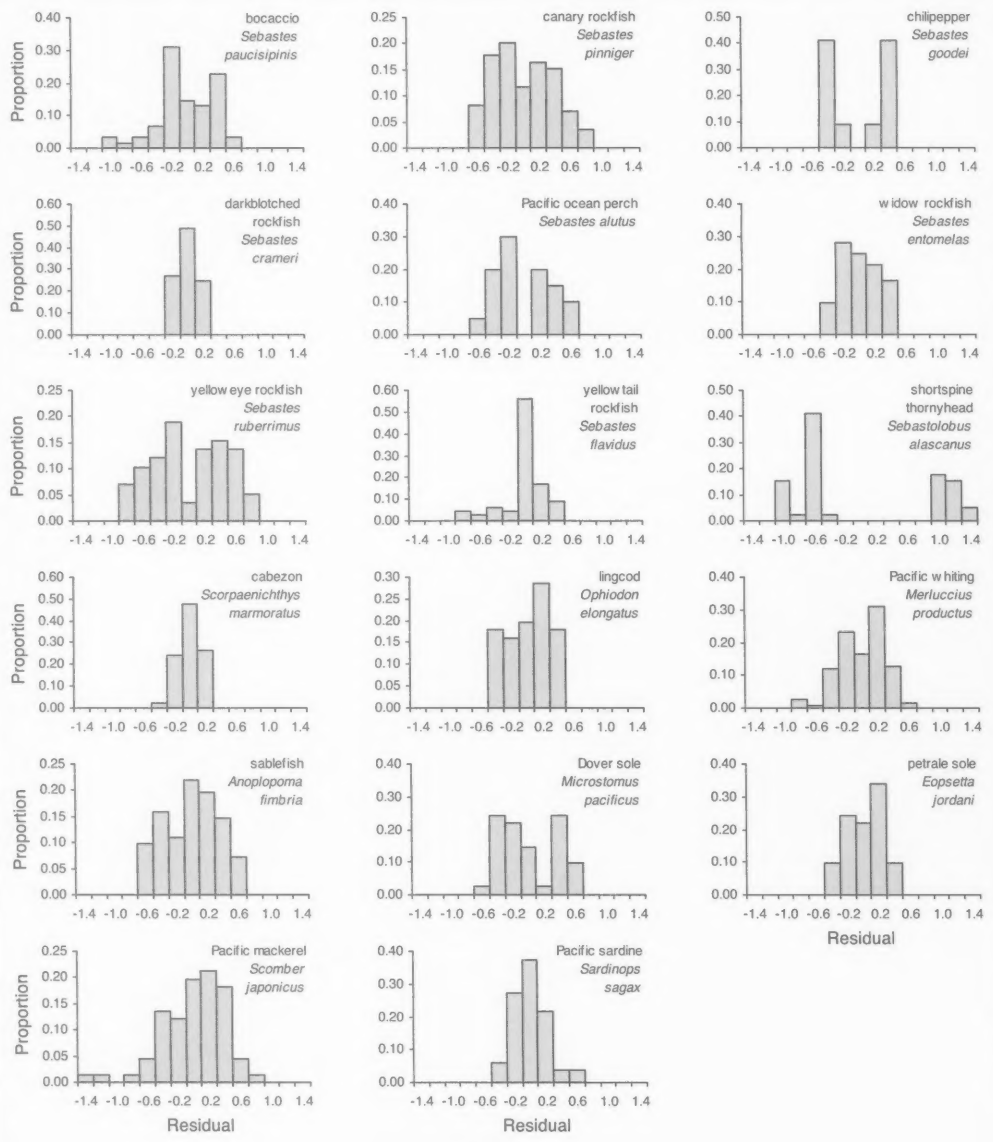

Figure 3

Frequency distributions of log-scale biomass deviations for selected groundfish and coastal pelagic species in stock assessments conducted for the Pacific Fishery Management Council. Residual deviations were calculated from annual means taken from the biomass time series presented in Figure 2 (**A** and **B**).

approach may prove useful for quantifying biomass uncertainty if it is applied in other geographical or management regions.

To illustrate how an estimate of log-scale variance can be used to form the basis of an ABC control rule, we exponentiate a lognormal distribution with a mean equal to zero and σ=0.36. Half of the probability density is then below a value of 1.00, which represents the median of the distribution. One can then select a cumulative probability less than 0.50 that maps onto a multiplier (=buffer) that can be interpreted as a reduction from the median of the distribution (Fig. 7). For example, 40% of the probability density is found at values ≤0.913. If one assumes that the median of

Table 2

Summary of stock-specific analyses of variation for estimates of terminal stock size from assessments of groundfish and coastal pelagic species. CV=coefficient of variation.

Stock group	Common name	Scientific name	No. of stock assessments	Squared deviations (n)	Log-scale standard deviation	Statistical uncertainty CV
Rockfish	bocaccio	*Sebastes paucispinis*	5	61	0.367	15%
	canary rockfish	*Sebastes pinniger*	8	85	0.375	15%
	chilipepper	*Sebastes goodei*	2	22	0.354	14%
	darkblotched rockfish	*Sebastes crameri*	3	45	0.103	13%
	Pacific ocean perch	*Sebastes alutus*	3	20	0.352	15%
	widow rockfish	*Sebastes entomelas*	5	61	0.241	31%
	yelloweye rockfish	*Sebastes ruberrimus*	4	58	0.492	14%
	yellowtail rockfish	*Sebastes flavidus*	6	66	0.269	24%
	shortspine thornyhead	*Sebastolobus alascanus*	3	39	0.923	9%
Roundfish	cabezon	*Scorpaenichthys marmoratus*	3	46	0.154	21%
	lingcod	*Ophiodon elongatus*	4	56	0.263	10%
	Pacific whiting	*Merluccius productus*	15	151	0.286	28%
	sablefish	*Anoplopoma fimbria*	7	82	0.340	10%
Flatfish	Dover sole	*Microstomus pacificus*	3	41	0.360	9%
	petrale sole	*Eopsetta jordani*	3	41	0.227	15%
Coastal pelagic	Pacific mackerel	*Scomber japonicus*	4	66	0.415	25%
	Pacific sardine	*Sardinops sagax*	3	51	0.206	41%

Table 3

Comparison of different methods of pooling stock-specific variance estimates. Method 1 weights each species equally, whereas method 2 weights each data point equally. In the table, σ is the standard deviation of log-scale anomalies from the mean.

Group	Number of stocks	σ Method 1	σ Method 2
rockfish	9	0.442	0.418
roundfish	4	0.269	0.281
flatfish	2	0.301	0.299
coastal pelagic	2	0.328	0.339
All stocks	17	0.337	0.358

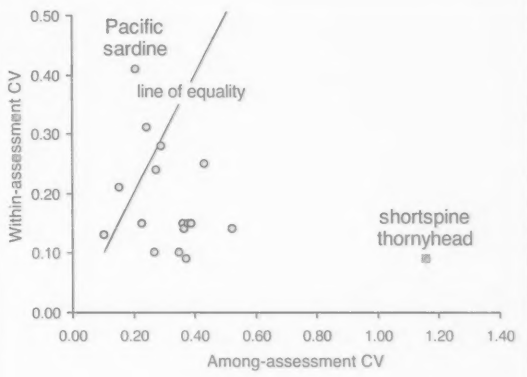

Figure 4

Relationship between the coefficients of variation (CV) calculated from biomass variation over multiple full stock assessments (x axis) and the CV based on the measurement error of the most recent analysis (y axis).

the lognormal distribution (1.00) is indicative of the best risk-neutral point estimate of catch (=OFL), 91% of that amount would be associated with a 0.40 probability of exceeding the true OFL.

Other approaches and future work

The approach outlined in this study is a pragmatic way to address the legislative requirement to calculate ABCs from OFLs, accounting for scientific uncertainty. Although the approach has been adopted and implemented as an ABC control rule for decision-making at the PFMC,[5] quantification of scientific uncertainty

[5] PFMC and NMFS. 2010. Proposed harvest specifications and management measures for the 2011–2012 Pacific Coast groundfish fishery and Amendment 16-5 to the Pacific Coast Groundfish Fishery Management Plan to update existing rebuilding plans and adopt a rebuilding plan for petrale sole: Draft environmental impact statement including Regulatory Impact Review and Initial Regulatory Flexibility Analysis. Pacific Fishery Management Council, Portland, OR (submitted to NOAA Fisheries Service), June 2010.

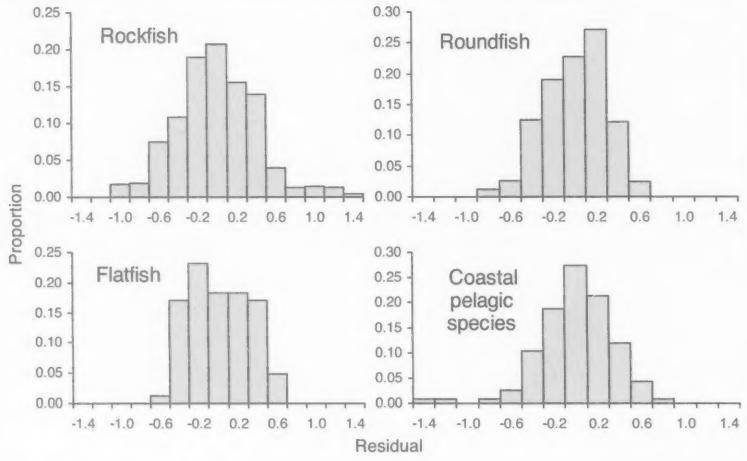

Figure 5

Composite distributions of log-deviations from the mean, pooled for four meta-analytic groupings (rockfish, roundfish, flatfish, and coastal pelagic species).

remains an active field of research. This fact is reflected by the range and changes over time in the ways that risk and uncertainty have been represented in fisheries assessments (see reviews by Francis and Shotton, 1997, and Patterson et al., 2001).

Our characterization of uncertainty does not include variability attributable to sources other than terminal-year biomass, which would tend to lead to negatively biased estimates of scientific uncertainty. Procedures for incorporating forecast uncertainty have been developed (Shertzer et al., 2008) and could be blended with our approach. Likewise, there is fertile ground to be explored with respect to uncertainty in F_{MSY}. Dorn (2002), for example, has developed a Bayesian prior for rockfish spawner-recruit steepness (h) that expresses uncertainty in estimates of stock productivity (see also Brooks et al., 2010). Because steepness maps almost directly onto F_{MSY} over a diverse range of groundfish life history patterns (Punt et al., 2008), a distribution of fishing mortality rates could be developed by mathematical composition of these functions, conditioned on the form of the stock-recruitment relationship. We assumed that estimates of F_{MSY} have negligible error and, as a consequence, uncertainty in OFL arises only from uncertainty in biomass estimates—an obvious simplification.

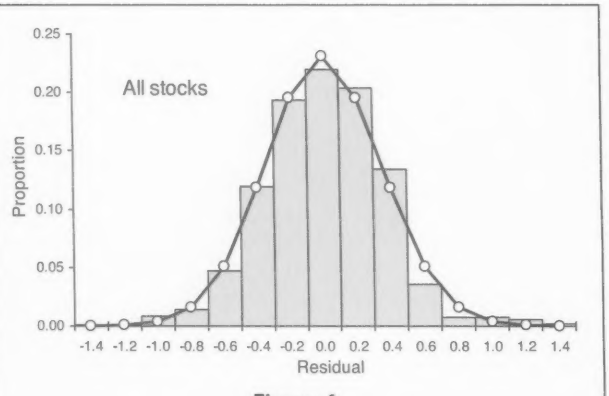

Figure 6

Aggregate distribution of log-deviations pooled over all 17 stocks with the fit of a normal distribution shown as the line with symbols (σ =0.36).

Although we elected to characterize uncertainty by analyzing variability in biomass estimates from historical stock assessments, an alternative approach might be to use decision table results, which are a required element in groundfish stock assessments. Specifically, the PFMC terms of reference for groundfish assessments[2] require the development of a decision table for use in characterizing uncertainty in stock assessments. The guidance states the following:

> Once a base model has been bracketed on either side by alternative model scenarios, which capture the overall degree of uncertainty within the assessment, a 2-way decision table analysis (states-of-nature versus management action) is the preferred way to present the repercussions of uncertainty to management. An attempt should be made to develop alternative model scenarios such that the base model is considered twice as likely as the alternative models, i.e., the ratio of probabilities should be 25:50:25 for the low stock size alternative, the base model, and the high stock size alternative.

It is therefore possible, in theory, to express uncertainty regarding biomass in a quantitative manner by appropriately weighting different states of nature presented in groundfish decision tables, which are derived through the collective expert opinion of the analytical team, the review panel, and the Scientific and Statistical Committee. A preliminary analysis of this approach has been completed, although a comprehensive analysis was not possible because of incomplete data in stock assessment documents. In particular, statistical weights for all three states of nature that are defined in the decision analysis (low, base, and high) have not always been explicitly expressed. When a characterization of the relative probabilities of the various states of nature under consideration is lacking, decision tables provide a type of risk assessment, but they are inadequate for risk management (*sensu* Francis and Shotton, 1997). Still, in three of the nine cases examined, variances from decision tables were greater than a CV=37%. We view these preliminary findings as promising and recommend that a thorough analysis of statistically weighted states of nature be considered as an alternative approach to characterization of scientific uncertainty in groundfish stock assessments.

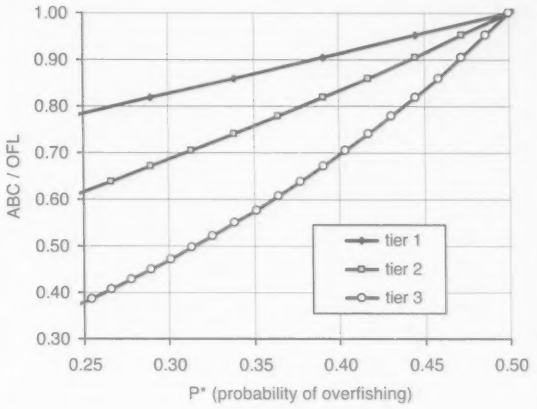

Figure 7

Relationship between the probability of overfishing (P^*) and an appropriate buffer between the allowable biological catch (ABC) and the overfishing level (OFL), based on varying amounts of uncertainty (σ=0.36, 0.72, and 1.44) assigned to different stock assessment tiers (1=data-rich, 2=data-moderate, and 3=data-poor), respectively.

Conclusions

Present and future management approaches for setting catch limits

This analysis was prepared in response to a pressing management need that arose from the requirements of the reauthorized MSA to implement ACLs by 2011. It is revealing to consider the ultimate impact of accounting for scientific uncertainty when setting catch limits at the PFMC. For all assessed groundfish species Table 4 provides the ABC and ACL as a percentage of the estimated F_{MSY} harvest level (OFL) as they were adopted by the PFMC in June 2010 (see footnote 5). Note that groundfish stocks are classified into three tiers based on the amount and quality of the information that is available for assessment modeling: tier-1 stocks are those for which there is data-rich information; tier-2 stocks are those for which there is data-moderate information; and tier-3 stocks are those for which there is data-poor information. Moreover, there was a consensus that scientific uncertainty cannot be lower for stocks that are more data limited. Hence, because σ=0.36 was derived from 81 tier-1 stock assessments, the Scientific and Statistical Committee recommended, and the PFMC elected to adopt, proxy estimates of uncertainty equal to double (0.72) and quadruple (1.44) σ for tier-2 and tier-3 stocks, respectively. This framework then provided a basis for separate ABC control rules for each tier. The PFMC then elected to adopt a P^*=0.45 for all tier-1 stocks and, with certain exceptions, P^*=0.40 for tier-2 and tier-3 stocks. Hence the scientific uncertainty buffers for the Council's data-rich stocks amounted to setting the ABC 4% below the OFL. Similarly, the adjustment for tier-2 stocks (σ=0.72 and P^*=0.40) was a 17% reduction (ABC=83% of the OFL) (Fig. 7). The differences between ACLs and ABCs shown in Table 4 reflect a variety of other factors, including 1) requirements for rebuilding overfished stocks; 2) harvest control rules for preventing stocks from becoming overfished; 3) socioeconomic considerations; 4) bycatch concerns for depleted species; 5) ecological considerations, and other factors.

Parsing scientific uncertainty in estimates of OFL from these other considerations was a particular challenge for the PFMC. Before the implementation of the new harvest specification framework recommended in the revised National Standard Guidelines, which were compelled by the reauthorized MSA, scientific and management uncertainties were considered jointly in setting optimum yields below the MSY harvest level. We have shown that quantifying scientific uncertainty in estimating exploitable biomass across multiple assessments through meta-analysis is a reasonable first approximation for explicitly accounting for uncertainty in preventing overfishing. Although all sources of error may not be have been considered with this approach, it was a helpful first step in the PFMC process. Importantly, with this approach the role of the Scientific and Statistical Committee in quantifying scientific uncertainty (by determining σ, a purely technical issue) and the role of the PFMC in deciding a preferred level of risk aversion to overfishing (by choosing P^*, which is a policy decision), are both duly respected. Coupling these two independent actions will help determine the ABC harvest level in a manner that is responsive to the mandates of the reauthorized MSA.

Table 4

Relative reductions from the overfishing limit (OFL) due to accounting for scientific and management uncertainty in setting 2011 groundfish allowable biological catches (ABCs) and annual catch limits (ACLs) at the Pacific Fishery Management Council (stocks in bold are overfished and their ACLs are based on rebuilding analyses). Tier 1=data rich; tier 2=data moderate; tier 3=data poor.

Stock/Complex	Tier	ABC ÷ OFL	ACL ÷ OFL
Bocaccio (*Sebastes paucispinis*)	1	96%	36%
Canary rockfish (*Sebastes pinniger*)	1	96%	17%
Cowcod (*Sebastes levis*)	2/3	76%	30%
Darkblotched rockfish (*Sebastes crameri*)	1	96%	59%
Pacific ocean perch (*Sebastes alutus*)	1	96%	18%
Widow rockfish (*Sebastes entomelas*)	1	96%	12%
Yelloweye rockfish (*Sebastes ruberrimus*)	1	96%	42%
Petrale sole (*Eopsetta jordani*)	1	96%	96%
Lingcod (OR & WA) (*Ophiodon elongatus*)	1	96%	96%
Lingcod (CA)	2	83%	83%
Pacific cod (*Gadus macrocephalus*)	3	69%	50%
Sablefish (*Anoplopoma fimbria*)	1	96%	77%
Shortbelly rockfish (*Sebastes jordani*)	2	83%	1%
Chilipepper (S 40°10′) (*Sebastes goodei*)	1	96%	96%
Splitnose rockfish (S 40°10′) (*Sebastes diploproa*)	1	96%	96%
Yellowtail rockfish (N 40°10′) (*Sebastes flavidus*)	1	96%	96%
Shortspine thornyhead (*Sebastolobus alascanus*)	1	96%	83%
Longspine thornyhead (*Sebastolobus altivelis*)	2	83%	70%
Black rockfish (WA) (*Sebastes melanops*)	1	96%	96%
Black rockfish (OR-CA)	1	96%	82%
California scorpionfish (*Scorpaena guttata*)	1	96%	96%
Cabezon (CA) (*Scorpaenichthys marmoratus*)	1	96%	96%
Cabezon (OR)	1	96%	96%
Dover sole (*Microstomus pacificus*)	1	96%	56%
English sole (*Parophrys vetulus*)	1	96%	96%
Arrowtooth flounder (*Atheresthes stomias*)	2	83%	83%
Starry flounder (*Platichthys stellatus*)	2	83%	75%
Longnose skate (*Raja rhina*)	1	96%	43%
Minor Nearshore rockfish North (species complex)	3	85%	85%
Minor Shelf rockfish North (species complex)	3	88%	44%
Minor Slope rockfish North (species complex)	3	91%	79%
Minor Nearshore rockfish South (species complex)	3	87%	87%
Minor Shelf rockfish South (species complex)	3	84%	32%
Minor Slope rockfish South (species complex)	3	92%	69%
Other Flatfish (species complex)	3	69%	48%
Other Fish (various) (species complex)	3	69%	50%

Acknowledgments

This study was generated, reviewed, and endorsed by members of the Pacific Fishery Management Council's Scientific and Statistical Committee, whom we would like to thank and acknowledge for their critical suggestions. In particular, members of the groundfish and coastal pelagic species subcommittees were most engaged in developing the analytical approach, including T. Barnes, L. Botsford, M. Dorn, S. Heppell, T. Jagielo, T. Tsou, and V. Wespestad. In addition, a number of people mined the primary PFMC stock assessment literature and provided us with a stock-specific time series of population abundance for use in the meta-analysis. In particular, we would like to offer our thanks to J. Cope (cabezon), P. Crone (Pacific mackerel), J. Field (bocaccio), M. Haltuch (petrale sole), X. He (widow rockfish), K. Hill (Pacific sardine), I. Stewart (canary rockfish, Pacific whiting, and yelloweye rockfish), and J. Wallace (yellowtail rockfish). Lastly, we appreciate the constructive reviews of this work that were provided by J. Cope, E.J. Dick, and A. MacCall. We also acknowledge the helpful comments of two anonymous reviewers and E. Williams who evaluated the manuscript for the journal.

Literature cited

Brandon, J., and P. R. Wade.
2006. Assessment of the Bering-Chukchi-Beaufort Seas stock of bowhead whales using Bayesian model averaging. J. Cet. Res. Manag. 8:225–239.

Brodziak, J., and K. Piner.
2010. Model averaging and probable status of North Pacific striped marlin, *Tetrapturus audax*. Can. J. Fish. Aquat. Sci. 67:793–805.

Brooks, E. N., J. E. Powers, and E. Cortés.
2010. Analytical reference points for age-structured models: application to data-poor fisheries. ICES J. Mar. Sci. 67:165–175.

Caddy, J. F., and R. McGarvey.
1996. Targets or limits for management of fisheries? N. Am. J. Fish. Manag. 16:479–487.

Cochran, W. G.
1977. Sampling techniques, 3rd ed., 429 p. John Wiley & Sons, New York.

Dorn, M. W.
2002. Advice on west coast rockfish harvest rates from Bayesian meta-analysis of stock-recruit relationships. N. Am. J. Fish. Manag. 22:280–300.

FAO (United Nations Food and Agriculture Organization).
1996. Precautionary approach to capture fisheries and species introductions. Technical guidelines for responsible fisheries, no. 2, 54 p. FAO, Rome.

Federal Register.
2009. Magnuson-Stevens Act Provisions; Annual Catch Limits; National Standard Guidelines; final rule. vol. 74, no. 11, January 16, p. 3178–3213. GPO, Washington, D.C.

Francis, R. I. C. C., and R. Shotton.
1997. "Risk" in fisheries management: a review. Can. J. Fish. Aquat. Sci. 54:1699–1715.

Hilborn, R., and C. J. Walters.
1992. Quantitative fisheries stock assessment—choice, dynamics, and uncertainty, 570 p. Kluwer Academic Publs., Boston.

IWC (International Whaling Commission).
1999. The report of the Scientific Committee, annex N. The revised management procedure (RMP) for baleen whales. J. Cet. Res. Manag. 1 (suppl.):251–258.

Kolody, D., T. Polacheck, M. Basson, and C. Davies.
2008. Salvaged pearls: lessons learned from a floundering attempt to develop a management procedure for southern bluefin tuna. Fish. Res. 94:339–350.

Johnson, N. L., and S. Kotz.
1970. Continuous univariate distributions, part 1, 300 p. Distributions in statistics. John Wiley & Sons, New York.

Methot, R. D.
2000. Technical description of the stock synthesis assessment program. NOAA Tech. Memo. NMFS-NWFSC-43, 46 p.

Patterson, K., J. Cook, C. Darby, S. Gavaris, L. Kell, P. Lewy, B. Mesnil, A. Punt, V. Restrepo, D. W. Skagen, and G. Stefansson.
2001. Estimating uncertainty in fish stock assessment and forecasting. Fish Fish. 2:125–157.

Pawitan, Y.
2001. In all likelihood—statistical modelling and inference using likelihood, 528 p. Oxford Univ. Press, Oxford.

PFMC (Pacific Fishery Management Council).
2010. FMP amendment addresses National Standard 1—annual catch limits, accountability measures. Pacific Council News 34(1):5. [Available at: http://www.pcouncil.org/wp-content/uploads/Spring_2010_Newsletter.pdf.]

Poole, D., G. H. Givens, and A. E. Raftery.
1997. A proposed stock assessment method and its application to bowhead whales, *Balaena mysticetus*. Fish. Bull. 97:144–152.

Prager, M. H., C. E. Porch, K. W. Shertzer, and J. F. Caddy.
2003. Targets and limits for management of fisheries: a simple probability-based approach. N. Am. J. Fish. Manag. 23:349–361.

Pribac, F., A. E. Punt, B. L. Taylor and T. I. Walker.
2005. Using length, age and tagging data in a stock assessment of a length selective fishery for gummy shark (*Mustelus antarcticus*). J. Northwest Atl. Fish. Sci. 35L:267–290.

Punt, A. E., and. G. Donovan.
2007. Developing management procedures that are robust to uncertainty: lessons from the International Whaling Commission. ICES J. Mar. Sci. 64:603–612.

Punt, A. E., M. W. Dorn, and M. A. Haltuch.
2008. Evaluation of threshold management strategies for groundfish off the U.S. west coast. Fish. Res. 94:251–266.

Punt, A. E., and R. Hilborn.
1997. Fisheries stock assessment and decision analysis: the Bayesian approach. Rev. Fish Biol. Fish. 7:35–63.

Quinn, T. J., II, and R. B. Deriso.
1999. Quantitative fish dynamics, 524 p. Oxford Univ. Press, New York.

Ralston, S.
2002. West coast groundfish harvest policy. N. Am. J. Fish. Manag. 22:249–250.

Restrepo, V. R., J. M. Hoenig, J. E. Powers, J. W. Baird, and S. C. Turner.
1992. A simple simulation approach to risk and cost analysis, with applications to swordfish and cod fisheries. Fish. Bull. 90:736–748.

Shertzer, K. W., M. H. Prager, and E. H. Williams.
2008. A probability-based approach to setting annual catch levels. Fish. Bull. 106:225–232.

Stewart, I. J., and O. S. Hamel.
2010. Stock assessment of Pacific hake, *Merluccius productus*, (a.k.a. whiting) in U. S. and Canadian waters in 2010, 290 p. [Available from Pacific Fishery Management Council, 7700 NE Ambassador Place, Suite 101, Portland, OR, 97220-1384.]

Wade. P. R.
1998. Calculating limits to the allowable human-caused mortality of cetaceans and pinnipeds. Mar. Mamm. Sci. 14:1–37.

Demographics by depth: spatially explicit life-history dynamics of a protogynous reef fish

Angela B. Collins (contact author)[1]
Richard S. McBride[2]

Email address for contact author: angela.collins@myfwc.com

[1] Florida Fish and Wildlife Conservation Commission
Fish and Wildlife Research Institute
100 8th Avenue SE
Saint Petersburg, Florida 33701

[2] Northeast Fisheries Science Center
National Marine Fisheries Service
National Oceanic and Atmospheric Administration
166 Water Street
Woods Hole, Massachusetts 02543

Abstract—Distribution and demographics of the hogfish (*Lachnolaimus maximus*) were investigated by using a combined approach of *in situ* observations and life history analyses. Presence, density, size, age, and size and age at sex change all varied with depth in the eastern Gulf of Mexico. Hogfish (64–774 mm fork length and 0–19 years old) were observed year-round and were most common over complex, natural hard bottom habitat. As depth increased, the presence and density of hogfish decreased, but mean size and age increased. Size at age was smaller nearshore (<30 m). Length and age at sex change of nearshore hogfish were half those of offshore hogfish and were coincident with the minimum legal size limit. Fishing pressure is presumably greater nearshore and presents a confounding source of increased mortality; however, a strong red tide occurred the year before this study began and likely also affected nearshore demographics. Nevertheless, these data indicate ontogenetic migration and escapement of fast-growing fish to offshore habitat, both of which should reduce the likelihood of fishing-induced evolution. Data regarding the hogfish fishery are limited and regionally dependent, which has confounded previous stock assessments; however, the spatially explicit vital rates reported herein can be applied to future monitoring efforts.

Manuscript submitted 29 September 2010.
Manuscript accepted 24 February 2011.
Fish. Bull. 109:232–242.

The views and opinions expressed or implied in this article are those of the author (or authors) and do not necessarily reflect the position of the National Marine Fisheries Service, NOAA.

Protogynous species require special management considerations when fishing reduces the probability of survival to the male phase. Selective harvesting of males may skew the sex ratio and reduce the reproductive capacity of a population by increasing the probability of sperm limitation (Hamilton et al., 2007). Also, selective removal of a particular sex or size class over many generations can have evolutionary consequences, including slower growth rates, reduced size at maturation, and earlier sexual transformation (Harris and McGovern, 1997; Adams et al., 2000; Brulé et al., 2003; Heppell et al., 2006). However, protogyny does not automatically imply elevated vulnerability to fishing if the population is able to compensate for reduced male survival (e.g., by earlier transition to the male phase). This ability to compensate is most likely to occur in species in which sex change is socially or environmentally mediated rather than constrained to a certain size or age (Alonzo and Mangel, 2005). Therefore, to predict stock dynamics and a species' response to fishing pressure, it is important not only to establish whether sex change occurs, but also to quantify the mechanisms that influence sex change and characterize the related demographics.

We synthesized data from *in situ* observations and life history collections to evaluate factors that could potentially influence the presence, density, and demographics of a reef fish. The hogfish (Labridae: *Lachnolaimus maximus*), which occurs from temperate to tropical waters of the western North Atlantic Ocean, Gulf of Mexico, and Caribbean Sea, was chosen for this study for several reasons. It is an economically important reef fish (for a list of total U.S. fishery landings and their estimated values see: www.st.nmfs.noaa.gov/st1/commercial/index.html, accessed February 2011), and a better understanding of its ecology will assist managers in evaluating regulatory options. The principal fishing method for this species is spearfishing (McBride and Richardson, 2007), which presents an opportunity to evaluate the effect of a single fishery sector with fewer confounding effects from other fishery sectors (e.g., hook-and-line). Hogfish can exceed 800 mm fork length (FL), weigh more than 10 kg, and live as long as 23 years (McBride and Richardson, 2007). These life-history characteristics allow a wide latitude for measuring differences in size and age. Finally, they are monandric, protogynous hermaphrodites (all fish begin life as female and can eventually change sex to male) (McBride and Johnson, 2007) that form harems, with a single male controlling 2–15 females (Davis, 1976; Colin, 1982; Claro et al., 1989). This mating system allowed for investigation of the effects of fishing, habitat, and other environmental variables on sex change and social structure.

Fishery regulations for hogfish were first implemented in 1994. The minimum size limit (305 mm FL) corresponded with the minimum length at sex change (Davis, 1976) and was established to protect spawning fish. However, concerns about the effectiveness of this size limit emerged when further research demonstrated that median size at sex change was significantly larger (~380 mm FL; McBride et al., 2008). Continual removal of the dominant male can impact the reproductive capacity of a population (Bannerot et al., 1987; Sluka and Sullivan, 1998). Under heavy fishing pressure, constant disruption of hogfish spawning harems could be problematic because several months are required to complete sex change (McBride and Johnson, 2007) and new males have lower reproductive success (Muñoz et al., 2010). A stock assessment in 2003 (Ault et al.[1]) stated that hogfish were undergoing overfishing in the U.S., but these findings were disputed because of concerns that catch and effort data were inadequate (Kingsley[2]). Under such conditions, demographic data may provide the only basis for setting management reference points (Brooks et al., 2010) and evaluating future monitoring strategies.

Data were collected through cooperation with the spearfishing community, and revealed abrupt, cross-shelf patterns in hogfish demographics. These findings highlight interactions between fishing operations and the environment on reef fish populations, specifically demonstrating that sex change mechanisms can be spatially explicit and that refuges may exist for larger spawners that survive long enough to reach offshore habitats.

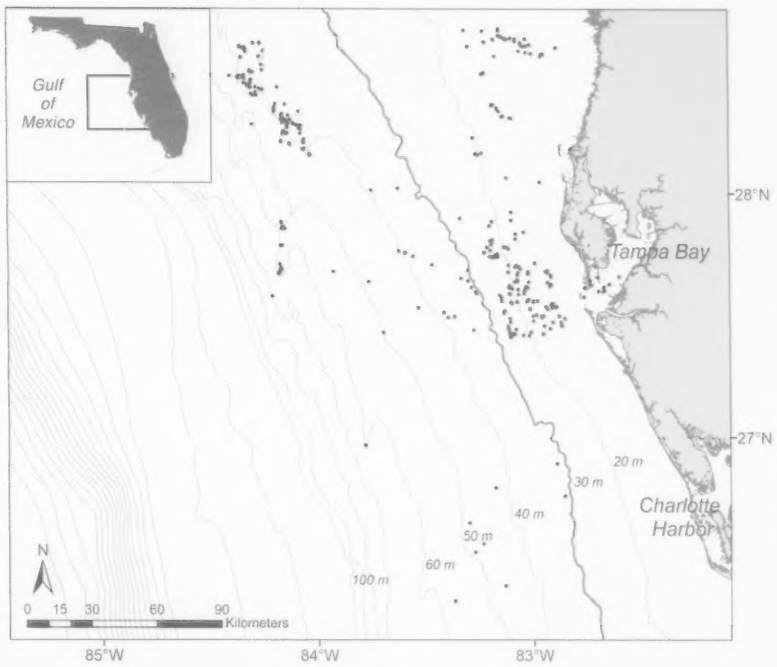

Figure 1

Study location in the central eastern Gulf of Mexico. Dive sites are indicated by dots (431 sites) and were surveyed for hogfish (*Lachnolaimus maximus*) between 2005 and 2007. Hogfish were harvested randomly from dive sites during scuba surveys. Bathymetry contours are isobaths and are labeled to 100 m; the 30-m isobath is bold and separates nearshore (<30 m) from offshore (≥30 m) sites.

Materials and methods

Sampling design

Visual observations and hogfish collections were made during scuba dives (to a depth of 69 m) in the central eastern Gulf of Mexico (Fig. 1). To investigate whether increasing depth and distance from shore affected hogfish distribution and demographics, scuba surveys were allocated to sample a range of depths and were categorized as nearshore (<30 m) or offshore (≥30 m). Thirty meters was chosen as the dividing point between the nearshore and offshore classification because many recreational divers do not exceed this depth on account of the reduced available bottom time and greater hazards associated with diving at deeper depths. Additionally, this 30-m depth corresponds roughly with a distance of 40–50 km from land, beyond which travel becomes more costly in terms of travel time, fuel expense, and risks associated with adverse weather. Sites were also examined by 10-m depth intervals to identify whether there were finer scale effects of depth on hogfish distribution.

Habitat was characterized into one of three major categories according to bottom type and relief: 1) natural habitat of rugose hard bottom with a maximum vertical relief >0.5 m, typically limestone outcroppings

[1] Ault, J. S., S. G. Smith, G. A. Diaz, and E. Franklin. 2003. Florida hogfish fishery stock assessment. Final report to Florida Fish & Wildlife Conservation Commission, 89 p. [Available from NOAA Southeast Fisheries Science Center, www.sefsc.noaa.gov/sedar/download/SEDAR6_RW4.pdf?id=DOCUMENT, accessed February 2011.]

[2] Kingsley, M. C. S., ed. 2004. The hogfish in Florida: Assessment review and advisory report. Southeast data and assessment review, 15 p. Prepared for the South Atlantic Fishery Management Council, the Gulf of Mexico Fishery Management Council, and the National Marine Fisheries Service. [Available at: http://www.sefsc.noaa.gov/sedar/download/SEDAR6_SAR2_hogfishall.pdf?id=DOCUMENT, accessed February 2011.]

or ledges; 2) natural habitat of flat hard bottom with low-relief (<0.5 m), typically limestone outcroppings and shallow potholes; or 3) artificial habitat, which was primarily shipwrecks but also included other non-natural structures (e.g., bridge pilings, building debris). Other habitats (seagrass, plain sand, or mud bottom) were uncommon and were grouped together.

Three to nine research trips were conducted monthly through all seasons: winter (January–March), spring (April–June), summer (July–September), and fall (October–December). Sampling effort was focused on rugose hard bottom as recommended by veteran divers with knowledge of hogfish distribution in the study area, and as indicated in published reports regarding hogfish ecology (Davis, 1976; Colin, 1982). Remaining habitats were systematically surveyed less often, mainly to confirm the expectations that hogfish occurred there less frequently or in lower abundance. Attempts were made to visit sites representative of each combination of habitat type and depth category at least quarterly.

Research dives

Hogfish are in general unwary of divers (Davis, 1976; Colin, 1982) and typically remain in an area when divers are present (senior author, personal observ.)—a characteristic that makes this species a good candidate for visual survey techniques (Jennings et al., 2001). Underwater observations using scuba were performed to record the presence, density, size distribution, and sex ratio of hogfish.

During each dive, a single observer (A. Collins) swam the length of a straight line 50-m transect three consecutive times. Transects were placed at the observer's discretion to maximize the length of the transect over the targeted habitat type (typically rugose hard bottom, where transects were laid in a straight line on top of the ledge). The observer waited at least one minute between setting the transect line and beginning the survey. Additionally, the observer waited one minute between the end of one replicate and the beginning of the next. During each replicate, the total number, size, and sex of hogfish observed within 3 m of the line were recorded (survey band=6×50 m, or 300 m^2). The greatest number of fish recorded during a single replicate was used to calculate hogfish density in the transect area.

Hogfish are dichromatic and dimorphic (McBride and Johnson, 2007). This attribute typically allowed visual identification of the sex of each fish. Fish were categorized as male, female, or, if sex was not obvious, sex unknown. Sex ratio (number of males divided by number of females) was calculated for each transect. The four cases in which a fish was designated as unknown were not included in the calculation of sex ratio. Maximum, minimum, and mean sizes of hogfish observed during each site visit were based on visual survey data (estimated FL, cm) as well as on harvested hogfish (measured FL, mm). Hogfish harvested from the survey area were identified during the survey and were measured only once.

Horizontal visibility was assessed by the observer during the survey. If visibility was less than 3 m, or if the site was too deep (>45 m) to allow for transect replicates, only data on fish presence were considered in further analyses (i.e., sex ratio and density were not calculated for these dives).

The binary relationship between hogfish presence (vs. absence) and habitat, depth, and season were investigated by using a general linear mixed model (GLIMMIX, SAS, vers. 9.1, SAS Inst., Cary, NC), and presence was modeled by using a binary distribution. General linear models (GLM and GLIMMIX) were also used to test for the effects of habitat, depth, and season upon each of the following variables: hogfish density, size, and sex ratio. Density was modeled with a Poisson distribution.

Life history

Hogfish were typically harvested from dive sites in accordance with fishing regulations; therefore most speared fish were greater than 305 mm FL. However, an effort was made to sample a number of small, sublegal-size fish during each season of the year. Harvested fish were otherwise randomly chosen throughout the dive. Length (FL, mm) and whole body weight (BW, to the nearest 0.25 kg) were measured for all harvested fish. Gonads were excised immediately after the diver surfaced, were wrapped in plastic, and stored on ice until they could be returned to the laboratory. Within 24 hours, gonads were weighed to the nearest 0.01 g, and a section of tissue approximately 1 cm long was removed from the middle of each gonad and placed in formalin. Histological processing followed the procedures described in McBride and Johnson (2007). Slides were examined (100–200× magnification) at least twice by an individual reader to identify reproductive class.

Reproductive class was assigned according to the method of McBride and Johnson (2007). Briefly, the most advanced oocyte stage or evidence of previous spawning (i.e., atretic advanced stage oocytes) were used to designate females as immature, mature resting, mature active, or postspawning (classes 1–4, respectively). Transitional-stage fish (class 5) were identified by the presence of seminiferous crypts along the boundary of the tunica. Males were classified by the dominant stage of spermatogenesis, the nature of the germinal epithelium, and the connection and size of sperm ducts and were designated as immature, mature inactive, ripening mature, ripe mature, or postspawning (classes 6–10, respectively).

Fish were aged by examining sectioned otoliths (sagittae). Age was independently assessed by two individual readers following the methods and criteria outlined in McBride and Richardson (2007). Growth was modeled with the von Bertalanffy growth equation:

$$FL = L_{\infty}(1 - e^{(-K[t - t_0])}),$$

where L_∞ = asymptotic fork length
K = the Brody growth coefficient; and
t_0 = the predicted age at which fish length is equal to zero.

Growth was modeled for the entire sample, as well as independently by depth category (nearshore vs. offshore).

To test for effects of fish age and depth on fish size, a 2-way analysis of variance (ANOVA) was used to compare size at age for age classes common to both depth categories (ages 3–6 yr). Size and age at female maturity and sex change were calculated with the logistic curve (binary logit model):

$$PM_t = e^{a + bX}/1 + e^{a + bX},$$

where PM_t is the probability of maturity at a particular age or length class;
a and b = constants; and
X is either length or age.

Size or age at 50% maturity = |a/b|. Model structure and fitting followed Allison (1999). Size and age at first maturity (i.e., class 1 vs. classes 2–4) and at sex change (i.e, classes 1–4 vs. classes 5–10) were modeled for each depth category, as well as for the aggregate sample.

Additional otoliths and gonads were collected opportunistically through spearfishing tournaments, trawl research cruises (Fisheries-Independent Monitoring Program of the Fish and Wildlife Research Institute), and independent diver donations. Fish were used for life history analyses only if the location and depth at capture within the central eastern Gulf of Mexico could be verified.

Results

Research dives

Hogfish presence was significantly related to habitat and depth. Fish were recorded most often and in highest densities nearshore over rugose hard bottom (Fig. 2A). Hogfish were present during 74% of all surveys (318/431) and were observed during all months of the year throughout the sampled depths and major habitat types (Tables 1 and 2). Hogfish density was greater nearshore (range 0–25; mean=5.4) than offshore (range 0–15; mean=1.3) during all seasons, and highest densities were recorded during summer (Fig. 2B). No significant relationship between presence and season was detected, nor was there a significant interaction between habitat and depth or season and depth (Table 2).

Hogfish observed during research dives nearshore were half the size of those offshore (nearshore mean=24 cm FL [range: 6–56 cm, n=1352]; offshore mean=51 cm FL [range: 18–77 cm, n=296]). Nearshore hogfish were larger in summer than in winter (P=0.0029), and offshore hogfish were larger in spring than in fall

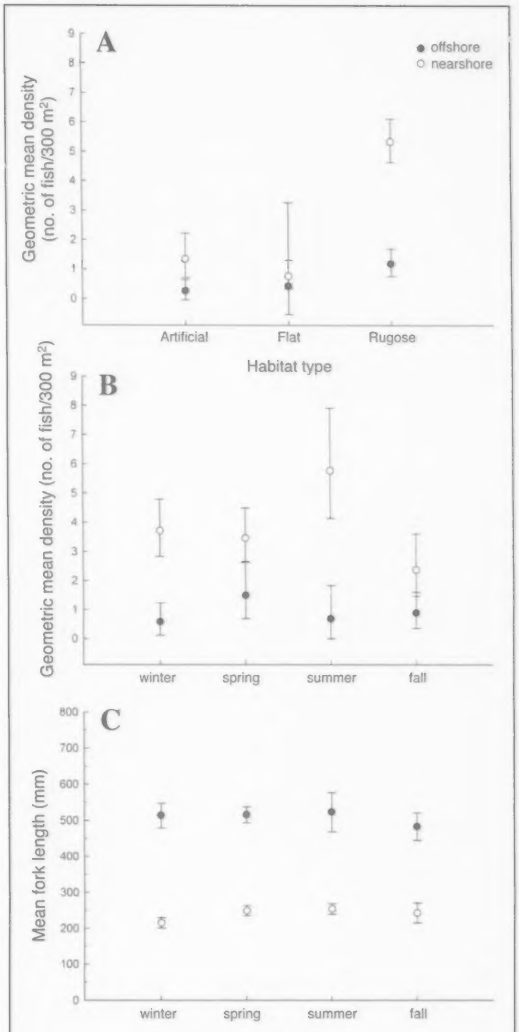

Figure 2

Geometric mean density of hogfish (*Lachnolaimus maximus*) recorded during visual transects (50×6 m bands with replication) by (**A**) habitat type and (**B**) season. (**C**) Mean fork length for hogfish observed over all seasons during all research dives. Depth categories were classified as nearshore (<30 m depth; open circles) or offshore (≥30 m depth; filled circles), and error bars represent 95% confidence limits.

(P=0.0141), but otherwise, no significant relationship was detected between fish size and season (Fig. 2C). Although density decreased with depth (P<0.0001; Fig. 3A), FL exhibited a positive relationship with depth (P<0.0001; Fig. 3B). Males were larger than females within each depth category (P<0.0001), but both sexes were larger offshore than nearshore (P<0.0001; Fig. 3B). Within depth categories, further analysis by

Table 1

Number of dives, visual transects, and hogfish (*Lachnolaimus maximus*) sampled (August 2005–August 2007) at nearshore (<30 m) and offshore (≥30 m) sites. Visual transects (research dives where replicates could be completed and visibility was ≥3 m) are indicated by habitat type as artificial (A), flat hard bottom (F), rugose hard bottom (R). The number of transects (No. of transects) during which at least one hogfish was observed (present) and the total number of transects performed (total) are listed for each month. Only seven dives were performed over other habitat (O); therefore this category was excluded from further analyses. Survey samples were harvested during research dives. Additional fish (included in the number of total fish sampled) were collected during spearfishing tournaments, trawl cruises or through private donations. *n* = number of fish sampled.

Month	No. of dives (near/offshore)	No. of transects (present/total)					*n* (survey)	Total *n* (near/offshore)
		Total	A	F	R	O		
Jan	38 (25/13)	29	2/2	3/5	19/20	0/2	46	46 (25/21)
Feb	32 (16/16)	23	0/1	0/1	10/18	0/3	28	28 (11/17)
Mar	56 (55/1)	47	7/11	2/5	28/31	0	31	36 (32/4)
Apr	63 (30/33)	32	0/2	2/5	22/25	0	65	110 (52/57)
May	34 (30/4)	26	0/2	1/3	21/21	0	26	75 (34/41)
Jun	37 (23/14)	22	2/3	0/1	17/18	0	25	33 (6/14)
Jul	27 (10/17)	14	2/3	0/1	10/10	0	25	29 (5/24)
Aug	21 (8/13)	10	0	1/2	7/8	0	21	115 (14/63)
Sep	20 (16/4)	18	0	1/2	14/16	0	16	38 (13/25)
Oct	31 (16/15)	17	2/4	3/5	8/8	0	44	80 (47/33)
Nov	31 (23/8)	22	3/9	0/3	8/8	0/2	24	27 (11/16)
Dec	41 (12/29)	23	3/7	1/2	11/14	0	35	36 (14/22)
Total	431(264/167)	283	21/44	14/35	175/197	0/7	386	653 (264/337)

Table 2

Relationship of hogfish (*Lachnolaimus maximus*) presence and density to habitat type, depth zone, and season (main effects), as well as the interaction effects between habitat type and depth zone. Hogfish were considered present if at least one individual was observed. Surveys where hogfish were present and the total survey number are indicated in parentheses (no. of surveys present/no. of surveys performed). Hogfish presence and density were significantly related to habitat and depth, and they were most common and abundant on shallow, rugose habitat. There were no significant seasonal effects on hogfish presence or density, or interactions between depth and habitat or season. LSM indicates least squares means.

	Hogfish presence				Hogfish density			
	$P>F$	F	LSM	$P>\|t\|$	$P>F$	F	LSM	$P>\|t\|$
Habitat	<0.0001*	32.38			<0.0001*	13.40		
Artificial (23/55)			0.3943	0.1797			0.9641	0.9003
Flat (16/43)			0.3248	0.0606			0.9847	0.9682
Rugose (278/324)			0.8734	<0.0001			3.5074	<0.0001
Depth zone	<0.0001*	8.7			<0.0001*	18.46		
Deep (112/166)			0.4284	0.3376			0.7591	0.3607
Shallow (205/256)			0.6904	<0.0001			2.9395	<0.0001
Season	0.6439	0.56			0.2998	1.23		
Fall (66/101)			0.5285	0.671			1.5843	0.0125
Spring (106/133)			0.5741	0.2902			1.2634	0.2131
Summer (53/68)			0.6387	0.1101			1.7192	0.0084
Winter (92/120)			0.5111	0.8787			1.4467	0.0424
Depth zone×habitat	0.4968	0.7			0.3469	1.06		
Depth zone×season	0.1488	1.79			0.0659	2.44		

10-m intervals did not reveal significant differences for density or size distribution (Fig. 3, A and B).

Hogfish aggregations varied in number and sex ratio. Females were most common and were recorded during 206 out of 283 transects (mean n=6), whereas males were recorded during only 103 out of 283 transects (mean n=1.5). As many as 25 individuals were recorded during a single transect. The maximum number of females observed during a transect was 23, and the maximum number of males observed was 4. Occasionally, more than four males were noted at a site beyond the boundaries of the transect, but typically, if males were observed, it was more common to see only one or two during the survey. When both sexes were present (n=94 transects), the largest fish observed were always males. Sex ratio (males:females) ranged from 0.0 to 1.0 (Fig. 4), with a mean of 0.14 (overall), 0.14 (nearshore), and 0.20 (offshore). Sex ratio showed no relationship to depth (P=0.90) or season (P=0.99).

Visual surveys were completed between November 2005 and June 2007, when bottom temperature, dissolved oxygen, and salinity were measured within the following ranges: 15.7–31.2°C, 6.0–9.6 mg/L, and 29–36 PSU, respectively.

Life history

Life history analyses supported visual survey observations, with hogfish size and age positively related to depth. Ages were assigned to 622/653 fish (95%), and ranged from 0 to 19 years old. Collection depth data were available for 92% of all harvested hogfish (601/653). Hogfish collected nearshore (n=264) ranged from 102 to 492 mm FL and from 0 to 8 years old; those from offshore (n=337) ranged from 319 to 774 mm FL and from 2 to 19 years old (Fig. 5). Fish at a common age were larger offshore, indicating that faster growing fish occur in deeper water (Fig. 6).

Reproductive classes were assigned to 472 aged individuals. As expected for a protogynous hermaphrodite, the majority of hogfish were female (classes 1–4; n=342). The remaining individuals were classified as transitional or immature males (class 5 or 6, respectively; n=61) or mature males (classes 7–10; n=92). Size and age at 50% maturity for females were 151.6 mm FL and 0.9 years. It is assumed that females completed maturation nearshore because immature females were not observed at depths >22 m.

Females were smaller and younger nearshore (means: 246 mm FL, 2.3 yr; n=159) than offshore (means: 479 mm FL, 6.7 yr; n=161) (P<0.0001). Sex change occurred across a wide range of sizes (197–727 mm FL) and ages (1–11 yr) and was observed both nearshore and offshore. Median size and age at sex change were significantly less nearshore (327 mm FL; 2.8 yr; n=15) than offshore (592 mm FL; 7.8 yr; n=18) (P<0.0001) (Fig. 7). The smallest transitional fish collected offshore was 449 mm FL. All fish >685 mm FL or older than 10.5 years were in the process of sex change or were already male.

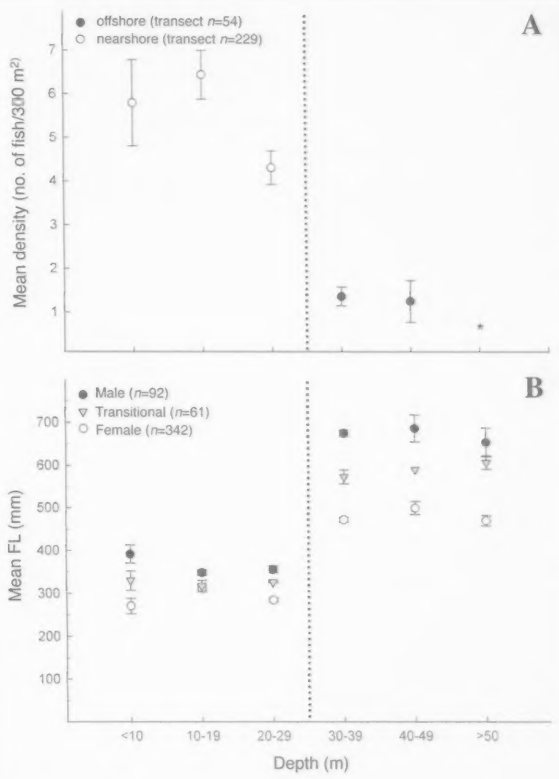

Figure 3

Mean observed densities and fork lengths (FL) for all sex phases of hogfish (*Lachnolaimus maximus*) as observed over increasing depths (by 10-m intervals). (**A**) Densities recorded during visual transects. Calculations were not performed for sites deeper than 45 m because of limited survey time, and are designated by *. (**B**) Mean fork lengths for each sex phase, as determined by histological examination. The dotted line separates nearshore and offshore data. Error bars indicate standard error of the mean.

Discussion

We identified distinct cross-shelf patterns in the presence and density of hogfish; both were greater nearshore. Hogfish were distributed widely, but not randomly. Across all depths sampled, their presence and density were greatest over complex, natural hard bottom habitats. In the Florida Keys, hogfish actively select habitat, preferring sandy rubble and gorgonian microhabitats (Muñoz et al., 2010).

The spatially explicit demographic patterns evident within this study were not detected in previous research in the eastern Gulf of Mexico, probably because the data were analyzed in aggregate from collections over a broad geographic area (McBride and Richardson, 2007; McBride et al. 2008). These new results reveal distinct demographic structure across the shelf. Nearshore, hogfish occurred in higher densities and were younger, smaller, and slower growing than those offshore. Moreover, fish changed sex at a smaller size and younger age nearshore—perhaps as a response to social cues that maintain harem structure and increase spawning success. Given these facts, the potential would be great for fishing-induced genetic shifts, except for the existence of larger, faster growing fish offshore. Potential mechanisms are evaluated in the following sections to synthesize these ecological findings and elucidate the resilience of these reef fishes to fishing and environmental factors.

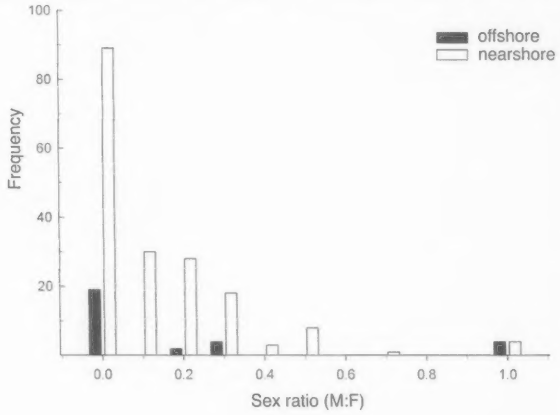

Figure 4

Frequency distribution of hogfish (*Lachnolaimus maximus*) sex ratio nearshore (<30 m depth; n=229 transects) and offshore (30–45 m depth; n=54 transects) recorded during visual transects. A value of 0.0 indicates that no males were observed; a value of 1.0 indicates that only males were observed. Sex ratios were not calculated for sites >45 m due to limited survey time.

Cross-shelf dynamics

Spatial variation in demographic parameters is not unusual for widely distributed reef fishes (Gust, 2004; DeVries, 2006; Allman, 2007; Lombardi-Carlson et al., 2008). It is likely that the underlying cross-shelf gradients of density and life history parameters observed for hogfish reflect their bipartite life cycle. Hogfish are broadcast pair-spawners whose larvae are planktonic for 30–45 d (Colin, 1982) before settling in shallow inshore habitat such as seagrass beds (Roessler, 1965; Victor, 1986; Lindeman et al., 2000). Along the west coast of Florida, juvenile hogfish use as nursery areas Tampa Bay, Charlotte Harbor, and the shallow inshore waters off Tarpon Springs and the Big Bend region (McMichael, unpubl. data[3]).

Ontogenetic migration offshore is suspected but is difficult to verify without tagging studies. Our research provides strong support for this hypothesis. Immature females were not collected from depths >22 m, and the youngest fish collected offshore (>30 m) was 2 years old, indicating that it takes at least two years to migrate from inshore settlement areas to offshore habitat. Although many reef fish have limited home ranges after settlement (e.g., Williams et al., 1994), ontogenetic habitat shifts to deeper water are not uncommon (e.g., surgeonfish [*Acanthurus chirurgus*] and parrotfish [*Scarus* spp.], Nagelkerken et al., 2000; gag grouper [*Mycteroperca microlepis*], Brulé et al., 2003; gray snapper [*Lutjanus griseus*], Faunce and Serafy, 2007).

It is likely that nearshore and offshore differences in maximum fish size and age were also, at least partially, related to the persistent, severe red tide (*Karenia brevis*) that occurred off the west coast of Florida during 2004–05, the year before this study began. Nearshore benthic communities in the study area suffered significant mortality during and following that red tide (Landsberg et al., 2009), when widespread fish kills and dead or reduced benthic fauna were reported in waters <30 m deep off Tampa Bay (Hu et al., 2006; Gannon et al., 2009).

During the last red tide outbreak of similar severity (in 1971), hogfish died or were displaced from many reefs in 13–30 m (Smith, 1975) but recolonized the affected areas within 4–10 months (Smith, 1979). Smith did not report length data, and therefore it was not possible to identify whether the source of recovery was new recruits or transient fish from unaffected reefs. Our findings regarding nearshore demographics may partially reflect the recovery of the population in that area after a major (but uncommon) toxic event.

Resiliency to localized environmental perturbations such as red tides is likely related to a species' distribution over a wide geographical range. The existence of large individuals in deep water offshore should provide a reservoir of spawning individuals to help replenish inshore areas (e.g., Simberloff, 1974). Although there were no reef-specific demographic data for the study area before the 2005 red tide, local divers recalled that the hogfish in shallow water were larger and more abundant before the toxic event. Additionally, greater numbers of relatively larger hogfish have been observed in shallow waters during research dives performed since the completion of this study (senior author, unpubl. data).

The pronounced size and age truncation observed nearshore is also likely related to greater fishing mor-

[3] McMichael, Robert. 2011. Unpubl. data. Fish and Wildlife Research Institute, Fisheries-independent monitoring group, 100 8th Avenue SE, Saint Petersburg, Florida 33701.

tality associated with increased accessibility of fish to fishing vessels. Hogfish feed on slow moving, benthic invertebrates (Randall and Warmke, 1967) and are less vulnerable to hook-and-line fishing methods than most other reef species in the region. Consequently, they are harvested primarily by spearfishing. Most recreational diving is done at depths <130 ft (40 m; PADI, 1999); at greater depths a diver's bottom time is limited and restricted to divers with higher skill levels. Additionally, because deep sites are farther from shore, fuel expense and travel time are greater. Together, these factors potentially contribute to decreased fishing-induced mortality of hogfish offshore. Tupper and Rudd (2002) noted a similar pattern in the Caribbean, where larger hogfish were present in deeper and unfished areas. This pattern has also been observed for other species in the Gulf of Mexico. Gray triggerfish (*Balistes capriscus*) exhibit decreasing mortality with increasing distance from shore (Ingram, 2001), and vermillion snapper (*Rhomboplites aurorubens*) display a spatial size dichotomy that has been related to higher exploitation rates within waters closer to shore (Allman, 2007).

Notably different patterns of sex change were observed for nearshore and offshore regions. In aggregate, sex change occurred over a broad range of ages and sizes (1–11 years and 197–727 mm FL), indicating that it is likely to be under social control (e.g., removal of the dominant male initiates sex change in a large female). The size advantage model predicts that sexual transition will occur at an earlier age in populations experiencing higher mortality (Warner, 1988), and it has often been observed that the continued removal of males results in reduced size at sex change and that size and age at the onset of sex change are lower in areas of greater fishing pressure (Warner 1975; Hawkins and Roberts, 2003; Hamilton et al., 2007). The smaller size and younger age of hogfish at sex change indicates shorter life spans and greater mortality in nearshore waters.

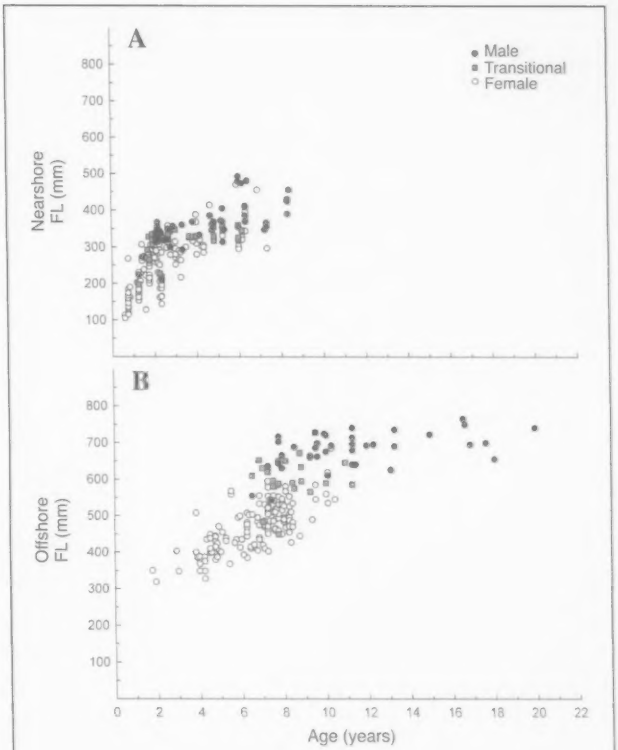

Figure 5

Hogfish (*Lachnolaimus maximus*) fork length (FL) at age for (**A**) nearshore (<30 m), and (**B**) offshore (≥30 m) collections. Gonad histology determined sexual classification as female (classes 1–4), transitional or immature male (classes 5–6), or mature male (classes 7–10). Estimated von Bertalanffy growth parameters: L_∞=380.5 mm, K=0.5614 and t_0=–0.1619 (nearshore) and L_∞=896 mm, K=0.0940 and t_0=–1.9752 (offshore).

In this study, median size at sex change nearshore (327 mm FL) just exceeded the legal minimum size (305 mm FL). These data indicate that many nearshore females are changing sex within one year after reaching legal size, since hogfish take about one year to complete sex change (McBride and Johnson, 2007). The probability of moving offshore may be related to an individual's growth rate because hogfish of the same age were larger offshore than nearshore. These faster-growing fish may have had greater energy reserves (perhaps by delaying sex change), allowing successful migration offshore. Alternately, resource (e.g., food, habitat) availability or another environmental factor may have allowed for faster growth within deeper habitat. The higher densities observed nearshore may result in an increased competition for food; however, a qualitative assessment of stomach fullness (stomach weight divided by total body weight) did not show any relationship with depth. A more quantitative assessment of prey availability and prey quality should be performed to address this question.

It is possible that differences in life history traits could reflect genetically distinct populations. Although this scenario was considered unlikely (because of the absence of immature hogfish offshore), DNA samples were collected from a subsample of individuals from both depth ranges (n=82; authors of this article, unpubl. data). Preliminary genetic analysis of microsatellite loci provided no evidence of separate stocks in our sampling area (Seyoum, unpubl. data[4]). The level of analysis available at this time cannot completely exclude the possibility, but it seems unlikely.

[4] Seyoum, Seifu. 2011. Unpubl. data. Fish and Wildlife Research Institute, 100 8th Avenue SE, Saint Petersburg, Florida 33701.

Spawning harems and management

Mature hogfish form harems; isolated males are sometimes observed but females tend to occur in pairs or groups (Davis, 1976; Colin, 1982; this study). Previous reports of hogfish sex ratios (0.1 M:F in Puerto Rico [Colin, 1982] and 0.2 M:F in Cuba [Claro et al., 1989]) coincided with the modal range that we observed (0.1–0.4 M:F). The variability in sex ratios reported herein was not related to season; therefore we conclude that harems are probably maintained throughout the year. Colin (1982) and Muñoz et al. (2010) reported high site fidelity and restricted home ranges for hogfish, at least during their spawning season (primarily winter–spring).

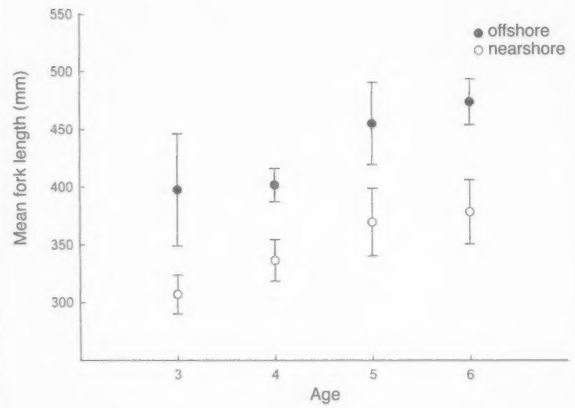

Figure 6

Mean fork length (mm) at age of hogfish (*Lachnolaimus maximus*) collected from nearshore (<30 m) and offshore (≥30 m) depths for four age classes commonly collected from both depth categories. Error bars represent 95% confidence limits.

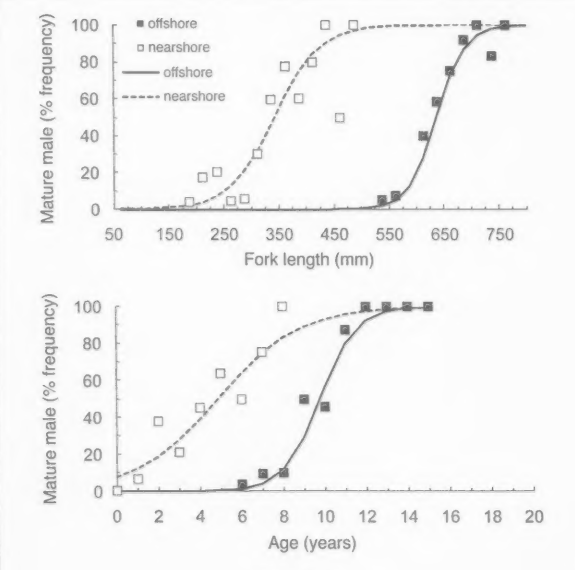

Figure 7

Maturity schedule for male hogfish (*Lachnolaimus maximus*) by fork length (top) and age (bottom). Nearshore (<30 m) hogfish are indicated by hollow squares and offshore (≥30 m) hogfish by filled squares. Lines indicate the predicted curve.

The wide range of sizes observed for transitional hogfish indicates the mechanism is under social (rather than genetic) control. Warner (1984) showed that female wrasse change sex at smaller sizes when densities are high because a single small male could not monopolize mating, increasing female incentive to change sex. However, large male size or low density discouraged competition, and sexual transition by females was postponed. Smaller sizes and higher densities of hogfish observed nearshore would indicate that social mechanisms were likely responsible for the cross shelf patterns of size and age at sex change for this protogynous fish.

Spawning success was much higher in a protected area of the Florida Keys than in an adjacent area open to fishing, even though the frequency of contact between sexes was the same in both areas (Muñoz et al., 2010). Muñoz et al. proposed that lower rates of mortality will create a familiar social order, facilitating courtship and increasing spawning rates. Higher levels of mortality in nearshore waters may thus potentially disrupt harem structure and reduce reproductive output in more heavily fished areas.

Conclusions

Although there is evidence of fishing effects in nearshore waters, the continued escapement of fast-growing fish to deeper waters reduces concerns about fishery-induced evolution of life history traits that could occur if fast growers were being harvested at such a rate that they could no longer spawn successfully. The maximum size and age of hogfish reported herein are similar to those reported for Cuban waters, where there is a relatively "unfished population" (Claro et al., 1989), and to those measured previously within the current study area (1995–2001; McBride and Richardson, 2007). The technical and logistic limits that prevent most spearfishing in offshore waters and the behavioral peculiarities that make hogfish less vulnerable to hook-and-line fisheries appear to support a *de facto* refuge for some of the faster growing and largest hogfish. Offshore females spawn for longer periods and produce larger batches of eggs than do nearshore females (authors of this article, unpubl. data), and therefore the persistent escape-

ment to offshore waters may contribute notably to the reproductive success of hogfish in the eastern Gulf of Mexico (Johannes, 1998; Birkeland and Dayton, 2005). Still, because the conspicuous nature and inquisitive behavior of hogfish make them very vulnerable to fishing, routine monitoring of fishing effort or fishing power by the spearfishing sector is warranted, as is periodic monitoring of spatially explicit densities, harem structure, and life history traits of this species.

Acknowledgments

This work could not have been completed without the dedication of the members of the Saint Petersburg Underwater Club (SPUC). D. O'Hern acted as the SPUC spokesman throughout this research. We would like to thank captains B. Bateman, L. Borden, W. Butts, J. DeLaCruz, C. Gardinal, C. Grauer, T. Grogan, B. Hardman, J. Hermes, S. Hooker, I. Lathrop, S. Lucas, M. Joswig, D. O'Hern, D. Palmer, H. Scarboro, C. Schnur, and R. Taylor. E. Leone, M. Murphy, and M. Greenwood provided statistical guidance. A. Richardson and K. McWhorter provided laboratory assistance. FWRI's Fisheries-Independent Monitoring Program provided trawl samples. D. DeVries served as the NOAA/NMFS partner and provided useful comments throughout the project. G. Shepherd, J. Colvocoresses, M. Murphy and three anonymous reviewers provided comments that improved this manuscript. The majority of the work described herein was funded by grant NA05NMF4540040 to the Florida Fish and Wildlife Conservation Commission from the National Oceanic and Atmospheric Administration's Cooperative Research Program.

Literature cited

Adams, S., B. D. Mapston, G. R. Russ, and C. R. Davies.
2000. Geographic variation in the sex ratio, sex specific size, and age structure of *Plectropomus leopardus* (Serranidae) between reefs open and closed to fishing on the Great Barrier Reef. Can. J. Fish. Aquat. Sci. 57:1448–1458.

Allison, P. D.
1999. Logistic regression using the SAS System, 288 p. SAS Institute, Inc., Cary, NC.

Allman, R.J.
2007. Small-scale spatial variation in the population structure of vermilion snapper (*Rhomboplites aurorubens*) from the northeast Gulf of Mexico. Fish. Res. 88:88–99.

Alonzo, S. H., and M. Mangel.
2005. Sex-change rules, stock dynamics, and the performance of spawning-per-recruit measures in protogynous stocks. Fish. Bull. 103:229–245.

Bannerot, S., W. W. Fox, and J. E. Powers.
1987. Reproductive strategies and the management of snappers and groupers. *In* Tropical snappers and groupers: biology and fisheries management (J. J. Polovina and S. Ralston, eds.), p. 561–603. Westview Press, Boulder, CO.

Birkeland, C., and P. K. Dayton.
2005. The importance in fishery management of leaving the big ones. Trends Ecol. Evol. 20:356–358.

Brooks, E. N., J. E. Powers, and E. Cortés.
2010. Analytical reference points for age-structured models: application to data-poor fisheries. ICES J. Mar. Sci. 67:165–175.

Brulé, T., C. Deniel, T. Colás-Marrufo, and M. Sanchez-Crespo.
2003. Reproductive biology of gag in the southern Gulf of Mexico. J. Fish Biol. 63:1505–1520.

Claro, R., A. Garcia-Cagide, and R. Fernández de Alaiza.
1989. Caracteristicas biológicas del pez perro, *Lachnolaimus maximus* (Walbaum), en el golfo de Batabanó, Cuba. Rev. Investig. Mar. 10:239–252. [In Spanish.]

Colin, P. L.
1982. Spawning and larval development of the hogfish, *Lachnolaimus maximus* (Pisces: Labridae). Fish. Bull. 80:853–862.

Davis, J. C.
1976. Biology of the hogfish, *Lachnolaimus maximus* (Walbaum), in the Florida Keys. M.S. thesis, 86 p. Univ. Miami, Coral Gables, FL.

DeVries, D. A.
2006. The life history, reproductive ecology, and demography of the red porgy, *Pagrus pagrus*, in the northeastern Gulf of Mexico. Ph.D. diss., 160 p. Florida State Univ., Tallahassee, FL.

Faunce, C. H., and J. E. Serafy.
2007. Nearshore habitat use by gray snapper (*Lutjanus griseus*) and bluestriped grunt (*Haemulon sciurus*): environmental gradients and ontogenetic shifts. Bull. Mar. Sci. 80:473–495.

Gannon, D. P., E. J. Berens McCabe, S. A. Camilleri, J. G. Gannon, M. K. Brueggen, A. A. Barleycorn, V. I. Palubok, G. J. Kirkpatrick, and R. S. Wells.
2009. Effects of *Karenia brevis* harmful algal blooms on nearshore fish communities in southwest Florida. Mar. Ecol. Prog. Ser. 378:171–186.

Gust, N.
2004. Variation in the population biology of protogynous coral reef fishes over tens of kilometres. Can. J. Fish. Aquat. Sci. 61:205–218.

Hamilton, S. L., J. E. Caselle, J. D. Standish, D. M. Schroeder, M. S. Love, J. A. Rosales-Casian, and O. Sosa-Nishizaki.
2007. Size-selective harvesting alters life histories of a temperate sex-changing fish. Ecol. Appl. 17:2268–2280.

Harris, P. J., and J. C. McGovern.
1997. Changes in the life history of red porgy, *Pagrus pagrus*, from the southeastern United States, 1972–1994. Fish. Bull. 95:732–747.

Hawkins, J. P., and C. M. Roberts.
2003. Effects of fishing on sex-changing Caribbean parrotfishes. Biol. Conserv. 115:213–226.

Heppell, S. S., S. A. Heppell, F. C. Coleman, and C. C. Koenig.
2006. Models to compare management options for a protogynous fish. Ecol. Appl. 16:238–249.

Hu, C., F. E. Muller-Karger, and P. W. Swarzenski.
2006. Hurricanes, submarine groundwater discharge, and Florida's red tides. Geophys. Res. Lett. 33 (L11601):1–5.

Ingram, G. W., Jr.
2001. Stock structure of gray triggerfish *Balistes capriscus* on multiple spatial scales in the Gulf of Mexico. Ph.D. diss., 228 p. Univ. South Alabama, Mobile, AL

Jennings, S. D., M. J. Kaiser, and J. D. Reynolds.
2001. Marine fisheries ecology, 417 p. Blackwell Science Ltd., Malden, MA.

Johannes, R. E.
1998. The case for data-less marine resource management: examples from tropical nearshore finfisheries. Trends Ecol. Evol. 13:243–246.
Landsberg, J. H., L. J. Flewelling, and J. Naar.
2009. *Karenia brevis* red tides, brevetoxins in the food web, and impacts on natural resources: Decadal advancements. Harmful Algae 8:598–607.
Lindeman, K. C., R. Pugliese, G. T. Waugh, and J. S. Ault.
2000. Developmental patterns within a multispecies reef fishery: management applications for essential fish habitats and protected areas. Bull. Mar. Sci. 66:929–956.
Lombardi-Carlson, L., G. Fitzhugh, C. Palmer, C. Gardner, R. Farsky, and M. Ortiz.
2008. Regional size, age and growth differences of red grouper (*Epinephelus morio*) along the west coast of Florida. Fish. Res. 91:239–251.
McBride, R. S., and M. R. Johnson.
2007. Sexual development and reproductive seasonality of hogfish (Labridae: *Lachnolaimus maximus*), an hermaphroditic reef fish. J. Fish. Biol. 71:1270–1292.
McBride, R. S., and A. K. Richardson.
2007. Evidence of size-selective fishing mortality from an age and growth study of hogfish (Labridae: *Lachnolaimus maximus*), a hermaphroditic reef fish. Bull. Mar. Sci. 80:401–417.
McBride, R. S., P. E. Thurman, and L. H. Bullock.
2008. Regional variations of hogfish (*Lachnolaimus maximus*) life history: Consequences for spawning biomass and egg production models. J. Northw. Atl. Fish. Sci. 41:1–12.
Muñoz, R. C., M. L. Burton, K. J. Brennan, and R. O. Parker.
2010. Reproduction, habitat utilization, and movements of hogfish (*Lachnolaimus maximus*) in the Florida Keys, U.S.A.: comparisons from fished versus unfished habitats. Bull. Mar. Sci. 86:93–116.
Nagelkerken, I., M. Dorenbosch, W. C. E. P. Verberk, E. Cocheret de la Morinière, and G. van der Velde.
2000. Importance of shallow-water biotopes of a Caribbean bay for juvenile coral reef fishes: patterns in biotope association, community structure and spatial distribution. Mar. Ecol. Prog. Ser. 202:175–192.
PADI (Professional Association of Diving Instructors).
1999. The PADI divemaster manual (D. Richardson , ed.), 200 p. International PADI, Inc., Santa Margarita, CA.
Randall, J. A., and G. L. Warmke.
1967. The food habits of the hogfish (*Lachnolaimus maximus*), a labrid fish from the western Atlantic. Caribb. J. Sci. 7:141–144.
Roessler, M.
1965. An analysis of the variability of fish populations taken by otter trawl in Biscayne Bay, Florida. Trans. Am. Fish. Soc. 94:311–318.
Simberloff, D. S.
1974. Equilibrium theory of island biogeography and ecology. Annu. Rev. Ecol. Syst. 5:161–182.
Sluka, R. D., and K. M. Sullivan.
1998. The influence of spear fishing on species composition and size of groupers on patch reefs in the upper Florida Keys. Fish. Bull. 96:388–392.
Smith, G. B.
1975. The 1971 red tide and its impact on certain reef communities in the mid-eastern Gulf of Mexico. Environ. Lett. 9:141–152.
1979. Relationship of eastern Gulf of Mexico reef-fish communities to the species equilibrium theory of insular biogeography. J. Biogeogr. 6:49–61.
Tupper, M., and M. A. Rudd.
2002. Species specific impacts of a small marine reserve on reef fish production and fishing productivity in the Turks and Caicos Islands. Environ. Conserv. 29:484–492.
Victor, B. C.
1986. Duration of the planktonic larval stage of one hundred species of Pacific and Atlantic wrasses (family Labridae). Mar. Biol. 90:317–326.
Warner, R. R.
1975. The reproductive biology of the protogynous hermaphrodite *Pimelometopon pulchrum* (Pisces: Labridae). Fish. Bull. 73:262–283.
1984. Deferred reproduction as a response to sexual selection in a coral reef fish: a test of the life historical consequences. Evolution 38:148–162.
1988. Sex change and the size-advantage model. Trends Ecol. Evol. 3:133–136.
Williams, D., McB., S. English, and M. J. Milicich.
1994. Annual recruitment surveys of coral reef fishes are good indicators of patterns of settlement. Bull. Mar. Sci. 54: 314–331.

Errata

Fishery Bulletin 109:20–33

Friess, Claudia, and George R. Sedberry

Age, growth, and spawning season of red bream (*Beryx decadactylus*) off the southeastern United States

Page 26, Table 1. Please note that in the column labeled Δ14C (‰) (±error) that some values were shown incorrectly as negative. The following table shows the correct values for that column.

Table 1

Summary of radiocarbon ($\Delta^{14}C$) results from red bream (*Beryx decadactylus*) otoliths collected off the southeast coast of the United States. NOSAMS accession no.= identification number assigned by the Woods Hole National Ocean Sciences Accelerator Mass Spectrometry Facility.

NOSAMS accession no.	Collection year	Birth year	Sample weight (mg)	Reading 1 age (yr)	Reading 2 age (yr)	Reading 3 (joint) age (yr)	$\Delta^{14}C$ (‰) (±error)
OS-67042	2007	1945	81.1	62	62	62	−61.5 (3.2)
OS-66866	2007	1951	40.6	58	59	56	−54.1 (4.0)
OS-66870	2006	1952	52	54	62	54	−62.1 (3.6)
OS-67041	2006	1958	56.5	48	50	48	−52.3 (2.9)
OS-66869	2007	1959	48.4	54	55	48	−67.7 (3.6)
OS-68036	2004	1959	74	38	43	45	−42.6 (3.3)
OS-68037	2005	1963	56.9	41	47	42	−67.8 (2.8)
OS-66868	2005	1964	86.6	44	50	41	−65.7 (3.2)
OS-68041	2004	1966	85.1	37	38	38	−18.7 (3.1)
OS-68142	2006	1966	152.3	40	43	40	25.3 (3.7)
OS-68035	2003	1967	75.3	24	32	36	14.4 (3.2)
OS-66867	2005	1969	42.7	33	38	36	48.6 (3.6)
OS-68038	2006	1970	99	38	42	36	−34.3 (3.2)
OS-66998	2004	1974	39.6	23	29	30	93.4 (4.1)
OS-68034	2005	1982	75.5	18	27	23	67.0 (3.6)
OS-67038	2004	1989	35.6	11	11	15	89.8 (4.1)
OS-68040	2003	1989	77.2	14	19	14	85.7 (5.1)
OS-67040	2005	1991	70.6	10	11	14	82.6 (3.4)

Fishery Bulletin

Guidelines for authors

Manuscript Preparation

Contributions published in *Fishery Bulletin* describe original research in marine fishery science, fishery engineering and economics, as well as the areas of marine environmental and ecological sciences (including modeling). Preference will be given to manuscripts that examine processes and underlying patterns. Descriptive reports, surveys, and observational papers may occasionally be published but should appeal to an audience outside the locale in which the study was conducted. Although all contributions are subject to peer review, responsibility for the contents of papers rests upon the authors and not on the editor or publisher. *Submission of an article implies that the article is original and is not being considered for publication elsewhere.* **Articles** may range from relatively short contributions (10–15 typed, double-spaced pages, tables and figures not included) to extensive contributions (20–30 typed pages). Manuscripts must be written in English; authors whose native language is not English are strongly advised to have their manuscripts checked by English-speaking colleagues before submission.

Title page should include authors' full names and mailing addresses and the senior author's telephone, fax number, and e-mail address, and a list of key words to describe the contents of the manuscript. **Abstract** should be limited to 200 words (one-half typed page), state the main scope of the research, and emphasize the author's conclusions and relevant findings. Do not review the methods of the study or list the contents of the paper. Because abstracts are circulated by abstracting agencies, it is important that they represent the research clearly and concisely. **Text** must be typed in 12 point Times New Roman font throughout. A brief introduction should convey the broad significance of the paper; the remainder of the paper should be divided into the following sections: **Materials and methods**, **Results**, **Discussion**, **Conclusions**, and **Acknowledgments**. Headings within each section must be short, reflect a logical sequence, and follow the rules of multiple subdivision (i.e., there can be no subdivision without at least two items). The entire text should be intelligible to interdisciplinary readers; therefore, all acronyms, abbreviations, and technical terms should be written out in full the first time they are mentioned. Include FAO common names for species in the list of keywords and in the introduction. Regional common names may be used throughout the rest of the text if they are different from FAO common names which can be found at http://www.fishbase.org/search.html. Follow the U.S. Government Printing Office Style Manual (2000 ed.) and Scientific Style and Format: the CSE Manual for Authors, Editors, and Publishers (7th ed.) for editorial style; for fish nomenclature follow the most current issue of the American Fisheries Society's Common and Scientific Names of Fishes from the United States, Canada, and Mexico, 6th ed. Dates should be written as follows: 11 November 2000. Measurements should be expressed in metric units, e.g., 58 metric tons (t); if other units of measurement are used, please make this fact explicit to the reader. Write out the numbers zero through nine unless they form part of measurement units (e.g., nine fish but 9 mm). Refrain from using the shorthand slash (/), an ambiguous symbol, in the general text.

Equations and mathematical symbols Set equations from a standard mathematical program (MathType) or tool (Equation Editor in MS Word). LaTex is acceptable for more advanced computations. For mathematical symbols in the general text (α, χ^2, π, $\pm$, etc.), use the symbols provided by the MS Word program and italicize all variables. Do not use the photo mode when creating these symbols in the general text.

Literature cited comprises published works and those accepted for publication in peer-reviewed literature (in press). Follow the name and year system for citation format in the "Literature cited" section (that is say, citations should be listed alphabetically by the authors' last names, and then by year if there is more than one citation with the same authorship). If there is a sequence of citations in the text, list chronologically: (Smith, 1932; Green, 1947; Smith and Jones, 1985). Abbreviations of serials should conform to abbreviations given in Cambridge Scientific Abstracts (http://www.csa.com/ids70/serials_source_list.php?ab=biolclast-set-c). Authors are responsible for the accuracy and completeness of all citations. Literature citation format: Author (last name, followed by first-name initials). Year. Title of report or manuscript. Abbreviated title of the series to which it belongs. Always include number of pages. Cite all software and special equipment or chemical solutions used in the study, not in a footnote but within parentheses in the text (e.g., SAS, vers. 6.03, SAS Inst., Inc., Cary, NC).

Tables are often overused in scientific papers; it is seldom necessary or even desirable to present all the data associated with a study. Tables should not be excessive in size and must be cited in numerical order in the text. Headings should be short but ample enough to allow the table to be intelligible on its own. All unusual symbols must be explained in the table legend. Other incidental comments may be footnoted with italic numeral footnote markers. Use asterisks to indicate significance in statistical data. Do not type table legends on a separate page; place them above the table data. *Do not submit tables in photo mode.*

Figures include line illustrations, photographs (or slides), and computer-generated graphs and must be cited in numerical order in the text. Graphics should aid in the comprehension of the text, but they should be limited to presenting patterns rather than raw data. Figures should not exceed one figure for every four pages of text. Figures must be labeled with author's

name and number of the figure. Avoid placing labels vertically (except for *y* axis). Figure legends should explain all symbols and abbreviations and should be double-spaced on a separate page at the end of the manuscript. Color is allowed in figures to show morphological differences among species (for species identification), to show stain reactions, and to show gradations in temperature contours within maps. Color is discouraged in graphs, and for the few instances where color may be allowed, the use of color will be determined by the Managing Editor.

- Zeros should precede all decimal points for values less than one.
- Sample size, *n*, should be italicized.
- Capitalize the first letter of the first word in all labels within figures.
- Do not use overly large font sizes in maps and for units of measurements along axes in figures.
- Do not use bold fonts or bold lines in figures.
- Do not place outline rules around graphs.
- Use a comma in numbers of five digits or more (e.g. 13,000 but 3000).
- Maps require a North arrow and degrees latitude-longitude (e.g., 170°E).

Failure to follow these guidelines and failure to correspond with editors in a timely manner will delay publication of a manuscript.

Copyright law does not apply to *Fishery Bulletin*, which falls within the public domain. However, if an author reproduces any part of an article from *Fishery Bulletin* in his or her work, reference to source is considered correct form (e.g., Source: Fish. Bull. 97:105).

Submission

Submit manuscript online at http://mc.manuscriptcentral.com/fisherybulletin. Commerce Department personnel should submit papers under a completed NOAA Form 25-700. For further details on electronic submission, please contact the Scientific Editorial Office directly at

julie.scheurer@noaa.gov

Once the manuscript has been accepted for publication, you will be asked to submit a final electronic copy of your manuscript. When requested, the text and tables should be submitted in Word format. Figures should be sent as PDF files, Windows metafiles, tiff files, or EPS files. Send a copy of figures in the original software if conversion to any of these formats yields a degraded version.

Questions? If you have questions regarding these guidelines, please contact the Managing Editor, Sharyn Matriotti, at

Sharyn.Matriotti@noaa.gov

Questions regarding manuscripts under review should be addressed to Julie Scheurer, Associate Editor.

Fishery Bulletin

Subscription form

Superintendent of Documents **Publications** Order Form

*5178

☐ YES, please send me the following publications:

____ Subscriptions to *Fishery Bulletin*
for $36.00 per year ($50.40 foreign)

The total cost of my order is $ _____ . Prices include regular domestic postage and handling and are subject to change.

_____
(Company or Personal Name) (Please type or print)

_____
(Additional address/attention line)

_____
(Street address)

_____
(City, State, ZIP Code)

_____
(Daytime phone including area code)

_____
(Purchase Order No.)

Charge your order. IT'S EASY!

VISA

MasterCard

Please Choose Method of Payment:

☐ Check Payable to the Superintendent of Documents

☐ GPO Deposit Account ☐☐☐☐☐☐☐–☐

☐ VISA or MasterCard Account

☐☐☐☐☐☐☐☐☐☐☐☐☐☐☐☐

☐☐☐☐ (Credit card expiration date)

To fax your orders (202) 512-2250

_____
(Authorizing Signature)

Thank you for your order!

Mail To: Superintendent of Documents
P.O. Box 371954, Pittsburgh, PA 15250-7954
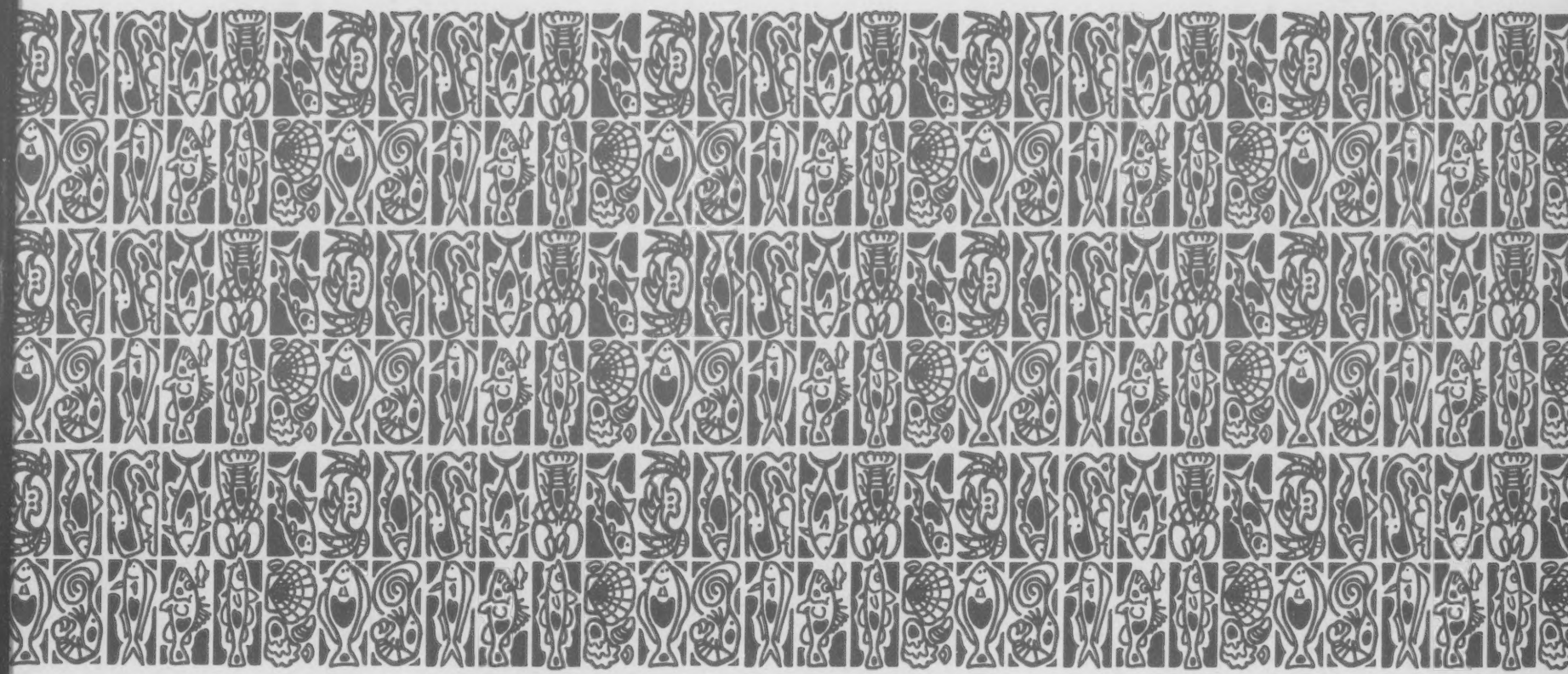
Also available online at http://bookstore.gpo.gov/collections/fishery-bulletin